CRETACEOUS/PALEOGENE BOUNDARY IN THE HAYMANA BASIN, CENTRAL ANATOLIA, TURKEY: MICROPALEONTOLOGICAL, MINERALOGICAL AND SEQUENCE STRATIGRAPHIC APPROACH

A THESIS SUBMITTED TO
THE GRADUATE SCHOOL OF NATURAL AND APPLIED SCIENCES
OF
MIDDLE EAST TECHNICAL UNIVERSITY

BY

SELEN ESMERAY

IN PARTIAL FULFILLMENT OF THE REQUIREMENTS
FOR
THE DEGREE OF MASTER OF SCIENCE
IN
GEOLOGICAL ENGINEERING

AUGUST 2008

Approval of the thesis:

CRETACEOUS/PALEOGENE BOUNDARY IN THE HAYMANA BASIN, CENTRAL ANATOLIA, TURKEY: MICROPALEONTOLOGICAL, MINERALOGICAL AND SEQUENCE STRATIGRAPHIC APPROACH

submitted by **SELEN ESMERAY** in partial fulfillment of the requirements for the degree of **Master of Science in Geological Engineering Department, Middle East Technical University** by,

Prof. Dr. Canan Özgen _____
Dean, Graduate School of **Natural and Applied Sciences**

Prof. Dr. Vedat Doyuran _____
Head of Department, **Geological Engineering**

Prof. Dr. Demir Altıner _____
Supervisor, **Geological Engineering Dept., METU**

Assoc. Prof. Dr. Sevinç Özkan Altıner _____
Co-Supervisor, **Geological Engineering Dept., METU**

Examining Committee Members:

Prof. Dr. Asuman Günal Türkmenoğlu _____
Geological Engineering Dept., METU

Prof. Dr. Demir Altıner _____
Geological Engineering Dept., METU

Assoc. Prof. Dr. Bora Rojay _____
Geological Engineering Dept., METU

Assist. Prof. Dr. İsmail Ömer Yılmaz _____
Geological Engineering Dept., METU

Dr. Zühtü Batı _____
Research Center, TPAO

Date: 22.08.2008

I hereby declare that all information in this document has been obtained and presented in accordance with academic rules and ethical conduct. I also declare that, as required by these rules and conduct, I have fully cited and referenced all material and results that are not original to this work.

Name, Last Name: Selen Esmeray

Signature:

ABSTRACT

CRETACEOUS/PALEOGENE BOUNDARY IN THE HAYMANA BASIN, CENTRAL ANATOLIA, TURKEY: MICROPALEONTOLOGICAL, MINERALOGICAL AND SEQUENCE STRATIGRAPHIC APPROACH

Esmeray, Selen

M. Sc., Department of Geological Engineering

Supervisor: Prof. Dr. Demir Altıner

Co-Supervisor: Assoc. Prof. Dr. Sevinç Altıner

August 2008, 271 pages

An integrated micropaleontological, mineralogical and sequence stratigraphical investigation was carried out across the Cretaceous/Paleogene (K/P) boundary in the Haymana basin, Turkey. A 29.41 m thick boundary section consisting of limestones and marls was measured and 90 samples were analyzed. Biostratigraphic and chronostratigraphic works are based on the planktonic foraminifera. 64 planktonic species were identified and 5 biozones were established. The biozones are, in ascending order, *Planoglobulina acervulinoides* zone, *Racemiguembelina fructicosa* zone, *Pseudoguembelina hariaensis* zone for the Late Maastrichtian; *Guembelitria cretacea* (P0) zone and *Parvulorugoglobigerina eugubina* (P1a) zone for the Early Danian.

In order to detect the mineralogical changes across the boundary bulk and clay minerals were analyzed using X-ray diffractometry (XRD). Calcite, quartz, feldspar and the clay minerals composed of smectite (montmorillonite) and chlorite are the main components of the rocks. A decrease in calcite and an increase in the detrital minerals (quartz, feldspar) and the clay minerals were detected in the boundary beds.

In order to find out the depositional history of the area a detailed microfacies study was performed and 10 microfacies type were determined. The microfacies types defined correspond to slope to basin environment. Based on microfacies analyses, the sequence stratigraphic framework of the boundary beds was constructed. K/P boundary beds were recorded in the transition of transgressive systems tract to highstand systems tract, coinciding with a maximum flooding surface. These beds show a similar pattern with many other K/P boundary beds in different locations of the world indicating eustatic sea-level variations overprint the tectonic control in the basin.

Keywords: Cretaceous/Paleogene Boundary, Planktonic Foraminifera, Microfacies Analysis and Sequence Stratigraphy, Bulk and Clay Mineralogy, Haymana Basin

ÖZ

HAYMANA HAVZASI'NDA (ORTA ANADOLU, TÜRKİYE) KRETASE/PALEOJEN SINIRI: MİKROPALEONTOLOJİK, MİNERALOJİK VE SEKANS STRATİGRAFİK YAKLAŞIM

Esmeray, Selen

Yüksek Lisans, Jeoloji Mühendisliği Bölümü

Tez Yöneticisi: Prof. Dr. Demir Altıner

Ortak Tez Yöneticisi: Doç. Dr. Sevinç Altıner

Ağustos 2008, 271 sayfa

Orta Anadolu'da yer alan Haymana Havzası'nda Kretase/Paleojen sınır tabakaları boyunca mikropaleontolojik, mineralojik ve sekans stratigrafik çalışmalar gerçekleştirilmiştir. Kireçtaşı ve marnlardan oluşan 29,41 metrelik bir kesit ölçülmüş ve bu kesit boyunca alınan 90 adet örnek incelenmiştir. Biyostratikrafik ve kronostratigrafik çalışmalar planktonik foraminiferlerle yapılmıştır. 64 adet tür tayin edilmiş ve 5 adet biyozon belirlenmiştir. Bu biyozonlar, aşağıdan yukarıya doğru, Maastrihtiyen'de *Planoglobulina acervulinoides* zonu, *Racemiguembelina fructicosa* zonu, *Pseudoguembelina hariaensis* zonu; Erken Daniyen'de ise *Guembelitria cretacea* (P0) zonu ve *Parvulorugoglobigerina eugubina* (P1a) zonudur.

Sınır birimleri boyunca görülen mineralojik değişimleri belirleyebilmek için, örneklerde X-ışını kırınımı (XRD) metodu ile tümkaya ve kil mineralleri incelenmiştir. Kayaçları oluşturan ana mineraller kalsit, kuvars, feldispat ve kil minerallerinden simektit (montmorillonit) ve klorittir. Sınır birimlerinde kalsit mineralinin yüzdesinde bir düşüş gözlemlenirken, kuvars ve feldispat gibi detrital minerallerde ve kil minerallerinde bir artış tespit edilmiştir.

Alanın çökelim tarihçesini belirleyebilmek için detaylı mikrofasiyes çalışmaları gerçekleştirlmiş ve 10 adet mikrofasiyes tipi belirlenmiştir. Belirlenen mikrofasiyes tipleri çökelimin yamaçtan havzaya doğru bir bölgede gerçekleştiğini göstermektedir. Mikrofasiyes analizleri temel alınarak sekans stratigrafisi çatısı oluşturulmuştur. Kretase/Paleojen sınır birimlerinin transgresif sistem çökelleri ile yüksek deniz seviyesi sistem çökelleri geçişinde, ve bir maksimum sellenme yüzeyine denk gelecek şekilde çökeldiği belirlenmiştir. Sınır birimleri, dünyanın farklı bölgelerdeki Kretase/Paleojen sınır birimleri ile benzerlik göstermekte, bu durum da havzadaki östatik deniz seviyesi değişimlerinin tektonik kontrollü değişimlerden daha baskın olduğuna işaret etmektedir.

Anahtar Kelimeler: Kretase/Paleojen Sınırı, Planktonik Foraminifer, Mikrofasiyes Analizi ve Sekans Stratigrafisi, Tümkaya ve Kil Mineralojisi, Haymana Havzası

To my beloved parents and sister

ACKNOWLEDGEMENTS

I would like to express my gratitude to my supervisor Prof. Dr. Demir ALTINER for his wisdom, clear guidance, critical vision, encouragements and endless support in every stage of this thesis. He has always been a role model for me with his scientific curiosity, endless eagerness to research and as well as with his motivating, sensitive and understanding approach towards to the people he works with. It is a great honor to feel his trust, support and appreciation.

I would like to express my appreciation to my co-supervisor Assoc. Prof. Dr. Sevinç ÖZKAN ALTINER for monitoring each step of this thesis with a great concern and supporting the progress of the work with her valuable advices. I am especially grateful for her clear guidance and her endless help during the micropaleontological work. It was a great chance for me to have had utilized her profound knowledge on the taxonomy of the planktonic foraminifera. Whenever I was discouraged she motivated me with a wise and affectionate manner and gave me the strength to continue my work.

I would like to thank Assist. Prof. Dr. İ. Ömer YILMAZ for his scientific support and encouragement during this study. His valuable advices about the mineralogical analyses were very useful for me.

I am grateful to Prof. Dr. Mevlüt ERTAN in the Department of Pharmacy at the Hacettepe University for his precious information about the disintegration techniques of the rocks. He has a great contribution to the improvement of the washing techniques.

I would like to express my gratitude to Prof. Dr. Asuman GÜNAL TÜRKMENOĞLU for her time, consideration and valuable advices for the interpretation of the XRD results.

I would like thank to Assist. Prof. Dr. Fatma TOKSOY KÖKSAL for allowing me kindly to use the equipments in the clay mineralogy laboratory and for her information related to the mineralogical analyses.

I am indebted to Prof. Dr. Isabella PREMOLI-SILVA for her help in identifications of certain species. It was an honor for me to have had discussions with her about the taxonomy of the planktonic foraminifera. I am also grateful to Prof. Dr. Gerta KELLER for the valuable information that she has given through e-mail.

I would like to thank to Dr. Doğan ALAYGUT for his help during the XRD analysis in the Research Center of TPAO and to Mr. Orhan KARAMAN for helping in the field studies and for preparing the thin sections.

I would like to thank to my dear friends Mrs. Ayşe ATAKUL ÖZDEMİR, Ms. Sabire Aslı OFLAZ and Ms. Hayriye ÇAKMAK for their motivation and to Mr. Elnur AMIROV for helping me in washing some samples.

I am grateful to Mr. Turgay SENLET for his endless help, technical support, patience and motivation during my study. Without his company and the bright and practical solutions he suggests to each problem, this study would not have been completed.

I would like to thank to the Scientific and Technological Research Council of Turkey (TÜBİTAK) for their scholarship during my M.Sc. study and to the METU Scientific Research Projects Coordination (BAP) for giving financial support for this study.

At last but definitely not the least, I would like to express my gratitude to my parents Mrs. Asuman ESMERAY & Mr. Mehmet ESMERAY, and my sister Ms. Müge ESMERAY for their encouragements, understanding and endless patience. I would like to thank also to my aunt Mrs. Yasemin ÖZBEK for her motivation during my study. Without the support of my family, this study would not have been accomplished.

TABLE OF CONTENTS

LIST OF TABLES

TABLES

LIST OF FIGURES

FIGURES

CHAPTER 1

INTRODUCTION

1.1 PURPOSE AND SCOPE

The objective of this thesis is to delineate the Cretaceous/Paleogene (K/P) boundary in a section measured in the Haymana basin, Turkey using planktonic foraminifera, to investigate the lithological and mineralogical changes across the boundary, to describe the evolution of the depositional environment using microfacies data and to interpret the stratal changes within the sequence stratigraphical framework.

K/P boundary event is one of the most significant global phenomena that has gained great attention worldwide. Different aspects of it have been studied by many authors in detail. This study aims to contribute to this international study by describing one of the K/P boundary sections in Turkey by using many disciplines.

K/P boundary marks the border between the Mesozoic and Cenozoic eras and corresponds to the 65 Ma. At the boundary, the earth has undergone very significant events after a meteoroid hit the Yucatan Peninsula, Mexico creating the Chicxulub crater (Alvarez *et al*., 1980). This impact event has caused the world suffer one of the five big mass extinctions (Raup and Sepkoski, 1982). The planktonic foraminifera have also experienced a great turnover at the boundary, especially in low latitudes. All keeled, large, ornamented forms like globotruncanids, racemiguembelinids and rugoglobigerinids have been extinct; new, very small, non-ornamented forms have been evolved. Only a few species could survive the K/P boundary. One of the main purposes of this study is to observe the changes in the planktonic foraminiferal fauna in the Haymana basin,

to construct a detailed taxonomy of the Late Cretaceous and Early Paleocene forms and determine a detailed planktonic foraminiferal biozonation. In order to achieve this goal the studied section has been measured twice. After determining the rough location of the boundary the section has been remeasured and new samples have been collected in cm-scale intervals. In order not to miss the first Danian forms, residues greater than 63μm size of the washed samples have been examined. This thesis is the first study carried out in Turkey that defines the first Danian planktonic foraminiferal biozonation with this resolution.

In order to find out the lithostratigraphic changes across the boundary, microfacies analyses have been carried out in addition to careful field investigations. Microfacies types in this study reflect the changing patterns of the depositional environment. This study also presents a sequence stratigraphical interpretation based on the detailed lithostratigraphic and microfacies analyses. Sequence stratigraphical approach aims to discuss the formation of the system tracts considering the eustatic sea-level fluctuations and the tectonic evolution of the basin.

Relative changes in bulk rock composition and clay mineral content are very important reflectors of the variations in sediment sources related to weathering, erosion, climate and sea-level changes. This study also aims to find out the compositional changes of the rocks across the K/P boundary. Therefore, relative percentages of the non-clay and clay minerals of the samples, taken from the 2 m interval including the boundary, have been determined with X-ray diffractometry (XRD) analysis. The results have been considered in terms of the depositional history and the global reflects of the K/P boundary event.

Briefly, the objective of this study is to describe the K/P boundary event using a variety of disciplines, to find out how this global event has been recorded in a tectonically active flyschoidal basin like the Haymana basin and to compare and contrast the results with the other K/P boundary localities of the world.

1.2 METHODS OF STUDY

The study has been initiated with a detailed literature survey and continued through field and laboratory studies. Throughout the study, more than 200 papers concerning the Haymana basin and the K/P boundary event have been gathered. The stratigraphical, sedimentological, paleontological, mineralogical as well as the geochemical changes across the K/P boundaries in various locations of the world have been examined.

On the first field study, 29.41 m thick section consisting of marls and limestones has been measured and 60 samples have been collected. Sample interval of the first measured section ranges from 10-100 cm. Each bed has been sampled carefully, oriented samples have been collected if possible and sampling interval has been narrowed towards to the expected level of the K/P boundary. After the first laboratory studies the K/P boundary has been placed roughly and another field study has been conducted accordingly. In the second field study, an interval measuring 2 m and including the boundary (1 m below and 1 m above the boundary) has been trenched and resampled. 30 new samples with the sample interval at about 2-10 cm were collected for a detailed micropaleontological and microfacies work. During the field studies the lithological, facies and faunal changes of the succession have been observed, described and photographed, important macrofossils have been collected.

Detailed micropaleontological and microfacies analyses have been carried out in the laboratory. For micropaleontological, mineralogical and microfacies analyses, thin sections from a total number of 90 samples were prepared in the thin section preparation laboratory of the Department of Geological Engineering, METU.

In the delineation of the K/P boundary, biostratigraphic ranges of the planktonic foraminifera have been used chiefly. In order to examine planktonic foraminiferal changes across the boundary both thin sections and washed samples have been examined. The great majority of the laboratory work of this

study consists of the preparation of the washed samples in order to obtain planktonic foraminifera and the construction of their taxonomy.

For the extraction of the foraminifera from the lithified rocks several washing techniques have been applied based on the composition and the hardness of the samples. Because of the hardness of the lithologies and the low species abundance of the samples, the extraction of the planktonic foraminifera was especially difficult in the study area. However, in order to get the best results in terms of the number and the preservation of the individuals a great number of methods in the literature have been utilized and also some new techniques have been improved. All the applied washing techniques and their results will be discussed in the Sample Preparation part of the Micropaleontology Chapter (Chapter 6).

The planktonic foraminifera have been picked from the washed samples under binocular microscope and mounted on microslides for a permanent record. All the planktonic foraminifera were identified and their stratigraphic ranges have been determined. Scanning electron microscope (SEM) and thin section photographs of the species have been taken and used in the taxonomical studies. The low species abundance did not allow a quantitative analysis. Deep benthic foraminifera in the samples were also picked and saved for the prospective studies in the future. Apart from the fossils, aggregates of the important clay minerals and spherule-like objects showing abundances at specific intervals have also been hand picked from the washed samples and analyzed.

For the microfacies analyses thin sections were examined and the rocks were classified based on their biological and mineralogical components. With the help of the detailed microfacies analyses paleoenvironmental properties of the samples in the area have been found out and a sequence stratigraphical model has been proposed accordingly.

In order to detect the mineralogical changes across the boundary semi-quantitative analyses of the bulk and clay minerals have been performed using

XRD. 12 samples collected within the 2 m interval enclosing the boundary have been analyzed in the XRD Laboratory of the Research Center of Turkish Petroleum Corporation (TPAO).

1.3 GEOGRAPHIC SETTING

The study area is located approximately 10 km southwest of the Haymana town, which is located 70 km southwest of Ankara (Figure 1). It is situated on the topographic map of Ankara-J28-b2 of 1/25.000 scale. The coordinates of the measured section is 03246543 E and 3940565 N and its elevation is 1256 m. The measured section is easily accessible from the road Ankara to Haymana.

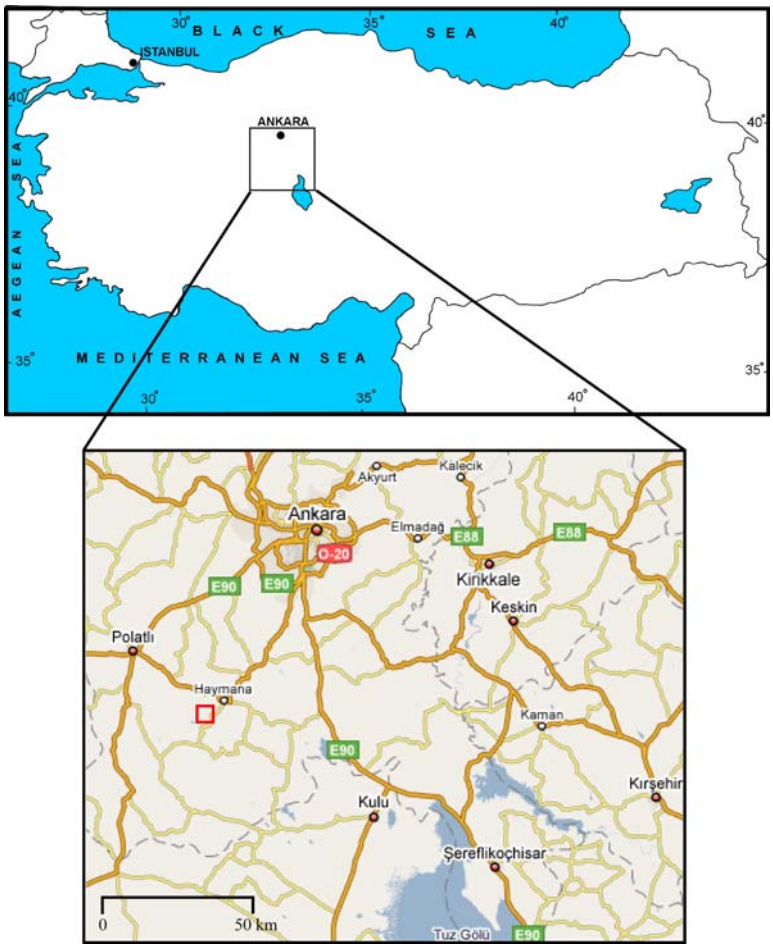

Figure 1. Geographic setting of the study area and the location of the measured section.

1.4 PREVIOUS WORK

1.4.1 Previous Work on the Haymana Basin

Haymana basin has been studied by various researches since the beginning of the early 1990s. The first studies in the basin were aiming to construct the lithostratigraphy of the basin. Chaput (1932, 1935a, b, 1936) initiated the studies in the region and worked on the Triassic to Eocene aged radiolorite, slate, limestone and flysch deposits. He realized the existence of Upper Cretaceous-Eocene rocks and claimed that the area has been folded in Tertiary. After Chaput, Lokman and Lahn (1946), Lahn (1949) and Egeran and Lahn (1951) tried to investigate the structural evolution of the Central Anatolia including the Haymana region. Lokman and Lahn (1946) and Lahn (1949) used the stratigraphical frame established by Chaput (1936) and identified the Upper Cretaceous, Paleocene and Eocene flyschoidal units with limestone intercalations. They defined several units in the succession of the Haymana region, such as, Senonian aged flysch with *Hippurites* and *Gryphea*; *Cyclolites*-bearing Maastrichtian marls; thinly bedded limestones in the Cretaceous-Paleocene transition; dark colored conglomerates in the Paleocene flysch and light colored Eocene limestones with *Nummulites* and *Assilina*. Lokman and Lahn (1946) focused on the structure of the Haymana region and claimed that orogenic events started before Early Cretaceous. They also recognized the unconformity between the Eocene and Neogene units related to the orogenic events in the area and reported the presence of the hydrothermal flows. In their opinion, Haymana region is similar to the other "arrière-fosse" examples in the Alpine orogeny and was formed due to the movements in the Late Mesozoic to Eocene.

In 1960s, Erol (1961) carried out very significant studies related to the structural evolution of the area. He reported Cenomanian-Turonian and Turonian-Santonian limestones underlying the Senonian flyschoidal deposits and interpreted this facies change as an evidence of the Sub-Hercynian

movements. He also observed the unconformity between the Eocene (Lutetian) and Neogene units and claimed that the area was covered by continental deposits after Lutetian.

In the early 1960s, there have been several studies in the region related to the petroleum potential of the basin. Rigo de Righi and Cortesini (1959), Reckamp and Özbey (1960), Schmidt (1960), and Akarsu (1971) carried out important studies in the Haymana basin. The studies performed by these petroleum geologists were very important for the construction of the stratigraphical frame of the area and can be considered as a base of works of Sirel (1975) and Ünalan *et al*. (1976).

Sirel (1975) studied in the Polatlı region and constructed the Upper Cretaceous-Eocene lithostratigraphy in the north and south of the Haymana region. The subdivisions of the formations proposed in this study were very important in terms of lithostratigraphy of the region. Sirel (1975) used micropaleontology for the age determination of units, made extensive taxonomical studies and constructed foraminiferal biozones for Cretaceous and Paleocene.

Ünalan *et al*. (1976) used also the lithostratigraphic definitions proposed by Rigo de Righi and Cortesini (1959), Reckamp and Özbey (1960), Schmidt (1960), and Akarsu (1971) and carried out a very important study in terms of the stratigraphy and paleogeography of the area. According to Ünalan *et al*. (1976), at the base of the Haymana basin there are 1) Triassic Temirözü Formation, which includes greywackes, metagreywackes and limestone blocks of Permian; 2) Upper Jurassic-Lower Cretaceous limestones of the Mollaresul Formation, which overlies the Temirözü Formation with an unconformity and 3) Dereköy Formation, which overlies the Mollaresul Formation with a discontinuity and includes serpentinite, limestone, radiolorite and volcanic blocks. In the Haymana basin, there are sandstones, conglomerates and shales of Maastrichtian age and these units are called the Haymana Formation. Overlying Beyobası Formation is represented by sandstones, conglomerates and fossiliferous

limestones. Paleocene units, showing lateral and vertical facies changes, have been divided into six formations. These are Kartal Formation, composed of conglomerates, sandstones and marls; Çaldağ Formation, consisting of algal limestones; Yeşilyurt Formation, represented by limestone blocks floating in marls; and Kırkkavak, Ilgınlıkdere and Eskipolatlı Formations, which have algal limestones and marls, conglomerates and sandstones and marls and limestones, respectively. Eocene units in the basin show also lateral and vertical facies changes and are represented by three formations. These are Beldede, Çayraz and Yamak Formations made up of conglomerates and sandstones, limestones and marls and conglomerates and sandstones, respectively. According to the Ünalan *et al*. (1976) deposition in the basin is almost continuous and the Neogene units cover all these formations unconformably. Ünalan *et al*. (1976) also interpreted the paleogeography of the basin and stated that there was a semicircle-shaped shelf near Haymana. Based on their idea, Çaldağ and Çayraz Formations were deposited on the shelf, partly continental formations like Kartal and Beldede were deposited behind the shelf and flyschoidal formations like Haymana, Yeşilyurt and Yamak were deposited in front of the shelf. Following Arıkan (1975), they also believed that the Haymana basin was joined with the Tuz Lake basin towards the southeast throughout Late Cretaceous-Early Paleogene and flyschoidal units were deposited in this part of the region. For Ünalan *et al*. (1976), this showed that the northern and western parts of the basin were filled with sediments and uplifted afterwards.

Gökçen (1976) carried out a detailed study related to the stratigraphical framework and tectonics of the southern Haymana region. In the map that he had prepared, he showed the structural units of the area and defined 8 lithostratigraphic units. He used different formation names than in Ünalan *et al*. (1976).

Görür (1981) made stratigraphical analyses in Haymana and Tuz lake basins and used the formation names in Ünalan *et al*. (1976). Consequently,

lithostratigraphic nomenclature of the area became more or less stabilized and has not been changed much after 1980s.

The paleontological studies play an important role in the investigation of the Haymana basin. Chronostratigraphic calibrations of the lithostratigraphic units were performed using paleontological data. Planktonic foraminifers, calcareous nannoplanktons and especially large benthic foraminifers have been studied in detail. The first studies were initiated by Dağer *et al*. (1963). They examined several stratigraphic sections in the vicinity of Ankara. According to their stratigraphy, Cenomanian-Turonian flysch-type rocks are overlain by reefal limestones of Senonian age. Tertiary rocks of lacustrine origin overlie both Paleozoic and Mesozoic rocks. In 1960s Dizer (1964, 1968) studied *Alveolina* and *Nummulites* populations in Eocene rocks. Sirel carried out very important studies in the Haymana basin. Sirel (1976a, b, c), Sirel and Gündüz (1976) focused on the taxonomy of *Alveolina*, *Nummulites*, *Ranikothalia* and *Assilina* in the Eocene rocks. Sirel continued his studies also in 1980s and 1990s. He worked on Beyobası, Kartal, Çaldağ and Kırkkavak Formations, studied the Cretaceous/Paleogene boundary and other stage boundaries and described many new benthic foraminifera genera (Sirel *et al*., 1986; Sirel 1998, 1999). Except Sirel, Meriç and Görür (1979-80) examined limestones of the Çaldağ Formation and determined its age as Montian and Thanetian. Matsumaru (1997) worked orbitoidal foraminifera in the Maastrichtian Beyobası Formation.

Calcareous nannoplankton and planktonic foraminifera studies in the Haymana basin have been initiated by Toker (1975, 1977). Toker (1977, 1979) studied Campanian to Maastrichtian Haymana and Kavak Formations and defined *Globotruncana elevata*, *Globotruncana havanensis*, *Globotruncana gansseri* and *Globotruncana mayaroensis* planktonic foraminifera biozones. Toker (1980) described with the nannoplankton biostratigraphy of the Cretaceous and Paleocene rocks in the Haymana basin. She basically followed the lithostratigraphic framework introduced by Yüksel (1970). In Toker's studies (1977, 1979, 1980) nannoplankton biozones were correlated with

planktonic foraminifera biozones and the paleobathymetry of the basin was introduced based on the microfossil content. Toker (1981) also described planktonic foraminifera biozonation for the Paleocene and Eocene formations. The biozones she defined, in ascending order, are *Globorotalia pseudobulloides*, *Globorotalia trinidadensis*, *Globorotalia uncinata*, *Globorotalia angulata*, *Globorotalia pusilla pusilla*, *Globorotalia pseudomenardii*, *Globorotalia velascoensis*, *Globorotalia subbotinae*, *Globorotalia formosa*, *Globorotalia aragonensis*, *Globorotalia pentacamerata* and *Globorotalia bullbrooki*.

In the recent years Özcan and Özkan-Altıner performed important paleontological studies in the Haymana region based on the planktonic foraminifera, large benthic foraminifera and calcareous nannofossils. Özcan and Özkan-Altıner (1997), Özcan and Özkan-Altıner (1999), Özcan and Özkan-Altıner (2001), Özcan *et al*. (2001) and Özcan (2002) dealt with the taxonomy of the large benthic foraminifera like *Orbitoides*, *Lepidorbitoides* and Orthophragminae in the Haymana, Beyobası, Kartal, Kırkkavak, Çaldağ, Eskipolatlı and Çayraz Formations in the Haymana basin. Özkan-Altıner and Özcan (1997) performed a project dealing with the microfacies variations around Cretaceous-Paleogene boundary. In their study, they conducted an integrated zonation of calcareous nannofossil, planktonic foraminifera and benthonic foraminifera in North, Northwest and Central Anatolian fore-arc basins. Özkan-Altıner and Özcan (1999) investigated the planktonic foraminiferal content of an Upper Cretaceous succession in the Haymana basin and calibrated the stratigraphic ranges of some important larger benthic foraminifera based on their early ontogenesis. Planktonic foraminiferal zonation they defined in Özkan-Altıner and Özcan (1997) and Özkan-Altıner and Özcan (1999), in ascending order, composed of *Dicarinella concavata*, *Dicarinella asymetrica*, *Globotruncanita elevata*, *Globotruncana ventricosa*, *Radotruncana calcarata*, *Globotruncanella havanensis*, *Globotruncana aegyptiaca*, *Gansserina gansseri*, *Abathomphalus mayaroensis* and *Morozovella pseudobulloides* zones.

Beside the foraminifera and calcareous nannoplankton studies in the area Özer (1986) studied Maastrichtian rudists in the Haymana Formation and Güngör (1975) carried out a study on the Eocene Campanile-type gastropoda in the Çayraz Formation. Duru and Gökçen (1990) studied ostracoda assemblages in the Lower Paleocene Kartal, Kırkkavak and Eskipolatlı Formations in the Polatlı region and established a detailed biozonation. According to their biostratigraphic and taxonomic study, the age of the Kartal Formation, Kırkkavak Formation and Eskipolatlı Formation are Montian, Thanetian and Cuisian; respectively. Based on the paleoenvironmental data obtained from the ostracoda species it has been stated that the Tertiary deposition started with continental units and passed into the marine deposits.

From the beginning of the 1970s sedimentology of the Haymana basin has also been studied by several researchers. The sedimentological studies carried out in the region were mostly in clastic sedimentary rocks. Norman and Rad (1971) studied Lower-Middle Eocene Harhor Formation which is above the *Nummulites*- and *Assilina*-bearing Çayraz Formation. They examined the mineralogy, grain size parameters and heavy mineral abundances of the formation and concluded that the sediments in the area were supplied from two different sources, one was from N-NW and the other was from S-SE. Norman (1973) studied Late Cretaceous-Early Paleogene sedimentation in Ankara, Yahşihan region. Ocakoğlu and Çiner (1995) studied the sedimentary evolution of the Paleocene-Lower Eocene continental deposits in the Orhaniye-Güvenç region which is situated in NW of Ankara and made some comparisons with the continental deposits in the Haymana basin. Gökçen (1977) focused on the provenance of resedimented deposits in the basin. Norman *et al*. (1980), and Gökçen and Kelling (1983) worked especially in the southern part of the region and defined the carbonate facies based on the mineralogical analysis in Cretaceous-Tertiary and Paleogene rocks respectively. Their study demonstrated that the sedimentation in the region has been derived from different provenances composed of different lithologies. Çetin *et al*. (1986) performed a sedimentological and petrological study on the Upper Cretaceous-Eocene

sequences in the northern flank of the Haymana anticline and found that the arenites in the region were derived from the north-northwest direction based on the paleocurrent analysis. Their data show that the sources of the siliciclastic sediments in the Upper Cretaceous-Paleocene units were mainly magmatics with metamorphic associates; whereas metamorphic sources became dominant in the Eskipolatlı and Yamak and Çayraz Formations although magmatic detritus was still being supplied. Çetin *et al*. (1986) also pronounced that the sediments in the basin are a subduction complex and fore-arc basin deposits. A similar study was carried out by Bayhan and Gökçen (1990) on the clastic sedimentary units in the Haymana, Tuz Lake and Kırıkkale-Yahşiyan basins. They found out that the sediments in the basins were derived from the magmatic and metamorphic rocks from the northern and southern directions. One of the latest sedimentological studies in the region was carried out by Demirel and Şahbaz (1994). According to their study, Haymana basin is a fore-arc basin and the majority of its clastic sediments were derived from the Kırşehir Massif and/or from the subduction complex at the base of the basin.

The hydrocarbon potential of the Haymana basin has also been attracting the attention of many researchers since the middle 1950s. The most important studies related to the oil exploration in the basin were carried out in a parallel continuum of the sedimentological studies. Arıkan (1975) carried out a detailed study about the geology and hydrocarbon potential of the Tuz Lake basin. In his study, both Tuz Lake and Haymana basins are defined as intercontinental basins and considered to be connected during Late Senonian to Middle Eocene. Gökçen (1978) made mineralogical, petrographical and clay mineralogical studies in the greywackes, calcarenites and reefal limestones in the southern parts of the Haymana region and carried out a provenance analysis. According to his findings, the sediments in the region were derived from one source area and/or a provenance composed of different lithologies. Şenalp and Gökçen (1978) examined the oil bearing channel fills of the submarine fan deposits in the Haymana Formation. One of the latest studies based on the petroleum potential of the Haymana basin has been performed by Coşkun *et al*. (1990).

They carried out a study on the region between Haymana-Mandıra and Dereköy towns in order to investigate the oil possibilities. In their study, Haymana and Ilgınlıkdere sandstones are considered as reservoir rocks, whereas Haymana and Yeşilyurt shales as possible source rocks. Hence they have concluded that Haymana basin is favorable for petroleum exploration. In one recent study related to the hydrocarbon potential of the area, Aydemir and Ateş (2006) made the structural interpretation of the basin by using seismic, gravity and aeromagnetic data and mentioned the possibility of hydrocarbon potential of the Haymana basin.

The sequence stratigraphy and cyclicity of the area has been studied only on the Eocene carbonates and on the Late Cretaceous clastic successions. Çiner (1992, 1993, 1996) and Çiner *et al*. (1993 a, b, 1996 a, b) examined the Middle Eocene carbonate platform of Çayraz Formation; alluvial fan, delta and shoreface deposits of Beldede Formation and turbidites of Yamak Formation. They examined the region with a sedimentological and sequence stratigraphical approach, carried out detailed studies on stratigraphic sections, divided the units into small scaled sedimentary packages and investigated the cyclicity and paleogeography of the area. Hüseynov (2007) studied the Upper Cretaceous siliciclastic submarine fan deposits in the Haymana Formation and defined the sedimentary cyclicity and the depositional sequences in the region.

Models and modern tectonic observations on the evolution of the Haymana basin were proposed after 1980s in the geology of Turkey. Chaput (1936), Blumenthal (1942), Lokman and Lahn (1946), Erol (1961), Ünalan *et al*. (1976) and several other authors had made regional and very general structural observations. However, Saner (1980) tried to explain the development of the western Pontide Mountains and adjacent basins in the northwestern Turkey based on the plate tectonic theory. In his study, he emphasized the common properties of Sivas, Çankırı-Çorum, Tuz Lake and Haymana basins. He stated that all these basins were formed on ophiolithic basements and composed of Upper Cretaceous-Eocene flysch deposits. In general, a regression took place in

Late Cretaceous and Paleocene and was followed by a transgression in Eocene. Tertiary molassic deposits are widespread, which have lateral transition and alternation with the continental deposits. Görür (1981) dealt with the evolution of the Haymana and Tuz Lake basins. Şengör and Yılmaz (1981) examined the area in the frame of plate tectonics. Another important study investigating the paleotectonic evolution of the Haymana basin considering the plate tectonics is Görür *et al*. (1984, 1998). In these studies, they studied the Tuz Lake basinal complex and considered Haymana and Tuz Lake basins to be coeval but independently evolved as two sub-basins in this complex. They stated that the Haymana basin was formed as a fore-arc basin along the active margins of the Sakarya continent. Turbidites accumulated in the basin interiors, with shallow marine and terrestrial deposition near the basin margins. The Late Paleocene-Early Eocene collision of the Menderes-Taurus block with the Sakarya continent and the Kırşehir block along the Inner Tauride suture, and the coeval collision of the Kırşehir block with the Rhodope-Pontide fragment along the Erzincan suture juxtaposed and deformed two sub-basins. Intra-continental collision continued during the Early-Middle Eocene, a single molasse basin was characterized by extensive red beds and evaporites.

Most recent studies related to the paleotectonic evolution of the Haymana basin were carried out by Koçyiğit *et al*. (1988), Koçyiğit (1991), Rojay and Süzen (1997), Çemen *et al*. (1999), Kaymakçı (2000), Okay *et al*. (2001) and Rojay *et al*. (2001, 2004). Based on the presence of Tertiary calcalkaline Galatean volcanism and ophiolithic basement in the basin, all these studies agree on the idea that the Haymana basin was developed on a fore-arc accretionary wedge which was active from the Late Cretaceous to the Late Eocene. After the Late Eocene the sediments of fore-arc basin and the rocks of the accretionary wedge were deformed, uplifted, and finally thrusted onto each other and also onto the younger fluvial to lacustrine sediments related to the continuing convergent events during Late Eocene to Early Oligocene.

After all these previous works, this study aims to delineate the Cretaceous/Paleogene boundary in the flyschoidal deposits of the Haymana basin using planktonic foraminifera with a high resolution approach, describe the lithological and geochemical changes across the boundary, analyze the microfacies changes and interpret the sequence stratigraphy of the biostratigraphically calibrated section.

1.4.2 Previous Works on the Cretaceous/Paleogene Boundary

Cretaceous/Paleogene boundary is widely known as the Cretaceous/Tertiary (K/T) boundary, however, International Commission on Stratigraphy (ICS) has been defined the boundary as Cretaceous/Paleogene (K/P) boundary in their annual report in 2003. Since then the term Cretaceous/Paleogene boundary is being used by the authors.

Cretaceous/Paleogene (K/P) boundary marks the end of the Cretaceous period and the beginning of the Tertiary period, i.e. the boundary between the Mesozoic and Cenozoic eras. This boundary corresponds to 65 million years before present. At Cretaceous/Paleogene boundary the earth underwent a mass extinction event which was one of the five big mass extinction events (Raup and Sepkoski, 1982). At the boundary the earth's ecosystem has been altered intensely. Land organisms like nonavian dinosaurs and marine organisms such as inoceramid and rudist bivalves, ammonites and belemnites all disappeared by the end of the period. On the other hand, some bird, marsupial and brachiopod species as well as foraminifera and palynoflora underwent drastic changes at the boundary. This idea has been first published by Alvarez *et al*. (1980). They proposed that an asteroid hit the Earth about 65 million years ago, creating the Chicxulub crater at the tip of Mexico's Yucatan Peninsula. According to their hypothesis, the impact would have penetrated the earth's crust, scattering dust and debris into the atmosphere, and causing huge fires, tsunamis, severe storms, acidic rains, seismic activities, and even volcanic activities. The impact could have caused chemical changes in the earth's atmosphere, increasing

concentrations of sulfuric acid, nitric acid, and fluoride compounds. The heat from the impact's blast would have affected all the life forms and the dust blocked most of the sunlight and lowered the temperature globally for months.

Except the extraterrestrial bolide impact hypothesis of Alvarez *et al*. (1980), there are some other scenarios explaining this catastrophic event like there are in the other mass extinction events. These are volcanism in Deccan traps in India, carbon dioxide poisoning, sea-level fluctuations and climate changes (Obaidalla, 2005 and references therein). Nevertheless, bolide impact is accepted as a major causal factor for the end-Cretaceous extinctions. There are irrefutable geochemical and geophysical evidences of a bolide impact, such as significant positive anomaly of the platinum-group element iridium at the K/P boundary in almost 100 locations in the world (Claeys *et al*., 2002) and the presence of a 10 km wide impact crater on the Mexico's Yucatan Peninsula.

Today we know that the K/P event is 65 Ma-old and coincides with a mass extinction that appears to be a catastrophic event related to the aftermaths of an approximately 10 km-diameter asteroid impact (Alvarez *et al*., 1980; Smit and Hertogen, 1980). Dust and fine ejecta covered the atmosphere and were deposited slowly, probably over months or a few years, forming a millimeter thick air fall layer worldwide (Smit, 1990; Hildebrand and Boynton, 1990). This layer contains evidence of the meteoritic impact including: an iridium anomaly, siderophile trace elements in chondritic proportions, osmium and chromium isotope anomalies, microdiamonds, nickel-rich spinels, shocked quartz, and altered microtektites (Smit, 1982; Robin *et al*., 1991; Carlisle and Braman, 1991; Shukolyukov and Lugmair, 1998; Arenillas *et al*., 2006).

Global Stratotype Section and Point (GSSP) of the K/P boundary were defined by the International Commission on Stratigraphy (ICS) in El Kef, NW Tunisia (Cowie *et al*., 1989). The El Kef section has been chosen as a stratotype section because of the presence and abundance of well-preserved calcareous and organic-walled microfossils, absence of bioturbation and its completeness, expansion, paleogeographical position, completeness and high sedimentation

rate (Ben Abdelkader *et al*., 1997). In El Kef section K/P boundary is marked by a millimeter-scale goethite-bearing clay layer (called "the boundary clay") containing Ir and Ni-rich spinels and with the drastic reduction (90-95%) of calcareous microfossils like coccoliths, foraminifers and ostracods (Ben Abdelkader *et al*., 1997). In many other complete Cretaceous/Paleogene sections similar geochemical and biostratigraphical changes are observed.

K/P event gained great interest from the public, as well as from the scientists and many papers have been published until today. There are great amount of scientific researches about the K/P event. The researches have been observing the lithological, geochemical, mineralogical, structural and most importantly paleontological changes across the K/P boundary and trying to delineate it.

Catastrophic and sudden change in the planktonic foraminifera has always played an important role in the delineation and description of the boundary. Although nannofossils, dinoflagellate cysts and some invertebrate marine organism like cephalopoda biozonations have been used in the placement of the K/P boundary, planktonic foraminiferal biozonation is most common one. The boundary is placed either at the first occurrence of Paleocene species, or at the mass extinction of Cretaceous species.

The mass extinction has been pointed out by many researchers since the early studies of the planktonic foraminifera. Luterbacher and Premoli-Silva (1964) performed a detailed biostratigraphic study in the K/P boundary of Gubbio section, Italy and described many new species as well as the new *Globigerina eugubina* biozone between the Maastrichtian and Danian, which is characterized by a planktonic foraminifera association completely different than found in the uppermost Maastrichtian assemblages. After the paper of Alvarez *et al*. (1980), Smit and Hertogen (1980) worked on the Caravaca section, Spain and documented that the planktonic foraminifera were severely affected by the K/P boundary event. They claimed that only one species, *Guembelitria cretacea*, survived. Initially Smit and many other specialists considered most of the

Maastrichtian taxa found in the lowermost Danian to be reworked specimens. However later studies showed that there are some survived species (Smit, 1982).

Although there is a wide consensus among the paleontologist that more than 50% of the planktonic foraminifera species have been affected at the K/P boundary, there are some questions about the catastrophic nature of the impact at the K/P boundary. Smit (1990) claimed that some Maastrichtian species survived and the final extinctions may have extended over a certain period of time, although he related the mass extinction to the bolide impact. Keller (1988, 1989a, b, 1996), Keller *et al*. (1993, 1994, 1995, 2002), Canudo *et al*. (1991), MacLeod and Keller (1994), Pardo *et al*. (1999), Karoui-Yaakoub *et al*. (2002) and Luciani (1997, 2002) suggested that 2/3 of the species declined prior to becoming extinct below or at the K/P boundary and about 1/3 of the species survived well into the Danian sequence. Hence they concluded that the mass extinction in planktonic foraminifera is gradual and this gradual pattern of the extinction cannot be attributed to the bolide impact. These authors believed that large, ornate, tropical-subtropical taxa disappeared at or near the K/P boundary in low-middle latitudes, whereas cosmopolitan taxa survived into the Danian. They claimed that the effect of extinction is negligible in high latitudes.

In order to find out the answer to the extinction pattern at the K/P boundary a blind sample test was suggested in 1992. A group of scientists re-sampled the El Kef stratotype section in Tunisia. Six unlabeled samples were studied by four paleontologists and the results were published (Lipps, 1997; Ginsburg, 1997, a, b; Smit and Nederbragt, 1997; Canudo, 1997; Masters, 1997; Olsson, 1997; Orue-Extebarria, 1997). The results did not help to solve the controversy as the data supported neither extinction pattern of extinction (Keller, 1997; Smit and Nederbragt, 1997). However the recent studies in Spain and Tunisia made by Molina *et al*. (1996) and Arenillas *et al*. (2000) suggest that the catastrophic mass extinction is coincident with the K/P boundary and related to the impact of the large asteroid. On the other hand, they explain the gradual extinction of some species in the basal Danian with the long term destructive

effect of the impact. Other recent and important surveys related to the behavior and the extinction pattern of the planktonic foraminifera at the K/P boundary are Obaidalla (2000, 2005), Arenillas *et al*. (2004, 2006) and Koutsoukos (1996, 2006).

The recent and important studies related to the geochemical record of the K/P boundary are Ben Abdelkader *et al*. (1997), Tantawy *et al*. (2001), Stüben *et al*. (2005), Yan *et al*. (2006) and Fornaciari *et al*. (2007). They studied the mineral and element changes, platinum group element anomalies and stable isotopes across the boundary. Pardo *et al*. (1999) analyzed clay mineralogy, Martinez-Ruiz *et al*. (2001, 2006) rare earth composition at the K/P boundary.

Smit (1999) gives the global stratigraphy of the K/P boundary impact ejecta and Claeys *et al*. (2002) present a database related to the mineralogical, sedimentological and geochemical information collected from 345 K/P boundary sites worldwide.

El Azabi and El Araby (2000), Ando (2003), El Kadiri *et al*. (2005) and Schulte *et al*. (2006) deal with the sedimentation pattern, depositional cycles and sequence stratigraphy across the K/P boundary.

K/P boundary has been studied by many researchers in different locations of Turkey as well. When we examine the K/P boundary studies carried out in Turkey, we see that they are mainly dealing with paleontological changes across the boundary. These studies are mainly conducted using planktonic foraminifera, calcareous nannoplanktons and large benthic foraminifera.

The planktonic foraminiferal studies across the K/P boundary started with Güvenç (1973). He worked in Kilis and defined *Globotruncana gagnebini* and *Globorotalia pseudobulloides* biozones as the last biozone in Maastrichtian and first biozone in Danian, respectively. Toker (1977, 1980) analyzed the Campanian-Lutetian nannoplankton and planktonic foraminifera biostratigraphy in the Haymana basin. In 1981, Dizer and Meriç studied the biostratigraphy of the K/P boundary in northwestern Turkey, whereas Meriç *et al*. (1987)

performed a study in the Adıyaman region and investigated the sedimentation and biostratigraphy of the boundary using foraminifera, ostracoda and nannoplankton. Özkan (1985) and Özkan and Altıner (1987) studied the K/P boundary in Gercüş area, SW Turkey. Tansel (1989) carried out a study in Ağva, İstanbul and delineated the K/P boundary using planktonic foraminifera. She defined the *Globigerina eugubina* biozone as a transition zone at the bottom of the Paleocene succession in between the *Abathomphalus mayaroensis* and *Morozovella pseudobulloides* biozones and claimed that the section in Ağva is continuous and conformable. She also pointed out the importance of the sampling interval for the K/P boundary studies and claimed that the *Globigerina eugubina* zone was missed by many authors in Turkey because of the inadequate sampling in the close vicinity of the boundary.

In 1990s and 2000s Yıldız carried out some studies related to the K/P boundary. Yıldız and Toker (1995) in Gürün region, Sivas; Yıldız *et al*. (2000) in Kalecik region, Ankara; Yıldız *et al*. (2001) in northwestern part of Tuz Lake basin and Yıldız and Gürel (2005) in eastern Pontides carried out paleontological analysis at the K/P boundary using mainly planktonic foraminifera and nannoplanktons.

Özkan-Altıner and Özcan (1997, 1999) performed important studies dealing with the microfacies and micropaleontological variations around the K/P boundary in North, Northwest and Central Anatolian fore-arc basins of Turkey. They performed an integrated zonation of calcareous nannofossil, planktonic foraminifera and benthonic foraminifera. On the other hand, Yakar (1993) studied the K/P transition in the Adıyaman region and delineated the boundary by using planktonic foraminifera. Güray (2006) carried out the planktonic foraminiferal taxonomy across the Campanian-Maastrichtian boundary in Kokaksu region, Bartın, and mentioned the presence of the K/P boundary in the section.

Şengüler *et al*. (1999) carried out a very important study on the hemipelagic successions of the western coast of the Black Sea and defined

detailed planktonic foraminifera and nannoplankton biozones. They identified the *Parvulorugoglobigerina eugubina* zone as the first Danian zone, which is absent in many K/P studies in Turkey and defined the triserial forms *Guembelitria cretacea* and *Guembelitria trifolia* as reworked species.

K/P transition has also been investigated by means of large benthic foraminifers. The most important studies carried out across the boundary are Sirel *et al*. (1986) and Sirel (1998) in Haymana basin; İnan and Temiz (1992) in Niksar region, Tokat; Akyazı *et al*. (1998) in Adriatic and Tauride platforms; İnan *et al*. (1999) in eastern Pontides. These studies provide extensive taxonomical information about the Late Cretaceous-Early Paleocene benthic foraminifera. However, they lack calibration with the endemic planktonic organisms. Therefore, it is hard to use the data provided in these studies in order to compare and contrast them with the K/P boundaries situated in different localities of the world.

Görmüş and Karaman (1992) and Kaya (1997) studied planktonic and large benthic foraminifera together in order to place the boundary in Çünür region (Isparta) and Niksar region (Tokat); respectively. Özer *et al*. (2001) worked the stratigraphy of the Upper Cretaceous-Lower Paleocene rocks of Menderes Massif and delineated K/P boundary using planktonic foraminifera, nannoplanktons and rudists.

There are also studies aiming to investigate the geochemical changes across the K/P boundary in Turkey. Bozkaya and Yalçın (1991a, b; 1992) and Yalçın and Bozkaya (1996) studied clay and carbonate mineralogy and geochemistry of the Hekimhan region, Malatya. Yalçın and İnan (1992 a, b) also studied benthic foraminiferal association in Tecer and Iğdır Formations in Sivas and carried out some mineralogical and geochemical investigations. Şengüler *et al*. (1999) examined the carbon and isotope changes in addition to carbonate percentages at the boundary. Arawaka *et al*. (2003) carried out an important study in Medetli, Gölpazarı region and found out element profiles as well as iridium concentrations of the K/P boundary in Medetli, Gölpazarı region.

Bayhan (2007) in her recent study focused on clay mineralogy in one of the Upper Cretaceous-Lower Paleogene sedimentary sequences of the Kalecik region.

Although other fossil groups are also used, planktonic foraminifera have always played a crucial role in the investigation of the K/P boundary. Therefore, the biozonation of the planktonic foraminifera at the boundary has been improved and specified by many planktonic foraminiferal specialists progressively. Now the biozonation of the foraminifera at the boundary is rather detailed and difficult to construct. The difficulty arises from the determination of the very minute and delicate first Danian species. Keller (1993) and Keller *et al*. (1995) have shown that the earliest Danian species are only present in 38-63 μm size fractions. Sampling interval is also crucial in the placement of the K/P boundary. In order to determine the first occurrences of the Early Danian planktonic foraminifera sample interval should be in cm-scale. If the sample interval is not dense enough it is very likely to miss the first occurrences of the Danian species. In order obtain a competent result; a very high resolution work should be carried out in K/P boundary studies.

Most of the planktonic foraminiferal K/P boundary studies in Turkey lack the identification of first Danian planktonic foraminifers and accordingly the first planktonic foraminiferal biozones in the Early Danian. The meter-scaled sample interval in many studies can not allow such kind of work anyway. Because of their inadequate sample interval most of the specialists have missed the very early forms of Danian and in general they defined the base of Paleocene with the first occurrence of *Parasubbotina pseudobulloides*.

This study aims to conduct a high resolution planktonic foraminiferal biozonation across the K/P boundary. Samples have been taken in cm interval around the transition. Small size fractions have been examined carefully in order not to miss early Danian forms in spite of poor preservation and rare occurrences of the planktonic foraminifers in the measured section.

1.5 REGIONAL GEOLOGICAL SETTING

The Haymana basin is located about 70 km SW of Ankara in Central Anatolia. It is a fore-arc basin formed during the Late Cretaceous to Late Eocene on the oceanic crust of the northern branch of Neo-Tethys, i.e. İzmir-Ankara suture zone (Figure 2, Figure 3). It has been formed by the convergence and collision of the Eurasian continent to the north, the Gondwana continent to the south, and overriding the Sakarya continent (Fourquin, 1975; Şengör and Yılmaz, 1981; Görür *et al*., 1984; Koçyiğit *et al*., 1988; Koçyiğit, 1991). The basin is surrounded by the Sakarya continent to the north-northwest, the metamorphic Kırşehir massif to the east and the Tauride-Anatolide block to the south (Figure 2, Figure 3).

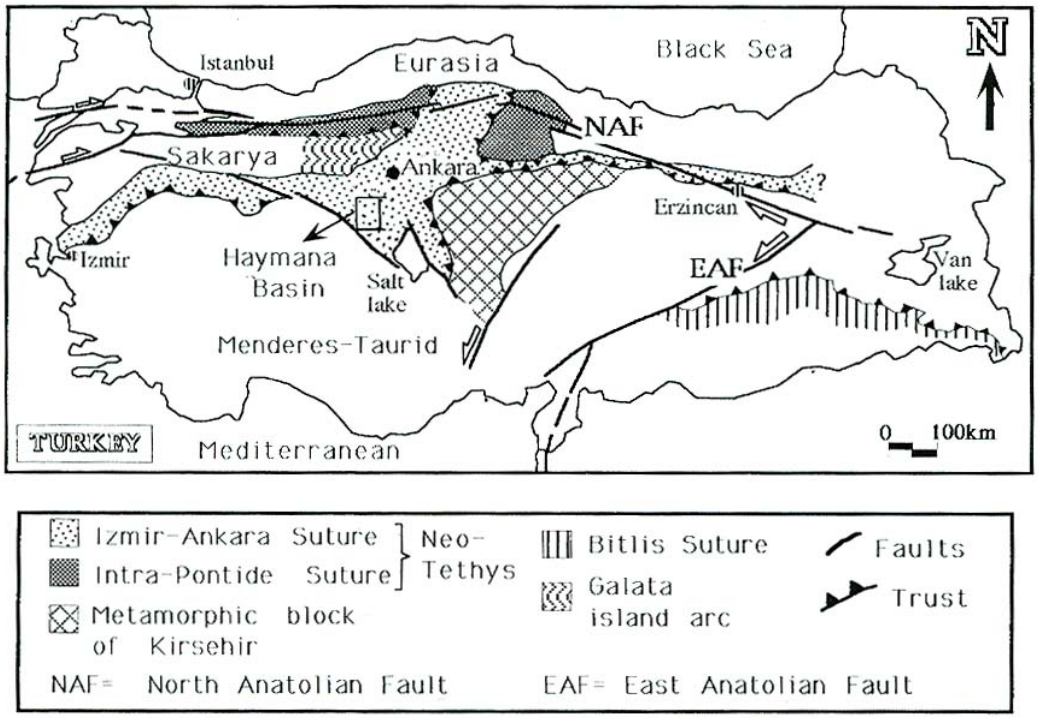

Figure 2. Main structural features of Turkey and the location of the Haymana basin (Çiner *et al*., 1996a).

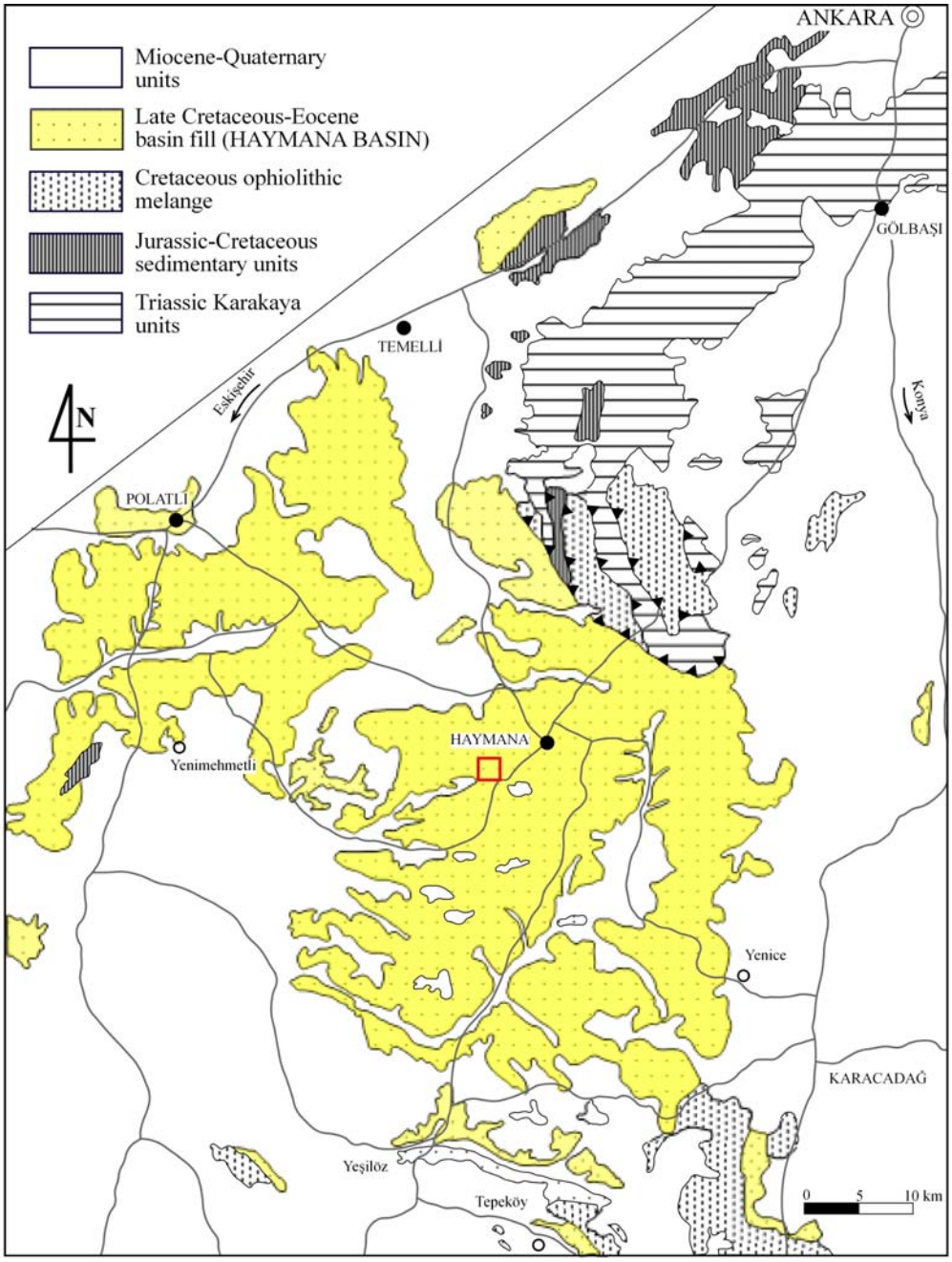

Figure 3. Generalized geological map of the Haymana basin and the location of the study area (modified and interpreted from 1/500.000 Turkey Map).

The existence of the calc-alkaline Galatean volcanics in the Pontides during the Tertiary and the ophiolithic basement in the basin made many researchers believe that the Haymana basin was developed on an accretionary wedge which was active from the Late Cretaceous to the Late Eocene (Şengör

and Yılmaz, 1981; Görür *et al*., 1984; Koçyiğit, 1991) (Figure 4). The arc activity in the Sakarya continent shows that the subduction was towards to the north (Fourquin, 1975; Şengör and Yılmaz, 1981).

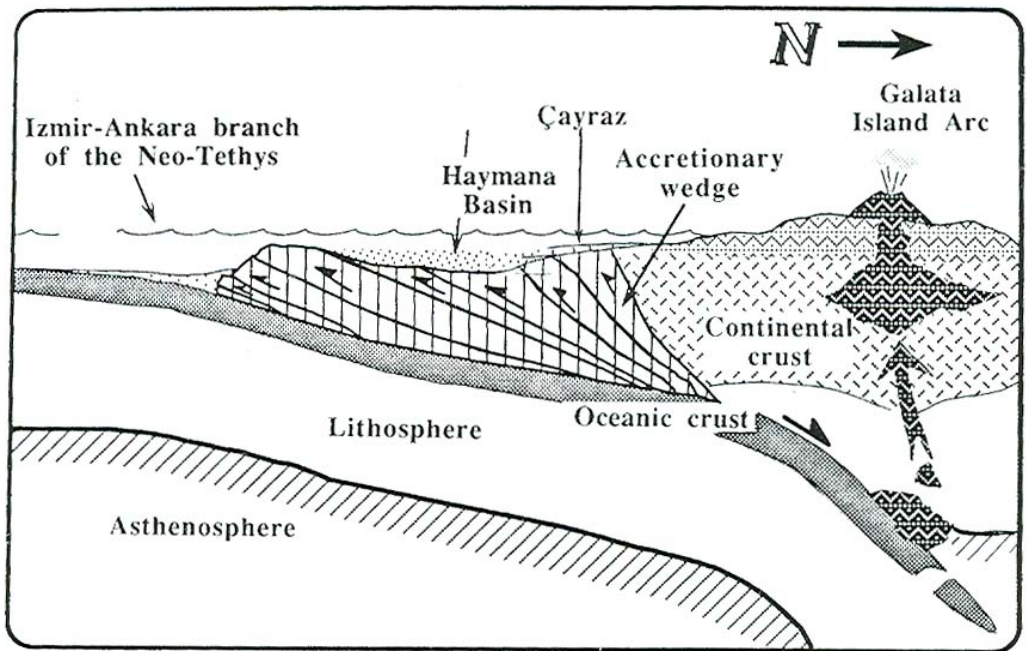

Figure 4. Schematic cross section (not to scale) showing the structural setting of the Haymana basin during Late Cretaceous to Middle Eocene (Çiner *et al*., 1996a).

Koçyiğit (1991) claimed that deformation continued until the Late Pliocene and the Haymana basin consists of a highly deformed sedimentary fill. The continuous Maastrichtian to Upper Eocene sedimentary sequence of the basin is more than 5 km thick (Ünalan *et al*., 1976; Görür, 1981). The deposition is dominated mostly by deep-marine flysch. The center of the basin mainly consists of turbidite sediments, whereas towards to the margins there are platform carbonates and continental red beds (Yüksel, 1970; Görür 1981; Çiner, 1992). It contains also local reefal build-ups and some volcanic intercalations (Görür, 1981; Koçyiğit and Lünel, 1987).

Görür *et al*. (1984) considered Haymana basin as a sub-basin in the Tuz Lake basinal complex and many other authors like Çemen *et al*. (1999) followed his idea. The two sub-basins of Tuz Lake basin complex, namely Haymana basin and Tuz Lake basin, evolved independently during the Late Cretaceous to the Eocene and have been integrated into one basin since the end of Eocene.

The basement of Haymana basin is composed of Jurassic-Early Cretaceous carbonate cover of Sakarya continent (Şengör and Yılmaz, 1981), the Karakaya complex forming a part of the pre Jurassic basement of Sakarya continent (Görür *et al*., 1984), and the Ankara mélange (Bailey and McCallien, 1953; Ünalan *et al*., 1976; Norman *et al*., 1980, Koçyiğit, 1991).

Ünalan *et al*., 1976 stated that above the composite basement, overlying an unconformity, Late Maastrichtian Haymana Formation starts (Figure 5). However, it has been changed by Hüseynov (2007). According to Hüseynov (2007), Haymana Formation rests on the reddish to pinkish beds of Kocatepe Formation which overlies the Seyran Formation unconformably comprising limestones, shales and breccias (Yüksel, 1970). On the other hand, the Seyran Formation overlies unconformably the thick bedded limestones of Çaltepe Formation which is probably a block embedded within a matrix of the ophiolithic mélange (Figure 6, Figure 7).

Haymana Formation is composed of turbidites made up of sandstones-shale alternations with frequent conglomerates, olistostromes and debris flow deposits (Figure 5, Figure 6, Figure 7). According to the Ünalan *et al*. (1976), Norman *et al*. (1980) and Görür *et al*. (1984) these clastics were derived from the basement ophiolithic rocks. However, Haymana Formation has also metamorphic rock fragments in it. Around the basin margins, these deep-sea deposits pass laterally and vertically into Upper Maastrichtian shallow marine sandstones, shales and limestones mainly with *Hippurites*, *Orbitoides*, *Cyclolites* and *Loftusia* and *Siderolites* (Ünalan *et al*., 1976). These lithologies have been gathered under the name Beyobası Formation by Ünalan *et al*. (1976), however Görür (Görür, 1981; Görür *et al*., 1984) preferred to use the name Asmaboğazı

Formation. Moreover, the Kavak Formation defined by Yüksel (1970) can also be correlated with this unit (Figure 5, Figure 6, Figure 7).

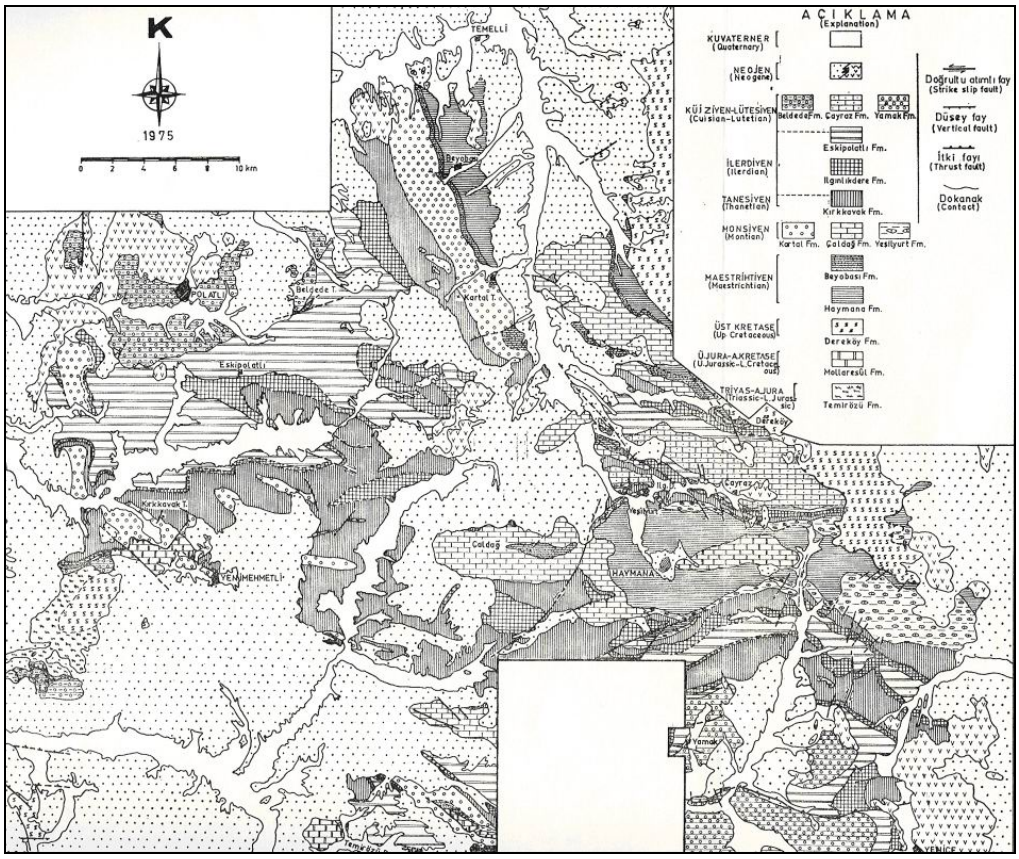

Figure 5. Geological map of the Haymana region (Ünalan *et al*., 1976).

Three main formations have been defined in Paleocene. Kartal Formation is composed of conglomeratic and sandy terrestrial red-beds and contains clasts of ophiolites, some coal and limestone bands. It shows a fluvial to supratidal depositional character containing plant and ostracoda fossils (Ünalan *et al*., 1976, Görür, 1981; Görür *et al*., 1984). Çaldağ Formation is characterized by reefal limestones and was developed at the basin edges. It is composed of limestones containing algae, echinodermata, corals, bryozoa and foraminifers (Ünalan *et al*., 1976, Görür, 1981; Görür *et al*., 1984). Kırkkavak Formation formed in the interior parts of the basin and exhibits shale-limestone intercalations.

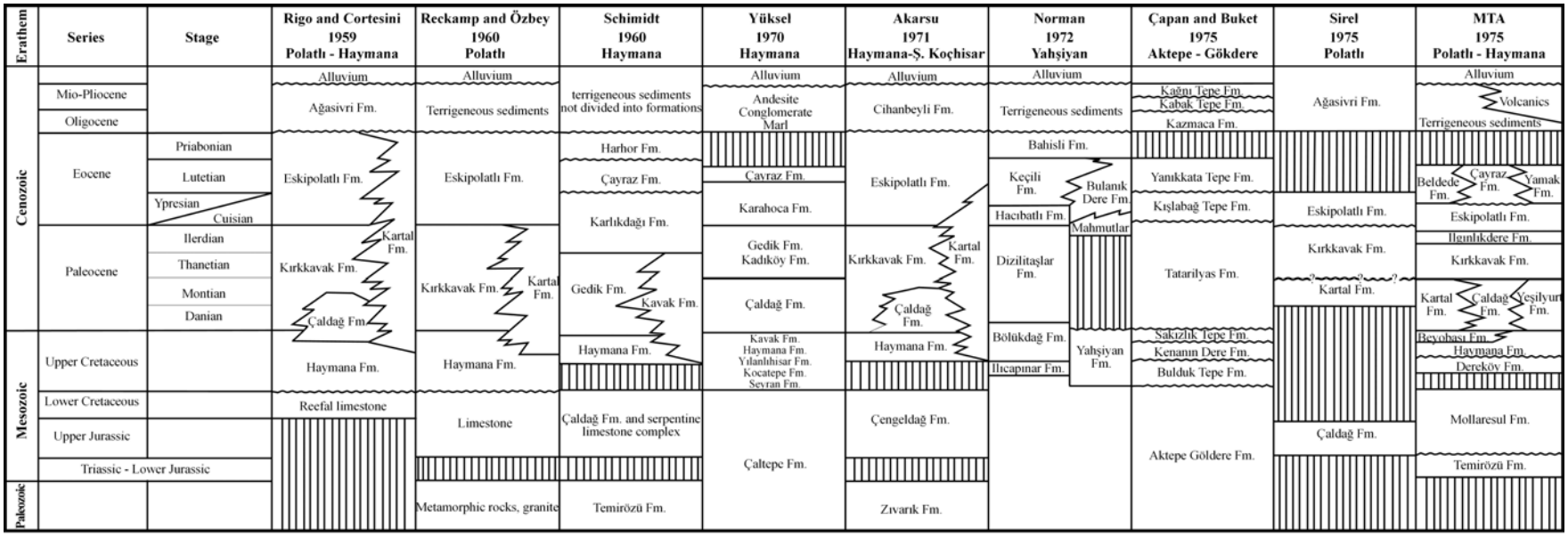

Figure 6. Correlation table of the lithostratigraphic units (Ünalan *et al*., 1976).

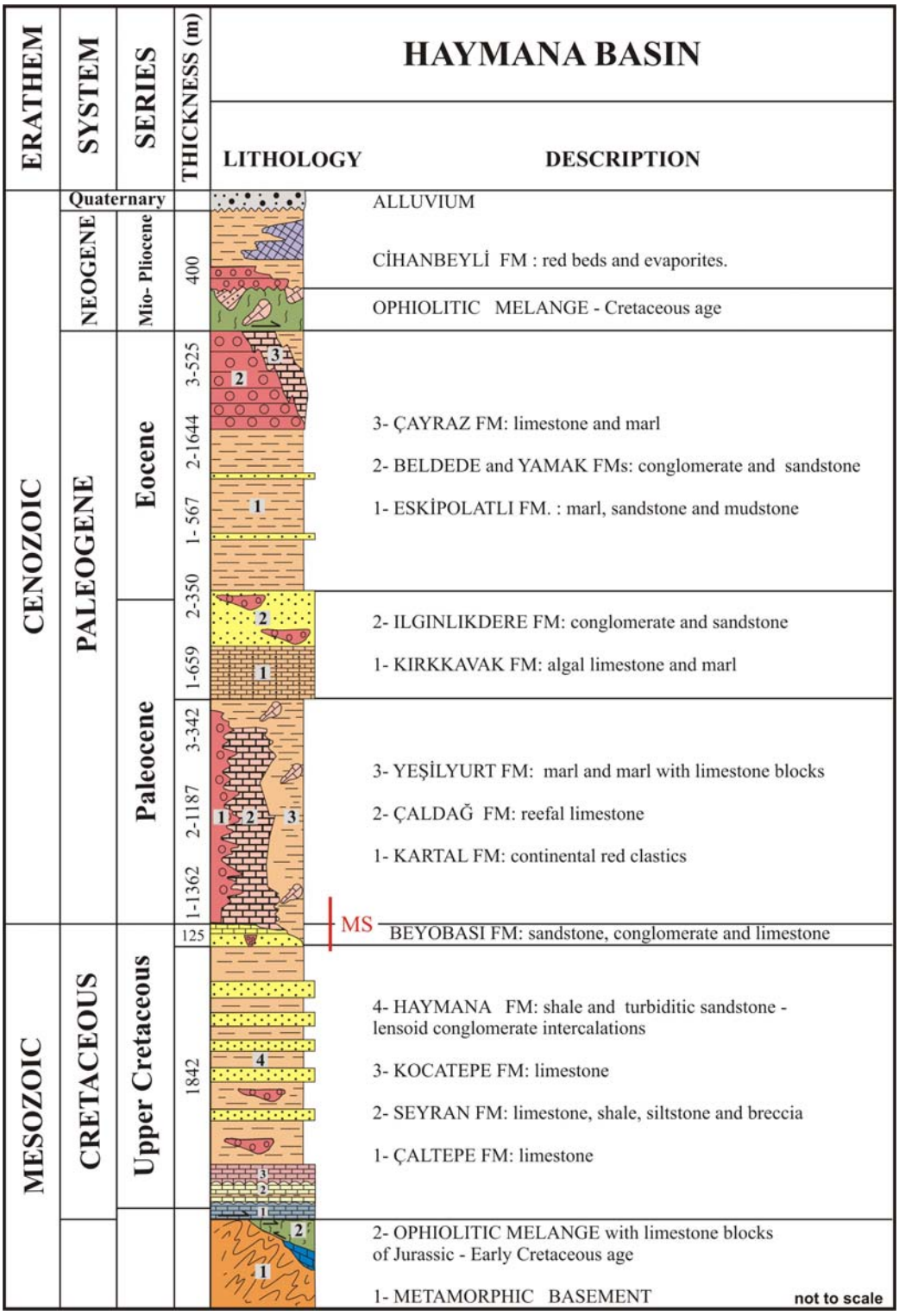

Figure 7. Generalized tectonostratigraphic columnar section of the Haymana basin indicating the level of the measured section (MS) (modified from Ünalan *et al*., 1976 and Yüksel, 1970).

Planktonic foraminifera found in the limestones of Kırkkavak Formation indicate a pelagic environment (Görür, 1981; Görür *et al*., 1984). Kartal, Çaldağ and Kırkkavak Formations depict lateral and vertical transitions. Ünalan *et al*., 1976 defined another formation called Yeşilyurt Formation at the transition zone between Çaldağ and Kırkkavak Formations (Figure 5, Figure 6, Figure 7). Turbiditic and planktonic foraminifera bearing shales and limestones of the Yeşilyurt Formation has not been defined as a separate unit by Görür (1981) and Görür *et al*. (1984) and placed into the Kırkkavak Formation.

The Early and Middle Eocene witnessed deposition of thick turbidite sequences in the central parts of the basin. Eocene turbidites choked the Çaldağ shelfal limestone and shoreline retreated away from the basin interior (Görür *et al*., 1984). The Eocene turbidites of the Haymana basin were described as the Eskipolatlı Formation. Shales and sandstones of Eskipolatlı Formation contain clasts of serpentinite, dunite, peridotite, diabase, basalt, radiolarian cherts, glaucophane schists derived from the ophiolites of the Ankara Mélange and Karakaya Complex (Görür *et al*., 1984). The conglomeratic level at the base of the Eskipolatlı Formation has been defined as the Ilgınlıkdere Formation by Ünalan *et al*. (1976).

Towards the end of the Middle Eocene, regression started at the basin and turbidite deposits began to shrink rapidly (Görür *et al*., 1984). Well-bedded shallow marine nummulitic limestones of the Çayraz Formation and terrestrial clastic sediments of the Beldede Formation started to deposit (Ünalan *et al*., 1976). Görür (1981) and Görür *et al*. (1984) considered those terrestrial clastic sediments as belonging to the Kartal Formation and claimed that the age of the Kartal Formation ranges from Maastrichtian to Eocene. Above the *Nummulites*- and *Assilina*-bearing Çayraz Formation turbiditic Yamak Formation was deposited (Ünalan *et al*., 1976). Finally, terrestrial conglomerates, sandstones, marls, tuffs and evaporites of the Mio-Pliocene deposits unconformably covered the Maastrichtian to Lutetian basin fill deposits (Ünalan *et al*., 1976, Görür, 1981 and Görür *et al*., 1984).

Within the regional geological frame, our studied section is located in the transition of the Beyobası (or Kavak or Asmaboğazı) Formation to Çaldağ Formation and the measured stratigraphic section represents the Cretaceous to Paleocene transition (Figure 7). Lithostratigraphic and biostratigraphic information about the section will be discussed in the following chapter.

CHAPTER 2

LITHOSTRATIGRAPHY AND BIOSTRATIGRAPHY

2.1 LITHOSTRATIGRAPHY

The studied section is situated in the transition of the Upper Cretaceous Beyobası Formation and Lower Paleocene Çaldağ Formation. Beyobası Formation has been defined first by Ünalan *et al*. (1976). In previous studies Upper Cretaceous rock units were also named as the Asmaboğazı Formation by Görür (Görür, 1981; Görür *et al*., 1984) and the Kavak Formation by Yüksel (1970) (Figure 7).

It has been stated by Ünalan *et al*. (1976) that the Beyobası Formation gives exposures near the Kavak, Temirözü and Erif villages, to the western part of the town Haymana, in the northern part of the Sarıgöl and between the villages Kayabaşı and Beyobası (Figure 5). Its type section is located in the northwestern part of the Beyobası village. The lithologic units of the formation from the older to the younger are sandstones, conglomerates, conglomeratic limestones and sandy marls. In general it is yellowish in color, quartz rich and fossiliferous. It contains foraminifera, pelecypoda and also some plant fossils. Its age has been determined as Maastrichtian by pervious authors based on the benthic foraminifera like *Orbitoides medius*, *Lepidorbitoides socialis*, *Siderolites calcitraposides*, *Cuvillieria sözerii*, *Omphalocyclus macroporous* (Sirel and Gündüz, 1976).

Beyobası Formation overlies the Haymana Formation and shows lateral transition to it in various localities (Figure 5, Figure 7). The age of the Haymana Formation has been determined as Maastrichtian with planktonic and benthic

foraminiferal data. It has wide exposures near the town of Haymana and is composed of gray shales with conglomerate and sand lenses and bands in them. Conglomeratic and sandy clastics have been derived mostly from the below lying ophiolithic mélange (Ünalan *et al*., 1976). Sandstone-shale alternations, the high ratio of the planktonic fauna to the benthic fauna and sedimentary structures like flute and load casts indicated that this formation has been formed in a slope to basin environment as flyschoidal deposits (Ünalan *et al*., 1976).

Beyobası Formation is underlying the Kartal Formation in the vicinity of Temelli and southern parts of Haymana, which is composed of semi-continental red siliciclastics. However in the vicinity of the town Haymana, Beyobası Formation shows lateral and vertical transition to the Çaldağ Formation (Figure 7). Çaldağ Formation is mainly composed of algae, coral, echinoderm, bryozoan and foraminifera rich packstones and grainstones. Its sparitic cement and fossil content indicate that the Çaldağ Formation was deposited in a shelfal environment with high energy (Ünalan *et al*., 1976).

Based on the fossil content and lithologies it can be concluded that Beyobası Formation represents a shallow marine environment in Maastrichtian. Towards to the end of the Maastrichtian shallowing is seen in the northern, southern and western parts of the basin and the Beyobası Formation was deposited on top of the flyschoidal Haymana Formation. However, the southeastern part of the basin was deeper in that time interval and Haymana Formation continued to deposit there (Ünalan *et al*., 1976).

Our studied section represents Cretaceous-Paleocene transition within the Beyobası Formation which overlies flyschoidal shales of the Haymana Formation and underlies the limestones of Çaldağ Formation (Figure 7). The total thickness of the measured section is 29.41 m. The first 60 samples collected from the measured section were named from HSE 1 to HSE 60. The interval between the samples HSE 48 and HSE 54, i.e. 2.32 m including the K/P boundary, has been resampled. The new 30 samples were named from KTS 1 to KTS 30. The stratigraphic levels of the samples HSE 48, HSE 49, HSE 50,

HSE 51, HSE 52, HSE 53 and HSE 54 correspond to the same stratigraphic levels of the samples KTS 1, KTS 4, KTS 13, KTS 15, KTS 16, KTS 24 and KTS 30; respectively (Figure 8).

The measured section begins with the yellowish colored, highly fractured, bioclastic limestone (Figure 9 A, B) and continues until the sample HSE 9 (Figure 8). This approximately 2 m measuring limestone is a packstone rich in large benthic foraminifera, calcareous red algae, bryozoans, mollusks and echinoderm fragments. It contains also Late Cretaceous planktonic foraminifera in minor amounts. Above this packstone, a grainstone consisting of very large hyaline benthic foraminifera, bryozoans, mollusks fragments and echinodermata spines is seen from the sample HSE 10 to HSE 11 (Figure 8). From the sample HSE 11 to HSE 27, through 5 meters, wackestone-packstone and wackestone alternation is observed (Figure 8). These wackestone-packstones and wackestones are also yellowish in color, highly fractured and rich in large benthic foraminifera, calcareous red algae, bryozoans, mollusks and echinoderm fragments (Figure 9 A, B). Between the samples HSE 27 and HSE 30, through 2 meters, quartz rich silty limestone was deposited (Figure 8). This silty limestone is rich in ammonites (Figure 9 C, D); and also large benthic foraminifera, calcareous red algae, bryozoans, mollusks and echinoderm fragments. Above the silty limestone, siliciclastic influx in the system increases and lead gray to greenish silty marls begin to deposit (Figure 9 E). This silty marl begins with the sample HSE 30, continues throughout the Maastrichtian, ends with the sample HSE 52 (=KTS 16) and last approximately 17 meters (Figure 8). Some parts of this silty marl is iron-oxide rich. As going younger, the number of large benthic foraminifera, algae, mollusks and echinoderm fragments decrease and the number of planktonic foraminifera and deep see agglutinated and hyaline benthics increase. At the uppermost part of the section, from the sample HSE 53 (=KTS 24) to the sample HSE 60, within an approximately 4 m interval, silty limestone-silty marl alternation is seen (Figure 8). Limestones seen at this part of the measured section are rich in silt size particles and clay minerals and contain planktonic and benthic foraminifera. The K/P boundary is in the

transition from the silty marls to the silty marl-silty limestone alternation (Figure 8, Figure 9). Lithologies and fossils content show that our section represents a slope to basin environment. As going younger deeper facies of slope to basin environment are seen and an overall transgression is observed.

The details of the faunal content and chronostratigraphy of the lithologies are given in the Biostratigraphy part of this chapter and detailed microfacies analyses and depositional environmental interpretations have been discussed in the Microfacies Analyses Chapter (Chapter 4).

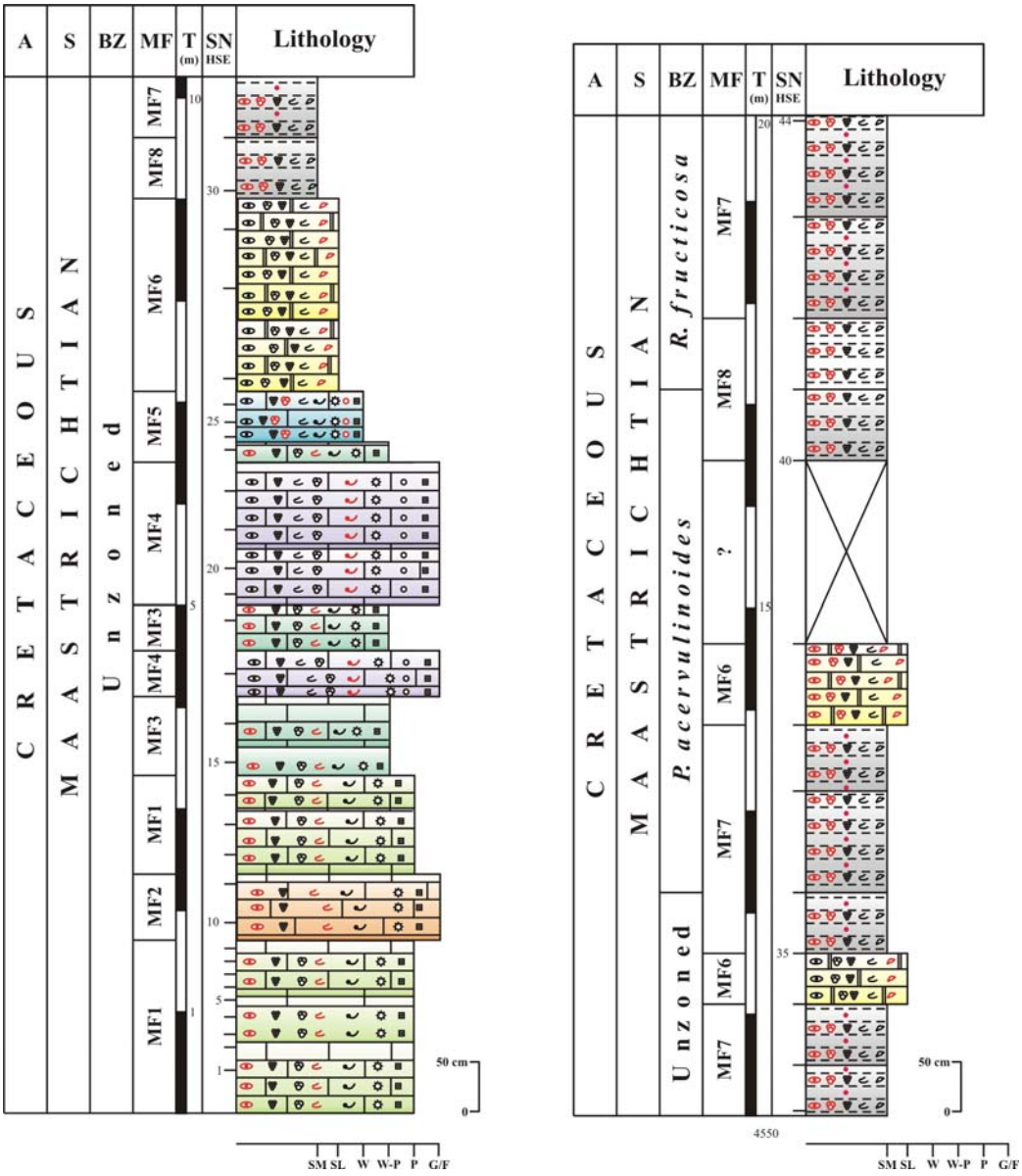

Figure 8. Lithostratigraphy of the measured section with planktonic foraminiferal biozones and microfacies types (The most abundant biogenic and abiogenic components are shown in red color).

Figure 8. Continued.

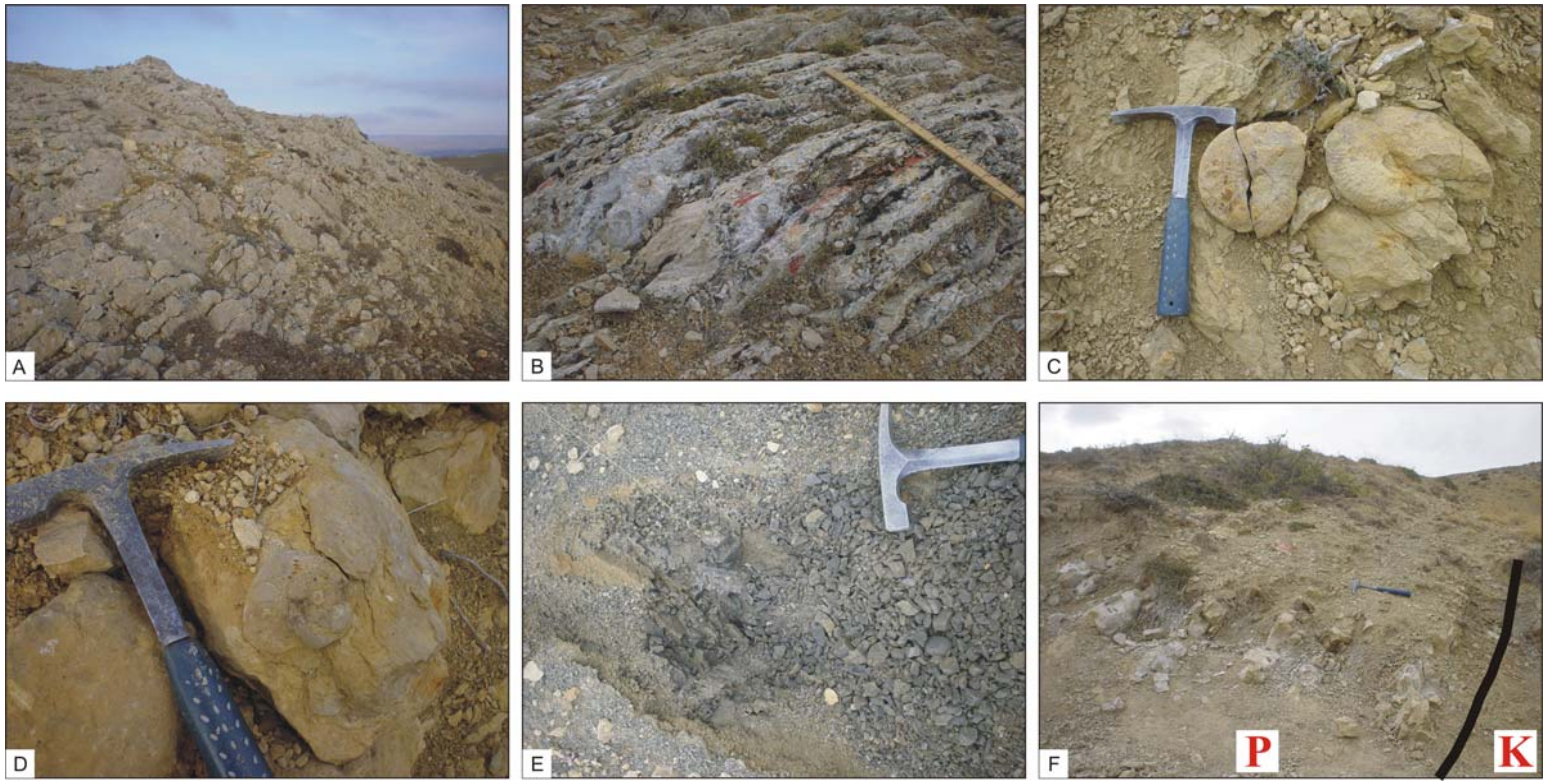

Figure 9. Photographs from the field area. **A., B.** Lowermost Upper Cretaceous fossiliferous limestone beds dipping towards southwest (HSE 1-26). **C., D.** Late Cretaceous ammonites in the limestones (HSE 27). **E.** Grayish silty marls (HSE 30). **F.** Transition from the Upper Cretaceous silty marls to the Lower Paleocene silty limestones (HSE 48-60, including all the KTS samples).

2.2 BIOSTRATIGRAPHY

Biostratigraphy is the most important tool in the determination of the stage boundaries. The International Commission on Stratigraphy defined the K/P boundary on the basis of unique biomarkers, the mass extinction of Cretaceous species and first appearance of Danian species. All other criteria, including lithological changes, geochemical signals, Ir content, and Ni-rich spinels are additional markers to identify the boundary, but by themselves do not define it (Stüben *et al*., 2005). In order to delineate the K/P boundary the most widely used microfossil group is planktonic foraminifera due to their use in global correlations. Therefore, in this study planktonic foraminifera biostratigraphy has been conducted in order to place the boundary and observe the faunal changes across the boundary. In Late Cretaceous 14 genera and 47 species; in Early Paleocene 10 genera and 17 species have been defined (Table 1).

The measured section contains also Late Cretaceous large hyaline benthic foraminifera like *Orbitoides*, *Lepidorbitoides*, *Siderolites*, *Sulcoperculina* and *Helonocyclina*; deep sea hyaline and agglutinated benthic foraminifera; mollusks shells; echinodermata spines; bryozoans; calcispheres and corallinacean and solenoporacean red algae. However, these fauna have not been used in the chronostratigraphic frame. They have only been used in order to determine the microfacies types, depositional environments and sequence stratigraphic system tracts (See Microfacies Analyses Chapter).

2.2.1 Planktonic Foraminiferal Biozonations

The biostratigraphy of the K/P boundary has been studied in detail in different latitudes of the world. The majority of the biostratigraphic studies on the K/P boundary sections are based on the planktonic foraminiferal turnover at the boundary. The high resolution studies have enhanced the planktonic foraminifera biozonation across the boundary, especially for the Early Danian

Table 1. Foraminiferal distribution chart

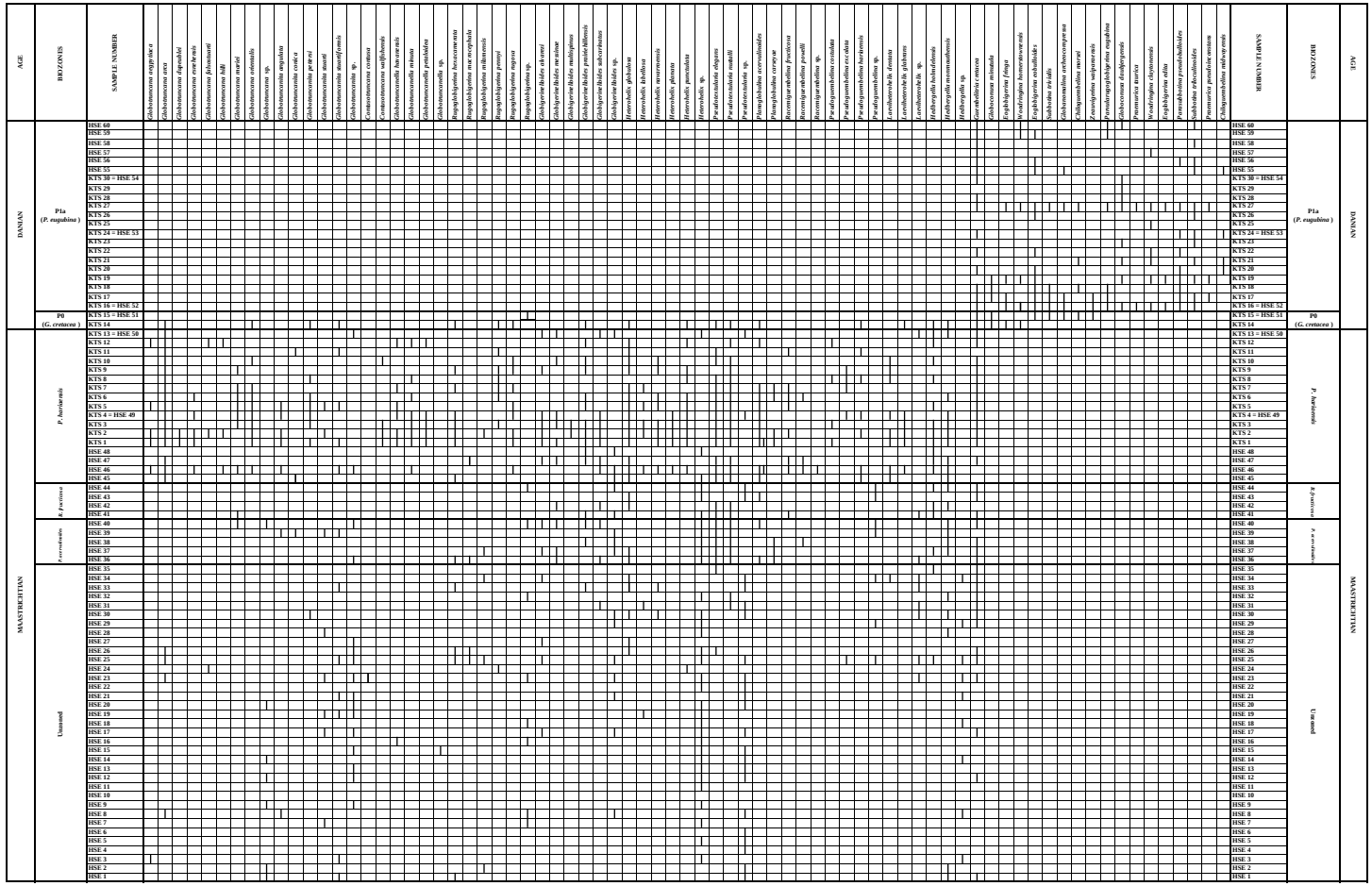

interval. Late Maastrichtian standard zonal schemes have also been improved in recent years.

The planktonic foraminiferal biozonation across the boundary is based on the last occurrences of the Maastrichtian fauna and the first appearances of the Danian fauna. At the boundary all the large, ornate, keeled forms of the genera *Globotruncana*, *Globotruncanita*, *Globotruncanella*, *Rugoglobigerina*, *Racemiguembelina*, *Pseudotextularia* and *Pseudoguembelina* disappeared and minute, delicate first Danian forms of the genera *Globoconusa*, *Eoglobigerina Globanomalina*, *Woodringina* started to appear. In order not to miss the first occurrences of the very Early Danian forms and to be able to construct a detailed biozonation across the boundary a high resolution work has been carried out in this study. After carrying out the first micropaleontological studies on the measured section the place of the K/P boundary has been determined within a 1 meter interval. In order to determine detailed planktonic foraminiferal biozonation across the boundary 2 m interval of the measured section including the boundary has been measured over again. 1 m below and 1 m above the boundary has been trenched and resampled. 30 samples with the sample interval at about 2-10 cm have been collected for detailed biostratigraphic work. Very detailed taxonomical work has been carried out in order to define the biozones. Criteria used in the definition of each species and all other taxonomical considerations are discussed in the Micropaleontology Chapter (Chapter 6) in detail.

In the early studies *Abathomphalus mayaroensis* total range zone, which was first defined by Brönnimann in 1952, was used as the uppermost Maastrichtian biozone (Bolli, 1966; Blow, 1979; Smit, 1982; Canudo *et al*., 1991; Berggren *et al*., 1995) (Figure 10). However, it has been found that this taxon is generally rare and often absent in the uppermost Maastrichtian strata (Blow, 1979; Keller, 1988; Canudo *et al*., 1991; Abramovich *et al*. 1998). It is especially hard to find this species in high latitude regions and relatively shallow water deposits. Because it has been found that *A. mayaroensis* is a problematic

taxon, other species have been used for the uppermost Maastrichtian interval. Instead of *A. mayaroensis* total range zone *Plummerita hantkeninoides* total range zone has been proposed by different authors (Keller 1989a, 1993; Pardo *et al*., 1996; Arenillas *et al*., 2000, Obaidalla, 2005) (Figure 10).

In the rareness or absence of the coiled index taxa uncoiled forms have also been used by many authors for the planktonic foraminiferal biozonations in the uppermost Maastrichtian strata (Keller, 1988; Luciani, 1997; Li and Keller, 1998; Robaszynski, 1998; Obaidalla, 2005) (Figure 10). In these heterohelicid biozonations stepwise first occurrences of the *Planoglobulina*, *Racemiguembelina* and *Pseudotextularia* species have been used by the authors.

In our samples index forms like *A. mayaroensis* and *P. hantkeninoides* have not been encountered, moreover keeled forms were also very rare. Therefore for the uppermost Maastrichtian part of the section heterohelicid biozonation has been proposed. In this study 5 biozones have been established from Late Maastrichtian to Early Danian based on the first and last appearances of the key planktonic species. These are from older to younger: *Planoglobulina acervulinoides* zone, *Racemiguembelina fructicosa* zone, *Pseudoguembelina hariaensis* zone, *Guembelitria cretacea* (P0) zone and *Parvulorugoglobigerina eugubina* (P1a) zone (Figure 10). This is the first study in Turkey which defines the Early Danian P0 and P1a zones.

It was not possible to zone the basal part of the measured section because of the rareness of the planktonic foraminifera due to the facies control. Figure 10 shows the comparison of the biozonation constructed in this study with the proposed biozonations for some complete international K/P boundary sections.

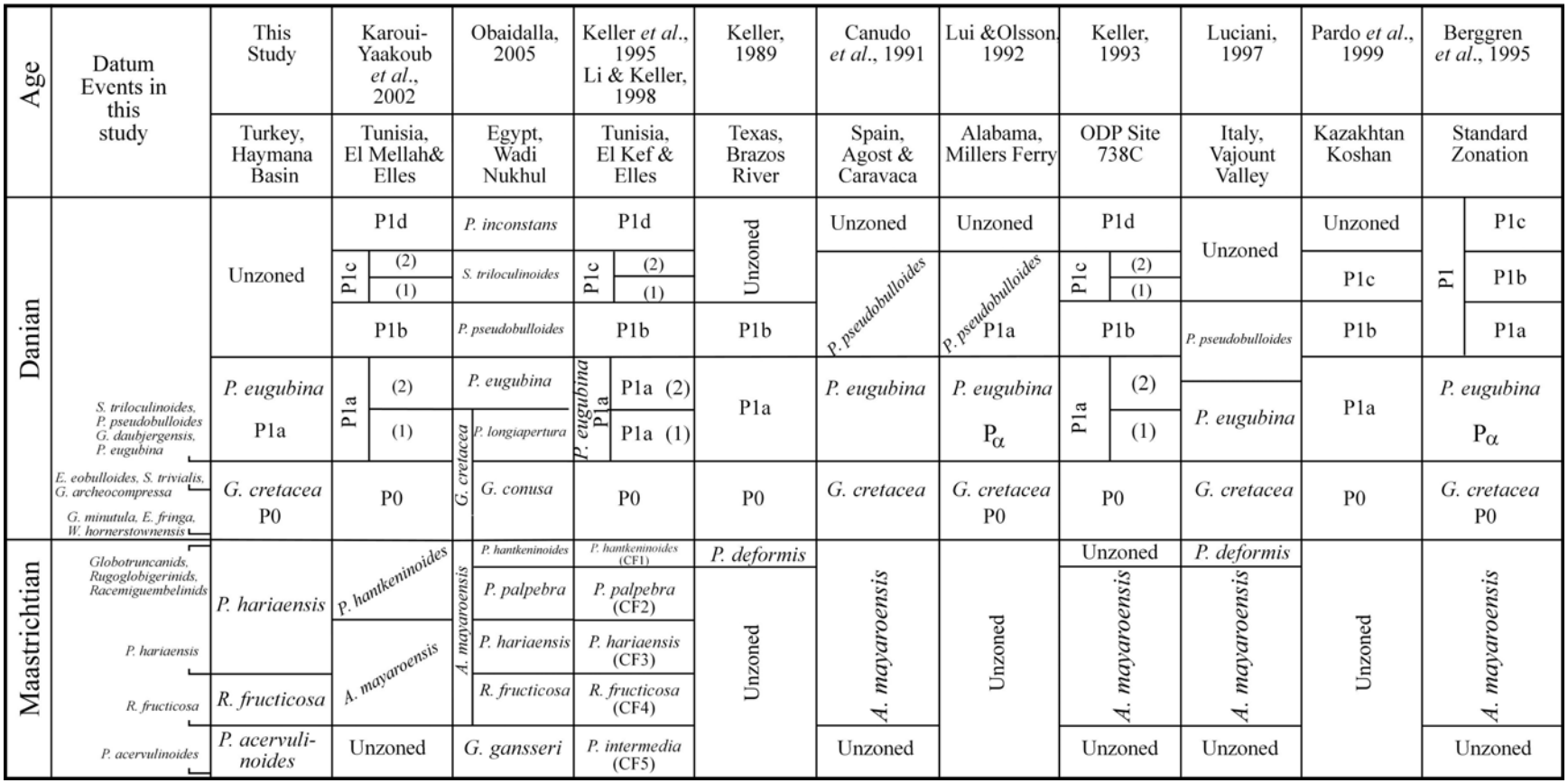

Figure 10. A comparison chart of the K/P boundary planktonic foraminiferal zonal schemes.

2.2.1.1 *Planoglobulina acervulinoides* Zone

Definition: Interval from the first appearance datum of the *Planoglobulina acervulinoides* to the first appearance datum of the *Racemiguembelina fructicosa* (Figure 10).

Author: ROBASZYNSKI, 1998

Remarks: This zone has been defined by Robaszynski (1998) above the *Pseudoguembelina excolata* zone. It covers approximately 5 meters. The lower part of the measured section, below the first appearance datum of the *Planoglobulina acervulinoides*, was left unzoned because the facies in the lowermost part of the measured section was not suitable for planktonic foraminiferal biozonation. It is overlain by the *Racemiguembelina fructicosa* zone.

Following species of planktonic foraminifera have been identified in this zone: *Globotruncana mariei*, *Globotruncana* sp., *Globotruncanita conica*, *Globotruncanita stuarti*, *Globotruncanita stuartiformis*, *Globotruncanita* sp., *Rugoglobigerina hexacamerata*, *Rugoglobigerina macrocephala*, *Rugoglobigerina milamensis*, *Globigerinelloides alvarezi*, *Globigerinelloides messinae*, *Globigerinelloides prairiehillensis*, *Globigerinelloides subcarinatus*, *Globigerinelloides* sp., *Heterohelix globulosa*, *Heterohelix* sp., *Pseudotextularia elegans*, *Pseudotextularia nuttalli*, *Planoglobulina acervulinoides*, *Planoglobulina carseyae*, *Racemiguembelina powelli*, *Pseudoguembelina* sp., *Laeviheterohelix* sp., *Hedbergella holmdelensis*, *Hedbergella monmouthensis* and *Guembelitria cretacea* (See Plates in Appendix).

Stratigraphic distribution: From the sample HSE 36 to the sample HSE 40.

Age: Middle-Late Maastrichtian

2.2.1.2 *Racemiguembelina fructicosa* Zone

Definition: Interval from the first appearance datum of the *Racemiguembelina fructicosa* to the first appearance datum of the *Pseudoguembelina hariaensis* (Figure 10).

Author: LI and KELLER, 1998

Remarks: This zone was defined by Li and Keller (1998) as the partial range of the nominate taxon between its first appearance datum and the first appearance datum of the *Pseudoguembelina hariaensis* (Figure 10). It has also been used with its above given definition by Robaszynski (1998). Obaidalla (2005) stated that *Racemiguembelina fructicosa* appeared at the same stratigraphic level with *A. mayaroensis* and placed this zone as a subzone at the bottom of the *A. mayaroensis* zone. This zone covers a 2.70 meter interval and overlain by the *Pseudoguembelina hariaensis* zone (Figure 10).

Following species of planktonic foraminifera have been identified in this zone: *Globotruncana mariei*, *Rugoglobigerina* sp., *Globigerinelloides messinae*, *Globigerinelloides prairiehillensis*, *Globigerinelloides subcarinatus*, *Globigerinelloides* sp., *Heterohelix globulosa*, *Heterohelix* sp., *Pseudotextularia elegans*, *Pseudotextularia nuttalli*, *Planoglobulina acervulinoides*, *Planoglobulina carseyae*, *Racemiguembelina fructicosa*, *Pseudoguembelina* sp., *Laeviheterohelix* sp., *Hedbergella holmdelensis*, *Hedbergella monmouthensis* and *Guembelitria cretacea* (See Plates in Appendix).

Stratigraphic distribution: From the sample HSE 41 to the sample HSE 44.

Age: Late Maastrichtian

2.2.1.3 *Pseudoguembelina hariaensis* Zone

Definition: Interval from the first appearance datum of the *Pseudoguembelina hariaensis* to the first appearance datum of the *Globoconusa minutula* (Figure 10).

Author: LI and KELLER, 1998

Remarks: This zone is the uppermost biozone in the Late Maastrichtian. It has been defined by Li and Keller (1998) as the total range of the nominate taxon (Figure 10). Its last appearance datum coincides with the first appearance datum of the first Paleocene forms and the mass extinction of the large and ornamented Cretaceous forms. Since we recognized *Pseudoguembelina hariaensis* in the first Danian sample together with the first Danian species we did not define this zone as a total range zone. Instead, an interval zone between the first appearance datum of the *Pseudoguembelina hariaensis* to the first appearance datum of the *Globoconusa minutula* has been preferred. With the initial occurrence of the first Danian forms K/P boundary has been placed. The *Pseudoguembelina hariaensis* zone in the measured section is approximately 5 meters and is relatively richer in planktonic foraminifera compared to other zones. However one crucial thing should be noted here. Normally we would expect to see lower diversity in the planktonic foraminifera while approaching to the K/P boundary due to the mass extinction of the large and ornamented forms. The increase in the diversity of planktonic foraminifera in this zone is not related to the age of the zone. In this study, facies control is the main reason for this increase. Because the facies is more suitable for planktonic foraminifera species it is seen that their diversity is increasing in this interval.

Following species of planktonic foraminifera have been identified in this zone: *Globotruncana aegpytiaca*, *Globotruncana arca*, *Globotruncana dupeublei*, *Globotruncana esnehensis*, *Globotruncana falsostuarti*, *Globotruncana hilli*, *Globotruncana mariei*, *Globotruncana orientalis*, *Globotruncanita angulata*, *Globotruncanita conica*, *Globotruncanita pettersi*, *Globotruncanita stuarti*, *Globotruncanita stuartiformis*, *Globotruncanita* sp., *Contusotruncana walfishensis*, *Globotruncanella havanensis*, *Globotruncanella minuta*, *Globotruncanella petaloidea*, *Rugoglobigerina hexacamerata*, *Rugoglobigerina macrocephala*, *Rugoglobigerina milamensis*, *Rugoglobigerina pennyi*, *Rugoglobigerina rugosa*, *Globigerinelloides alvarezi*,

Globigerinelloides messinae, *Globigerinelloides multispinus*, *Globigerinelloides prairiehillensis*, *Globigerinelloides subcarinatus*, *Globigerinelloides* sp., *Heterohelix globulosa*, *Heterohelix labellosa*, *Heterohelix navarroensis*, *Heterohelix planata*, *Heterohelix punctulata*, *Heterohelix* sp., *Pseudotextularia elegans*, *Pseudotextularia nuttalli*, *Pseudotextularia* sp., *Planoglobulina acervulinoides*, *Planoglobulina carseyae*, *Racemiguembelina fructicosa*, *Racemiguembelina powelli*, *Pseudoguembelina costulata*, *Pseudoguembelina excolata*, *Pseudoguembelina hariaensis*, *Laeviheterohelix dentata*, *Laeviheterohelix glabrans*, *Laeviheterohelix* sp., *Hedbergella holmdelensis*, *Hedbergella monmouthensis* and *Guembelitria cretacea* (See Plates in Appendix).

Stratigraphic distribution: From the sample HSE 45 to the sample HSE 50 = KTS 13.

Age: Latest Maastrichtian

2.2.1.4 *Guembelitria cretacea* (P0) Zone

Definition: Interval between the first appearance datum of the *Globoconusa minutula* to the first appearance datum of the *Parvularugoglobigerina eugubina* (Figure 10).

Author: SMIT, 1982

Remarks: The lowermost strata of the Danian were first defined by the first appearance datum of *Parvularugoglobigerina eugubina* by Luterbacher and Premoli-Silva (1964). Smit (1982) first introduced *Guembelitria cretacea* Zone (P0 Zone) to define the interval from the K/P boundary to the first appearance datum of *Globoconusa minutula* before the first appearance datum of *Parvularugoglobigerina eugubina*. *Guembelitria cretacea* is one of the opportunistic species that survives across the boundary hence initial zone of the Early Danian has been named as *Guembelitria cretacea* zone or P0 zone. After Smit (1982) *Guembelitria cretacea* Zone (P0 Zone) has been defined by various

authors between the first occurrences of Early Danian forms to the first appearance of *Parvularugoglobigerina eugubina* (Smit, 1982; Canudo *et al*., 1991; Liu and Olsson, 1992; Berggren *et al*., 1995; Luciani, 1997; Keller, 1988; Keller *et al*., 1995; Arenillas *et al*., 2004; Obaidalla, 2005) (Figure 10). In this study *Guembelitria cretacea* zone (P0 zone) has been defined from the first appearance datum of the initial Danian forms like *Globoconusa minutula*, *Eoglobigerina fringa* and *Woodringina hornerstownensis* to the first appearance datum of the *Parvularugoglobigerina eugubina*. P0 Zone in this study lasts 20 cm.

The initial Danian forms observed in this interval are *Globoconusa minutula*, *Eoglobigerina fringa*, *Woodringina hornerstownensis*, *Eoglobigerina eobulloides*, *Subbotina trivialis*, *Globanomalina archeocompressa*, *Chiloguembelina morsei* and *Zeauvigerina waiparaensis* (See Plates in Appendix).

Reworked or survived species in the initial Danian sediments?

Besides these first Paleocene forms some Cretaceous forms are also observed in the first Danian sample (KTS 14). These are *Globotruncana arca*, *Globotruncana orientalis*, *Globotruncanita pettersi*, *Globotruncanita stuartiformis*, *Rugoglobigerina hexacamerata*, *Rugoglobigerina pennyi*, *Rugoglobigerina rugosa*, *Globigerinelloides prairiehillensis*, *Globigerinelloides* sp., *Heterohelix globulosa*, *Heterohelix punctulata*, *Pseudotextularia elegans*, *Pseudotextularia nuttalli*, *Planoglobulina acervulinoides*, *Pseudoguembelina hariaensis*, *Laeviheterohelix glabrans*, *Hedbergella holmdelensis*, *Hedbergella monmouthensis*, *Guembelitria cretacea*.

Species survivorship concept across the K/P boundary has been discussed by various authors and this subject is still in debate. In the early studies many foraminiferal researchers reported that almost all the Cretaceous species extinct at the K/P boundary. However, some authors observed dwarfed Late Cretaceous genera such as *Rugoglobigerina*, *Planomalina*, *Globigerinelloides* and

Hedbergella. The presence of these small Late Cretaceous species in the early Tertiary sediments was generally assumed to be due to reworking or bioturbation. However Keller (1988) proposed that some small Cretaceous forms such heterohelicids, pseudotextularids and hedbergellids are survivors. After Keller (1988), which claims some Cretaceous species survived the K/P boundary, many other studies have been carried out related to this phenomenon. Many recent studies agree that all the large, complex, ornamented, tropical Cretaceous forms like globotruncanids, racemiguembelinids and rugoglobigerinids are extinct at the boundary; small, robust, dwarfed forms like heterohelicids, pseudotextularids, hedbergellids and guembelitrids survived across the boundary and small, primitive, cosmopolitan Danian forms evolved above the boundary (Keller, 1988, 1989a, 1989b; Keller *et al*., 1995; Canudo *et al*., 1991; MacLeod and Keller, 1994; Pardo *et al*., 1996; Luciani, 1997, 2002; Pardo *et al*., 1999; Karoui-Yaakoub *et al*., 2002; Keller and Pardo, 2004; Paul, 2005) (Figure 11). On the other hand some micropaleontologists believe that only three of the Cretaceous species survived the K/P boundary. These are *Hedbergella holmdelensis*, *Hedbergella monmouthensis* and *Guembelitria cretacea* (Olsson *et al*., 1999; Premoli-Silva and Verga, 2004).

Reworked specimens are difficult or often impossible to identify unless they are discolored, show differential preservation or huge age difference with the rest of the faunal assemblage. The Cretaceous species in our Early Danian samples do not show distinct characteristics that may help us to decide whether they are survived or reworked species. Although survivorship concept is still a matter of intense debate, it is now accepted that at least certain number of species may have survived the K/P extinction. Therefore it might be considered that small cosmopolitan surface-water dweller forms such as *Heterohelix*, *Laeviheterohelix*, *Pseudoguembelina*, *Globigerinelloides*, *Hedbergella* and *Guembelitria* in the first Danian sample (KTS 14) are survived species. All of these have small morphology with little or no surface ornamentation and resemble the newly evolving Early Danian fauna (Luciani, 2002).

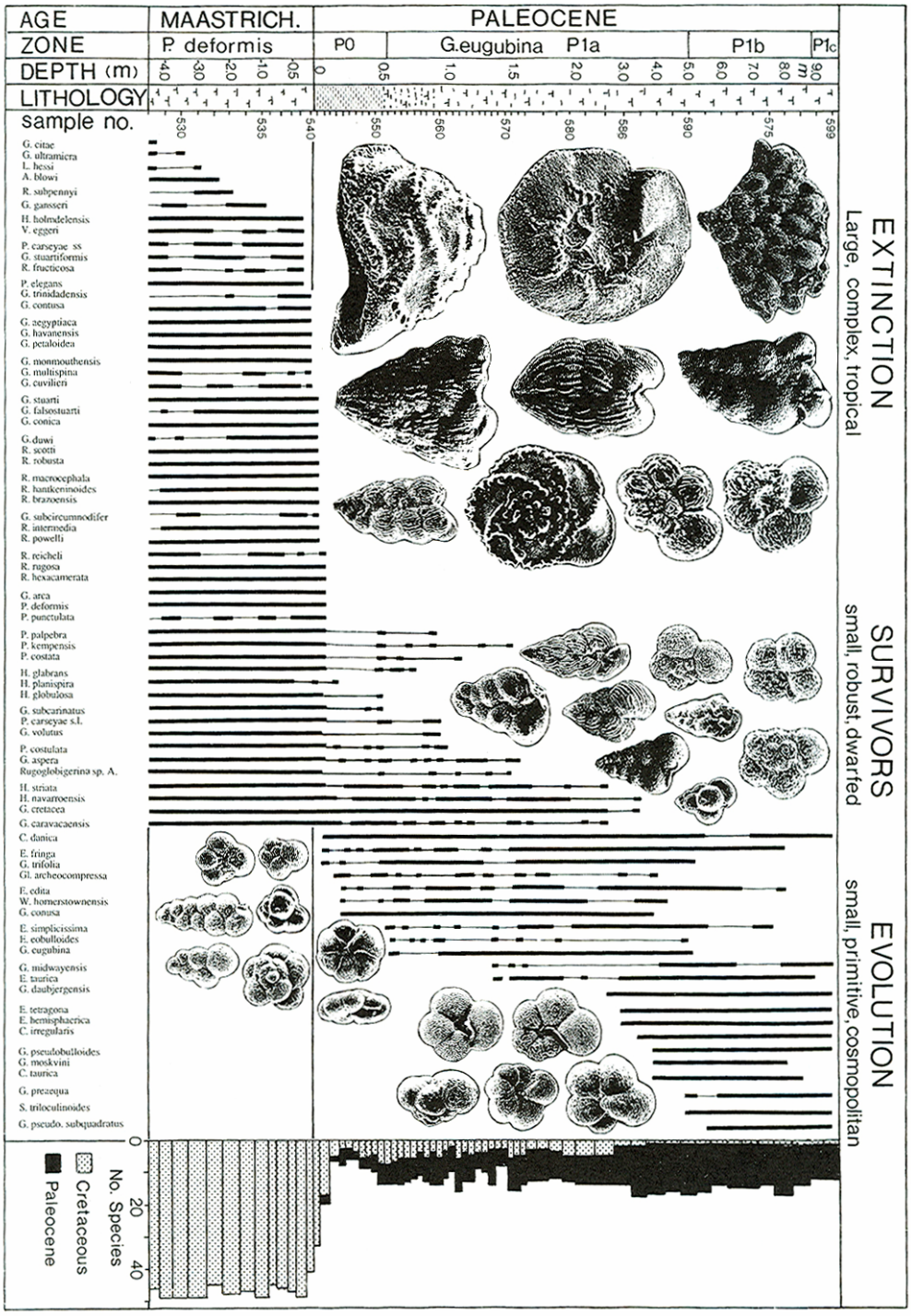

Figure 11. Stratigraphical ranges of planktonic foraminiferal species across the K/P boundary at El Kef with scanning electron microscope illustrations of characteristic extinct, surviving, and evolving species at their relative sizes (Keller, 1988 in MacLeod and Keller, 1996).

On the other hand, keeled deeper dwellers and larger forms like *Globotruncana*, *Globotruncanita*, *Rugoglobigerina* and *Planoglobulina* in the first Danian samples (KTS 14 and KTS 15) should be considered as reworked species.

Stratigraphic distribution: From the sample KTS 14 to the sample KTS 15 = HSE 51.

Age: Early Danian

2.2.1.5 *Parvularugoglobigerina eugubina* (P1a) Zone

Definition: Interval from the first appearance datum of the *Parvularugoglobigerina eugubina* to end of the measured section (Figure 10).

Author: LUTERBACHER and PREMOLI-SILVA, 1964

Remarks: This zone has been restricted with the taxon range zone of the species *Parvularugoglobigerina eugubina*. It has also been named as Pα zone by various authors (Berggren *et al*., 1995; Liu and Olsson, 1992; Olsson *et al*., 1999) (Figure 10). However, in the majority of the recent works it is seen that P1a is a more common name for this taxon range zone. Therefore, in this study the name P1a has been preferred. The *Parvularugoglobigerina eugubina* zone (P1a zone) defined here is very similar to the P1a zones defined by Keller *et al*. (1995), Karoui-Yaakoub *et al*. (2002), Obaidalla (2005) and Darvishzad *et al*. (2007) and covers approximately 1 m interval. Because the last appearance datum of the species *Parvularugoglobigerina eugubina* have not been encountered in the measured section the upper limit of this zone was not defined.

P1a zone has been divided into two subzones, P1a (1) and P1a (2), with the first occurrences of *Parasubbotina pseudobulloides* by Keller *et al*. (1995), Pardo *et al*. (1996), Li and Keller (1998) and Karoui-Yaakoub *et al*. (2002) (Figure 10). However in this study it was not possible to subdivide the P1a zone into two subzones, as the first appearance datum of *Parasubbotina*

pseudobulloides and *Parvularugoglobigerina eugubina* coincide in the sample KTS 16. The first occurrence of *Subbotina triloculinoides* also happens in the same sample. In various studies the researchers claimed that the first occurrence of the *Subbotina triloculinoides* is after the extinction of the *Parvularugoglobigerina eugubina*. In other words, *Subbotina triloculinoides* and *Parvularugoglobigerina eugubina* do not overlap (Olsson *et al*., 1999; Arenillas *et al*., 2000; Obaidalla, 2005). However in this study it has been observed that first occurrence of *Subbotina triloculinoides* is in the P1a zone and it occurs together with *Parvularugoglobigerina eugubina*. The studies of MacLeod and Keller (1991), Keller *et al*. (1995), Pardo *et al*. (1996), Luciani (1997), Li and Keller (1998) and Karoui-Yaakoub *et al*. (2002) also suggest that the first appearance datum of *Subbotina triloculinoides* is in P1a and support our observation. On the other hand, stepwise first occurrences of *Parvularugoglobigerina eugubina*, *Parasubbotina pseudobulloides* and *Subbotina triloculinoides* observed in the above mentioned studies can not be observed in the samples of the Haymana basin, even though the sampling interval was in cm-scale.

Following species of planktonic foraminifera have been identified in the *Parvularugoglobigerina eugubina* (P1a) zone: *Guembelitria cretacea*, *Globoconusa minutula*, *Eoglobigerina fringa*, *Woodringina hornerstownensis*, *Eoglobigerina eobulloides*, *Subbotina trivialis*, *Globanomalina archeocompressa*, *Chiloguembelina morsei*, *Zeauvigerina waiparaensis*, *Parvularugoglobigerina eugubina*, *Globoconusa daubjergensis*, *Praemurica taurica*, *Woodringina claytonensis*, *Eoglobigerina edita*, *Parasubbotina pseudobulloides*, *Subbotina triloculinoides*, *Praemurica pseudoinconstans* and *Chiloguembelina midwayensis* (See Plates in Appendix).

Stratigraphic distribution: From the sample KTS 16 = HSE 52 to the sample HSE 60.

Age: Early Danian

CHAPTER 3

MINERALOGICAL ANALYSES

Relative changes in bulk rock mineralogical composition and clay mineral content are very important reflectors of the variations in sediment sources related to weathering, erosion, climate and sea-level changes. In order to find out the compositional changes across the K/P boundary various studies were conducted related to the bulk and clay mineralogy by several authors. Although mineralogical compositions exhibit great variability based on the paleogeography and depositional environments, some similar properties were observed in various K/P boundary beds. These similar patterns have been mostly interpreted as conclusions of the impact event and/or the mass extinction of the great number of calcareous microfossils (Ben Abdelkader *et al*., 1997; Luciani, 2002).

In order to observe the bulk and clay mineralogical changes across the boundary 12 samples have been analyzed using X-ray diffractometry (XRD). The samples have been selected from the close vicinity of the K/P boundary (approximately 1 m below and 1 m above the boundary). The sampling interval is ranging from 5 to 50 cm. The samples analyzed are KTS 1, KTS 5, KTS 7, KTS 12, KTS 13, KTS 14, KTS 16, KTS 17, KTS 21, KTS 25, KTS 28 and KTS 30 (Figure 12, Figure 13).

The samples have been prepared and analyzed at the Research Center of Turkish Petroleum Corporation (TPAO). All of them have been crushed, and for the clay mineral analysis the crushed samples have been treated further both mechanically and chemically. For the XRD-bulk analysis and XRD-clay analysis Rigaku D/Max-2200 Ultima^{+}/PC generator has been used and the

scanning speed was 2°/min. The obtained diffractograms have been analyzed using Jade-7.0 software based on the Inorganic Crystal Structure Database (ICSD) of the International Center for Diffraction Data (ICCD) by the Research Center. The non-clay and clay mineral composition of the samples and their relative percentages have been determined with ± 3% error.

In the measured section the sediments are primarily composed of calcite, clay minerals and detrital minerals like quartz, plagioclase and K-feldspar (Figure 12, Figure 13). Calcite content averages between 33 to 70% in volume. Clay minerals made up approximately 17 to 30% of the rocks in volume and are mainly smectites and chlorites. Quartz is a minor constituent for some of the samples with the 3% volume but its percentage can reach to 20% in some of the samples. The relative percentages of the plagioclase and K-feldspar range between 3 to 14%. There are also some amphiboles, illite and smectites-chlorite mixed layers in the samples with very minor amounts (Figure 12, Figure 13).

Calcite is the main component of the samples. In the first sample (KTS 1) the percentage of calcite mineral is 42% in volume. Towards the boundary its percentage slightly increases and reaches 50%. However, in the first sample of Danian (KTS 14) its percentage suddenly drops to 39% percentage in volume (Figure 12). After the K/P boundary, the average percentage of the calcite mineral increases and reaches maximum 70% in volume in the samples KTS 21 and KTS 28.

The decrease in the calcite mineral has been observed in many K/P boundary beds in various localities. Carbonate content drops to low percentages (generally less than 10%) through the *Globigerina eugubina* (P1a) zone (Keller, 1988). In the K/P boundary stratotype section El Kef, Tunisia calcite drops to 0% percentage at the boundary above the 40-50% calcite containing marly unit (Ben Abdelkader *et al*., 1997). At the boundary a dark clayey unit, the "boundary clay", is seen. The $CaCO_3$ content in most of the K/P sections of the Deep Sea Drilling Project cores record also values very close to zero in the boundary clay.

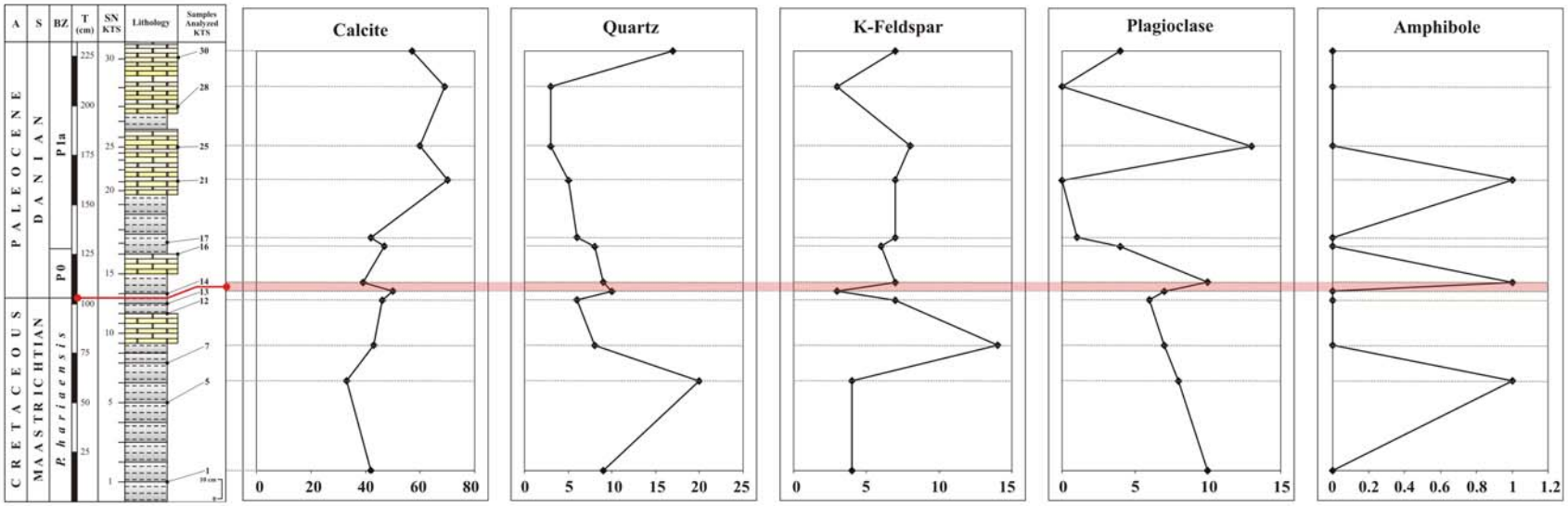

Figure 12. Composite illustration of the bulk minerals of the measured section (KTS) determined from X-ray diffractometry (All have given in relative percentages in a constant volume. The key to the lithological symbols is given in Figure 8).

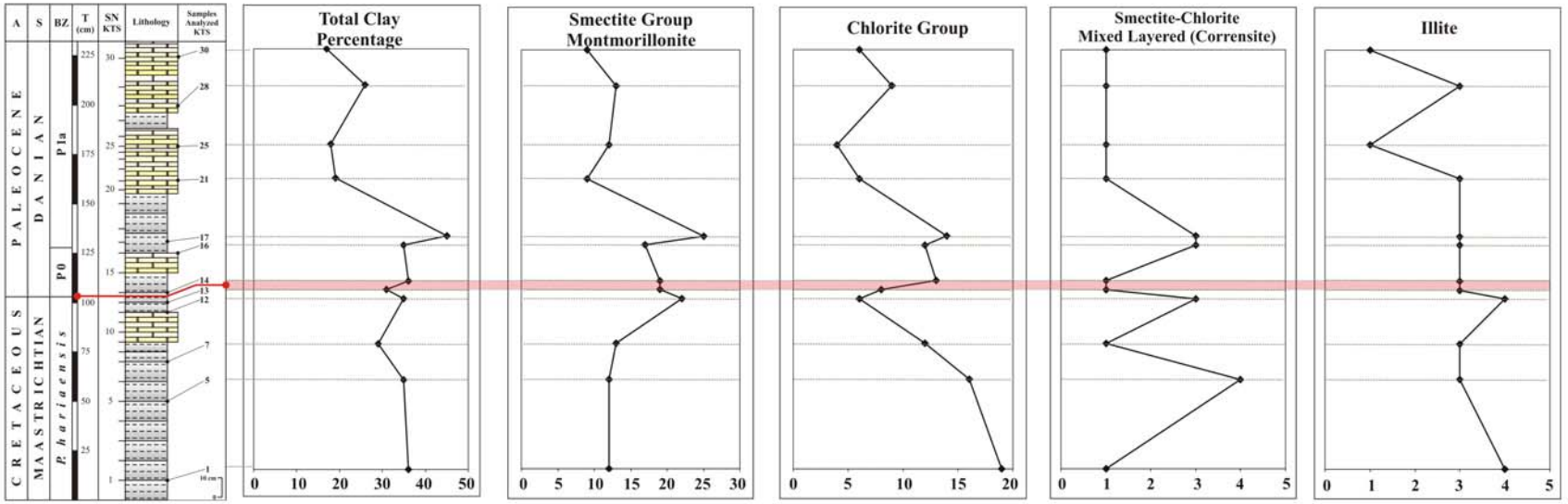

Figure 13. Composite illustration of the clay minerals of the measured section (KTS) determined from X-ray diffractometry (All have given in relative percentages in a constant volume. The key to the lithological symbols is given in Figure 8).

Some other K/P boundary sections with a significant decrease in the calcite content at the boundary clay are: Gubbio section in Italy (Luterbacher and Premoli-Silva, 1964), El Melah, Elles and Seldja sections in Tunisia (Adatte *et al*., 2002a); Erto section in Italy (Luciani, 2002); and Caravaca section in Spain (Arenillas *et al*., 2006). The decrease in the carbonate content is interpreted as reflecting principally the crisis in post-boundary productivity. It is interrelated generally with the decrease of the carbonate production after the mass extinction of the calcareous microfossils like foraminifers, ostracods and coccoliths.

In our section, a marked drop in carbonate content (11%) is recorded at the base of the P0 zone (Figure 12). However, the percentage of $CaCO_3$ is still too high (39%) at the boundary for properly defining the boundary clay. This behavior of $CaCO_3$ could indicate that the carbonate/clastic sedimentation ratio in the measured section does not merely reflect the primary productivity of carbonate plankton. Since the section was measured in the tectonically active Haymana basin, the change in the carbonate content may also be related to sea-level fluctuations and terrestrial sediment input related to tectonic pulses. On the other hand, the increase of the carbonate content in the P1a zone may indicate newly reestablished calcareous plankton ecosystem or decrease of the sediment influx to the basin (Figure 12).

Quartz is another main component in the samples. Its percentage increases from 9% to 20% from the sample KTS 1 to KTS5 (Figure 12). Then it drops to 6% close to the boundary (KTS 12). In the boundary beds the percentage of quartz volume reaches approximately 10%. It coincides with the decrease in the carbonate content. Above the boundary beds the percentage decreases around 5% and it increases again up to 17% to the end of the P1a zone (Figure 12).

If the patterns of calcite and quartz percentages are examined, it will be seen that there is a strong opposite relationship between their

behaviors (Figure 12). This opposite relation may be explained with the sea-level fluctuations and related changes in the rate of terrestrial influx to the basin.

The other detrital minerals plagioclase and K-feldspar are in lesser amounts when compared to quartz. Their percentages reach maximum 14% in the rock volumes. Just at the boundary (between the samples KTS 13 and KTS 14) both K-feldspar and plagioclase increase (Figure 12). On the other hand, amphibole, which is generally associated with volcanic material, is seen as a trace mineral with less then 3% in few of the samples (Figure 12).

Clay minerals are very important since their assemblages reflect continental morphology, tectonic activity, as well as climate evolution and associated sea-level fluctuations. The most abundant clay minerals recorded in the measured section are smectite group minerals, namely montmorillonites. Montmorillonite is the most common member of the smectite group. Its unit cell consists of one aluminous octahedral sheet sandwiched between two tetrahedral sheets (Berner, 1971).

In the samples the average percentage of smectite is 15%. In the Cretaceous samples the percentage of smectite is around 12%. As approaching to the K/P boundary its proportion in the samples increases and reaches to 22%. At the base of the P1a zone (KTS 17), approximately 25 cm above the K/P boundary, it reaches its maximum value and becomes 25% in volume (Figure 13).

Smectite group minerals commonly reflect weathering and transport (Flügel, 2004). Therefore, the increase in the smectites, namely montmorillonites, can be explained with the increase in sediment influx around the boundary. This result can also be correlated with the increase in the other detrital minerals like quartz and plagioclase (Figure 12, Figure 13).

As a consequence of different transport behaviors, clay minerals are deposited in the ocean at different distances from the coast. Smectite group minerals are deposited in general in deeper, more offshore settings than the other

detrital minerals like kaolinite or illite (Flügel, 2004; Adatte *et al*., 2002a). Since smectite group minerals consists of fine particles they are easily carried into slope and basin environments (Adatte and Rumley, 1989; Chamley, 1989; Weaver, 1989). This information also supports our idea about the depositional environments based on the microfacies analyses. The constant presence of smectite in the measured section indicates also the absence of a strong diagenetic overprint owing to burial. It also implies a detrital origin that may reflect local uplift and/or variations in weathering processes and soil formation in the bordering continental areas (Chamley, 1989; Weaver, 1989).

Chlorite is the other common clay mineral in the samples. It is an aluminosilicate of magnesium and iron and a common detrital clay mineral (Berner, 1971). The average percentage of chlorite is approximately 10% in the samples. It shows its maximum amounts in the Cretaceous samples, in the *P. hariaensis* zone (12-19%). Then close to the boundary its percentage is dropped to the values of 6%. In the boundary beds, chlorite shows also an increase like smectite does. In the first Danian sample (KTS 14) its percentage is 13%. In the lower part of P1a (in KTS 17), approximately 25 cm above the K/P boundary, it reaches 14% in volume (Figure 13). After that, it shows a decrease throughout the P1a zone.

Smectite-chlorite mixed layer has also been recorded in the samples. It shows a corrensite character. Smectite is generally transformed into chlorite-like phyllosilicates forming chlorite-smectite mixed layers. This diagenetic alteration is explained by the degradation and partial destruction of smectite by organic acids under strongly reducing conditions (Chamley, 1989). The average percentage of smectite-chlorite mixed layer is very low in our samples. It ranges between 1 and 4% showing that the amount of degradation is low in our samples. If the transformation from smectite to chlorite was intense in the samples, an inverse trend would have been observed in their relative percentages. However, in our samples their values show very similar patterns,

especially in the Danian (Figure 13). In the samples there is also illite in very minor amounts. Its percentage is changing from 1 to 4% (Figure 13).

Total clay mineral percentage makes 17 to 30% of the rocks volume. In the *P. hariaensis* zone the value of the total clay minerals are around 35%. It displays an increasing trend around the K/P boundary and reaches its maximum percentage in the sample KTS 17, which is located approximately 25 cm above the boundary (Figure 13). Then it shows a decreasing trend and end up with 17% in the sample KTS 30.

As a summary, our mineralogical analyses on the K/P boundary beds demonstrate that some minerals like calcite and clay minerals can be used to interpret the boundary. In other words, some mineralogical changes allow correlating the K/P boundary beds located in different locations of the world. However, in a tectonically active basin like Haymana all the factors affecting the mineralogy of the rocks should be taken into consideration.

CHAPTER 4

MICROFACIES ANALYSES

4.1 MICROFACIES TYPES AND DEPOSITIONAL ENVIRONMENTS

The microfacies term has been originally defined as the petrographic and paleontological data studied in thin sections. However, today, microfacies is regarded as the total of all sedimentological and paleontological data which can be described and classified from thin sections, peels, polished slabs and rock samples (Flügel, 2004). Grain types and frequency, matrix types, depositional fabrics, fossils and depositional texture types should be considered in the determination of the microfacies types (Flügel, 2004).

The microfacies study in this work aims to understand the depositional history of the area by examining the sedimentological and paleontological characteristics of the samples. Microfacies analyses have been performed by examining the main components, textures, macro-, and microfossil associations of the samples. Lithological variations observed in the outcrop have also been considered. In addition, most frequently used facies models have been examined and the depositional environments of the rocks have been determined.

For the naming of the carbonate rocks Dunham Classification of Carbonate Rocks (1962) has been utilized (Figure 14). The original classification of Dunham includes five textural classes. Two major groups are distinguished (1) carbonates whose original components were originally bound together during deposition (boundstones), and (2) carbonates whose original components were not originally bound. The second group is subdivided according to mud-support (mudstone and wackestone) or grain-support

(packstone and grainstone). The subdivision of the mud-supported rocks is based on the < or > 10% grain bulk boundary. Embry and Klovan (1971) expanded the classification of Dunham and proposed two other rock names for the carbonates whose original components were not organically bound during the deposition. These are floatstone (mud-supported) and rudstone (grain-supported). Both floatstone and rudstone should contain more than 10% of grains larger than 2 mm (Figure 14).

<table>
<tr><th colspan="9">CLASSIFICATION OF LIMESTONES (DUNHAM, 1962)</th></tr>
<tr><td colspan="5">DEPOSITION TEXTURE RECOGNIZABLE</td><td colspan="4" rowspan="3">DEPOSITIONAL TEXTURE
NOT RECOGNIZABLE

CRYSTALLINE CARBONATE
(Subdivide according classification designed to bear on physical texture and diagenesis)</td></tr>
<tr><td colspan="5">Original components not bound together during deposition</td></tr>
<tr><td colspan="3">Contains mud
(particles of clay and fine silt size)</td><td rowspan="2">Lacks mud and is grain-supported</td><td rowspan="2">Original components were bound together during deposition as shown by intergrown or lamination contrary to gravity, sediment-floored cavities that are roofed over by organic or questionable organic matter and are too large to be interstices</td></tr>
<tr><td colspan="2">Mud-supported</td><td>Grain-supported</td></tr>
<tr><td>less than 10% grains</td><td>more than 10% grains</td><td></td><td></td><td></td><td colspan="4"></td></tr>
<tr><td>MUDSTONE</td><td>WACKESTONE</td><td>PACKSTONE</td><td>GRAINSTONE</td><td>BOUNDSTONE</td><td colspan="4"></td></tr>
<tr><th colspan="9">EXPANDED CLASSIFICATION (EMBRY and KLOVAN, 1971)</th></tr>
<tr><td colspan="6">ALLOCHTHONOUS LIMESTONE
ORIGINAL COMPONENTS NOT ORGANICALLY ORIGINAL
BOUND DURING DEPOSITION</td><td colspan="3">AUTOCHTHONOUS LIMESTONE
COMPONENTS ORGANICALLY
BOUND DURING DEPOSITION</td></tr>
<tr><td colspan="2">Less than 10% > 2 mm components
contains lime mud (< 0.03 mm)</td><td>no lime mud</td><td colspan="3">Greater than 10% > 2mm components</td><td colspan="3">by organisms which</td></tr>
<tr><td colspan="2">Mud-supported</td><td colspan="2" rowspan="2">Grain-supported</td><td rowspan="2">Matrix-supported</td><td rowspan="2">> 2 mm component supported</td><td rowspan="2">build a rigid framework</td><td rowspan="2">encrust and bind</td><td rowspan="2">act as bafflers</td></tr>
<tr><td>less than 10% grains (> 0.03 mm and < 2 mm)</td><td>greater than 10% grains</td></tr>
<tr><td colspan="6"></td><td colspan="3">BOUNDSTONE</td></tr>
<tr><td>MUDSTONE</td><td>WACKESTONE</td><td>PACKSTONE</td><td>GRAINSTONE</td><td>FLOATSTONE</td><td>RUDSTONE</td><td>FRAMESTONE</td><td>BINDSTONE</td><td>BAFFLESTONE</td></tr>
</table>

Figure 14. Dunham classification (1962) of carbonate rocks and its expanded version by Embry and Klovan (1971).

For the mixed siliciclastic-carbonate rocks, there is not a recent classification used frequently by the authors. However a descriptive classification system was proposed by Mount (1985) using for components. These are (1) siliciclastic sand (sand-sized quartz, feldspar etc.), (2) non-carbonate mud (mixtures of silt and clay), (3) carbonate grains or allochems (peloids, ooids, bioclasts, intraclasts) and (4) carbonate mud (micrite) (Flügel, 2004). In this classification the name of the sediment type reflects both the dominant grain type and the most abundant antithetic component (Figure 15). Although the classification of Mount is not a common classification, it is quite

applicable for naming of the marls and no other alternative has been encountered in the recent publications. It has been observed that many sedimentologists prefer to give names to the mixed siliciclastic-carbonate rocks like “silty limestone”, “sandy limestone”, “calcareous sandstone” , “silty marl” etc. In this study, the mixed siliciclastic-carbonate rocks have been named both using the common names in the papers and using the principles proposed in the Mount (1985) classification.

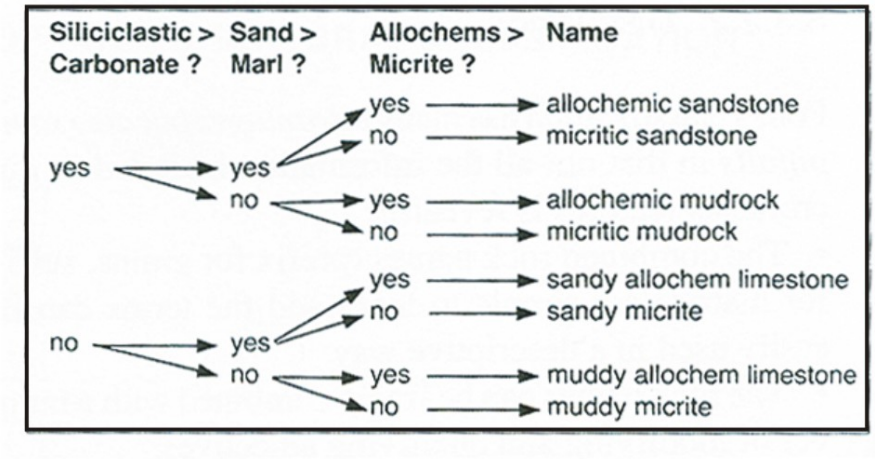

Figure 15. Classification of mixed siliciclastic-carbonate rocks (Mount, 1985).

The assemblages of the micro and macrofossils play important role in the determination of the microfacies types. Therefore, all the major fossil groups in the samples have been studied carefully in order to make correct identifications. In the determination of the major fossil groups the explanations and photographs in Flügel (2004), Scholle and Ulmer-Scholle (2003) and Horowitz and Potter (1971) have been utilized.

In order to understand the depositional environments of the lithologies the most applicable and detailed microfacies models have been examined. One of the most detailed and frequently used facies model has been developed by Wilson (1975). Wilson (1975) has defined 10 Standard Facies Zones (FZ) describing idealized facies belts along an abstract transect from open-marine

deep basin across a slope, a platform marginal rim (characterized by reefs or zone with sand shoals), and an inner platform to the coast (Figure 16). Although it is limited to tropical and subtropical platforms and does not include the affect of climatic control and sea-level fluctuations, the model of Wilson has been used successfully by many authors involved in basin analyses and reservoir studies.

Flügel (2004) has also established a facies model describing the sedimentation on a rimmed carbonate shelf and warm-water platform-reef environments in tropical latitudes. Within this model he has described 26 Standard Microfacies Types (SMF) (Figure 16). He has also gathered information from various case studies related to unrimmed and ramp carbonate shelves and proposed 30 Ramp Microfacies Types (RMF) (Figure 17). The facies zones in RMF and SMF can be correlated in certain cases. In this study Standard Facies Zones (FZ) proposed by Wilson (1975), and Standard Microfacies Types (SMF) and Ramp Microfacies Types (RMF) established by Flügel (2004) have been examined when determining the microfacies types and depositional environments. However, it should be noted that, these models are composite and strongly generalized. Therefore, it is not always possible to see the microfacies types described in these models with the same order and character in the studied section.

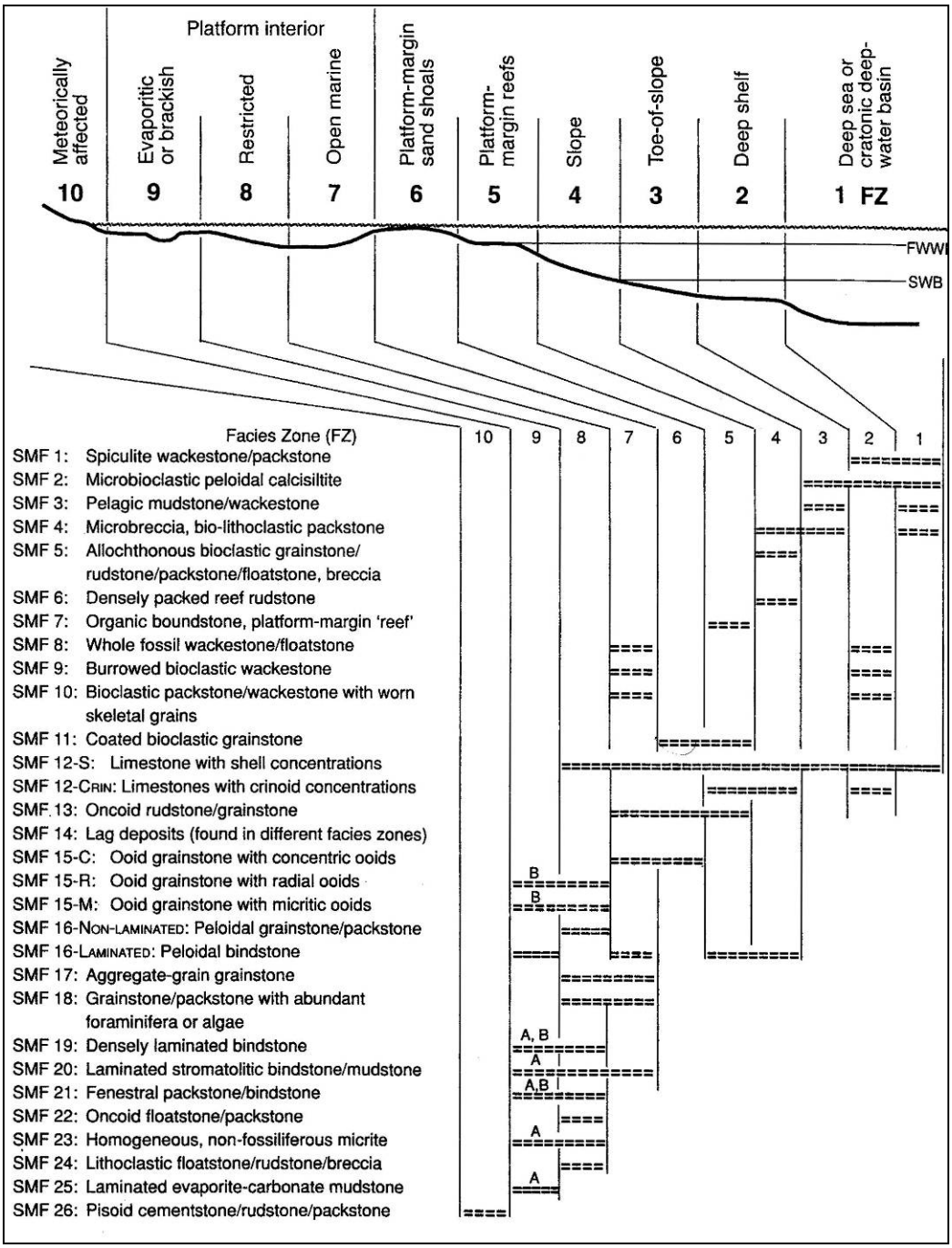

Figure 16. Distribution of Standard Microfacies (SMF) types in the Facies Zones (FZ) of Wilson (1975) on a rimmed carbonate platform model (Flügel, 2004) (A: evaporitic, B: brackish).

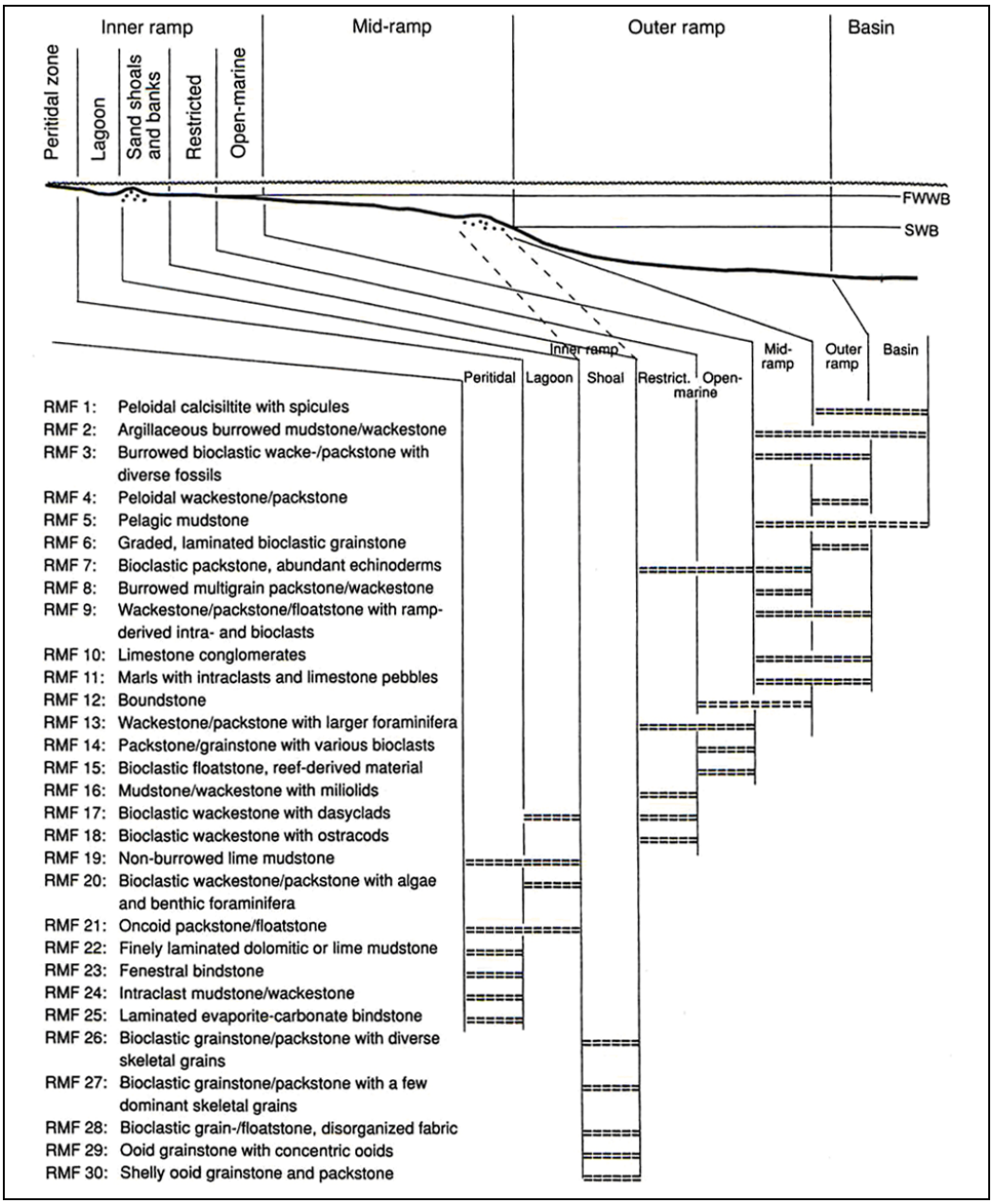

Figure 17. Generalized distribution of microfacies types (RMF) in different parts of a homoclinal carbonate ramp (Flügel, 2004).

Based on the above explained criteria, 10 microfacies (MF) types have been determined in this study. The MF types defined in this study correspond to basically carbonate shelf to open marine environment. Most of them show slope to basin character. It is difficult to determine the type of the shelf. Nonetheless, with the obtained observations it can be concluded that some of the facies belts show very similar characteristics with the ramp facies and unrimmed, open shelf platform facies defined by various authors. The abundance of the mixed siliciclastic-carbonate rocks in the system and the gradual transition of the facies belts observed from inner shelf to the outer shelf and from outer shelf to the basin are evidences of that. However, in order to be sure about the shelf type further sedimentological studies are needed.

The MF types determined in this study are namely: bioclastic packstone with large benthic foraminifera and calcareous red algae, grainstone with large benthic foraminifera and calcareous red algae, bioclastic wackestone-packstone with benthic foraminifera and calcareous red algae, bivalved floatstone, wackestone with planktonic organisms, quartz-rich silty limestone with benthic and planktonic foraminifera and calcareous red algae, iron-rich silty marl with planktonic and benthic foraminifera, silty marl with planktonic and benthic foraminifera, silty marl with large clay minerals and spheroid grains, silty limestone with planktonic and benthic foraminifera. Table 2 summarizes the main features of the microfacies types; Figure 18 shows the stratigraphical distribution of the major fossil groups throughout the measured section, and Figure 19 and Figure 20 show the thin section photographs of the major fossil group identified within the frame of the microfacies analyses. It should be noted that the taxonomy of these forms are beyond the scope of this study. These fossil groups have been treated only as biogenetic constituents of the rocks and only been used in the microfacies interpretations.

Table 2. Microfacies types, corresponding depositional environments and systems tracts.

No	MFT	Field Description	Main Component	Depositional Environment	System Tract
1	bioclastic packstone with large benthic foraminifera and calcareous red algae	yellowish bioclastic limestone	large hyaline benthic foraminifera, calcareous red algae, agglutinated benthic foraminifera, mollusk fragments, echinodermata fragments	inner shelf to slope	HST
2	grainstone with large benthic foraminifera and calcareous red algae	yellowish bioclastic limestone with abundant large benthic foraminifera	large hyaline benthic foraminifera, calcareous red algae, agglutinated benthic foraminifera, mollusk fragments, echinodermata fragments	platform interior to open marine	HST
3	bioclastic wackestone-packstone with benthic foraminifera and calcareous red algae	yellowish bioclastic limestone	large hyaline benthic foraminifera, calcareous red algae, agglutinated benthic foraminifera, mollusk fragments, echinodermata fragments, planktonic foraminifera	shelf to slope	HST
4	bivalved floatstone	pelecypoda-rich yellowish limestone	mollusk fragments, benthic foraminifera, planktonic foraminifera, calcispheres	slope	HST
5	wackestone with planktonic organisms	yellowish limestone	planktonic foraminifera, benthic foraminifera, calcispheres	deeper shelf to slope	HST

Table 2. Continued.

No	MFT	Field Description	Main Component	Depositional Environment	System Tract
6	quartz-rich silty limestone with benthic and planktonic foraminifera and calcareous red algae	dark gray marl	quartz, hyaline smaller benthic foraminifera, planktonic foraminifera, calcareous red algae, agglutinated benthic foraminifera	slope to basin/ outer ramp	SMW
7	iron-rich silty marl with planktonic and benthic foraminifera	lead to dark gray marl	iron-oxide minerals, quartz and feldspar, planktonic foraminifera, smaller benthic foraminifera,	slope to basin/ outer ramp	TST
8	silty marl with planktonic and benthic foraminifera	greenish gray marl	clay minerals, iron-oxide minerals, planktonic foraminifera, benthic foraminifera	toe of slope/ outer ramp	TST
9	silty marl with large clay minerals and spheroid grains	greenish gray marl	large clay minerals, quartz, feldspar, spheroid grains, planktonic foraminifera, large agglutinated benthic foraminifera, smaller hyaline benthic foraminifera	slope to basin	TST - HST
10	silty limestone with planktonic and benthic foraminifera	yellowish-brownish limestone	very small planktonic foraminifera, smaller hyaline benthic foraminifera, iron-oxide minerals	close to the basin	HST

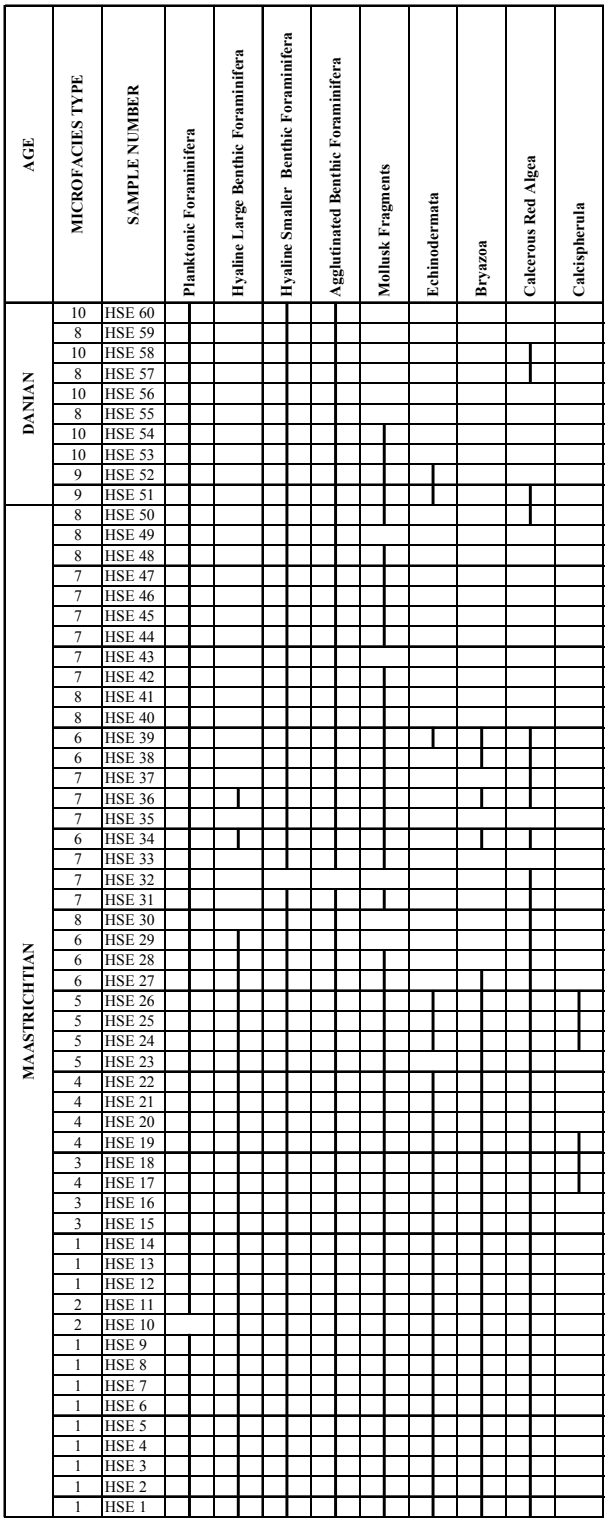

Figure 18. Stratigraphical distribution of the major fossil groups and the microfacies types throughout the measured section**.**

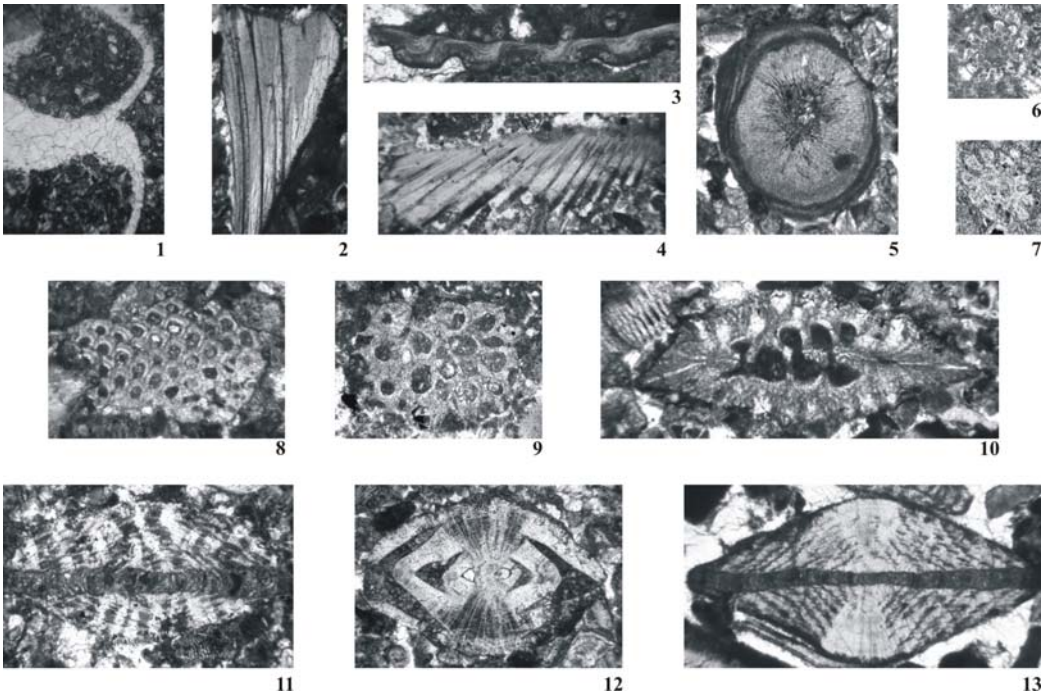

Figure 19. Thin section photographs of the major fossil group identified within the frame of the microfacies analyses. **1.** gastropoda shell, X6 (HSE 21). **2.** pelecypoda shell, X10 (HSE 1). **3.** pelecypoda shell, X15 (HSE 11). **4.** pelecypoda shell, X7 (HSE 4). **5.** echinodermata spine, X16 (HSE 7). **6.** echinodermata spine, X40 (HSE 19). **7.** echinodermata spine, X50 (HSE 26). **8.** bryozoan shell, X25 (HSE 8). **9.** bryozoan shell, X12 (HSE 17). **10.** bryozoan shell, X20 (HSE 8). **11.** hyaline large benthic foraminifera, X20 (HSE 1). **12.** hyaline smaller benthic foraminifera, X18 (HSE 3). **13.** hyaline large benthic foraminifera, X15 (HSE 11).

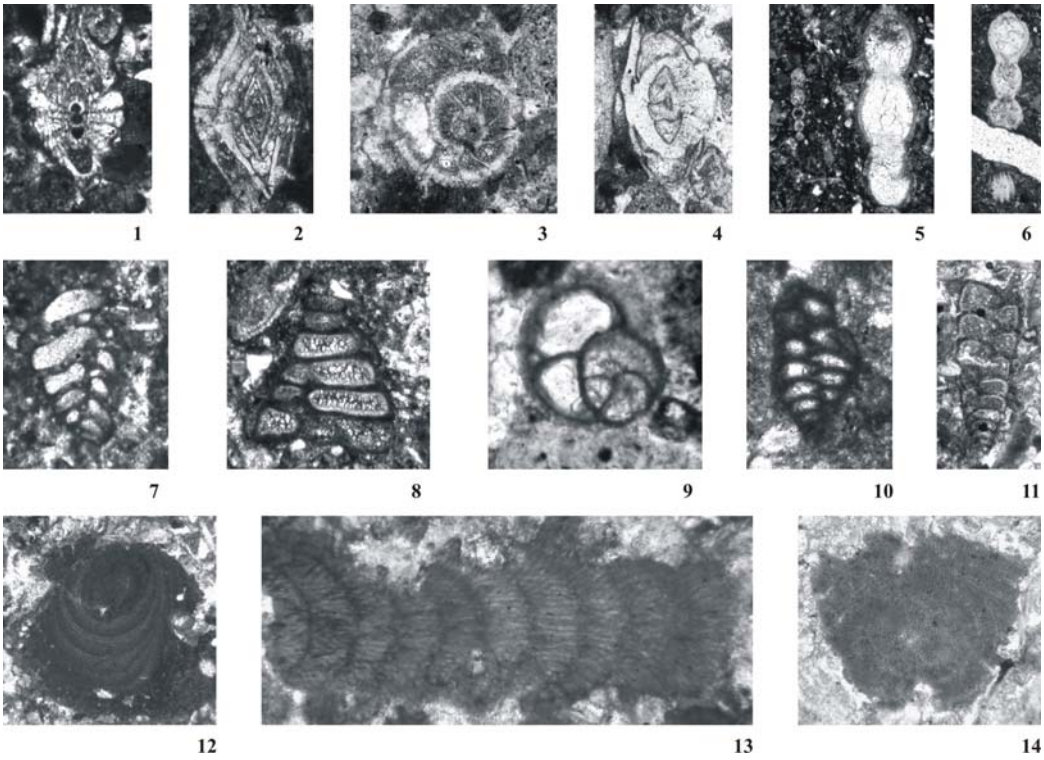

Figure 20. 1. hyaline large benthic foraminifera, X25 (HSE 1). **2.** hyaline smaller benthic foraminifera, X33 (HSE 2). **3.** hyaline smaller benthic foraminifera, X52 (HSE 13). **4.** hyaline smaller benthic foraminifera, X26 (HSE 1). **5.** hyaline smaller benthic foraminifera, X12 (HSE 14). **6.** hyaline smaller benthic foraminifera, X10 (HSE 25). **7.** agglutinated benthic foraminifera, X20 (HSE 16). **8.** agglutinated benthic foraminifera, X35 (HSE 24). **9.** agglutinated benthic foraminifera, X84 (HSE 22). **10.** agglutinated benthic foraminifera, X38 (HSE 15). **11.** agglutinated benthic foraminifera, X 18 (HSE 6). **12.** calcareous red algae, X13 (HSE 2). **13.** calcareous red algae, X45 (HSE 4). **14.** calcareous red algae, X30 (HSE 2).

4.1.1 MF 1, Bioclastic Packstone with Large Benthic Foraminifera and Calcareous Red Algae

In the field the lithology of this microfacies has been described as yellowish colored bioclastic limestone and it occurs in the lowermost part of the measured section in the samples HSE 1-9 and HSE 12-14 (Figure 8, Figure 9 A, B). In thin sections MF 1 is characterized by its abundant micro- and macrofossil content within a micritic matrix (Figure 21). The rock is grain-supported and grains made up of more than 50% of the whole composition. Therefore packstone is a suitable name for this limestone. Large hyaline benthic

foraminifera like *Orbitoides*, *Lepidorbitoides*, *Siderolites*, *Sulcoperculina* and *Helonocyclina* (Figure 22) are quite abundant. Agglutinated uncoiled benthic foraminifera are also common. Corallinacean and Solenoporacean calcareous red algae with the large benthic foraminifera occupy a great volume of the rock. Besides the foraminifera and red algae mollusk fragments (pelecypoda, gastropoda and cephalopoda pieces), echinodermata fragments and spines, bryozoans and calcareous green algae are seen in this microfacies type. There are also some planktonic foraminifera, but they are very scarce. In MF 1 the size of the allochems are quite big and the percentage of the micritic matrix shows variability within the microfacies. In certain samples sparite is also seen in little amounts.

Large rotaliinid benthic foraminifera are seen in shelf and shelf slope deposits. They are abundant and rock-forming in the restricted and open marine environments in the platform interiors and inner ramps (Figure 16, Figure 17). On the other hand, calcareous red algae need light penetration and are seen in the platform edges, upper slope environments or mid-ramp settings (Flügel, 2004). Bryozoans, mollusks and echinoderms are seen also in inner and mid-ramp settings and platform interior to slope environments. Presence of the planktonic foraminifera is very important, because it shows that this facies is affected by the open marine conditions. When all these data are considered, it is concluded that MF 1 corresponds to a place in the transition of the inner shelf to slope.

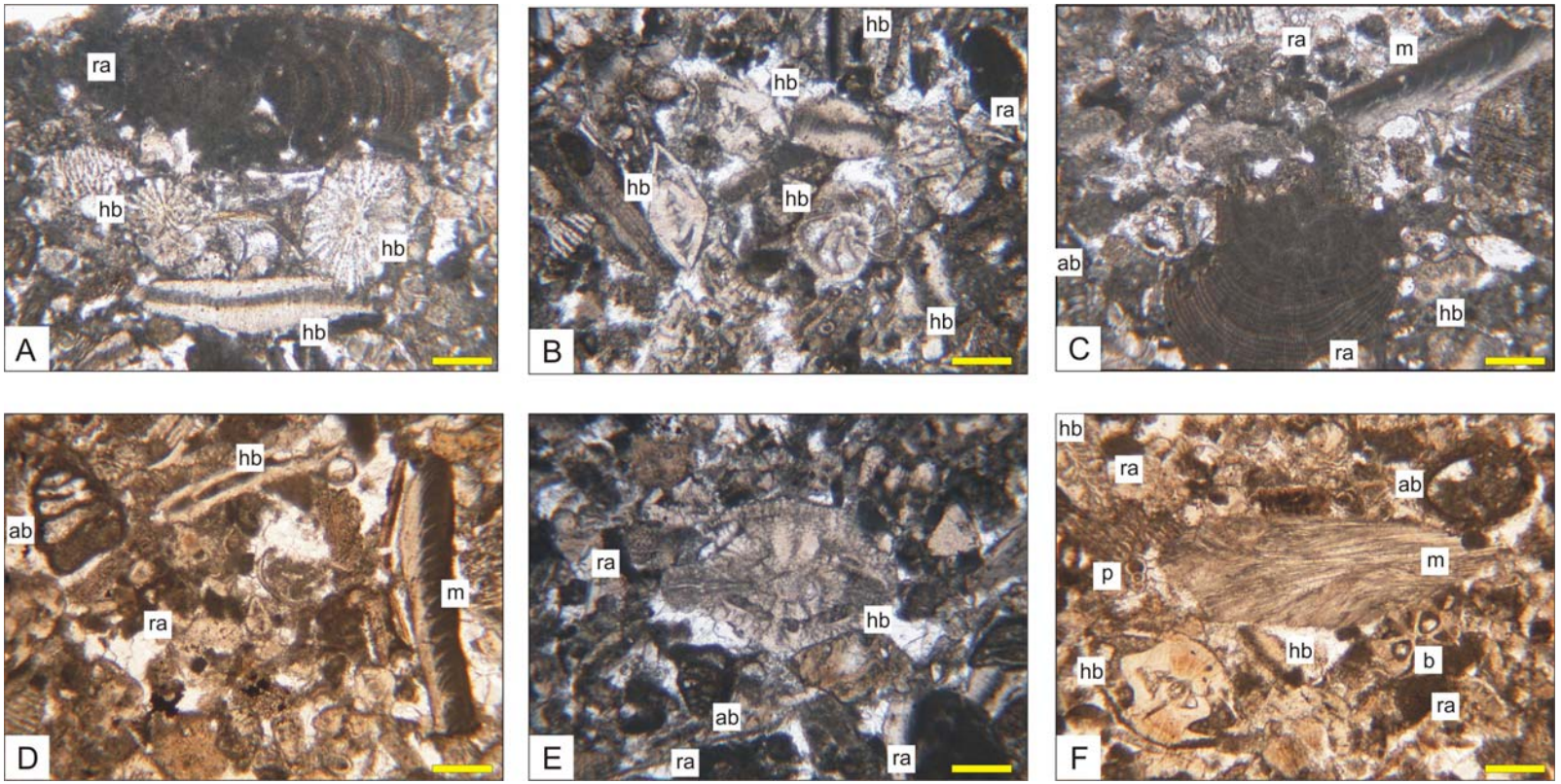

Figure 21. Photomicrographs of the bioclastic packstone with large benthic foraminifera and calcareous red algae (MF 1). (hb: hyaline benthic foraminifera, ab: agglutinated benthic foraminifera, p: planktonic foraminifera, ra: calcareous red algae, m: mollusk fragment, b: bryozoan). **A.** HSE 1. **B.** HSE 2. **C.** HSE 5. **D.** HSE 8. **E.** HSE 7. **F.** HSE 7. (Scale bar is 0.25 mm).

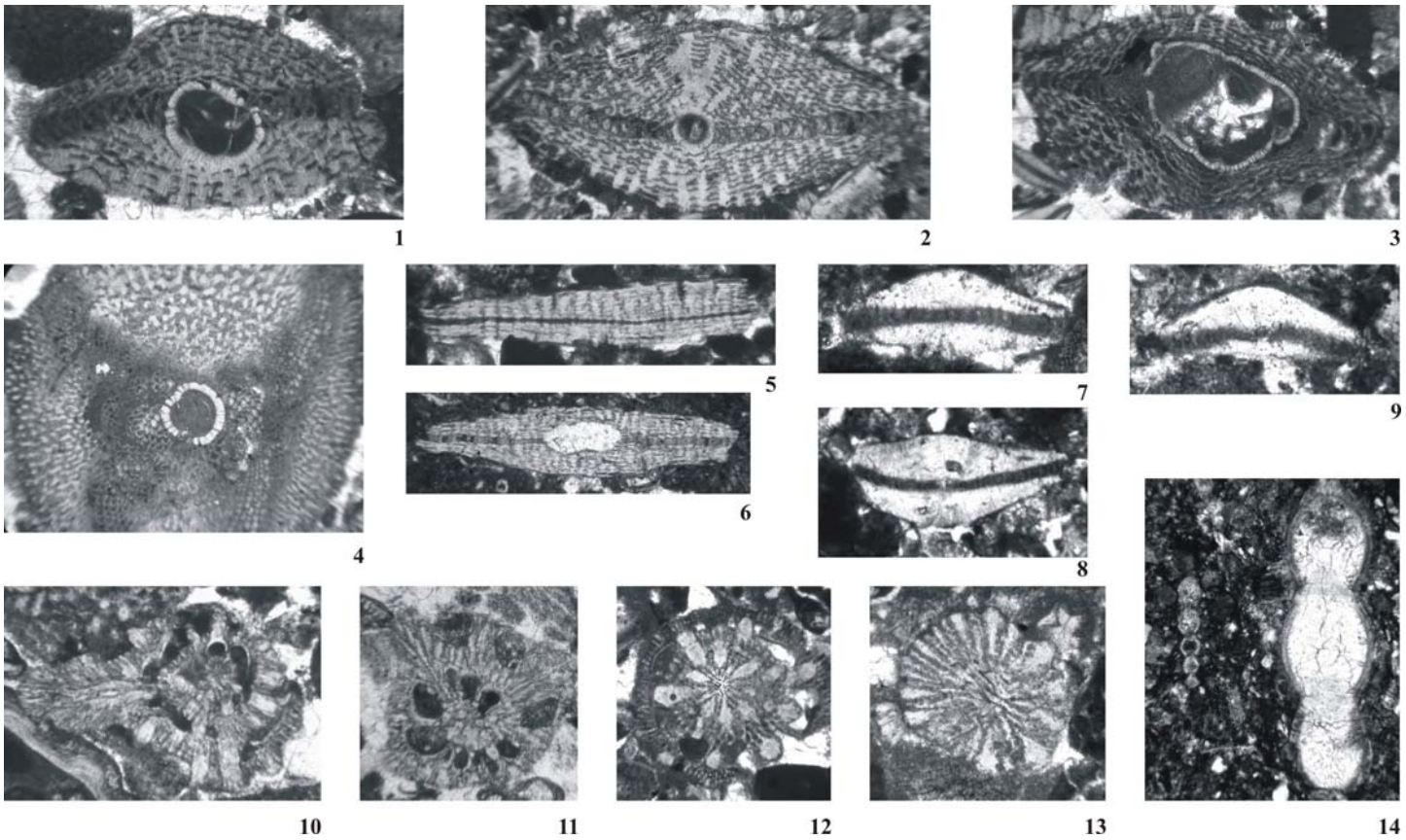

Figure 22. 1. *Orbitoides*, X33 (HSE 10). **2.** *Orbitoides*, X27 (HSE 13). **3.** *Orbitoides*, X27 (HSE 10). **4.** *Orbitoides*, X15 (HSE 10). **5.** *Lepidorbitoides*, X26 (HSE 6). **6.** *Lepidorbitoides*, X21 (HSE 4). **7.** *Helonocyclina*, X52 (HSE 1). **8.** *Helonocyclina*, X29 (HSE 1). **9.** *Helonocyclina*, X81 (HSE 1). **10.** *Siderolites*, X24 (HSE 18). **11.** *Siderolites*, X27 (HSE 11). **12.** *Siderolites*, X31 (HSE 11). **13.** *Siderolites*, X35 (HSE 11). **14.** *Nodosaria*, X24 (HSE 14).

This microfacies is quite similar to SMF 18-FOR (bioclastic grainstones and packstones with abundant benthic foraminifera or calcareous algae, "FOR" denotes abundance of foraminifera) and RMF 13 (packstone with abundant larger foraminifera) defined by Flügel (2004). It also corresponds to the FZ 7 (platform interior to open marine environment) of Wilson (1975) (Figure 16, Figure 17).

4.1.2 MF 2, Grainstone with Large Benthic Foraminifera and Calcareous Red Algae

This microfacies has been noticed in the field as a limestone with abundant large benthic foraminifera and occurs in the lower parts of the measured section in the samples HSE 10-11 (Figure 8). It is characterized by the abundant large benthic foraminifera and calcareous red algae within a sparitic cement (Figure 23). Therefore the rock has been called as grainstone. The most common large benthic foraminifera in this facies are *Orbitoides*, *Lepidorbitoides*, *Omphalocyclus*, *Siderolites*, *Sulcoperculina* and *Helonocyclina*. In MF 2 bryozoans and agglutinated benthic foraminifera are quite common. Mollusk and echinodermata fragments are also observed.

MF 2 is quite similar to MF 1 and can also be correlated with the SMF 18-FOR (bioclastic grainstones and packstones with abundant benthic foraminifera or calcareous algae) defined by Flügel (2004). It corresponds to the FZ 7 (platform interior to open marine environment) of Wilson (1975) (Figure 16, Figure 17).

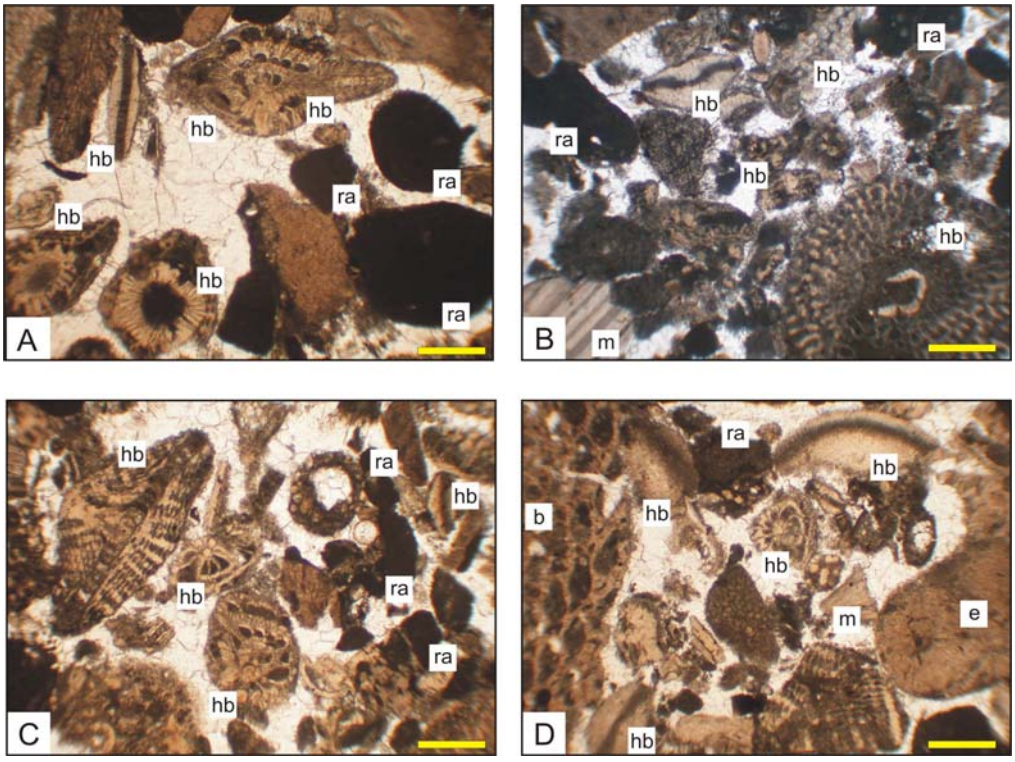

Figure 23. Photomicrographs of the grainstone with large benthic foraminifera and calcareous red algae (MF 2). (hb: hyaline benthic foraminifera, ab: agglutinated benthic foraminifera, p: planktonic foraminifera, ra: calcareous red algae, m: mollusk fragment, b: bryozoan, e: echinodermata spine). **A.** HSE 10. **B.** HSE 10. **C.** HSE 10. **D.** HSE 10. (Scale bar is 0.50 mm).

4.1.3 MF 3, Bioclastic Wackestone-Packstone with Benthic Foraminifera and Calcareous Red Algae

This microfacies type is seen in the lower parts of the measured section in the samples HSE 15, HSE 16, and HSE 18-23, and similar to MF 1 (Figure 8). Hyaline benthic foraminifera and calcareous red algae are also abundant in this microfacies (Figure 24). However in MF 3, the amount of micrite is increased and the size and the abundance of the allochems are decreased. The number of hyaline large benthic foraminifera is also diminished. Agglutinated benthic foraminifera, echinoderm spines, bryozoans and mollusk fragments are quite common in this microfacies. Calcareous green algae and some calcispheres are also observed. Planktonic foraminifera are rare to common in this microfacies type.

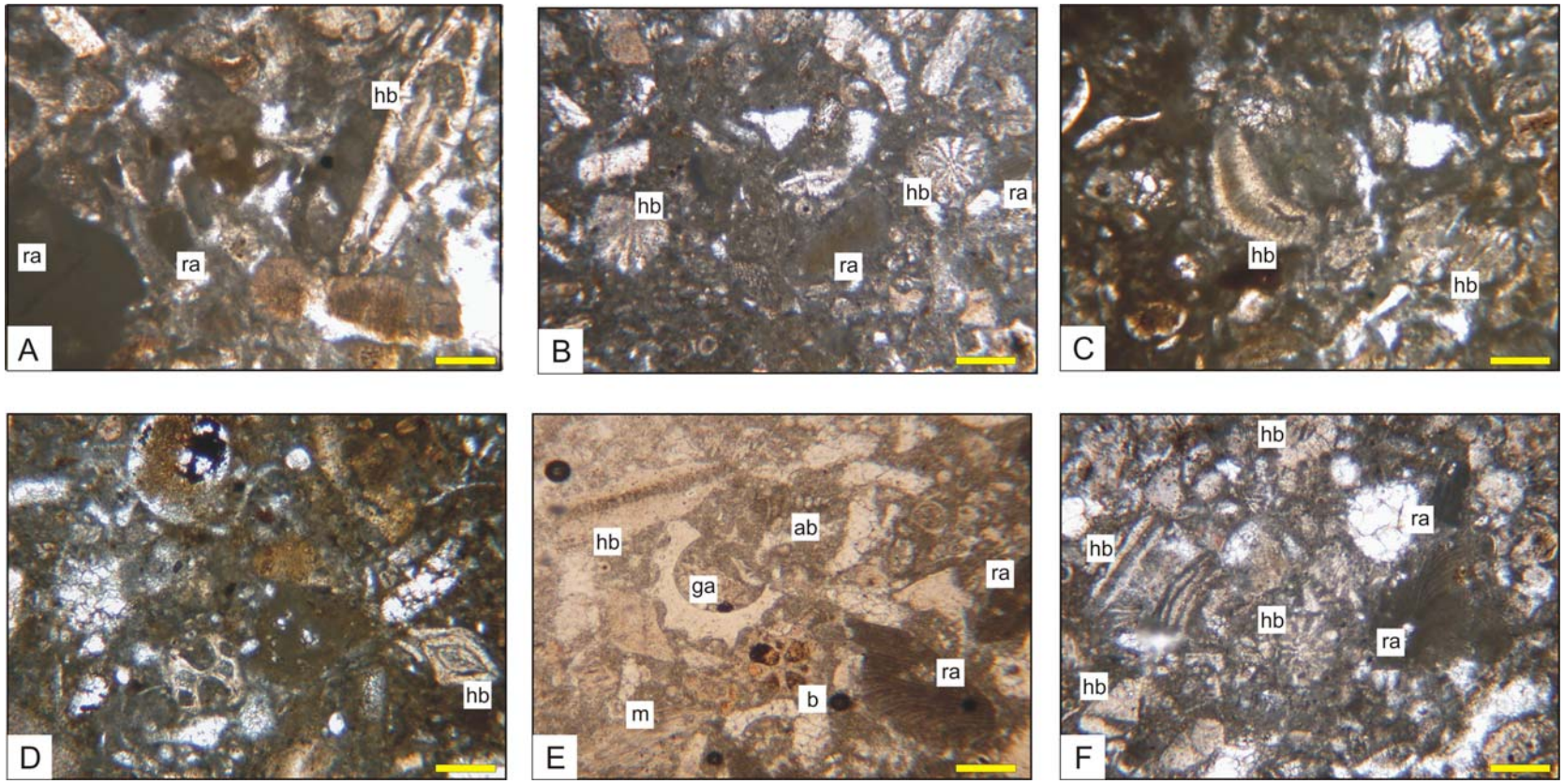

Figure 24. Photomicrographs of the bioclastic wackestone-packstone with benthic foraminifera and calcareous red algae (MF 3). (hb: hyaline benthic foraminifera, ab: agglutinated benthic foraminifera, ra: calcareous red algae, ga: calcareous green algae, m: mollusk fragment, b: bryozoan). **A.** HSE 15. **B.** HSE 16. **C.** HSE 18. **D.** HSE 23. **E.** HSE 18. **F.** HSE 21. (Scale bar is 0.25 mm).

Considering its textural appearance and fossil content it can be said that this microfacies type is observed on the shelf to the slope and corresponds to SMF 18-FOR and RMF 13 of the Flügel's model like MF 1 does (Figure 16, Figure 17). However, the slight increase in the abundance of the planktonic foraminifera may indicate the proximity of this facies to the basin.

4.1.4 MF 4, Bivalved Floatstone

This facies has been described in the field as pelecypoda-rich limestone in the samples HSE 17, and HSE 19-22 (Figure 8). Thin section studies supported the descriptions made on the field. The lithologies belonging to this facies are composed of large mollusk, especially bivalve fragments (Figure 25). The size of the shell fragments exceeds 2 mm in size and they constitute almost 50% of the rock embedded within a micritic matrix. Therefore, the rock has been named as bivalved floatstone. The places in between the bivalve fragments are composed of planktonic and benthic foraminifera and micritic lime containing calcispheres. The size of the foraminifera and other bioclasts within the shell pieces are very small. Besides bivalves, foraminifera and calcispheres; echinodermata, bryozoans, calcareous red and green algae are also very common in this facies. On the other hand large hyaline benthic foraminifera are rare.

MF 4 is very similar to the SMF 12-Bs defined by Flügel (2004). This standard microfacies defined as bioclastic rudstones or densely packed floatstones is characterized by accumulations of one-type shell concentrations. If shells belong to bivalves, the abbreviation "Bs" is used. Rock-building concentrations of shells may originate in various environments from coast to the deep sea. Based on the facies model proposed by Flügel (2004) bivalve shell beds are formed in platform interior settings (FZ 8), open platforms (FZ 7), reefs and slopes (FZ 5 and FZ 4) and toe-of-slope and deep marine settings (FZ 3, FZ 2, FZ 1). Because the shell concentrations are seen within a micritic matrix abundant in pelagic organisms, it can be concluded that this facies has been

deposited in a slope environment. Therefore, FZ 4 of Wilson (1975) is the most suitable facies zone for this MF type (Figure 16).

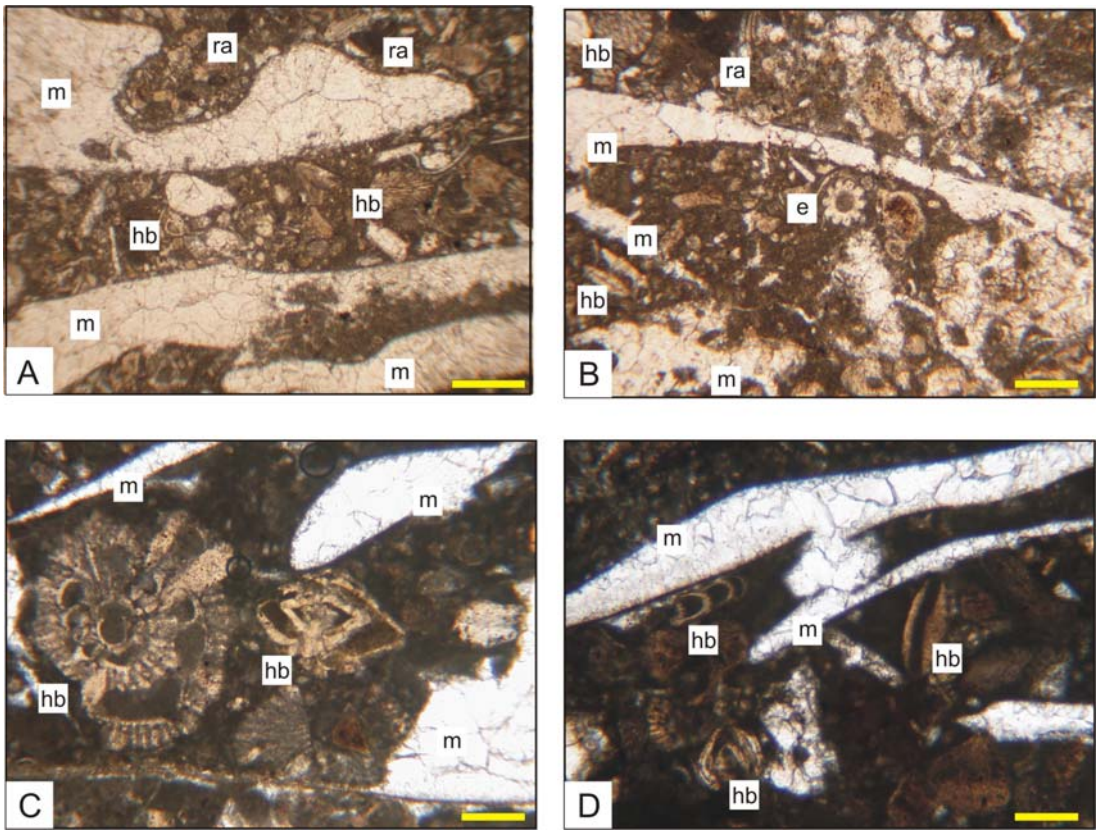

Figure 25. Photomicrographs of the bivalved floatstone (MF 4). (hb: hyaline benthic foraminifera, ra: calcareous red algae, m: mollusk fragment, e: echinodermata spine). **A.** HSE 19. **B.** HSE 19. **C.** HSE 22. **D.** HSE 22. (Scale bar is 0.50 mm for A, 0.25 mm for B-D).

4.1.5 MF 5, Wackestone with Planktonic Organisms

This facies has been described as a yellowish limestone in the field and seen in the lower parts of the measured section in the samples HSE 24-26 (Figure 8). The most important characteristic of the MF 5 is its very fine micritic matrix containing abundant planktonic foraminifera and calcispheres. Besides these planktonic organisms, it also contains hyaline and agglutinated benthic foraminifera, calcareous red algae, mollusk fragments, bryozoans and

echinoderms (Figure 26). This facies is similar with SMF 3 of Flügel (2004). However it is not exactly the same microfacies described (Figure 16). Here, we see planktonic foraminifera in association with algae and benthic foraminifera. Although the number of planktonics increases in this facies benthic large benthic foraminifera like *Helenocyclina* are still common. Deep sea hyaline benthics like *Nodosaria* are also seen in this MF. *Nodosaria* in association with planktonic foraminifers indicate a deeper shelf environment (Geel, 2000). Hence, we may conclude that MF 5 has been deposited in a deeper shelf to slope environment.

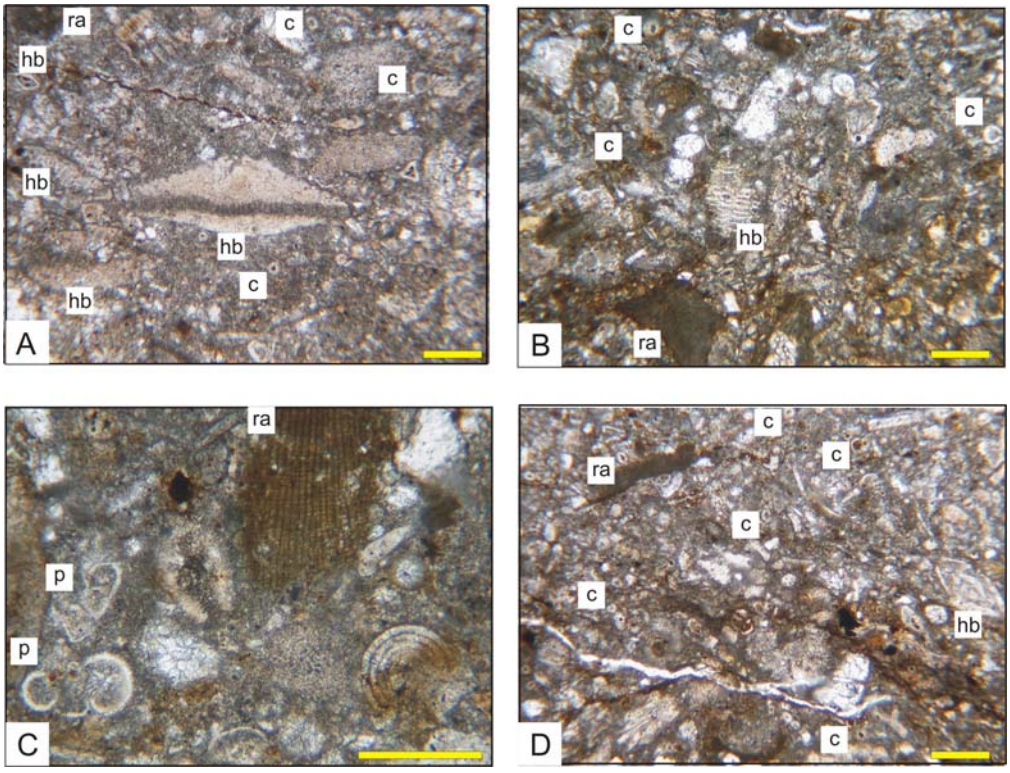

Figure 26. Photomicrographs of the wackestone with planktonic organisms (MF 5). (hb: hyaline benthic foraminifera, p: planktonic foraminifera, ra: calcareous red algae, c: calcisphere). **A.** HSE 24. **B.** HSE 24. **C.** HSE 25. **D.** HSE 25. (Scale bar is 0.25 mm).

4.1.6 MF 6, Quartz-Rich Silty Limestone with Benthic and Planktonic Foraminifera and Calcareous Red Algae

This facies has been described as dark gray marl in the field and seen in the middle part of the measured section in the samples HSE 27-29, and HSE 34-38 (Figure 8). It is quartz-rich and silty however $CaCO_3$ matrix is the dominant constitute. Therefore, the rock has been named as silty limestone. The facies is quite fossiliferous and contains agglutinated benthic foraminifera, hyaline smaller benthic foraminifera, planktonic foraminifera, bryozoan, mollusk fragments, echinoderm spines and red algae (Figure 27). Especially, benthic foraminifera and calcareous red algae are dominant and their sizes are large. The number of the deeper sea smaller benthics like *Nodosaria* increases in the facies relative to its abundance in the older levels in the measured section.

According to the classification made by Mount (1985) the rock can be named as muddy allochems limestone (Figure 15). Because, it has been determined that the amount of carbonates exceeds siliciclastic material, the amount mud-size siliciclastics exceeds sand-size siliciclastics and the amount of allochems exceeds calcite micrite.

Based on textural and compositional properties, it can be concluded that MF 6 has been deposited in proximal outer ramp settings or slope to basin environment. The model established by El Gadi and Brookfield (1999) and the RMF model proposed by Flügel (2004) place the marly facies in the outer ramp settings. Heldt *et al*. (2008) has also defined the silty limestone facies with planktonic and small benthic foraminifera and shell fragments in proximal outer ramp settings.

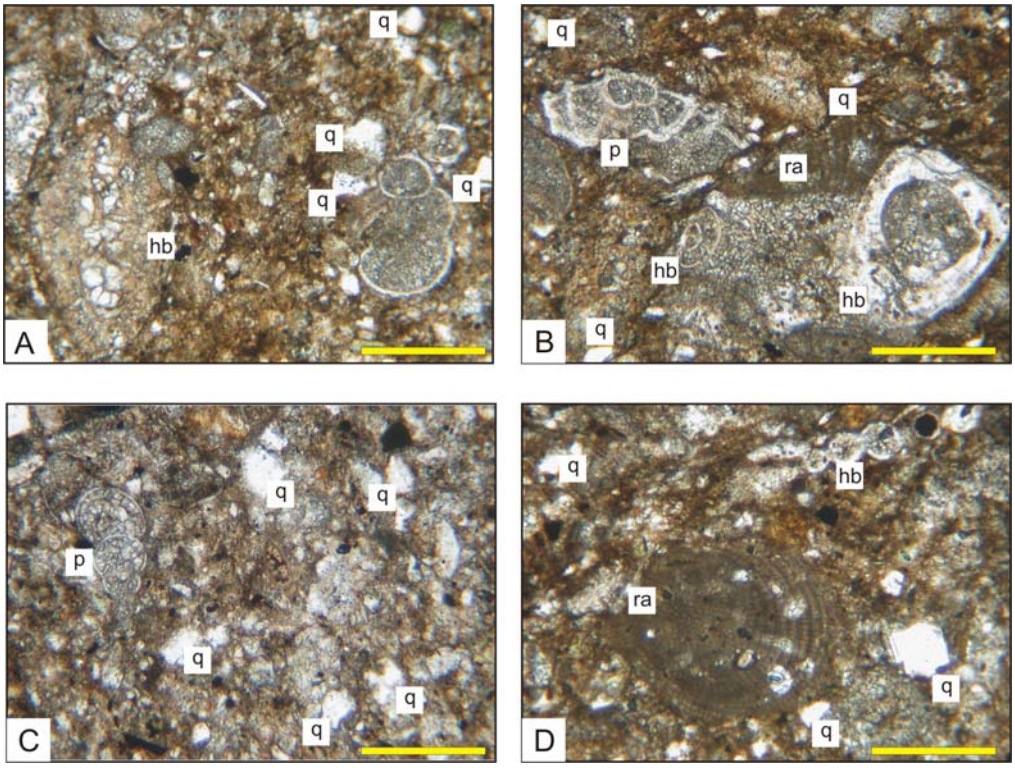

Figure 27. Photomicrographs of quartz-rich silty limestone with benthic and planktonic foraminifera and calcareous red algae (MF 6). (hb: hyaline benthic foraminifera, p: planktonic foraminifera, ra: calcareous red algae, c: calcisphere, q: quartz). **A.** HSE 34. **B.** HSE 34. **C.** HSE 38. **D.** HSE 38. (Scale bar is 0.25 mm).

4.1.7 MF 7, Iron-Rich Silty Marl with Planktonic and Benthic Foraminifera

This facies has been defined in the field as lead to dark gray marl. It is one of the most common MF types in the studied section and has been observed from the Upper Cretaceous sediments towards to the Cretaceous-Paleogene boundary beds in the samples HSE 31-33, HSE 35-37, and HSE 42-47 (Figure 8). Most distinguishable feature of this MF is its very dark color in thin sections (Figure 28). Iron and clay minerals are very rich and most organism shells are filled with iron-oxide minerals. Quartz and feldspar grains are also frequent in the facies. Sizes of quartz grains are usually larger than those of quartz grains seen in the MF 6. Although there are some red algae and other bioclast fragments, MF 7 is rich in smaller benthic and planktonic foraminifera.

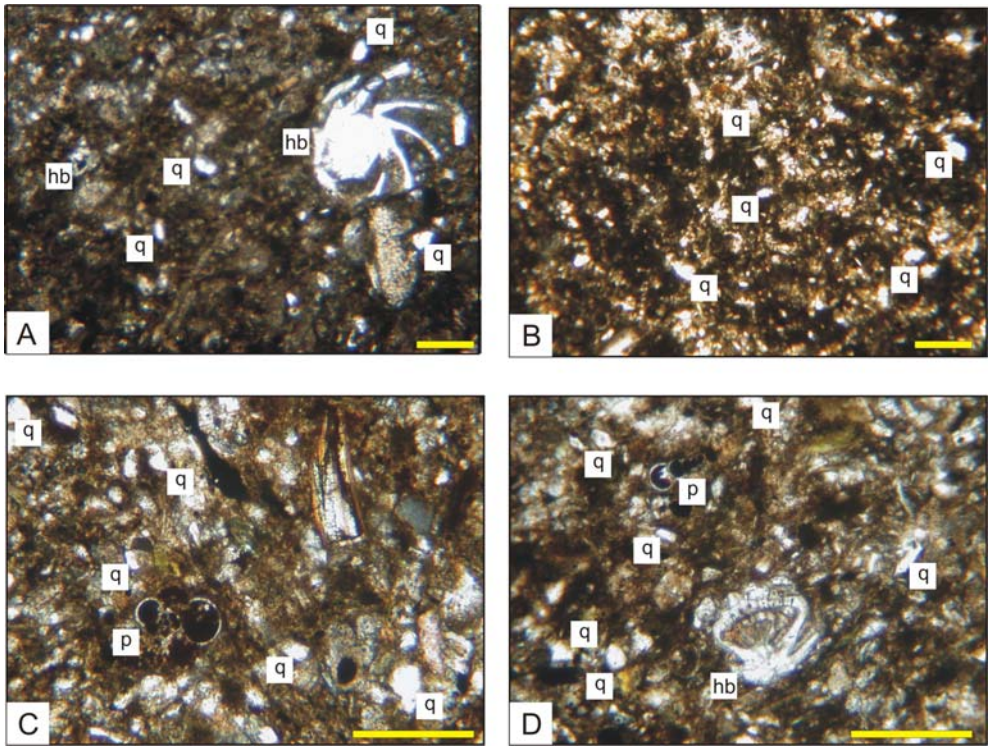

Figure 28. Photomicrographs of the iron-rich silty marl with planktonic and benthic foraminifera (MF 7). (hb: hyaline benthic foraminifera, p: planktonic foraminifera, q: quartz). **A.** HSE 31. **B.** HSE 35. **C.** HSE 37. **D.** HSE 37. (Scale bar is 0.25 mm).

According to the Mount (1985) classification the rocks of this facies can also be named as micritic mudrock (Figure 15). Because, in MF 7 the amount of siliciclastics exceeds carbonate material, the amount mud-size siliciclastics exceeds sand-size siliciclastics and the amount of micrite exceeds allochems. This marly facies is considered to be deposited in outer ramp facies in low energy settings or slope to basin setting when the shelf is an unrimmed, open platform type.

4.1.8 MF 8, Silty Marl with Planktonic and Benthic Foraminifera

This facies has been defined as greenish gray marl and corresponds in general to the uppermost Maastrichtian to lowermost Danian beds. It is seen in the samples HSE 30, HSE 40-41, KTS 1-9, KTS 12, KTS 16-18 and in KTS 27 (Figure 8). MF 8 is quite similar to the MF 7 in terms of its texture and

composition. MF 8 is also in marl character consisting of silt size siliciclastic particles and calcium carbonate matrix. It can also be named as micritic mudrock according to the Mount (1985) classification and rich in planktonic and smaller benthic foraminifera (Figure 29). The main difference between MF 7 and MF 8 is their iron-oxide mineral composition. Although iron minerals are seen in MF 8 they are not as abundant as in MF 7. On the other hand, lithologies in this facies have lighter color. MF 8 has a greenish color most probably due to the enrichments in clay minerals. MF 8 has also been considered as an outer ramp or toe of slope facies.

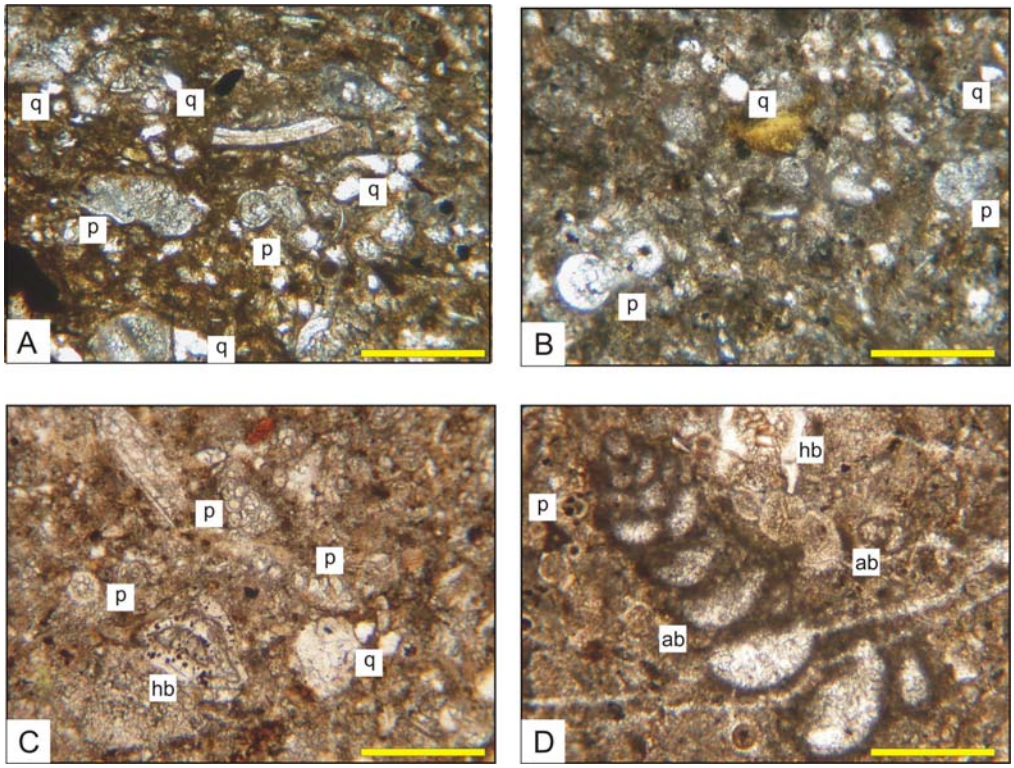

Figure 29. Photomicrographs of the silty marl with planktonic and benthic foraminifera (MF 8). (hb: hyaline benthic foraminifera, ab: agglutinated benthic foraminifera, p: planktonic foraminifera, q: quartz). **A.** HSE 40. **B.** HSE 50. **C.** HSE 55. **D.** HSE 59. (Scale bar is 0.25 mm).

4.1.9 MF 9, Silty Marl with Large Clay Minerals and Spheroid Grains

This facies correspond to the boundary beds in the samples HSE 51=KTS 15 and HSE 52=KTS 16 (Figure 8). In the field no remarkable property of these beds have been observed however in thin sections it has been realized that these beds are quite different in terms of texture and composition. It is a marly unit that has both micritic matrix and silt-size siliciclastic material.

This facies is characterized with benthic and planktonic foraminifera. The large agglutinated non-coiled benthic foraminifera are common. Hyaline deep sea benthic foraminifera displaying various sizes are also present. On the other hand, planktonic foraminifera (Early Danian) in this microfacies are in very small sizes and often filled with iron-oxide minerals. In MF 9 quartz and feldspar grains are very abundant (Figure 30).

Many big, green clay minerals have invaded these beds showing rounded to angular shapes (Figure 31). These clay minerals were so abundant that they have been also hand-picked from the washed residues during the micropaleontological study (Figure 31). The grains are very similar or identical to smectite-glauconite minerals collected from the clay boundary bed just at the Cretaceous/Paleogene boundary in Furlo Section, Italy (http://www.geo.vu.nl/~smit/microkrystites/microkrystites.html) (Figure 31).

In this facies, just above the boundary, some rounded grains of unknown origin have been countered. In washed residue these grains are rounded to ellipsoidal in shape and yellowish in color. Under the microscope they are dark and brownish and probably composed of iron oxide rich material containing some silicate minerals (Figure 32, Figure 33). It has been questioned whether these spheroids might be microtektites, i.e. impact generated spherules found at the Cretaceous-Paleogene boundary in various localities of the world. We have referred to the opinion of Prof. Dr. Gerta Keller at Princeton University, who has various valuable studies related to the Cretaceous/Paleogene boundary, about these objects (Keller, 2001; Keller *et al*., 2003). Through e-mail she has

stated that these spherules have no relation with Chicxulub impact and they might be proto-ooids that form on the seafloor in gently agitated waters. However, we find still problematic to see the presence of such objects nowhere but in boundary beds and think that the origin of these objects should be investigated in further researches. MF 9 is considered to be deposited in a slope to basin environment.

4.1.10 MF 10, Silty Limestone with Planktonic and Benthic Foraminifera

This facies has been observed as yellowish-brownish limestone in the field corresponding to the uppermost Maastrichtian and Paleocene beds. It is in the samples KTS 9-11, KTS 15, KTS 20-26, KTS 28-30, HSE 56, HSE 58, and HSE 60 (Figure 8). It is a limestone with clay minerals and planktonic foraminifera. The Early Paleocene planktonic foraminifera are quite small and often filled with iron minerals. Small hyaline and agglutinated benthic foraminifera in the facies are also present but they are rare when compared to the planktonic species.

This facies can be named as muddy micrite according to the Mount (1985) classification (Figure 15). Because, in this facies the amount of carbonates exceeds siliciclastic material in a great extent, the amount mud-size siliciclastics exceeds sand-size siliciclastics and the amount of calcite micrite exceeds allochems. Based on its textural and compositional properties, MF 10 is considered to be deposited in outer ramp to basin facies in low energy settings. It is deposited most probably very close to the basin. Greater abundance of planktonic foraminifera than that of benthic foraminifera indicates open marine conditions.

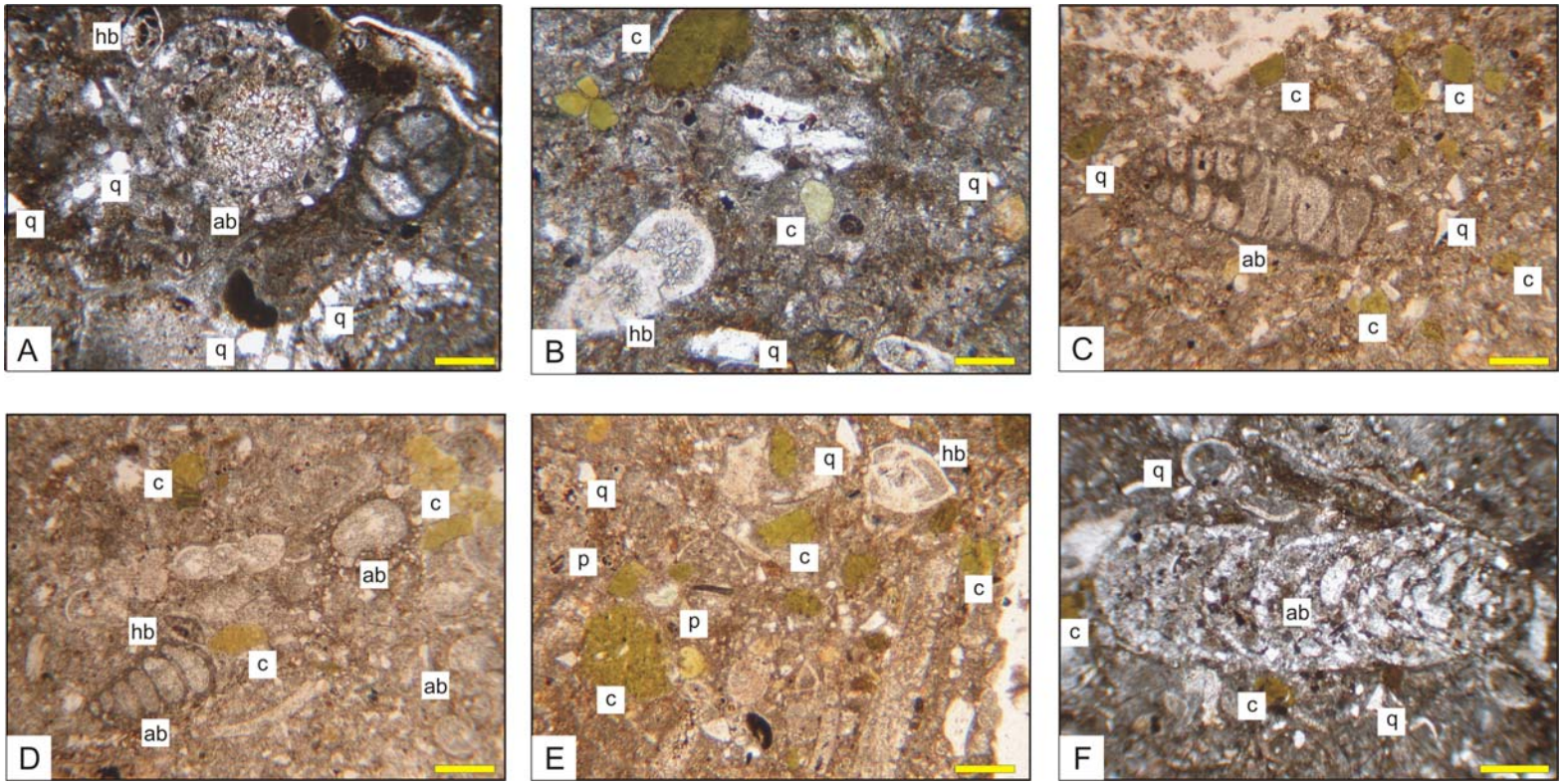

Figure 30. Photomicrographs of the silty marl with large clay minerals and spheroid grains (MF 9). (hb: hyaline benthic foraminifera, ab: agglutinated benthic foraminifera, p: planktonic foraminifera, q: quartz, c: clay minerals). **A.** HSE 51. **B.** HSE 51. **C.** HSE 51. **D.** HSE 51. **E.** HSE 51. **F.** HSE 51. (Scale bar is 0.25 mm for A-E, 0.50 mm for F).

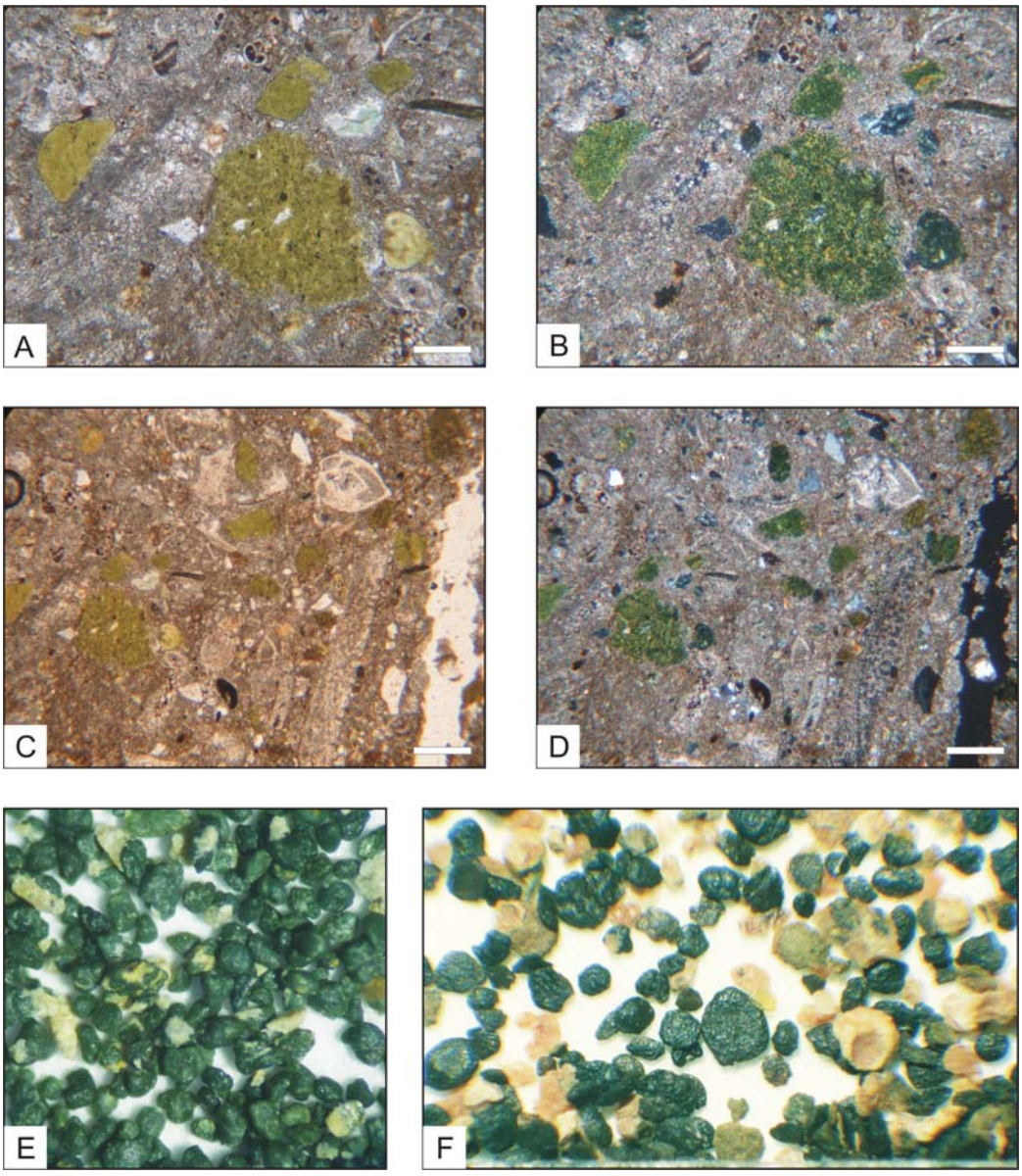

Figure 31. A-D. Thin section photographs of clay minerals just above the K/P boundary in uncrossed and crossed polar (HSE 51), (Scale bar: 0.25 mm). **E.** Binocular microscope photographs of the clay minerals which were hand-picked from the residue of the washed samples (KTS 15). **F.** Clay minerals found just at the K/P boundary in the Furlo section, Italy (http://www.geo.vu.nl/~smit/microkrystites/microkrystites.html).

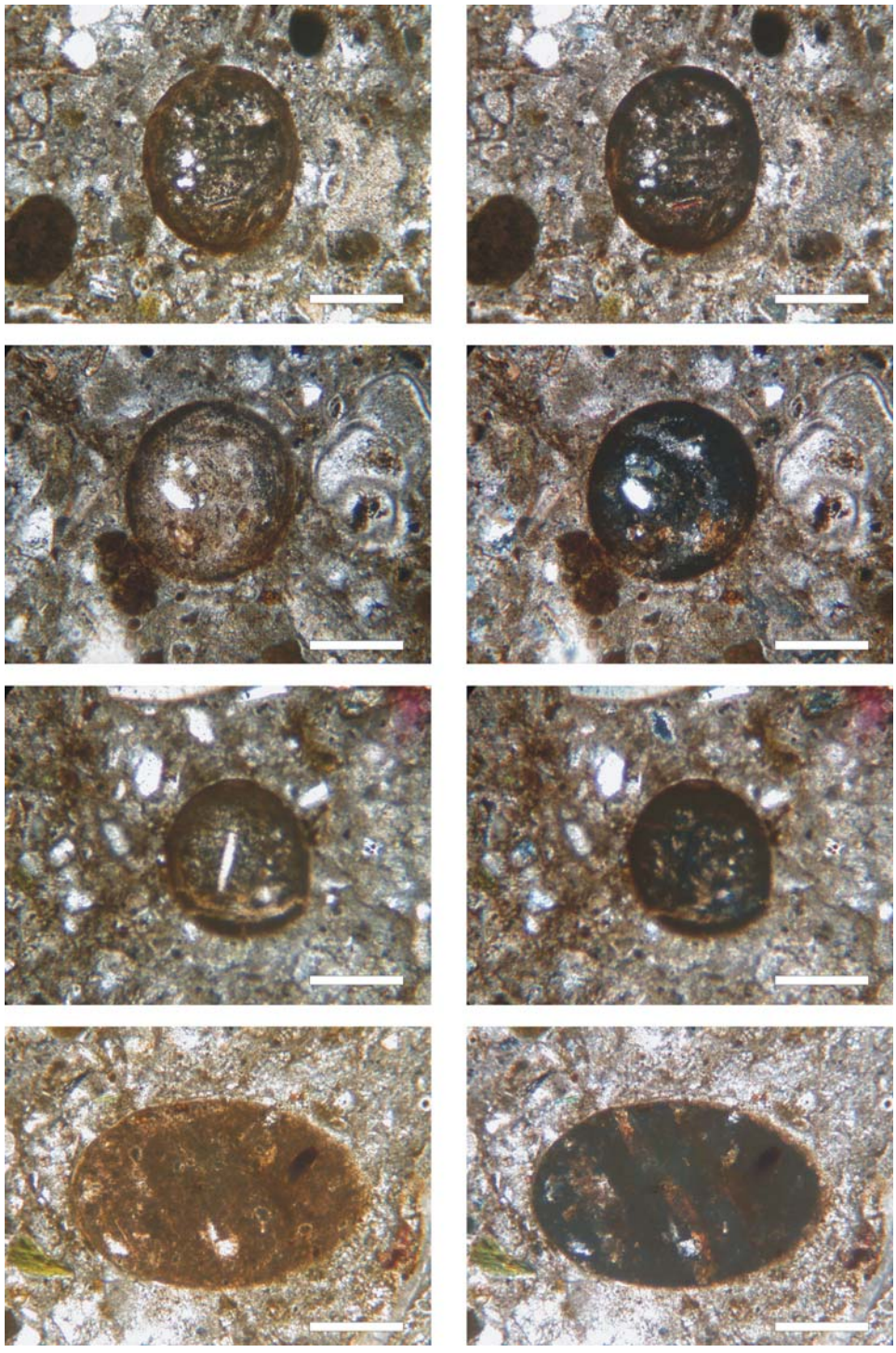

Figure 32. Thin section photographs of spheroid grains in uncrossed and crossed polar. All have taken from the same sample just above K/P boundary (HSE 51), (Scale bar: 0.25 mm).

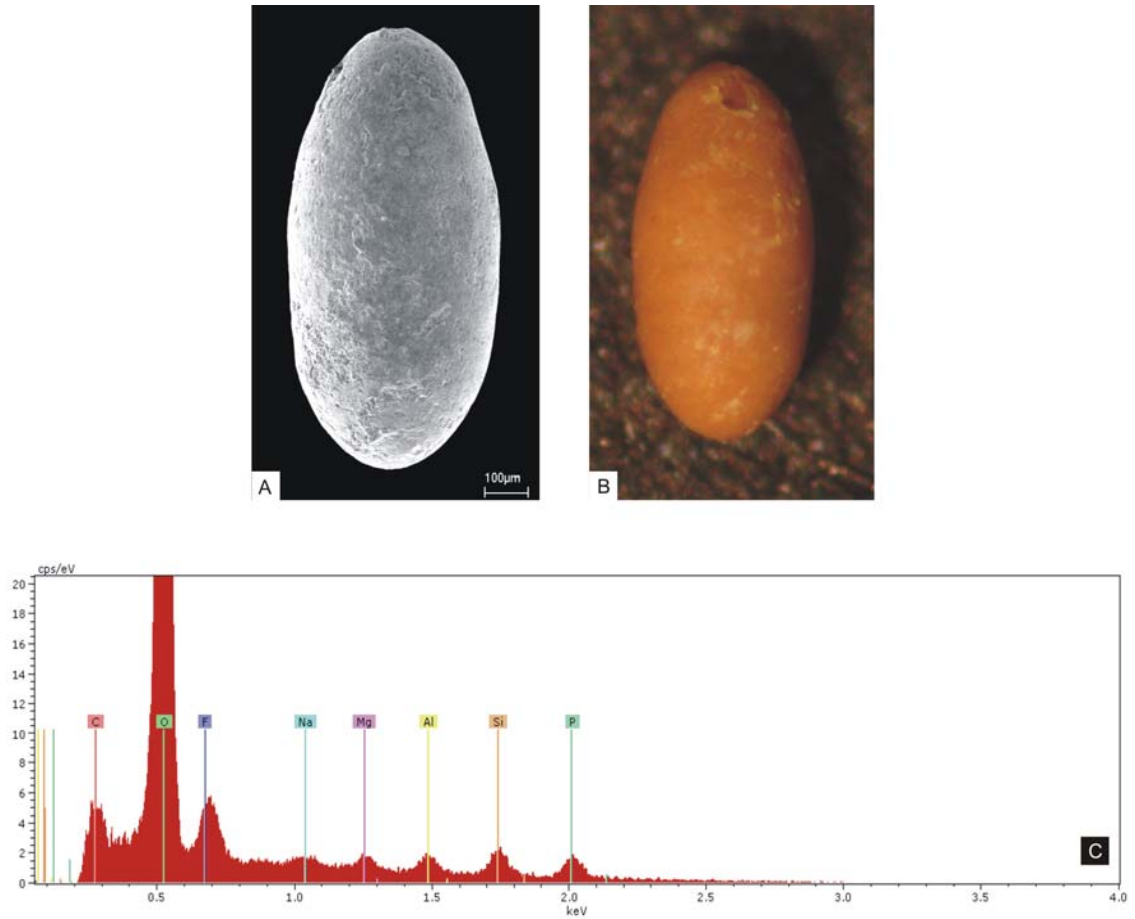

Figure 33. Spheroid grain taken from a sample just at the K/P boundary (KTS 13). **A.** SEM photograph. **B.** binocular microscope photograph **C.** elemental composition of the grain.

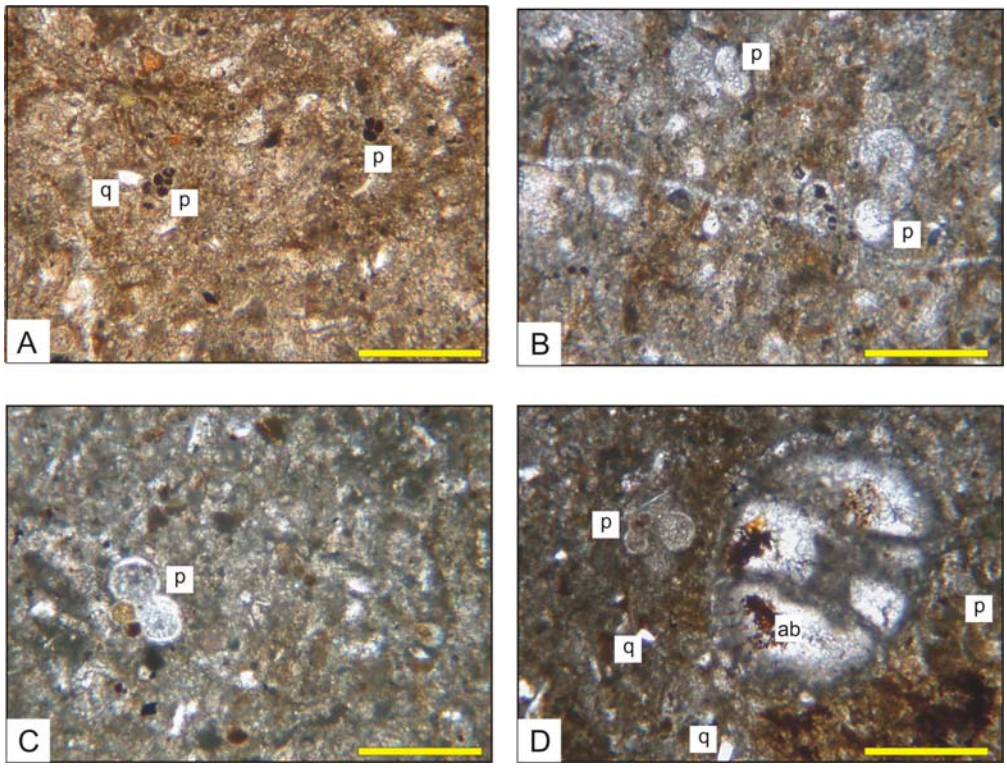

Figure 34. Photomicrographs of the silty limestone with planktonic and benthic foraminifera (MF 10). (ab: agglutinated benthic foraminifera, p: planktonic foraminifera, q: quartz). **A.** HSE 54. **B.** HSE 54. **C.** HSE 60. **D.** HSE 60. (Scale bar is 0.25 mm).

CHAPTER 5

SEQUENCE STRATIGRAPHY

5.1 BACKGROUND ON SEQUENCE STRATIGRAPHY

Sequence stratigraphy is a subdiscipline of stratigraphy evolved in the 1970s from seismic stratigraphy. It is a highly successful exploration technique for the natural resources and used widely by both industry and academic practitioners.

The idea subdividing the depositional sequences into genetically related packages first proposed by Vail *et al*. (1977). Vail *et al*. (1977) and Vail and Mitchum, 1977 used seismic stratigraphy in order to define the depositional sequences. Mitchum *et al*., 1977 has defined a depositional sequence as a stratigraphic unit composed of a relatively conformable succession of genetically related strata and bounded at its top and base by unconformities or their correlative conformities. With this definition they have changed the sequence definition of Sloss (1963), who defined the sequence as an unconformity bounded rock-stratigraphic unit. With this change the meaning of the depositional sequence was narrowed and more specified. Afterwards, in Vail *et al*. (1984) eustatic sea-level changes were emphasized as the controlling mechanism for sequence development. In 1987, Haq *et al*. global sea-level cycle chart was published, which is a great tool in many applications of exploration.

Sequence stratigraphy was introduced initially as a stratigraphic methodology using only the combination of seismic stratigraphy and global sea-level cycle charts. However, Posamentier *et al*. (1988) and Van Wagoner *et al*. (1988) introduced the incorporation of outcrop and well data.

Van Wagoner *et al*. (1988) defined the sequence stratigraphy as the study of rock relationships within a chronostratigraphic framework of repetitive, genetically related strata bounded by surfaces of erosion or nondeposition, or their correlative conformities. Sequence is the fundamental unit of sequence stratigraphy and is subdivided into systems tracts which are composed of depositional systems, i.e. 3-D assemblages of lithofacies (Van Wagoner *et al*., 1988). Systems tracts are defined by stacking patterns of parasequence sets or cycles. According to the Van Wagoner *et al*. (1988), a cycle consists of relatively conformable succession of genetically related beds or bed sets bounded by marine flooding surfaces and their correlative surfaces.

Weimer and Posamentier (1993) compiled some important recent publications and presented new studies related to the siliciclastic sequence stratigraphic concepts and tried to refine the conceptual models. They focused on the application of the sequence stratigraphy in the field of petroleum geology. In 1998, the global eustasy model is widely used for sequence stratigraphic analysis of the European basins (de Graciansky *et al*., 1998).

Although it was initially defined for siliciclastic systems, sequence stratigraphy is also applied to carbonate systems. Sarg (1988) discussed carbonate sequence stratigraphy and cyclicity on carbonate rocks. Biostratigraphy, chronostratigraphy and sedimentology are the disciplines contribute to sequence stratigraphic approach. In 1991, Loucks and Sarg dealt with the developments and the applications of the carbonate sequence stratigraphy and showed the diverse response of carbonate platforms to subsidence, relative changes in sea-level, and the related changes in environment and sediment supply. They have also emphasized the unique responses of carbonates to the tectonic subsidences and sea-level changes. Schlager (2005) is also one of the important publications related to the carbonate sequence stratigraphy. He approached sequence stratigraphy based on the sedimentologic background. Schlager (2005) claimed that carbonate sedimentation, in contrast to siliciclastic sedimentation, is largely governed by

chemistry and biota of the ocean and therefore sequence stratigraphic interpretations should consider all these characteristics of the carbonate systems.

One the most recent studies related to sequence stratigraphy is Coe (2003). In this publication both siliciclastics and carbonates are taken into consideration and theory of the sequence stratigraphy and the mechanism of the sea-level changes are discussed. In 2006, Catuneanu presented all the sequence stratigraphic models and showed how they relate to each other and how their applicability may vary with the case study.

The sequence stratigraphy deals basically with the depositional history of the sequences. The formation of the systems tracts in a depositional sequence is based to the accommodation space available. In other words, the geometry and stacking patterns of the strata are affected by the available place for the sedimentary accumulation. The available place for the sedimentation is determined basically with the relative sea-level changes. Relative sea-level changes are controlled by the combination of the eustatic sea-level changes and the tectonic controls in the sedimentary basins. In order to observe the stacking patterns and determine the systems tracts by using the outcrop data detailed field observations and microfacies analyses are needed. In this study, in order to construct the sequence stratigraphical model of the measured section both the results of the detailed microfacies analyses and field observations were utilized.

5.2 SEQUENCE STRATIGRAPHIC INTERPRETATION

The measured section is composed of basically 3 main sedimentary packages. The first package is composed of carbonate rocks and covers the interval from the sample HSE 1 to HSE 29 (Figure 35). The MF types observed in this package are: bioclastic packstone with large benthic foraminifera and calcareous red algae (MF 1), grainstone with large benthic foraminifera and calcareous red algae (MF 2), bioclastic wackestone-packstone with benthic foraminifera and calcareous red algae (MF 3), bivalved floatstone (MF 4) and

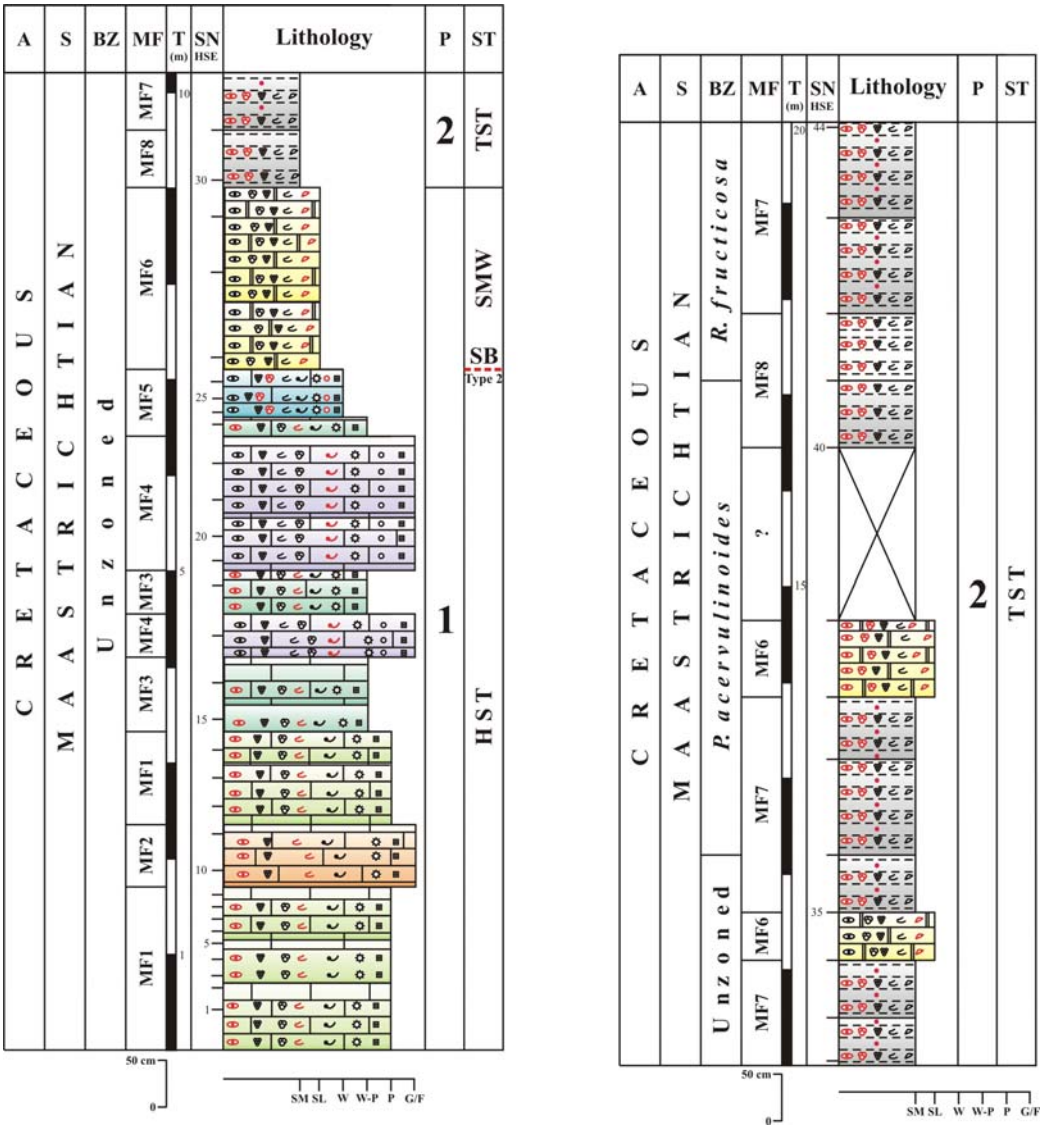

Figure 35. Sequence stratigraphical construction of the measured section showing systems tracts, sedimentary packages and important surfaces.

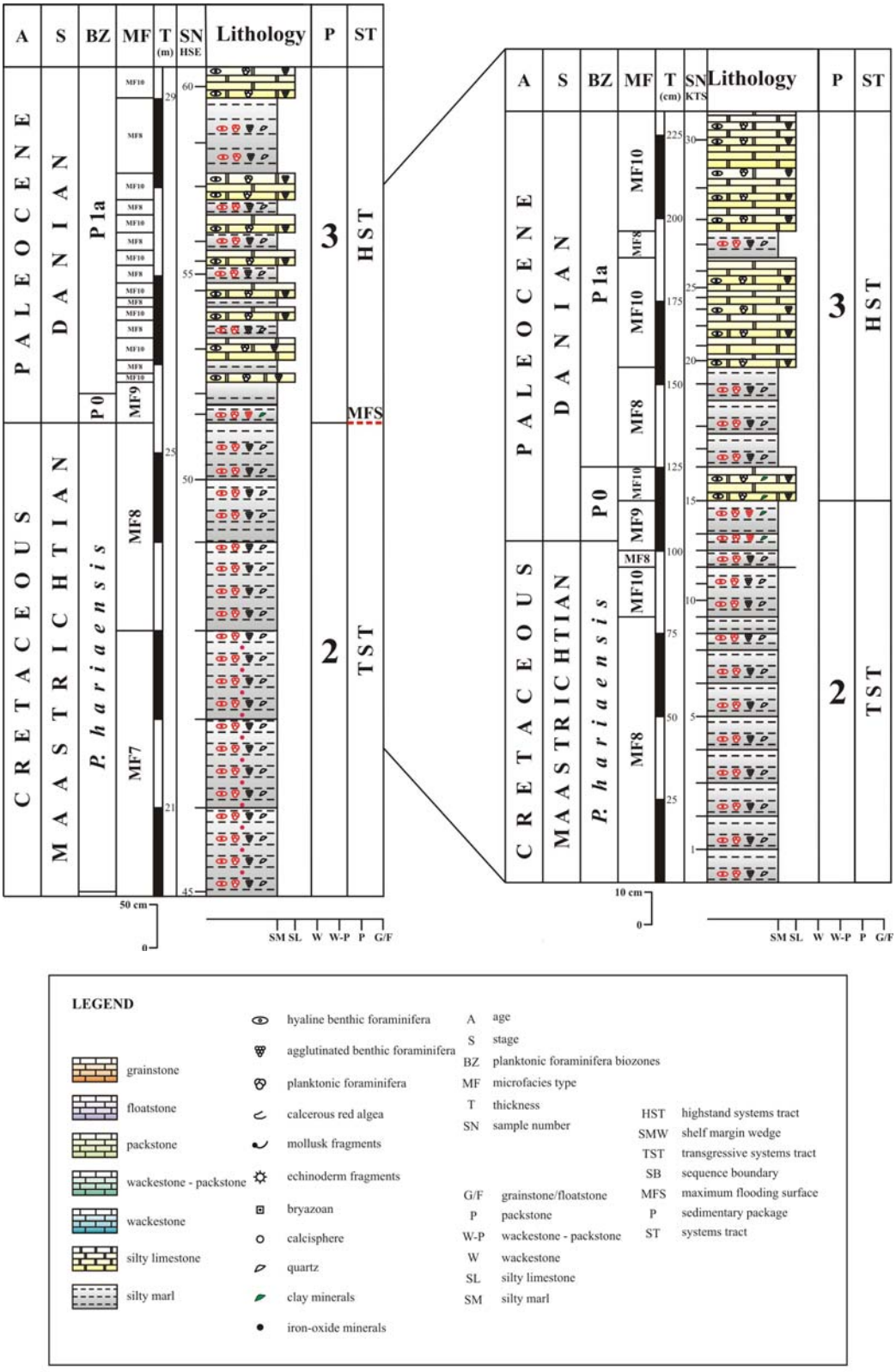

Figure 35. Continued.

wackestone with planktonic organisms (MF 5). The second package is composed of silty limestones and silty marls and covers the interval from the sample HSE 30 to HSE 50 (Figure 35). In this marly sequence, quartz-rich silty limestone with benthic and planktonic foraminifera and calcareous red algae (MF 6), iron-rich silty marl with planktonic and benthic foraminifera (MF 7), silty marl with planktonic and benthic foraminifera (MF 8) are observed. The third package is composed of silty marl (MF 8)-silty limestone (MF 9) alternation and seen between the samples HSE 51 and HSE 60 (Figure 35). In brief, the bottom of the measured section is composed of carbonate rocks (first package), above them a thick marly succession is seen (second package) and at the top again carbonate rocks (third package) are deposited.

The basic approach for the sequence stratigraphic interpretation of the section lies behind the fact that the carbonate rocks have a prograding character into the basin from a carbonate uphill when the accommodation space is getting narrow and there is not enough space for the carbonate growth (Figure 36). Based on this idea, the first carbonate package consisting of mainly packstones and grainstones was deposited during a highstand systems tract (HST). According to the carbonate systems depositional model of Emery and Myers (1996), carbonate grow will be limited by the creation of accommodation. In HST, when the carbonate production exceeds the rate of creation of accommodation space, carbonates are shed off the platform top to the slope and basin. This phase is called 'keep up' (Neumann and Macintyre, 1985). In the keep up phase high energy carbonates like packstones and grainstones are expected to deposit. The deposition of carbonates from a platform or an uphill top to the slope and the basin is referred to as 'highstand shedding' (Emery and Myers, 1996). A carbonate platform tends to shed most sediment during HST as the rate of creation of accommodation declines. In the Haymana basin this carbonate source, which prograded into the basin during highstand systems tracts might be the reefal and algal limestones of the Çaldağ Formation (Ünalan *et al*., 1976) (Figure 36).

Above the carbonate sequence containing packstones, grainstones and wackestones, the top of the MF 5 is interpreted as a sequence boundary (SB) (Figure 35). The SB is at the bottom of the sample HSE 27, where quartz-rich silty limestone (MF 6) starts to deposit. The drastic change from the packstones, grainstones and wackestones to the quartz-rich limestone is an evidence for a SB. With the relative sea-level fall detrital materials reach the slope to basin environment. Since no evidence for subaerial exposure is seen, this SB is considered as a correlative conformity.

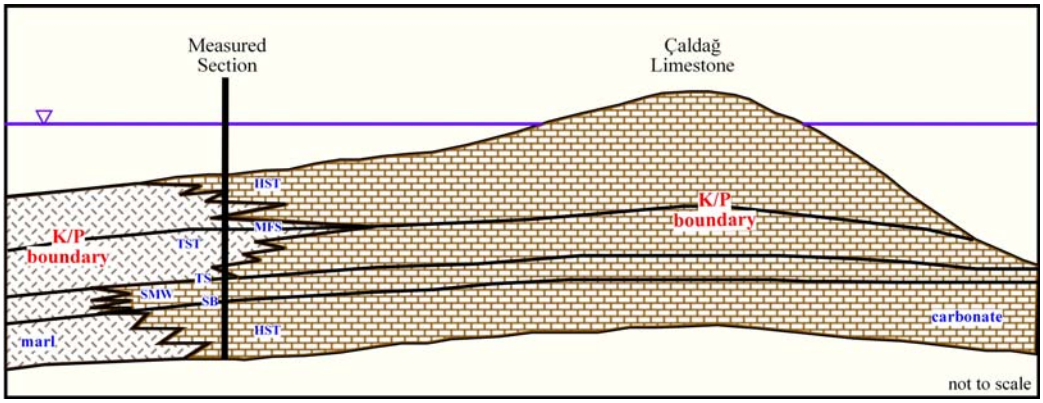

Figure 36. Model showing the sequence stratigraphical interpretation of the measured section.

The type of the SB is determined as a Type 2 SB. A type 2 sequence boundary is marked by a subaerial exposure and a downward shift in coastal onlap landward of the depositional shoreline break; however, it lacks both subaerial erosion associated with stream rejuvenation and a basinward shift in facies (Van Wagoner *et al*., 1988). No coarse-grained sediments indicating stream rejuvenation associated with the lowstand systems tract (LST) are seen in the measured section. On the contrary, the sediments above the SB is silty limestone showing an aggradational pattern and can be associated with a shelf margin wedge (SMW) defined just above the Type 2 sequence boundary facies (Van Wagoner *et al*., 1988). The deposition of the SMW is represented with the

MF 6 which is a silty limestone rich in quartz, planktonic and benthic foraminifera and ammonites.

With the sample HSE 30 silty marls (second package) start in the measured section (Figure 35). The decrease in the carbonate content indicates that the carbonate rocks can not reach the section location anymore where the section is measured (Figure 36). In other words, their progradation ceases, since there is enough accommodation for their growth. This can be associated with a relative sea-level rise and accordingly with the transgressive systems tract (TST). The bottom of the first silty marl sample (HSE 30) can be regarded as a transgressive surface. During the TST a continuous marl deposition is seen with very minor silty limestone depositions (sample HSE 34 and HSE 38) in them (Figure 35). The TST is continues until the level within the samples HSE 50 and HSE 51, namely until the sample KTS 14, which is the first sample of the Danian.

With the sample HSE 51 (=KTS 15) carbonates appear in the measured section (third package) again (Figure 35). That means that in the early Danian highstand shedding started once more indicating a shrinking accommodation space during the latest part of a relative sea-level rise or the earliest part of a relative sea-level fall. Therefore, the carbonate-marl succession in the Early Danian is considered as an early HST (Figure 36).

Based on the defined systems tracts, K/P boundary beds in the Haymana basin were deposited during the transition from the TST to HST, in other words they coincide most probably with a maximum flooding surface (MFS). This result is quite similar with the other K/P boundary localities of the world indicating that the eustatic sea-level control overprints the tectonic controls in the Haymana basin. In the following part of this chapter eustatic sea-level fluctuations at the K/P boundary will be discussed in detail.

5.3 EUSTATIC SEA-LEVEL FLUCTUATIONS AT THE K/P BOUNDARY

Eustatic sea-level fluctuations and their relation with the K/P boundary extinction have been studied by many authors. In the cycle chart by Vail *et al*. (1977) a major eustatic sea-level fall, in the order of 150-200 m, marks the K/P boundary, which is followed by a gradual rise in the early Paleocene. A large number of papers supported the long term sea-level fall or regression at the end of the Cretaceous (Hancock and Kauffman, 1979; Matsumoto 1980; Ekdale and Bromley, 1984; Hultberg and Malmgren, 1986; Peypouquet *et al*., 1986, Speijer and Van Der Zwaan, 1996, de Graciancky *et al*., 1998).

In the revised cycle chart (Haq *et al*. 1987, 1988) a prominent 100 m sea-level fall is situated well below the K/Pg boundary (*G. contusa* zone; sequence boundary age 68 Ma), and is followed by a rapid 75 m eustatic rise. A relatively minor fall (10-20m) marks the uppermost Maastrichtian (*A. mayaroensis* zone; sequence boundary at 67 Ma) and is followed by a 25 m sea-level rise from the K/Pg boundary onwards (Speijer and Van Der Zwaan, 1996) (Figure 37).

Keller and Stinnesbeck (1996) is one of the recent important studies supporting a global review of the sea-level changes across the K/P boundary with quantitative estimates. The stratigraphic sections that they deal with span a wide range of marine environments, from near shore to inner neritic through middle and outer shelf to continental slope and bathyal. They also review the distribution of coarse clastic deposits at the K/P boundary, which were deposited in some shallower water regions. Based on the detailed quantitative studies of benthic and planktonic foraminifera, spores and pollen, dinoflagellates and macrofossils they have proposed a consistent pattern of global sea-level changes (Figure 38). The pattern they proposed suggest that following a major late Maastrichtian fall, there was a rise in sea-level in about the last 50-100 ka of the Maastrichtian, with two short-term lowstands in the early Danian, marked by hiatuses and/or condensed sections. The inferred sea-level changes are consistent in both magnitude and timing, suggesting global control, with only

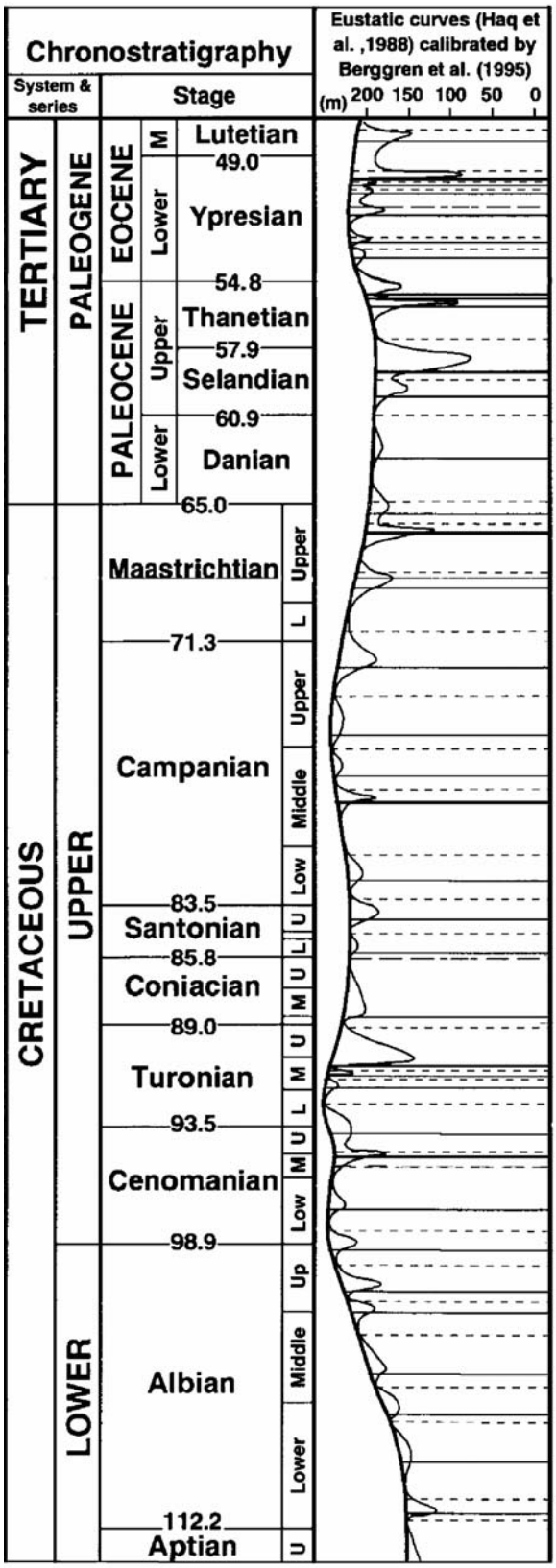

Figure 37. Eustatic sea-level curve proposed by Haq *et al*., 1988 with the calibration of Berggren *et al*., 1995 (taken from Ando, 2003).

minor local tectonic overprint. According to the authors, most continental shelf and slope sections indicate a major sea-level lowstand, often accompanied by hiatuses, in the latest Maastrichtian, about 2-300 ka below the K/P boundary.

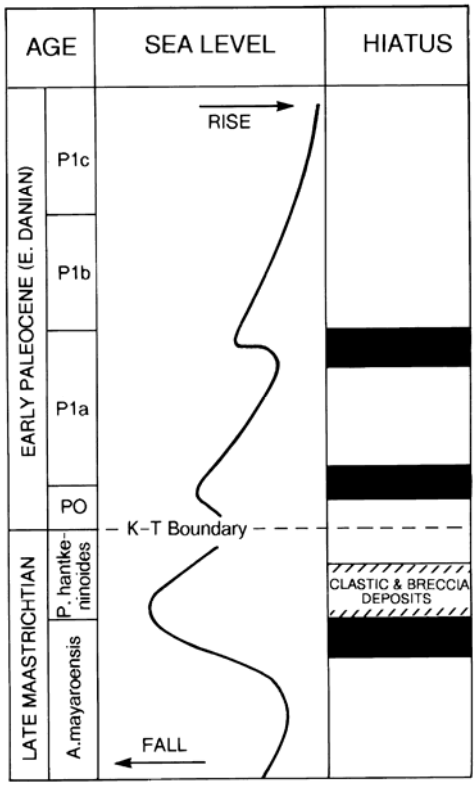

Figure 38. Eustatic sea-level changes across the K/P boundary with the planktonic foraminiferal biozones, simplified from Keller and Stinnesbeck 1996 by Hallam and Wignall (1999).

The curve of Haq *et al.* (1987) compares well with that of Keller and Stinnesbeck (1996) in showing a major latest Maastrichtian fall quickly followed by a rise immediately prior to the K/P boundary. The fall suggested by Haq *et al.*(1987) was greater than anything in the previous 25 million years and the estimated magnitude is close to the of Keller and Stinnesbeck's findings (Hallam and Wignall, 1999) (Figure 37, Figure 38).

Adatte *et al*. (2002) carried out a very important study in five sections (El Melah, El Kef, Elles, Ain Settara and Seldja) in Tunisia and examined the K/P boundary transition. Based on bulk rock and clay mineralogy, biostratigraphy and lithology they defined the sea-level fluctuations. The Tethyan sea-level falls identified by Adatte *et al*. (2002) at 68.9-68.3 Ma, 70.7-70.3 Ma and ~74.2 Ma coincide with major eustatic sea-level falls identified by Haq *et al*. (1987) (Figure 37). Therefore, they suggested that these fluctuations are of eustatic origin. Adatte *et al*. (2002) recognized also the late Maastrichtian seal level low at 65.45 Ma, which is also likely of eustatic origin as indicated by Keller and Stinnesbeck (1996).

In brief, a sea-level transgression marks the end of the Maastrichtian and maximum flooding coincides with the K/P boundary (Donovan *et al*., 1988; Baum and Vail, 1988; Keller and Stinnesbeck, 1996; Stinnesbeck *et al*., 1996; Adatte *et al*., 2002). The basal Danian planktonic foraminiferal zone P0 nearly always consists of grey-black organic-rich clay containing faunas tolerant of oxygen deficiency, which corresponds to the sea-level highstand (Hallam and Wignall, 1999). Since very similar results were obtained in this study, it can be concluded that the eustatic sea-level control overprint the tectonic controls in the Haymana basin.

CHAPTER 6

MICROPALEONTOLOGY

6.1 SAMPLE PREPARATION

Extraction of the foraminifera from the lithified rocks has always been an important phenomenon. There are some basic methods explaining the extraction techniques of the foraminifera in the literature. However these methods need adjustments depending on the facies and the lithology of the section studied. Although, in general similar chemicals are used, the dilution and the amount of the solvents and the time duration of the experiments vary in a large extent. Because there is no unique solution, micropaleontologists should modify the methods and find out the most suitable technique for their samples considering the composition and the preservation of the fossils and the hardness of the enclosing sediment. Finding out the appropriate method might be a very long-lasting and overwhelming task especially for the hard and lithified rocks like limestone.

For the uncemented, loosely consolidated and soft sediments washing and sieving only with tap water might be sufficient. Zepeda (1998), Pardo *et al*. (1999), Arenillas *et al*. (2000), Karoui-Yaakoub *et al*. (2002) and Abramovich *et al*. (2003) and Abramovich and Keller (2003) have used tap water in order to obtain foraminifera from their samples. Nevertheless, if the samples are firmly lithified sieving with water will be ineffective and a disintegration process using chemical solvents will be essential. The harder the sample is, the harsher the preparation treatment required (Green, 2001).

Because of the hardness of the lithologies and the low species abundance of the samples, the extraction of the planktonic foraminifera was especially

difficult in the study area. However, in order to get the best results in terms of the number and the preservation of the individuals a great number of methods in the literature have been utilized and also some new techniques have been improved. Table 3 summarizes all the methods applied in this study.

During this study it has been observed that the amount of residue obtained, amount of fossils found in the residue and quality of the preservation of the forms change greatly based on the method applied. The same sample washed with different techniques gives different results. Therefore most of the samples have been washed more than once applying different methods until finding the finest results. The aim was to improve the number of the fossils obtained and to enhance the preservation quality.

Our studied section consists of marls and limestones. For the marls and limestones diverse methods had to be applied. The most common method used in the extraction of the planktonic foraminifera from the softer sedimentary rocks like shales, claystones and marls is the hydrogen peroxide (H_2O_2) washing technique. For the marly samples we have also applied this method (Table 3). In the H_2O_2 treatment the samples are crushed into pieces and soaked into diluted H_2O_2 solution. Gebhardt (1999), Petrizzo (2000), Arenillas *et al*. (2000, 2006), Karoui-Yaakoub *et al*. (2002), Luciani (2002), Verga and Premoli-Silva (2003), Coccioni *et al*. (2006), Coccioni and Marsili (2007) are some of the studies which used diluted H_2O_2 for the extraction of the foraminifera. Because 35% diluted H_2O_2 was not sufficient to disintegrate our samples 50% diluted H_2O_2 has been used. For the all samples 25 g of rock has been washed. The ratio of the samples to the solution has been fixed to 1:10, i.e. for 25 g of the sample 250 ml H_2O_2 solution has been used. The solvent used should be plentiful enough. In cases where the amount of solvent used to cover the rock fragments is not sufficient, the sample absorbs all the solvent and hardens (Lirer, 2000). Time duration of the experiment has been changed according to the character of the rocks. Because of the stiffness of the rocks, the samples have been left in the H_2O_2 solution at least for 2 days. For most of the marly samples even one week

was essential in order to obtain disintegrated residues (Table 3). It has been also observed that the size of the crushed pieces plays an important role in the disintegration of the rocks. If the rocks are too durable big pieces remained unchanged after the treatment. Therefore the samples have been crushed into very small pieces (2-5 mm^3) in order to obtain more disintegrated residue (Lirer, 2000). Breaking the samples into smaller pieces increases the interaction surface of the sample with the solvent and the disintegration is enhanced.

Shaking the solution during the experiment affects also the degree of breakdown and the time required. Considering this fact we have tried a new technique for the softer marls. The solutions have been shaken during the whole experiment with the help of the magnetic splitters. In the treatments with magnetic splitter 30-60 minutes were enough in order to obtain disintegrated residues. 45 minutes was the optimum time duration for most of the softer marly samples (Table 3). Shaking the solution with the magnetic splitter does not only drop the experiment time, it also prevents the fossils from the damaging affect of the solution reducing the exposure time. After the treatment the disintegrated residues have been washed under running water through the sieves of 425, 250, 125, 63 and 38 microns and dried in an oven at 50° C.

With the diluted H_2O_2 treatment sometimes weak detergents are also used for the extraction of the foraminifera (Pardo *et al*., 1996; Schulte *et al*., 2006). Desogen (a tensio-active chemical product) (Coccioni *et al*., 2006; Coccioni and Marsili, 2007; Luciani, 1997), Calgon (sodium hexametaphosphate) (Keller, 1988; Hart *et al*., 2005) and Quaternary-O (an industrial detergent) (Morris, 1971; Smith and Buzas, 1986) are some of the common products used in the disintegration of the soft sedimentary rocks. They provide the breakdown of the rocks by causing the separation of clay particles. Although it is not that common kerosene is another chemical material used in the disintegration of the carbonate rocks (Said and Kenawy, 1956; Morris, 1971; Nagy and Johansen, 1991; MacLeod *et al*., 2007). Since we have obtained good results from the hydrogen peroxide treatment, we did not try these methods.

Table 3. Applied washing techniques to the different type of lithologies (Best methods obtained are highlighted with orange color).

Lithology	Solvent Type	Time Duration	Magnetic Splitter
Softer Marls	H_2O_2 (50% diluted)	1 day	–
	H_2O_2 (50% diluted)	2 days	–
	H_2O_2 (50% diluted)	3 days	–
	H_2O_2 (50% diluted)	7 days	–
	H_2O_2 (50% diluted)	30 minutes	used
	H_2O_2 (50% diluted)	**45 minutes**	**used**
	H_2O_2 (50% diluted)	60 minutes	used
Harder Marls	H_2O_2 (50% diluted)	1 day	–
	H_2O_2 (50% diluted)	2 days	–
	H_2O_2 (50% diluted)	3 days	–
	H_2O_2 (50% diluted)	**7 days**	–
	H_2O_2 (50% diluted)	30 minutes	used
	H_2O_2 (50% diluted)	45 minutes	used
	H_2O_2 (50% diluted)	60 minutes	used
Limestones	CH_3COOH (50% diluted) with Chloroform	1 hour	–
	CH_3COOH (50% diluted) with Chloroform	2 hours	–
	CH_3COOH (50% diluted) with Chloroform	4 hours	–
	CH_3COOH (50% diluted) with Chloroform	6 hours	–
	CH_3COOH (50% diluted) with Chloroform	8 hours	–
	CH_3COOH (50% diluted) with Chloroform	12 hours	–
	CH_3COOH (50% diluted) with Chloroform	16 hours	–
	CH_3COOH (50% diluted) with Chloroform	24 hours	–
	CH_3COOH (65% diluted) with Chloroform	1 hour	–
	CH_3COOH (65% diluted) with Chloroform	2 hours	–
	CH_3COOH (65% diluted) with Chloroform	4 hours	–
	CH_3COOH (65% diluted) with Chloroform	6 hours	–
	CH_3COOH (65% diluted) with Chloroform	8 hours	–
	CH_3COOH (65% diluted) with Chloroform	12 hours	–
	CH_3COOH (65% diluted) with Chloroform	16 hours	–
	CH_3COOH (65% diluted) with Chloroform	24 hours	–
	CH_3COOH (65% diluted) with Chloroform	2 hours	–
	CH_3COOH (80% diluted)	5 hours	–
	CH_3COOH (80% diluted)	10 hours	–
	80% H_2O_2 (50% diluted) + 20% CH_3COOH (50% diluted)	30 minutes	used
	80% H_2O_2 (50% diluted) + 20% CH_3COOH (50% diluted)	45 minutes	used
	80% H_2O_2 (50% diluted) + 20% CH_3COOH (50% diluted)	60 minutes	used
	70% H_2O_2 (50% diluted) + 30% CH_3COOH (50% diluted)	30 minutes	used
	70% H_2O_2 (50% diluted) + 30% CH_3COOH (50% diluted)	45 minutes	used
	70% H_2O_2 (50% diluted) + 30% CH_3COOH (50% diluted)	60 minutes	used
	60% H_2O_2 (50% diluted) + 40% CH_3COOH (50% diluted)	30 minutes	used
	60% H_2O_2 (50% diluted) + 40% CH_3COOH (50% diluted)	45 minutes	used
	60% H_2O_2 (50% diluted) + 40% CH_3COOH (50% diluted)	60 minutes	used
	50% H_2O_2 (50% diluted) + 50% CH_3COOH (50% diluted)	30 minutes	used
	50% H_2O_2 (50% diluted) + 50% CH_3COOH (50% diluted)	45 minutes	used
	50% H_2O_2 (50% diluted) + 50% CH_3COOH (50% diluted)	**60 minutes**	**used**
	40% H_2O_2 (50% diluted) + 60% CH_3COOH (50% diluted)	30 minutes	used
	40% H_2O_2 (50% diluted) + 60% CH_3COOH (50% diluted)	45 minutes	used
	40% H_2O_2 (50% diluted) + 60% CH_3COOH (50% diluted)	60 minutes	used
	30% H_2O_2 (50% diluted) + 70% CH_3COOH (50% diluted)	30 minutes	used
	30% H_2O_2 (50% diluted) + 70% CH_3COOH (50% diluted)	45 minutes	used
	30% H_2O_2 (50% diluted) + 70% CH_3COOH (50% diluted)	60 minutes	used
	20% H_2O_2 (50% diluted) + 80% CH_3COOH (50% diluted)	30 minutes	used
	20% H_2O_2 (50% diluted) + 80% CH_3COOH (50% diluted)	45 minutes	used
	20% H_2O_2 (50% diluted) + 80% CH_3COOH (50% diluted)	60 minutes	used

Extraction of the foraminifera from the more lithified and harder rocks needs stronger chemicals like acetic acid (CH_3COOH). In our study acetic acid treatment was necessary for limestones (Table 3). There are two important methods utilizing acetic acid in the preparation of the isolated planktonic foraminifera. These are Knitter method (Knitter, 1979) and Lirer method (Lirer, 2000). In the Knitter method, the crushed pieces of the sample is covered with 50-65% of acetic acid and chloroform is added in 1: 1 ratio (for example for 25 g. of sample 25 ml chloroform is added). On the contrary, in the recently proposed Lirer method, samples were processed using a solution with 80% acetic acid and 20% H_2O and the time of disintegration varies from 1-10 hours depending on the lithology. Arenillas *et al*. (2006), Coccioni *et al*. (2006) and Fornaciari *et al*. (2007) are the studies which preferred to use Lirer method. Both acetic acid treatments have been utilized in this study. For the Knitter method different time durations beginning from 1 hour to 24 hours (1, 2, 4, 6, 8, 12, 16, 24 hours) have been tried (Table 3). In order to find out an optimum condition different dilutions (50% and 65%) of the acetic acid have been used with different time intervals. For the Lirer method the dilution of the acetic acid (80%) has not been changed, only various time intervals (2, 5, 10 hours) has been tried. The results of these two methods were similar. For the short experiment times no disintegration has been obtained. On the other hand, if the experiment time is increased it has been seen that the walls of the foraminifers are totally destroyed. Consequently, none of the methods provided successful results.

Since no satisfying results have been obtained from the Knitter and Lirer methods a new technique, which has not been mentioned in the literature yet, has been developed and applied in order to acquire foraminifera from the hard limestone samples. This new washing technique has been developed owing to the personal communication with the Prof. Dr. Mevlüt Ertan, Department of Pharmacy, Hacettepe University. In this method samples of 25 g are broken down into very small pieces (2-5 mm^3) and are soaked into a mixture of 50% diluted H_2O_2 and 50% diluted acetic acid. The ratio of the sample to the solution

is again 1:10, i.e. for 25 g of the sample 250 ml mixture. The mixture is shaken with the help of the magnetic splitter 30-60 minutes. The ratio of the H_2O_2 to the acetic acid in the mixture is one of the most important factors in this method. Based on the hardness of the rocks the ratio of the H_2O_2 to the acetic acid is changed. Several ratios has been tried in order to obtain the best result for different samples (80% acetic acid to 20% H_2O_2, 70% acetic acid to 30% H_2O_2, 60% acetic acid to 40% H_2O_2, 50% acetic acid to 50% H_2O_2, 40% acetic acid to 60% H_2O_2, 30% acetic acid to 70% H_2O_2, 20% acetic acid to 80% H_2O_2) (Table 3). It has been seen that best result is obtained with the ratio 50% of 50% diluted H_2O_2 to 50% of 50% diluted acetic acid in 60 minutes for the most of the limestones. The mixture of 50% of 50% diluted H_2O_2 and 50% of 50% diluted acetic acid has also been tried in the disintegration of the marly samples but the results were not satisfying. After this treatment again the residues were washed under running water through the sieves of 425, 250, 125, 63 and 38 microns and dried in an oven at 50° C.

Extraction of the foraminifera from the lithified limestones has always been difficult. In most of the cases acetic acid treatment is also not successful. For the hard limestones it should be waited for long time intervals in order to acquire disintegration. However during this long time duration the walls of the foraminifera usually get destroyed. Our observations proved that using H_2O_2 with acetic acid together diminishes the destruction effect of the acetic acid up to some level and increases the rate of breakdown. On the other hand, using magnetic splitter enhances the interaction of the sample with the solvent and therefore reduces the experiment time. Because the experiment time is dropped the exposure of the foraminifera to the acetic acid is also reduced. So using the mixture of H_2O_2 and acetic acid as a solvent and shaking the solution with the help of the magnetic splitter is a new and successful method in the preparation of the washed foraminifera species.

In most of the cases disintegration techniques are not sufficient to obtain clean individuals free from the sediments. In such circumstances ultrasonic

treatment is one of the efficient methods. It is used to clean encrusted specimens to assist identification (Luciani, 1997; Zepeda, 1998; Pardo *et al*., 1996 and 1999; Lirer, 2000; Adatte *et al*., 2002b; Abramovich *et al*. 2003; Nielsen and Jakobsen, 2004; Schulte *et al*., 2006). Especially the forms obtained from the H_2O_2 treatment needs cleaning (Lirer, 2000; Nielsen and Jakobsen, 2004). The treatment can be performed with water or with water diluted chemicals like Desogen (Lirer, 2000). Since the obtained species were not clean enough ultrasonic treatment was also completed in our study. Especially for the samples washed with H_2O_2 ultrasonic agitation was essential in order to facilitate identification. The treatment was performed with water and several time durations have been tried. By looking at the degree of the sediment encrustation around the fossils it is determined how much time ultrasonic agitation is required. However while deciding on the duration of the treatment it should be noted that too much agitation might destroy the fossils. In the literature it can be seen that time duration for this treatment is rather variable (10-15 seconds in Canudo (1997) and Pardo *et al*. (1996), 1-3 hours in Lirer (2000)). After applying different time intervals ranging 1-30 minutes it has been seen that 5-7 minutes for the robust Cretaceous forms and 4 minutes for the fragile Paleocene forms are the optimum time durations for our samples. After the treatment the fossils were dried under sunlight. It should be highlighted that the ultrasonic cleaning was very efficient and useful for our samples and eased the identification of the taxa in a great amount.

6.2 SYSTEMATIC TAXONOMY

The systematic taxonomy of the planktonic foraminifera has been carried out analyzing both washed residues and the thin sections of the systematically collected samples. The classification of the planktonic foraminifera is mainly based on the coiling mode, wall structure, peripheral shape, primary and secondary apertures, shape and arrangement of the chambers, sutures, presence or absence of keels, number of keels and ornamentations of the taxa. Because of the poor preservation after the washing treatment it was difficult to observe some properties of the specimens, such as wall structure, umbilical system (tegilla and portici) and apertures. Therefore, our classification is primarily based on the coiling mode; peripheral shape; shape, arrangement and number of the chambers; presence or absence of keels, number of the keels and sutural properties.

The systematic taxonomy of the planktonic foraminifera has been studied by various authors for several decades. Our identifications are based on the most important and most recent taxonomical studies related to the Cretaceous and Paleocene planktonic foraminifera. For the identification of the Cretaceous foraminifera Loeblich and Tappan (1988), Postuma (1971), The Ellis and Messina Catalogue of Foraminifera (1941-2004), Robaszynski *et al*. (1984), Nederbragt (1991) and Premoli-Silva and Verga (2004) have been utilized. In addition to these publications the database in the web site Chronos Portal has been used.

Unless otherwise is stated the stratigraphic ranges given for the Cretaceous foraminifera are based on the studies of Premoli-Silva and Verga (2004) and Nederbragt (1991). However there are some contradictions about the stratigraphic ranges of a few Late Cretaceous forms. It has been discussed whether they are extinct species or K/P boundary survivors. For the stratigraphic ranges of such species different ideas have been presented.

For the Paleocene species, type descriptions in The Ellis and Messina Catalogue of Foraminifera (1941-2004), in the Atlas of Paleocene Planktonic Foraminifera (Olsson *et al*., 1999) and at the web site Chronos Portal have been used. The classification of the Paleocene foraminifera in the Atlas of Paleocene Planktonic Foraminifera prepared by Olsson *et al*. (1999) is mainly based on the wall structure of the species. This type of classification is not applicable unless the specimens are very well preserved. Even if the specimens are very well preserved binocular microscope will not be sufficient to see the details of the wall structure and scanning electron microscope photographs will be necessary. Therefore in order to describe the Paleocene species, similar to what has been done for the Cretaceous species, morphologic features observable under binocular microscope have been used. The global stratigraphic ranges of the Paleocene forms have been given based on the study of Olsson *et al*. (1999). Different ideas about the first and last appearances of the species have also been discussed.

It should be noted that taxonomic work given in this part consists of short portraits of the forms rather than complete descriptions. The remarks of the author explaining the main identification criteria, difficulties encountered during the taxonomical study and suggestions for further studies have been presented and a synonym list comprising the most recent studies has been given.

Order FORAMINIFERIDA EICHWALD, 1830

Suborder GLOBIGERININA DELAGE and HÉROURARD, 1896

Superfamily GLOBOTRUNCANACEA BROTZEN, 1942

Family GLOBOTRUNCANIDAE BROTZEN, 1942

Subfamily GLOBOTRUNCANINAE BROTZEN, 1942

Genus *Globotruncana* CUSHMAN, 1927

Type species: *Pulvinulina arca* CUSHMAN, 1926

***Globotruncana aegpytiaca* NAKKADY, 1950**

Pl. 2, fig. 7, 8

1950. *Globotruncana aegpytiaca* NAKKADY; p. 690, pl. 80, fig. 20.

1956. *Globotruncana aegpytiaca* NAKKADY; SAID and KENAWY, p. 169, pl. 5, fig. 19.

1984. *Globotruncana aegpytiaca* NAKKADY; ROBASZYNSKI *et al*., p. 179, pl. 2, fig.1-6; p. 181, pl. 3, fig. 1-4.

1987. *Globotruncana aegyptiaca* NAKKADY; ÖZKAN and ALTINER, p. 269, pl. 1, fig. 13-15.

1988. *Globoruncana aegyptiaca* NAKKADY; KELLER, p. 250, pl. 1, fig. 6.

1997. *Globotruncana aegyptiaca* NAKKADY; LUCIANI, p. 804, text fig. 3, fig. 4; p. 816, text fig. 8, fig. 5.

1998. *Globotruncana aegyptiaca* NAKKADY; NEDERBRAGT, p. 399, pl .1, fig. 6, 7; p. 401, pl. 2, fig. 1.

1999. *Globotruncana aegyptiaca* NAKKADY; ÖZKAN-ALTINER and ÖZCAN, p. 292, text fig. 4, fig. 11.

2002. *Globotruncana aegyptiaca* NAKKADY; KELLER *et al*., p. 280, pl. 3, fig. 14.

2003. *Globotruncana aegyptiaca* NAKKADY; ABDELGHANY, p. 400, text fig. 9, fig. 6.

2003. *Globotruncana aegyptiaca* NAKKADY; ABRAMOVICH *et al*., p. 14, pl. 5, fig. 8.

2004. *Globotruncana aegyptiaca* NAKKADY; CHACON *et al*., p. 589, text fig. 3, fig. E.

2004. *Globotruncana aegyptiaca* NAKKADY; KASSAB *et al*., p. 432, fig. 3, fig. 1-2.

2004. *Globotruncana aegyptiaca* NAKKADY; PREMOLI-SILVA and VERGA, p. 103, pl. 33, fig. 1-4; p. 240, pl. 10, fig. 4-8.

2007. *Globotruncana aegyptiaca* NAKKADY; DARVISHZAD *et al*., p. 141, pl. 1, fig. 6.

Remarks:

Globotruncana aegyptiaca is identified on the spiral side with its lobate outline, raised and beaded sutures and four chambers in the last whorl increasing rapidly in size. Most distinguishable features of the *G. aegyptiaca* are its asymmetrical profile, with an almost flat spiral side and a convex umbilical side and its double keels present on all chambers. When the latest Maastrichtian globotruncanids are examined it is seen that there are only two forms having double keels and planoconvex appearance with a flat spiral side. These are *G. aegyptiaca* and *Gansserina wiedenmayeri*. *G. aegyptiaca* is differentiated from *G. wiedenmayeri* easily with lesser number of chambers in the last whorl.

Stratigraphic Distribution:

The stratigraphic distribution of *G. aegyptiaca* ranges from the *G. aegyptiaca* zone (Campanian) to the end of the *Abathomphalus mayaroensis* zone (K/P boundary). In our samples this species is very rare and has been encountered from the beginning of the measured section until the K/P boundary.

Globotruncana arca CUSHMAN, 1926

Pl. 1, fig. 1, 2; Pl. 13, fig. 1-4

1926. *Pulvinulina arca* CUSHMAN; p. 23, pl.3, fig.1.

1984. *Globotruncana arca* CUSHMAN; ROBASZYNSKI *et al*., p. 183, pl. 4, fig. 1-3.

1988. *Globotruncana arca* CUSHMAN; KELLER, p. 250, pl. 1, fig. 7, 8, 11.

1998. *Globotruncana arca* CUSHMAN; NEDERBRAGT, p. 401, pl. 2, fig. 2.

1998. *Globotruncana arca* CUSHMAN; ZEPEDA, p. 124, text fig.3, fig. 1-5.

1999. *Globotruncana arca* CUSHMAN; PARDO *et al*., p. 258, pl. 3, fig. 1-4.

2000. *Globotruncana arca* CUSHMAN; ARENILLAS *et al*., p. 208, pl. 1, fig. 3, 4.

2000. *Globotruncana arca* CUSHMAN; PETRIZZO, p. 503, text fig. 17, fig. 2a-c.

2002. *Globotruncana arca* CUSHMAN; KELLER *et al*., p. 280, pl. 3, fig. 13.

2003. *Globotruncana arca* CUSHMAN; ABRAMOVICH *et al*., p. 15, pl. 5, fig.1, 2.

2004. Globotruncana arca CUSHMAN; CHACON *et al*., p. 589, text fig. 3, fig. F.

2004. *Globotruncana arca* CUSHMAN; PREMOLI-SILVA and VERGA, p. 104, pl. 34, fig. 3,4; p.105, pl. 35, fig. 1; p. 240, pl. 10, fig. 11-15; p. 241, pl. 11, fig. 1-4.

2005. *Globotruncana arca* CUSHMAN; BERTLE and SUTTNER, p. 503, text fig. 5, fig. G.

2005. *Globotruncana arca* CUSHMAN; OBAIDALLA, p. 217, pl. 2, fig. 1, 2.

2007. *Globotruncana arca* CUSHMAN; BABAZADEH *et al*., p. 452, text fig. 6, fig. 1.

2007. *Globotruncana arca* CUSHMAN; DARVISHZAD *et al*., p. 141, pl. 1, fig. 15.

Remarks:

The spiral side *Globotruncana arca* has a lobate to subcircular outline with 6-7 chambers increasing moderately in size and in general its early sutures are more raised and beaded than the later ones. Very well developed double keel is easily distinguishable in lateral as well as in umbilical views. The inequally biconvex appearance, high trochospire, curved and U-shaped sutures and well developed adumbilical ridges on the umbilical side are the most important features used in the identification of the *G. arca*. *G. arca* is very similar to *G. mariei* and *G. orientalis*. It is differentiated from *G. mariei* with its slower increase in chamber size and greater number of chambers in the last whorl. Double keel is also marked easier in *G. arca* than in *G. mariei*. It is differentiated from *G. orientalis* with its wider spaced keels and often more curved and more beaded sutures on the spiral side. However, for some of the individuals it is really difficult to distinguish between *G. arca* and *G. orientalis*.

Stratigraphic Distribution:

The stratigraphic distribution of *G. arca* ranges from the *Dicarinella asymetrica* zone (Santonian) to the end of the *Abathomphalus mayaroensis* zone (K/P boundary). It is one of the most common species in the studied material and has been identified from the beginning of the measured section until the first sample of the Danian.

Globotruncana dupeublei CARON, GONZALEZ DONOSO, ROBASZYNSKI and WONDERS, 1984

Pl. 2, fig. 6

1984. *Globotruncana dupeublei* CARON *et al*.; pl. 7, fig. 1.

1984. *Globotruncana dupeublei* CARON *et al*.; ROBASZYNSKI *et al*., p. 189, pl. 7, fig. 1-2.

1987. *Globotruncana dupeublei* CARON *et al*.; ÖZKAN and ALTINER, p. 269, pl. 1, fig. 1-3.

1997. *Globotruncana dupeublei* CARON *et al*.; LUCIANI, p. 816, text fig. 8, fig. 7.

1998. *Globotruncana dupeublei* CARON *et al*.; ZEPEDA, p. 125, text fig. 4, fig. 3.

1999. *Globotruncana dupeublei* CARON *et al*.; ÖZKAN-ALTINER and ÖZCAN, p. 292, text fig. 4, fig. 7.

2002. *Globotruncana dupeublei* CARON *et al*.; KELLER *et al*., p. 280, pl. 3, fig. 7, 8.

2004. *Globotruncana dupeublei* CARON *et al*.; PREMOLI-SILVA and VERGA, p. 106, pl. 36, fig. 1, 2.

Remarks:

Globotruncana dupeublei is identified with its large number of chambers in the last whorl. It has usually 7-9 trapezoidal to rectangular chambers showing very slow increase rate in size. It has variable trochospire height and can be equally biconvex to umblico-convex. One-keeled *G. dupeublei* differs from *G. esnehensis* in having distinctly slower increase in chamber size. With its peripheral outline, chamber size in the last whorl and similar trochospire height *G. dupeublei* is very similar to *G. falsostuarti*. However *G. dupeublei* owns a single keel, while *G. falsostuarti* has double keels.

Stratigraphic Distribution:

The stratigraphic distribution of *G. dupeublei* ranges from the *Gansserina gansseri* zone (Late Campanian-Early Maastrichtian) to the end of the *Abathomphalus mayaroensis* zone (K/P boundary). In this study *G. dupeublei* has been very rarely recorded (only in two samples in the *P. hariaensis* zone).

Globotruncana esnehensis NAKKADY, 1950

Pl. 2, fig. 9

1950. *Globotruncana arca* CUSHMAN var. *esnehensis* NAKKADY; p. 690, pl. 90, fig. 23-26.

1956. *Globotruncana esnehensis* NAKKADY; SAID and KENAWY, p. 169, pl. 5, fig. 21.

1984. *Globotruncana esnehensis* NAKKADY; ROBASZYNSKI *et al*., p. 193, pl. 9, fig. 1-4.

1987. *Globotruncana esnehensis* NAKKADY; ÖZKAN and ALTINER, p. 275, pl. 5, fig. 1, 2, 10.

2004. *Globotruncana esnehensis* NAKKADY; PREMOLI-SILVA and VERGA, p. 106, pl. 36, fig. 3, 4.

2007. *Globotruncana esnehensis* NAKKADY; DARVISHZAD *et al*., p. 141, pl. 1, fig. 2.

Remarks:

Globotruncana esnehensis is another single-keeled species under the genus *Globotruncana*. It has spiro-convex appearance with a trochospire of moderate height and raised and beaded sutures. It is distinguished from the single-keeled *G. dupeublei* with its rapidly increasing chamber size and more convex spiral side. In most of the G. *esnehensis* species the single keel is missing on the first chamber of the last whorl. It is distinguishable for *G. esnehensis*, however difficult to notice.

Stratigraphic Distribution:

The stratigraphic distribution of *G. esnehensis* ranges from the *G. aegyptiaca* zone (Campanian) to the end of the *Abathomphalus mayaroensis* zone (K/P boundary). In this study it is rather rare and has been identified in the *P. hariaensis* zone.

Globotruncana falsostuarti SIGAL, 1952

Pl. 13, fig. 10-12

1952. *Globotruncana falsostuarti* SIGAL; p. 43, text fig. 46.

1984. *Globotruncana falsostuarti* SIGAL; ROBASZYNSKI *et al*., p. 195, pl. 10, fig. 1-3.

2004. *Globotruncana falsostuarti* SIGAL; CHACON *et al*., p. 589, text fig. 3, fig. G.

2004. *Globotruncana falsostuarti* SIGAL; PREMOLI-SILVA and VERGA, p. 107, pl. 37, fig. 1, 2; p. 241, pl. 11, fig. 13-15; p. 242, pl. 12, fig. 1-6.

2007. *Globotruncana falsostuarti* SIGAL; DARVISHZAD *et al*., p. 141, pl. 1, fig. 12.

Remarks:

One of the most characteristic features of the *Globotruncana falsostuarti* is its large number of chambers in the final whorl. It possesses 7-8 petaloid chambers in the last whorl increasing slowly in size. Another important property of *G. falsostuarti* is the manner of joining of sutures. It has also raised and beaded sutures like the other *Globotruncana* forms but sutures join at acute angles, sometimes at right angles at the end of the last whorl. It resembles *G. dupeublei* but differs from it in its double-keeled profile and the acute mode of joining of sutures.

Stratigraphic Distribution:

The stratigraphic distribution of *G. falsostuarti* ranges from the *Globotruncana ventricosa* zone (Campanian) to the end of the *Abathomphalus mayaroensis* zone (K/P boundary). In this study it has been observed in the *P. hariaensis* zone.

Globotruncana hilli PESSAGNO, 1967

Pl. 13, fig. 7-9

1967. *Globotruncana hilli* PESSAGNO; p. 343, pl. 64, fig. 9-14.

2000. *Globotruncana hilli* PESSAGNO; PETRIZZO, p. 503, text fig. 18, fig. 3.

2004. *Globotruncana hilli* PESSAGNO; PREMOLI-SILVA and VERGA, p. 107, pl. 37, fig.3, 4; p. 242, pl. 12, fig. 7-12.

Remarks:

Globotruncana hilli is identified with its 5 chambers in the last whorl and beaded sutures on the spiral side. The nature and position of its double keel help us to differentiate this form from the other globotruncanids. Its chambers in the early whorls and several chambers of the posterior part of the final whorl are spherical and lack double keel; whereas remaining chambers forming anterior part of the final whorl are abruptly truncated peripherally by wide double keel of *Globotruncana linneiana* type.

Stratigraphic Distribution:

The stratigraphic distribution of *G. hilli* ranges from the *Globotruncana ventricosa* zone (Campanian) to the end of the *Abathomphalus mayaroensis* zone (close to the K/P boundary). In this study it has been identified in the *P. hariaensis* zone until the K/P boundary.

Globotruncana mariei BANNER and BLOW, 1960

Pl. 12, fig. 3-5; Pl. 13, fig. 5, 6

1960. *Globotruncana mariei* BANNER and BLOW; pl. 11, figs.6.

1984. *Globotruncana mariei* BANNER and BLOW; ROBASZYNSKI *et al.*, p. 205, pl. 15, figs. 1-6.

1987. *Globotruncana mariei* BANNER and BLOW; ÖZKAN and ALTINER, p. 271, pl. 2, figs. 13-15.

2004. *Globotruncana mariei* BANNER and BLOW; PREMOLI-SILVA and VERGA, p. 110, pl. 40, fig.1-3; p. 244, pl. 14, fig. 1.

Remarks:

Globotruncana mariei is distinguished with its double-keeled biconvex profile and few chambers. It has 4-5 chambers in the last whorl and chambers increase considerably rapidly in size as added. This high rate of increase in chamber size helps to distinguish this form from *G. arca* and *G. orientalis*. Its trochospire is also lower than *G. arca* and *G. orientalis*. It is differs from *Globotruncana rosetta* in the presence of two keels on all chambers and often more convex spiral side.

Stratigraphic Distribution:

The stratigraphic distribution of *G. mariei* ranges from the beginning of the *Globotruncanita elevata* zone (Campanian) to the uppermost part of the *Abathomphalus mayaroensis* zone (Late Maastrichtian). In this study *G. mariei* is one of the common forms and has been identified from the *P. acervulinoides* zone to the upper part of the *P. hariaensis* zone.

***Globotruncana orientalis* EL NAGGAR, 1966**

Pl. 1, fig. 3-5; Pl. 2, fig. 1, 2

1966. *Globotruncana orientalis* EL NAGGAR; p. 125, pl. 12, fig. 4.

1984. *Globotruncana orientalis* EL NAGGAR; ROBASZYNSKI *et al*., p. 207, pl. 16, fig. 1-3; p. 209, pl 17, figs 1-4.

1987. *Globotruncana orientalis* EL NAGGAR; ÖZKAN and ALTINER, p. 271, pl. 2, fig. 4-6.

1997. *Globotruncana orientalis* EL NAGGAR; LUCIANI, p. 816, text fig. 8, fig. 8.

1999. *Globotruncana orientalis* EL NAGGAR; ÖZKAN-ALTINER and ÖZCAN, p. 292, text fig. 4, fig. 6.

2000. *Globotruncana orientalis* EL NAGGAR; PETRIZZO, p. 503, text fig. 17, fig. 3.

2003. *Globotruncana orientalis* EL NAGGAR; ABDELGHANY, p. 400, text fig. 9, fig. 7.

2003. *Globotruncana orientalis* EL NAGGAR; ABRAMOVICH *et al*., p. 15, pl. 5, fig. 7.

2004. *Globotruncana orientalis* EL NAGGAR; PREMOLI-SILVA and VERGA, p. 110, pl. 40, fig. 4; p. 111, pl. 41, fig. 1, 2; p. 244, pl. 14, fig. 2-9.

Remarks:

Globotruncana orientalis is identified with its double keels and moderately high trochospire. It has a slightly lobate to subcircular outline, 5-7 chambers in the last whorl, raised and beaded sutures on the spiral side and well developed adumbilical ridges on the umbilical side. With the all above explained features it resembles *G. arca* in a great extent. However, it differs from it in its closely-spaced keels, in its less lobate periphery and its more raised and noticeable sutures on the spiral side.

Stratigraphic Distribution:

The stratigraphic distribution of *G. orientalis* ranges from the middle part of the *Globotruncanita elevata* zone (Campanian) to the uppermost part of the *Abathomphalus mayaroensis* zone (Late Maastrichtian). *G. orientalis* is one of the most frequent keeled forms in this study and has been identified in the *P. hariaensis* zone until the first sample of the Danian.

Genus *Globotruncanita* REISS, 1957

Type species: *Rosalina stuarti* DE LAPPARENT, 1918

Globotruncanita angulata TILEV, 1951

Pl. 3, fig. 2, 3; Pl. 13, fig. 28

1951. *Globotruncanita lugeoni* TILEV var. *angulata* TILEV; p. 46, pl. 3, fig. 1, 13.

1984. *Globotruncanita angulata* TILEV; ROBASZYNSKI *et al*., p. 221, pl. 23, fig. 1-5.

1998. *Globotruncana angulata* TILEV; ZEPEDA, p. 125, text fig. 4, fig. 2.

2003. *Globotruncanita angulata* TILEV; ABRAMOVICH *et al*., p. 15, pl. 5, fig. 9.

2004. *Globotruncanita angulata* TILEV; PREMOLI-SILVA and VERGA, p. 115, pl. 45, fig. 1, 2; p. 247, pl. 17, fig. 1-5.

2007. *Globotruncanita angulata* TILEV; DARVISHZAD *et al*., p. 141, pl. 1, fig. 8.

Remarks:

Globotruncanita angulata is one of the single-keeled umbilico-convex forms. It differs from *Gansserina gansseri* in the well developed adumbilical ridges and trapezoidal chambers in the spiral side. *G. angulata* also differs from *G. pettersi* in having more trapezoidal chambers on the spiral side and a less lobate outline due its slower increase in chamber size.

Stratigraphic Distribution:

The stratigraphic distribution of *G. angulata* ranges from the end of the *G. aegyptiaca* zone (Late Campanian) to the end of the *Abathomphalus*

mayaroensis zone (K/P boundary). In this study *G. angulata* has been observed from the *P. acervulinoides* zone to the middle part of the *P. hariaensis* zone.

Globotruncanita conica WHITE, 1928

Pl. 13, fig. 16, 17

1928. *Globotruncana conica* WHITE; p. 285, pl. 38, fig. 7.
1984. *Globotruncanita conica* WHITE; ROBASZYNSKI *et al*., p. 227, pl. 26, fig. 1-3.
2003. *Globtruncanita conica* WHITE; ABDELGHANY, p. 400, text fig. 9, fig.11.
2004. *Globotruncanita conica* WHITE; CHACON *et al*., p. 589, text fig. 3, fig. J.
2004. *Globotruncanita angulata* TILEV; PREMOLI-SILVA and VERGA, p. 116, pl. 46, fig. 2-4; p. 247, pl. 17, fig. 7-13.
2005. *Globotruncanita conica* WHITE; OBAIDALLA, p. 217, pl. 2, fig. 4, 5.

Remarks:

Globotruncanita conica can easily be identified with its almost circular outline, very strongly convex spiral side and trapezoidal to rectangular chambers on the spiral side. With its single keel it can be differentiated from *Contusotruncana* forms. This form has been initially classified under the genus *Globotruncanita* by Robaszynski *et al*. (1984) for the reason that its umbilical system is composed of portici. However, it is very difficult to observe this feature in our samples.

Stratigraphic Distribution:

The stratigraphic distribution of *G. conica* ranges from the *Gansserina gansseri* zone (Late Campanian-Early Maastrichtian) to the end of the

Abathomphalus mayaroensis zone (K/P boundary). In this study, it has been identified from the *P. acervulinoides* zone to the *P. hariaensis* zone.

Globotruncanita pettersi GANDOLFI, 1955

Pl. 13, fig. 4

1955. *Globotruncana* (*Globotruncana) rosetta* CARSEY subsp. *pettersi* GANDOLFI; p. 68, pl.6, fig. 3.
1984. *Globotruncanita pettersi* GANDOLFI; ROBASZYNSKI *et al*., p. 233, pl. 29, fig. 1-5.
1987. *Globotruncanita pettersi* GANDOLFI; ÖZKAN and ALTINER, p. 273, pl. 3, fig. 1-3.
1999. *Globotruncanita pettersi* GANDOLFI; ÖZKAN-ALTINER and ÖZCAN, p. 294, text fig. 5, fig. 5.
2004. *Globotruncanita pettersi* GANDOLFI; PREMOLI-SILVA and VERGA, p. 117, pl. 47, fig. 3, 4; p. 118, pl. 48, fig. 1; p. 248, pl. 18, fig. 11-12.

Remarks:

Globotruncanita pettersi has a distinctly asymmetrical profile; spiral side flat to slightly convex; umbilical side strongly convex. With its single-keeled and umbilico-convex profile it resembles *G. angulata*. However, it differs from it in having more elongated chambers in the last whorl and more lobate outline. The umbilical side of *G. pettersi* is also more convex than *G. angulata*. *G. pettersi* has also well developed adumbilical ridges which make us easier to differentiate it from *Gansserina gansseri*.

Stratigraphic Distribution:

The stratigraphic distribution of *G. pettersi* ranges from the *Gansserina gansseri* zone (Late Campanian-Early Maastrichtian) to the end of the

Abathomphalus mayaroensis zone (K/P boundary). In this study it has been identified below the *P. acervulinoides* zone until the K/P boundary.

***Globotruncanita stuarti* de LAPPARENT, 1918**

Pl. 3, fig. 5; Pl. 13, fig. 18-19

1918. *Rosalina stuarti* de LAPPARENT; p. 11, text fig. 4, lower 3 figures.
1984. *Globotruncanita stuarti* de LAPPARENT; ROBASZYNSKI *et al*., p. 235, pl. 30, fig. 1-3; p. 237, pl. 31, fig. 1-3.
1987. *Globotruncanita stuarti* de LAPPARENT; ÖZKAN and ALTINER, p.273, pl. 3, fig. 4-6.
1988. *Globotruncana stuarti* de LAPPARENT; KELLER, p. 250, pl. 1, fig. 4.
1997. *Globotruncanita stuarti* de LAPPARENT; LUCIANI, p. 804, text fig. 3, fig. 11, 12.
1998. *Globotruncanita stuarti* de LAPPARENT; NEDERBRAGT, p. 403, pl. 3, fig. 2-4.
1999. *Globotruncanita stuarti* de LAPPARENT; ÖZKAN-ALTINER and ÖZCAN, p. 292, text fig. 4, fig. 8.
2002. *Globotruncanita stuarti* de LAPPARENT; KELLER *et al*., p. 280, pl. 3, fig. 9-11.
2003. *Globotruncanita stuarti* de LAPPARENT; ABDELGHANY, p. 400, text fig. 9, fig.12, 13.
2003. *Globotruncanita stuarti* de LAPPARENT; ABRAMOVICH *et al*., p. 15, pl. 5, fig. 10, 11.
2004. *Globotruncanita stuarti* de LAPPARENT; PREMOLI-SILVA and VERGA, p. 118, pl. 48, fig. 3, 4; p. 119, pl. 49, fig. 1; p. 248, pl. 18, fig. 13-15; p. 249, pl. 19, fig. 1-7.
2007. *Globotruncanita stuarti* de LAPPARENT; DARVISHZAD *et al*., p. 141, pl. 1, fig. 11.

Remarks:

Globotruncanita stuarti is marked by its circular outline, trapezoidal to rectangular chambers and high trochospire. Its raised and beaded sutures are straight and join almost at right angles. This property is one of the diagnostic features of *G. stuarti*. It differs from *G. stuartiformis* in having almost rectangular chambers on the spiral side, more circular outline and slower increase rate in chamber size.

Stratigraphic Distribution:

The stratigraphic distribution of *G. stuarti* ranges from the *Gansserina gansseri* zone (Late Campanian-Early Maastrichtian) to the end of the *Abathomphalus mayaroensis* zone (K/P boundary). In this study *G. stuarti* has been very common and has been identified from the beginning of the measured section until the middle part of the *P. hariaensis* zone.

***Globotruncanita stuartiformis* DALBIEZ, 1955**

Pl. 3, fig. 6; Pl. 13, fig. 21-27

1955. *Globotruncana* (*Globotruncana) elevata* BROTZEN subsp. *stuartiformis* DALBIEZ; p. 169, text fig 10.
1984. *Globotruncanita stuartiformis* DALBIEZ; ROBASZYNSKI *et al*., p. 239, pl. 32, fig. 1-4.
1987. *Globotruncanita stuartiformis* DALBIEZ; ÖZKAN and ALTINER, p. 273, pl. 3, fig. 7-9.
2003. *Globotruncanita stuartiformis* DALBIEZ; ABRAMOVICH *et al*., p. 6, pl. 1, fig. 1, 2.
2004. *Globotruncanita stuartiformis* DALBIEZ; PREMOLI-SILVA and VERGA, p. 119, pl. 49, fig. 2-4; p. 249, pl. 19, fig. 8-15.
2007. *Globotruncanita stuartiformis* DALBIEZ; DARVISHZAD *et al*., p. 141, pl. 1, fig. 10.

Remarks:

Globotruncanita stuartiformis is identified with its subcircular outline and 5-8 subtriangular chambers in the last whorl. Its sutures are raised, beaded and join the spiral suture at acute angles. When *G. stuartiformis* is compared with *Globotruncanita stuarti*, it is seen that *G. stuartiformis* has a more lobate outline, its chambers are triangular instead rectangular and its sutures join the spiral sutures at very acute angles instead right angles.

Stratigraphic Distribution:

The stratigraphic distribution of *G. stuartiformis* ranges from the *Dicarinella asymetrica* zone (Santonian) to the end of the *Abathomphalus mayaroensis* zone (K/P boundary). In this work *G. stuartiformis* has been encountered frequently from the first sample of the measured section until the K/P boundary.

Genus *Contusotruncana* KORCHAGIN, 1982

Type species: *Pulvinulina arca* var. *contusa* CUSHMAN, 1926

Contusotruncana contusa CUSHMAN, 1926

Pl. 13, fig. 13

1926. *Pulvinulina arca* CUSHMAN var. *contusa* CUSHMAN; p. 23, no type figure given.
1984. *Rosita contusa* CUSHMAN; ROBASZYNSKI *et al*., p. 247, pl. 36, fig. 1-2; p. 249, pl. 37, fig. 1-3.
1987. *Rosita contusa* CUSHMAN; ÖZKAN and ALTINER, p. 275, pl. 4, fig. 4-6.
1988. *Globotruncana contusa* CUSHMAN; KELLER, p. 250, pl. 1, fig. 9.

1997. *Contusotruncana contusa* CUSHMAN; LUCIANI, p. 804, text fig. 3, fig. 1.

1998. *Contusotruncana contusa* CUSHMAN; ZEPEDA, p. 126, text fig. 5, fig. 3.

1999. *Contusotruncana contusa* CUSHMAN; ÖZKAN-ALTINER and ÖZCAN, p. 294, pl. 2, fig. 2.

2002. *Rosita contusa* CUSHMAN; KELLER *et al*., p. 279, pl. 2, fig. 9, 10.

2004. *Contusotruncana contusa* CUSHMAN; CHACON *et al*., p. 590, text fig. 4, fig. C, D.

2004. *Globotruncana contusa* CUSHMAN; PREMOLI-SILVA and VERGA, p. 78, pl. 8, fig. 1-2; p. 233, pl. 3, fig. 1-12.

Remarks:

Contusotruncana contusa is easily identified with its high convexity in the spiral side. Besides its high trochospire it is also identified with its distinctly U-shaped adumbilical ridges and closely spaced double keels. *C. contusa* is identified in thin sections with its high trochospiral axial view.

Stratigraphic Distribution:

The stratigraphic distribution of *C. contusa* ranges from the *Gansserina gansseri* zone (Late Campanian-Early Maastrichtian) to the end of the *Abathomphalus mayaroensis* zone (K/P boundary). In this work *C. contusa* has been very rare and encountered only in few samples below the *P. acervulinoides* zone and in the middle part of the *P. hariaensis* zone.

Contusotruncana walfishensis TODD, 1970

Pl. 3, fig. 1; Pl. 13, fig. 14, 15

1970. *Globotruncana walfishensis* TODD; p. 153, pl. 5, fig. 8.

1984. *Rosita walfishensis* TODD; ROBASZYNSKI *et al*., p. 259, pl. 42, fig. 1-4.

1987. *Rosita walfishensis* TODD; ÖZKAN and ALTINER, p. 273, pl. 3, fig. 13-15; p. 277, pl. 5, fig. 11.

1997. *Contusotruncana walfishensis* TODD; LUCIANI, p. 804, text fig. 3, fig. 2.

1998. *Contusotruncana walfishensis* TODD; ZEPEDA, p. 126, text fig. 5, fig. 4.

2003. *Rosita walfischensis* TODD; ABRAMOVICH *et al*., p. 15, pl. 5, fig. 19.

2004. *Contusotruncana walfischensis* TODD; CHACON *et al*., p. 589, text fig. 3, fig. B; p. 590, text fig. 4, fig. E, F.

2004. *Contusotruncana walfischensis* TODD; PREMOLI-SILVA and VERGA, p. 81, pl. 11, fig. 2-4; p. 235, pl. 5, fig. 1-3.

Remarks:

Contusotruncana walfischensis has a very high trochospire and is identified with its strongly convex spiral side. Its outline is subcircular to polygonal and its almost equally developed two keels are closely spaced. *C. walfischensis* has a special lateral view. Its profile is like a dome with a flattened apex. *C. walfischensis* differs from *C. contusa* in its distinctly smaller size and from *C. contusa* and *C. plicata* in having large number of globular chambers making up a large portion of the spiral side.

Stratigraphic Distribution:

The stratigraphic distribution of *C. walfischensis* ranges from the *Gansserina gansseri* zone (Late Campanian-Early Maastrichtian) to the end of

the *Abathomphalus mayaroensis* zone (K/P boundary). In this study this species has been identified in the *P. hariaensis* zone.

Subfamily GLOBOTRUNCANELLINAE MASLAKOVA, 1964

Genus *Globotruncanella* REISS, 1957

Type species: *Globotruncana citae* BOLLI, 1951 (= *Globotruncana havanensis* VOORWIJK, 1937 = *Globorotalia pschadae* KELLER, 1946)

Globotruncanella havanensis VOORWIJK, 1937

Pl. 4, fig. 7, 8; Pl. 14, fig. 10, 11

1937. *Globotruncana havanensis* VOORWIJK; p. 195, pl. 1, fig. 25, 26, 29.

1984. *Globotruncanella havanensis* VOORWIJK; ROBASZYNSKI *et al*., p. 267, pl. 44, fig. 4-6.

1988. *Globotruncanella havanensis* VOORWIJK; KELLER, p. 250, pl.1, fig. 10.

1998. *Globotruncanella havanensis* VOORWIJK; ZEPEDA, p. 127, text fig. 6, fig. 4.

1999. *Globotruncanella havanensis* VOORWIJK; ÖZKAN-ALTINER and ÖZCAN, p.294, text fig. 4, fig. 9.

2003. *Globotruncanella havanensis* VOORWIJK; ABRAMOVICH *et al*., p. 10, pl. 3, fig. 15.

2004. *Globotruncanella havanensis* VOORWIJK; PREMOLI-SILVA and VERGA, p.113, pl. 43, fig. 1, 2; p. 246, pl. 16, fig. 1-9.

2005. *Globotruncanella havanensis* VOORWIJK; OBAIDALLA, p. 217, pl. 2, fig. 6.

2007. *Globotruncanella havanensis* VOORWIJK; DARVISHZAD *et al*., p. 141, pl. 1, fig. 1.

Remarks:

Globotruncanella havanensis is marked by its more than 4 triangular to trapezoidal, compressed chambers among the other *Globotruncanella* species. Chambers of the last whorl are increasing rapidly in size as added and the test outline is lobate. Its surface can contain pustules and sometimes rugosities. It has a spiro-convex profile but its spiral side is not convex as the spiral side of *G. petaloidea*. Moreover, it has a less lobate profile than other *Globotruncanella* forms.

Stratigraphic Distribution:

The stratigraphic distribution of *G. havanensis* ranges from the *G. havanensis* zone (Campanian) to the end of the *Abathomphalus mayaroensis* zone (K/P boundary). In this study this species has been encountered from the lower part of the *P. acervulinoides zone* toward to the K/P boundary.

***Globotruncanella minuta* CARON and GONZALEZ DONOSO, 1984**

Pl. 4, fig. 9; Pl. 14, fig. 9

1984. *Globotruncanella minuta* CARON and GONZALEZ DONOSO; p. 263, pl. 43, fig. 5.

1984. *Globotruncanella minuta* CARON and GONZALEZ DONOSO; ROBASZYNSKI *et al*., p. 263, pl. 43, fig. 5-8.

2003. *Globotruncanella minuta* CARON and GONZALEZ DONOSO; ABDELGHANY, p. 400, text fig. 9, fig.14.

2004. *Globotruncanella minuta* CARON and GONZALEZ DONOSO; PREMOLI-SILVA and VERGA, p.113, pl. 43, fig. 3, 4; p. 246, pl. 16, fig. 10, 11.

Remarks:

Globotruncanella minuta is differentiated from the other *Globotruncanella* species by its chamber shape. Both *G. havanensis* and *G. petaloidea* have petaloid chambers, whereas *G. minuta* has globular ones. It has a more lobate outline than *G. havanensis*. Its trochospire is very low tending to become planispiral. With its nearly planispiral appearance and globular chambers showing very rapid increase in size, it resembles *Hedbergella monmouthensis*. However it differs from it in having pustulose and hispid chamber surface.

Stratigraphic Distribution:

The stratigraphic distribution of *G. minuta* ranges from the *Gansserina gansseri* zone (Late Campanian-Early Maastrichtian) to the end of the *Abathomphalus mayaroensis* zone (K/P boundary). In this study, *G. minuta* is rather common in the samples and has been recognized in the *P. hariaensis* zone.

***Globotruncanella petaloidea* GANDOLFI, 1955**

Pl. 4, fig. 10-12; Pl. 14, fig. 12

1955. *Globotruncana* (*Rugoglobigerina*) *petaloidea* GANDOLFI subsp. *petaloidea* GANDOLFI; p. 52, pl. 3, fig. 13.
1984. *Globotruncanella petaloidea* GANDOLFI; ROBASZYNSKI *et al*., p. 267, pl. 44, fig. 1-2.
1988. *Globotruncanella petaloidea* GANDOLFI; KELLER, p. 250, pl.1, fig. 12, 13.
1997. *Globotruncanella petaloidea* GANDOLFI; LUCIANI, p. 804, text fig. 3, fig. 7.
2002. *Globotruncanella petaloidea* GANDOLFI; KELLER *et al*., p. 277, pl. 1, fig. 8.

2003. *Globotruncanella petaloidea* GANDOLFI; ABDELGHANY, p. 400, text fig. 9, fig.15.

2004. *Globotruncanella petaloidea* GANDOLFI; PREMOLI-SILVA and VERGA, p.114, pl. 44, fig. 1, 2; p. 246, pl. 16, fig. 12.

2005. *Globotruncanella petaloidea* GANDOLFI; OBAIDALLA, p. 214, pl. 1, fig. 5.

2007. *Globotruncanella petaloidea* GANDOLFI; DARVISHZAD *et al*., p. 141, pl. 1, fig. 9.

Remarks:

Globotruncanella petaloidea has a moderately to very high trochospiral and spiroconvex test. It has 4 distinctly petaloid chambers in the last whorl increasing very rapidly in size and its peripheral outline is strongly lobate. *G. petaloidea* is very similar to *G. havanensis*; however it differs from it in having always 4 petaloid chambers in the last whorl, in a strongly lobate outline and in rapidly increasing chamber size.

Stratigraphic Distribution:

The stratigraphic distribution of *G. petaloidea* ranges from the *Gansserina gansseri* zone (Late Campanian-Early Maastrichtian) to the end of the *Abathomphalus mayaroensis* zone (K/P boundary). In this study this species has been encountered in *P. hariaensis* zone rather frequently.

Family RUGOGLOBIGERINIDAE SUBBOTINA, 1959

Genus *Rugoglobigerina* BRONNIMANN, 1952

Type species: *Globigerina rugosa* PLUMMER, 1927

Rugoglobigerina hexacamerata BRONNIMANN, 1952

Pl. 4, fig. 1; Pl. 14, fig. 1, 2

1952. *Rugoglobigerina* (*Rugoglobigerina*) *reicheli hexacamerata* BRONNIMANN; p. 23, pl. 2, fig. 10-12.

1984. *Rugoglobigerina hexacamerata* BRONNIMANN; ROBASZYNSKI *et al*., p. 283, pl. 49, fig. 8.

1988. *Rugoglobigerina hexacamerata* BRONNIMANN; KELLER, p. 252, pl. 2, fig. 16, 17.

1997. *Rugoglobigerina hexacamerata* BRONNIMANN; LUCIANI, p. 804, text fig. 3, fig. 5.

1998. *Rugoglobigerina hexacamerata* BRONNIMANN; NEDERBRAGT, p. 405, pl. 4, fig. 1-4.

2002. *Rugoglobigerina hexacamerata* BRONNIMANN; KELLER *et al*., p. 279, pl. 2, fig. 5-7.

2003. *Rugoglobigerina hexacamerata* BRONNIMANN; ABRAMOVICH *et al*., p. 10, pl. 3, fig. 11.

2004. *Rugoglobigerina hexacamerata* BRONNIMANN; KASSAB *et al*., p. 432, text fig. 3, fig. 5.

2004. *Rugoglobigerina hexacamerata* BRONNIMANN; PREMOLI-SILVA and VERGA, p.199, pl. 129, fig. 1, 2; p. 269, pl. 39, fig. 1, 2.

2007. *Rugoglobigerina hexacamerata* BRONNIMANN; DARVISHZAD *et al*., p. 142, pl. 2, fig. 8.

Remarks:

Rugoglobigerina hexacamerata is quite different from the other *Rugoglobigerina* species and therefore is easy to identify. First of all, its trochospire is much lower than the other species. Secondly, it has 6 chambers in the last whorl. Lastly, the rate of increase in the chamber size is lower than the other species of this genus.

Stratigraphic Distribution:

The stratigraphic distribution of *R. hexacamerata* ranges from the *G. havanensis* zone (Campanian) to the end of the *Abathomphalus mayaroensis* zone (K/P boundary). In this study *R. hexacamerata* has been quite common and has been identified from the first sample of the measured section until K/P boundary.

***Rugoglobigerina macrocephala* BRONNIMANN, 1952**

Pl. 4, fig. 3; Pl. 14, fig. 3, 4

1952. *Rugoglobigerina* (*Rugoglobigerina*) *macrocephala macrocephala* BRONNIMANN; p. 25, pl. 2, fig. 1-3.
1984. *Rugoglobigerina macrocephala* BRONNIMANN; ROBASZYNSKI *et al*., p. 283, pl. 49, fig. 7.
1988. *Rugoglobigerina macrocephala* BRONNIMANN; KELLER, p. 250, pl. 1, fig. 3.
2000. *Rugoglobigerina macrocephala* BRONNIMANN; ARENILLAS *et al*., p. 208, pl. 1, fig. 9, 10.
2003. *Rugoglobigerina macrocephala* BRONNIMANN; ABDELGHANY, p. 400, text fig. 9, fig.17, 18.
2004. *Rugoglobigerina macrocephala* BRONNIMANN; KASSAB *et al*., p. 432, text fig. 3, fig. 3.

2004. *Rugoglobigerina macrocephala* BRONNIMANN; PREMOLI-SILVA and VERGA, p. 200, pl. 130, fig. 1-4; p. 269, pl. 39, fig. 3, 4.

Remarks:

Rugoglobigerina macrocephala has 3 globular chambers in the last whorl and they are covered by thick rugosities and costellae. It is distinguished easily from the all other *Rugoglobigerina* species with its much larger last chamber. The rate of increase in chamber size is so high that the last chamber makes about half the volume of the test.

Stratigraphic Distribution:

The stratigraphic distribution of *R. macrocephala* ranges from the *G. aegyptiaca* zone (Campanian) to the end of the *Abathomphalus mayaroensis* zone (K/P boundary). In this study this species has been found first in the unzoned part of the measured section until the lower part of the *P. hariaensis* zone.

***Rugoglobigerina milamensis* SMITH and PESSAGNO, 1973**

Pl. 14, fig. 5

1973. *Rugoglobigerina milamensis* SMITH and PESSAGNO; p. 56, pl. 24, fig. 4-7.
1984. *Rugoglobigerina milamensis* SMITH and PESSAGNO; ROBASZYNSKI *et al*., p. 287, pl. 50, fig. 3.
1998. *Rugoglobigerina milamensis* SMITH and PESSAGNO; ZEPEDA, p. 129, text fig. 8, fig. 1-4.
2004. *Rugoglobigerina milamensis* SMITH and PESSAGNO; PREMOLI-SILVA and VERGA, p. 201, p. 131, fig. 1; p. 269, pl. 39, fig. 5, 6.

Remarks:

Rugoglobigerina milamensis has 5-6 globular chambers in the last whorl. In the early whorls chambers increase very rapidly in size; on the other hand in the last whorl the increase in chamber size is very slow, if it exists. It has very convex spiral side due to its high trochospire and this feature is the most discernible feature of this form among other *Rugoglobigerina* species.

Stratigraphic Distribution:

The stratigraphic distribution of *R. milamensis* ranges from the *Gansserina gansseri* zone (Late Campanian-Early Maastrichtian) to the end of the *Abathomphalus mayaroensis* zone (K/P boundary). In the measured section, *R. milamensis* is rare. It has been found from the first sample until the middle part of the *P. hariaensis* zone.

***Rugoglobigerina pennyi* BRONNIMANN, 1952**

Pl. 4, fig. 2; Pl. 14, fig. 6, 7

1952. *Rugoglobigerina* (*Rugoglobigerina*) *rugosa pennyi* BRONNIMANN; p. 34, pl. 4, fig. 1-3.
1984. *Rugoglobigerina pennyi* BRONNIMANN; ROBASZYNSKI *et al*., p. 287, pl. 50, fig. 1.
1998. *Rugoglobigerina pennyi* BRONNIMANN; ZEPEDA, p. 128, text fig. 7, fig. 1-4.
2004. *Rugoglobigerina pennyi* BRONNIMANN; PREMOLI-SILVA and VERGA, p. 201, pl. 131, fig. 2-4; p. 269, pl. 39, fig. 7.

Remarks:

Rugoglobigerina pennyi can be considered as an intermediate form between *R. rugosa* and *R. milamensis*. It has also 5-6 globular chambers in its

last whorl like *R. milamensis* does, but its trochospire is lower. On the other hand, the main difference between *R. pennyi* and *R. rugosa* is that *R. pennyi* has more chambers in the last whorl and much slower increase in the chamber size.

Stratigraphic Distribution:

The stratigraphic distribution of *R. pennyi* ranges from the *G. aegyptiaca* zone (Campanian) to the end of the *Abathomphalus mayaroensis* zone (K/P boundary). In this study this species has been found first in the unzoned part of the measured section until the K/P boundary.

***Rugoglobigerina rugosa* PLUMMER, 1926**

Pl. 4, fig. 3-6; Pl. 14, fig. 8, 9

1926. *Globigerina rugosa* PLUMMER; p. 38, pl. 2, fig. 10 a.
1984. *Rugoglobigerina rugosa* PLUMMER; ROBASZYNSKI *et al*., p. 283, pl. 49, fig. 4, 6.
1988. *Rugoglobigerina rugosa* PLUMMER; KELLER, p. 252, pl. 2, fig. 14.
1997. *Rugoglobigerina rugosa* PLUMMER; LUCIANI, p. 804, text fig. 3, fig. 6.
1998. *Rugoglobigerina rugosa* PLUMMER; ZEPEDA, p. 130, text fig. 9, fig. 4.
2000. *Rugoglobigerina rugosa* PLUMMER; PETRIZZO, p. 501, text fig. 14, fig. 5.
2002. *Rugoglobigerina rugosa* PLUMMER; KELLER *et al*., p. 279, pl. 2, fig. 1, 2.
2003. *Rugoglobigerina rugosa* PLUMMER; ABRAMOVICH *et al*., p. 6, pl. 1, fig. 4, 16.
2004. *Rugoglobigerina rugosa* PLUMMER; CHACON *et al*., p. 590, text fig. 4, fig. L.

2004. *Rugoglobigerina rugosa* PLUMMER; PREMOLI-SILVA and VERGA, p. 202, pl. 132, fig. 1-3; p. 269, pl. 39, fig. 8-11.

2005. *Rugoglobigerina rugosa* PLUMMER; OBAIDALLA, p. 217, pl. 2, fig. 3.

2007. *Rugoglobigerina rugosa* PLUMMER; DARVISHZAD *et al*., p. 142, pl. 2, fig. 10.

Remarks:

Rugoglobigerina rugosa has 4-5 globular chambers in its last whorl which are covered with thick rugosities and costellae like the chambers of the other *Rugoglobigerina* species. The main difference of *R. rugosa* from the other species of this genus is its almost flat spiral side because of low trochospire, 4-5 chambers in the last whorl and rapid increase in chamber size. Besides, it is sometimes so robust that it is difficult to see its sutures clearly.

Stratigraphic Distribution:

The stratigraphic distribution of *R. rugosa* ranges from the *Globotruncanita elevata* zone (Campanian) to the end of the *Abathomphalus mayaroensis* zone (K/P boundary). In our samples *R. rugosa* is one of the most frequent forms and has been found in the *P. hariaensis* zone.

Superfamily PLANOMALINACEA BOLLI, LOEBLICH and TAPPAN, 1957

Family GLOBIGERINELLOIDIDAE LONGORIA, 1974

Subfamily GLOBIGERINELLOIDINAE LONGORIA, 1974

Genus *Globigerinelloides* CUSHMAN & ten DAM, 1948

Type species: *Globigerinelloides algeriana* CUSHMAN and ten DAM, 1948

Globigerinelloides alvarezi ETERNOD OLVERA, 1959

Pl. 5, fig. 1; Pl. 15, fig. 1-5

1959. *Planomalina alvarezi* ETERNOD OLVERA,?

2004. *Macroglobigerinelloides alvarezi* ETERNOD OLVERA; PREMOLI-SILVA and VERGA, p. 153, pl. 83, fig. 1-3; p. 254, pl. 24, fig. 8-13.

Remarks:

Globigerinelloides alvarezi is one of the many chambered species of the genus *Globigerinelloides*. It has 7-8 globular chambers in the final whorl which increase gradually in size. Its biumbilicate nature also helps us to differentiate it.

Stratigraphic Distribution:

The stratigraphic distribution of *G. alvarezi* ranges from the *Globotruncana ventricosa* zone (Campanian) to the end of the *Abathomphalus mayaroensis* zone (K/P boundary). In this study *G. alvarezi* is a common species like the other *Globigerinelloides* forms and has been encountered first in the unzoned part of the measured section and continued until the K/P boundary.

Globigerinelloides messinae BRONNIMANN, 1952

Pl. 5, fig. 3; Pl. 15, fig. 6-8

1952. *Globigerinella messinae messinae* BRONNIMANN; p. 42, pl. 1, fig. 6, 7; text fig. 20a-q.

1964. *Globigerinella messinae messinae* BRONNIMANN; OLSSON, p. 187, pl. 7, fig. 6 (not 7, 8).

2000. *Globigerinelloides messinae* BRONNIMANN; PETRIZZO, p. 499, text fig. 10, fig. 5.

2004. *Macroglobigerinelloides messinae* BRONNIMANN; PREMOLI-SILVA and VERGA, p. 155, pl. 85, fig. 4-6; p. 256, pl. 26, fig. 1, 2.

Remarks:

Globigerinelloides messinae is distinguished by its small, compressed and closely coiled test which is more or less lobate. The last whorl comprises five, rarely six, chambers. They are peripherally rounded and increase rapidly in size. There is a great size difference between the first and last chambers. The outline of the chambers is elongate to ellipsoidal in the apertural view and subcircular in the umbilical view. It differs from *G. alvarezi* in having less number of chambers and greater increase rate in chambers size.

Stratigraphic Distribution:

The stratigraphic distribution of *G. messinae* ranges from the *Dicarinella asymetrica* zone (Santonian) to the end of the *Abathomphalus mayaroensis* zone (K/P boundary). In this study this species has been identified from the beginning of the *P. acervulinoides* zone until the end of the *P. hariaensis* zone.

Globigerinelloides multispinus LALICKER, 1948

Pl. 5, fig. 4

1943. *Globigerinelloides multispina* LALICKER; p. 624, pl. 92, figs 1.

2000. *Globigerinelloides multispinus* LALICKER; PETRIZZO, p. 499, text fig. 10, fig. 6.

2001. *Globigerinelloides multispinus* LALICKER; PETRIZZO, p. 855, text fig. 10, fig. 4, 6.

2004. *Macroglobigerinelloides multispinus* LALICKER; PREMOLI-SILVA and VERGA, p. 156, pl. 86, fig. 1-3; p. 256, pl. 26, fig 3.

Remarks:

Globigerinelloides multispinus is one of the involute and planispiral forms that is easily recognized among the other *Globigerinelloides* species. Most distinguishable characteristic of the form is that its last chamber is divided into two globular chambers which are on the each side of the plane of coiling.

Stratigraphic Distribution:

The stratigraphic distribution of *G. multispinus* ranges from the *Dicarinella asymetrica* zone (Santonian) to the end of the *Abathomphalus mayaroensis* zone (K/P boundary). In this study this species has been very rarely recorded in few samples of the *P. hariaensis* zone.

***Globigerinelloides prairiehillensis* PESSAGNO, 1967**

Pl. 5, fig. 2; Pl. 15, fig. 9-16

1967. *Globigerinelloides prairiehillensis* PESSAGNO; p. 277, pl. 60, fig. 2, 3; pl. 80, fig. 1; pl. 90, fig. 1, 2-4; pl. 97, fig. 3, 4.

1996. *Globigerinelloides prairiehillensis* PESSAGNO; p. 311, pl. 1, fig. 2.

2000. *Globigerinelloides prairiehillensis* PESSAGNO; PETRIZZO, p. 499, text fig. 10, fig. 7.

2004. *Macroglobigerinelloides prairiehillensis* PESSAGNO; PREMOLI-SILVA and VERGA, p. 156, pl. 86, fig. 4-6; p. 256, pl. 26, fig. 4-9.

Remarks:

Globigerinelloides prairiehillensis has a lobate outline and a biumbilicate (like an hourglass) side view. Although in the definition of the form it is stated that there are 6-7 chambers in the last whorl, we have observed in general 5-6 chambers in our samples. Its spherical chambers increase in size but rate of increase is less than those the other *Globigerinelloides* species.

Stratigraphic Distribution:

The stratigraphic distribution of *G. prairiehillensis* ranges from the *Radotruncana calcarata zone* (Campanian) to middle part of the *Abathomphalus mayaroensis* zone (Late Maastrichtian). Although in the literature last appearance datum of this form is below the K/P boundary, we have encountered this species frequently until the last sample of Maastrichtian.

***Globigerinelloides subcarinatus* BRONNIMANN, 1952**

Pl. 5, fig. 5, 6; Pl. 15, fig. 17, 18

1952. *Globigerinella messinae subcarinata* BRONNIMANN; p. 44, pl. 1, fig. 10, 11; text fig. 21a-m.

1964. *Globigerinelloides subcarinatus* BRONNIMANN; OLSSON, p. 187, pl. 7, fig. 9, 10.

1967. *Globigerinelloides subcarinatus* BRONNIMANN; PESSAGNO, p. 278, pl. 62, fig. 12, 13.

1988. *Globigerinelloides subcarinatus* BRONNIMANN; KELLER, p. 252, pl. 2, fig. 2.

1998. *Globigerinelloides subcarinatus* BRONNIMANN; ZEPEDA, p. 127, text fig. 6, fig. 2.

2001. *Globigerinelloides subcarinatus* BRONNIMANN; PETRIZZO, p. 855, text fig. 10, fig 5.

2002. *Globotruncanella subcarinatus* BRONNIMANN; KELLER *et al*., p. 277, pl. 1, fig. 7.

2003. *Globigerinelloides subcarinatus* BRONNIMANN; ABRAMOVICH *et al*., p. 10, pl. 3, fig. 3.

2004. *Macroglobigerinelloides subcarinatus* BRONNIMANN; PREMOLI-SILVA and VERGA, p. 157, pl. 87, fig. 1-3; p. 256, pl. 26, fig. 10-13.

Remarks:

Globigerinelloides subcarinatus is the one of the easiest forms to identify. Its planispiral and lobate test is very compressed and the shape of the chambers is elongate to ellipsoid in the apertural view. In general there are 5 chambers in the last whorl and most distinguishingly the end chamber of the last whorl is occasionally not larger or even smaller than the penultimate one. Sometimes we see ornamentation on the surface and it is stronger in the earlier stage of the last whorl.

Stratigraphic Distribution:

The stratigraphic distribution of *G. subcarinatus* ranges from the *Globotruncanita elevata* zone (Campanian) to the end of the *Abathomphalus mayaroensis* zone (K/P boundary). In this study *G. subcarinatus* is rather frequent and seen firstly in the unzoned part of the measured section. It also disappeared at the K/P boundary.

Superfamily ROTALIPORACEA SIGAL, 1958

Family HEDBERGELLIDAE LOEBLICH and TAPPAN, 1961

Subfamily HEDBERGELLINAE LOEBLICH and TAPPAN, 1961

Genus HEDBERGELLA BRONNIMANN and BROWN, 1958

Type species: *Anomalina lorneiana* d'ORBIGNY var. *trochoidea* GANDOLFI, 1942

Hedbergella holmdelensis OLSSON, 1964

Pl. 5, fig. 10, 11; Pl. 14, fig. 21-28

1964. *Hedbergella holmdelensis* OLSSON; p. 160, pl. 1, fig. 2a-c.

1998. *Hedbergella holmdelensis* OLSSON; ZEPEDA, p. 127, text fig. 6, fig. 3.

1999. *Hedbergella holmdelensis* OLSSON; PARDO *et al*., p. 258, pl. 3, fig. 13, 14.

2000. *Hedbergella holmdelensis* OLSSON; PETRIZZO, p. 498, text fig. 8, fig. 3.

2002. *Hedbergella holmdelensis* OLSSON; LUCIANI, p. 312, pl. 1, fig. 22-23.

2004. *Hedbergella holmdelensis* OLSSON; ARENILLAS *et al*., p. 82, text fig. 4, fig. D, E.

2004. *Muricohedbergella holmdelensis* OLSSON; PREMOLI-SILVA and VERGA, p. 166, pl. 96, fig. 3-5; p. 260, pl. 30, fig. 6-8.

2005. *Hedbergella holmdelensis* OLSSON; OBAIDALLA, p. 217, pl. 2, fig. 9.

2007. *Hedbergella holmdelensis* OLSSON; DARVISHZAD *et al*., p. 142, pl. 2, fig. 12.

Remarks:

Hedbergella holmdelensis shows very low trochospiral (nearly planispiral) coiling and a lobate periphery. It has 5-6 chambers in the last whorl increasing considerably rapidly in size. It is differentiated from *H. monmouthensis* with its ovate and elongated chambers. Especially in axial view the chambers are seen compressed and ovate. Another difference between *H. holmdelensis* and *H. monmouthensis* is that the rate of increase in chambers size in the last whorl is less in *H. holmdelensis*.

Stratigraphic Distribution:

The stratigraphic distribution of *H. holmdelensis* is from Early Maastrichtian to lower P0 zone (Early Danian). There is an agreement among the micropaleontologists that this species has survived the K/P mass extinction event. In the samples this form is quite commonly recorded, from the unzoned interval of Maastrichtian age through *P. acervulinoides* zone and disappeared in the *G. cretacea* (P0) zone.

***Hedbergella monmouthensis* OLSSON, 1960**

Pl. 5, fig. 8, 9; Pl. 14, fig. 14-20

1960. *Globorotalia monmouthensis* OLSSON; p. 47, pl. 9, fig. 22-24.

1999. *Hedbergella monmouthensis* OLSSON; PARDO *et al*., p. 258, pl. 3, fig. 9, 10.

2002. *Hedbergella monmouthensis* OLSSON; KELLER *et al*., p. 277, pl. 1, fig. 5, 6.

2002. *Hedbergella monmouthensis* OLSSON; LUCIANI, p. 312, pl. 1, fig. 18-21.

2004. *Muricohedbergella monmouthensis* OLSSON; PREMOLI-SILVA and VERGA, p. 167, pl. 97, fig. 1-4; p. 260, pl. 30, fig. 9, 10.

2005. *Hedbergella monmouthensis* OLSSON; OBAIDALLA, p. 217, pl. 2, fig. 8.

2007. *Hedbergella monmouthensis* OLSSON; DARVISHZAD *et al*., p. 142, pl. 2, fig. 9.

Remarks:

Hedbergella monmouthensis displays a similar coiling pattern and a test shape with *H. holmdelensis*. *H. monmouthensis* differs from *H. holmdelensis* in having a more rapid increase in size of the chambers of the last whorl. Rate of chamber size increase is so much that the last two chambers make up over 1/2 of the test and overall periphery becomes distinctly lobate. It has globular to subglobular chambers and this is also distinctive for this species. Easiest way to differentiate *H. monmouthensis* from *H. holmdelensis* is to examine their shape of chambers. While *H. monmouthensis* has globular chambers, *H. holmdelensis* has ovate and compressed chambers and this is especially easy to differentiate by looking at their profile view.

Stratigraphic Distribution:

H. monmouthensis is also one of the survived species and several authors agree with this idea. It ranges from Upper Maastrichtian to lower P0 (Early Danian). In this study *H. monmouthensis* has been frequently recorded from the lowest part of the measured section and to the middle part of the *G. cretacea* (P0) zone.

Superfamily HETEROHELICACEA CUSHMAN, 1927

Family HETEROHELICIDAE CUSHMAN, 1927

Subfamily HETEROHELICINAE CUSHMAN, 1927

Genus *Heterohelix* EHRENBERG, 1843

Type species: *Textularia americana* EHRENBERG, 1843

Heterohelix globulosa EHRENBERG, 1840

Pl. 6, fig. 1-6; Pl. 16, fig. 1-7

1840. *Textularia globulosa* EHRENBERG; p. 135, pl. 4, fig. 2b, 4b, 5b, 7b, 8b.

1938. *Guembelina reussi* EHRENBERG; CUSHMAN, p. 11, pl. 2, fig. 6-9.

1991. *Heterohelix globulosa* EHRENBERG; NEDERBRAGT, p. 347, pl. 2, fig. 1, 2.

1997. *Heterohelix globulosa* EHRENBERG; LUCIANI, p. 804, text fig. 3, fig. 20.

1998. *Heterohelix globulosa* EHRENBERG; ZEPEDA, p. 132, text fig. 11, fig. 7, 8.

1999. *Heterohelix globulosa* EHRENBERG; PARDO *et al*., p. 254, pl. 1, fig. 1-6.

2000. *Heterohelix globulosa* EHRENBERG; PETRIZZO, p. 500, text fig. 11, fig. 3.

2002. *Heterohelix globulosa* EHRENBERG; KELLER *et al*., p. 277, pl. 1, fig. 10-13.

2002. *Heterohelix globulosa* EHRENBERG; LUCIANI, p. 312, pl. 1, fig. 7-10

2003. *Heterohelix globulosa* EHRENBERG; ABDELGHANY, p. 399, text fig. 8, fig. 13.

2003. *Heterohelix globulosa* EHRENBERG; ABRAMOVICH *et al*., p. 8, pl. 2, fig. 1, 2.

2004. *Heterohelix globulosa* EHRENBERG; KELLER and PARDO, p. 97, pl. 1, fig. 17, 18.

2004. *Heterohelix globulosa* EHRENBERG; PREMOLI-SILVA and VERGA, p. 140, pl. 70, fig. 5-7; p. 252, pl. 22, fig. 13, 14.

2005. *Hetrohelix globulosa* EHRENBERG; OBAIDALLA, p. 214, pl. 1, fig. 10.

2007. *Heterohelix globulosa* EHRENBERG; DARVISHZAD *et al*., p. 142, pl. 2, fig. 14.

Remarks:

Heterohelix globulosa is one of the most common biserial forms. The number of pairs and its surface ornamentations depict considerable variation in the literature. However it is distinguished with its globular chambers, lobate periphery throughout and gradual size increase towards to the last chamber. Especially the last chamber is noticeably big in most of the individuals.

During the washing treatments surface ornamentations like striations might get destroyed and are often very difficult to recognize under the binocular microscope. Therefore it was not possible to differentiate *H. striata* from *H. globulosa* in this study. However, some forms classified as *H. globulosa* under the microscope showed distinct striations in the SEM images (Pl. 6, fig. 5).

Stratigraphic Distribution:

There are different ideas about the stratigraphic distribution of this species. According to Nederbragt (1991) and Premoli-Silva and Verga (2004) *H. globulosa* appeared in the Turonian and disappeared at the K/P boundary. However some authors suggest that it survived into the Danian (Keller, 1988, 1989a, 1989b; Keller *et al*., 1995; Canudo *et al*., 1991; MacLeod and Keller, 1994; Pardo *et al*., 1996; Luciani, 1997, 2002; Pardo *et al*., 1999; Karoui-Yaakoub *et al*., 2002; Keller and Pardo, 2004; Paul, 2005). In this study *H. globulosa* is very common in the samples and seen first in the unzoned part

of the measured section. The stratigraphic distribution ranges across the boundary and *H. globulosa* has been recovered in the first Danian sample.

***Heterohelix labellosa* NEDERBRAGT, 1991**

Pl. 6, fig. 8; Pl. 16, fig. 14, 15

1991. *Heterohelix labellosa* NEDERBRAGT; p. 347, pl. 2, fig. 3-5.
2003. *Heterohelix labellosa* NEDERBRAGT; ABRAMOVICH *et al*., p. 8, pl. 2, fig. 3.
2004. *Heterohelix labellosa* NEDERBRAGT; PREMOLI-SILVA and VERGA, p. 141, pl. 71, fig. 1-3.

Remarks:

There are two important features that set apart *Heterohelix labellosa* from the other species of *Heterohelix*. These are its subglobular to reniform chambers and the distinct and continuous costae which cover the test. Its sides are rapidly flaring in the juvenile stage and becoming subparallel in the adult stage. Even if some individuals of the species *H. globulosa* show similar ornamentations, *H. labellosa* is differentiated from it with its more reniform chambers.

Stratigraphic Distribution:

H. labellosa ranges from the Campanian to the end of the Maastrichtian. In our samples *H. labellosa* appeared in the unzoned part of the measured section and continued towards to the middle part of the *P. hariaensis* zone.

Heterohelix navarroensis LOEBLICH, 1951

Pl. 6, fig. 7; Pl. 16, fig. 8-12

1854. *Spiroplecta americana* EHRENBERG; p. 854, pl. 32II, fig. 25.

1951. *Heterohelix navarroensis* LOEBLICH; p. 107, 108, pl. 12, fig. 1-3; text fig. 2.

1988. *Heterohelix navarroensis* LOEBLICH; KELLER, p. 252, pl. 2, fig. 5.

1991. *Heterohelix navarroensis* LOEBLICH; NEDERBRAGT, p. 349, pl. 3, fig. 5.

1999. *Heterohelix navarroensis* LOEBLICH; PARDO *et al*., p. 254, pl. 1, fig. 15.

2002. *Heterohelix navarroensis* LOEBLICH; KELLER *et al*., p. 277, pl. 1, fig. 9.

2002. *Heterohelix navarroensis* LOEBLICH; LUCIANI, p. 312, pl. 1, fig. 1.

2004. *Heterohelix navarroensis* LOEBLICH; KELLER and PARDO, p. 97, pl. 1, fig. 19.

2004. *Heterohelix navarroensis* LOEBLICH; PREMOLI-SILVA and VERGA, p. 141, pl. 71, fig. 8-10.

2007. *Heterohelix navarroensis* LOEBLICH; DARVISHZAD *et al*., p. 142, pl. 2, fig. 11.

Remarks:

The most important diagnostic feature of *Heterohelix navarroensis* is the presence of an initial coiled part. Although Nederbragt (1991) claimed that some forms without an initial coil can also be included to *H. navarroensis* provided that they have the same overall morphology. In our study, we have classified the *Heterohelix* species as *H. navarroensis* only if they have an initial coiled part.

Stratigraphic Distribution:

There are different ideas about the stratigraphic distribution of this species. According to Nederbragt (1991) and Premoli-Silva and Verga (2004), *H. navarroensis* is seen throughout the Maastrichtian and extinct at the K/P boundary. However some authors believe that *H. navarroensis* is one of the survived species (Keller, 1988, 1989a, 1989b; Keller *et al*., 1995; Canudo *et al*., 1991; MacLeod and Keller, 1994; Pardo *et al*., 1996; Luciani, 1997, 2002; Pardo *et al*., 1999; Karoui-Yaakoub *et al*., 2002; Keller and Pardo, 2004; Paul, 2005). In our samples *H. navarroensis* appeared in the unzoned interval of the measured section and continued towards to the upper part of the *P. hariaensis* zone.

Heterohelix planata CUSHMAN, 1938

1938. *Guembelina planata* CUSHMAN; p.12, 13, pl. 2, fig. 13, 14.
1991. *Heterohelix planata* CUSHMAN; NEDERBRAGT, p. 349, pl. 3, fig. 3-4.
1998. *Heterohelix planata* CUSHMAN; ZEPEDA, p. 131, text fig. 10, fig. 8.
2000. *Heterohelix planata* CUSHMAN; PETRIZZO, p. 500, text fig. 11, fig. 5.
2003. *Heterohelix planata* CUSHMAN; ABRAMOVICH *et al*., p. 8, pl. 2, fig. 4.
2004. *Heterohelix planata* CUSHMAN; PREMOLI-SILVA and VERGA, p. 142, pl. 72, fig. 7-9.

Remarks:

Heterohelix planata have ovate chambers. Its test is covered by thin and discontinuous costae. In our samples costae on the test was not observable because of the poor preservation. The main criteria in our classification were the ovate chambers and the compressed test of the species.

Stratigraphic Distribution:

H. planata ranges from the uppermost part of the *Dicarinella asymetrica* zone (Santonian) to the end of the *Abathomphalus mayaroensis* zone (K/P boundary). In this study this species is rather rarely recorded in the *P. hariaensis* zone.

Heterohelix punctulata CUSHMAN, 1938

Pl. 6, fig. 9; Pl. 16, fig. 13

1938. *Guembelina punctulata* CUSHMAN; p. 13, pl. 2, fig. 15, 16.
1988. *Pseudoguembelina punctulata* CUSHMAN; KELLER, p. 252, pl. 2, fig. 10.
1991. *Heterohelix punctulata* CUSHMAN; NEDERBRAGT, p. 349, pl. 3, fig. 6.
1999. *Heterohelix punctulata* CUSHMAN; PARDO *et al.*, p. 254, pl. 1, fig. 7, 8.
2003. *Heterohelix punctulata* CUSHMAN; ABRAMOVICH *et al.*, p. 6, pl. 1, fig. 9; p. 8, pl. 2, fig. 5.
2004. *Heterohelix punctulata* CUSHMAN; PREMOLI-SILVA and VERGA, p. 143, pl. 73, fig. 1-5; p. 253, pl. 23, fig. 5.

Remarks:

The biserial test of *Heterohelix punctulata* is rapidly flaring in the juvenile stage and then its sides become subparallel towards to the adult stage. Therefore, its later portion has more or less the same width. The test of *Heterohelix punctulata* is quite broad and rounded. With its large and robust appearance it is easy to identify it.

Stratigraphic Distribution:

H. punctulata ranges from the uppermost part of the *Dicarinella asymetrica* zone (Santonian) to the end of the *Abathomphalus mayaroensis* zone (K/P boundary). In our samples *H. punctulata* is rather frequent and appeared in the unzoned interval, continued until the K/P boundary and is seen also in the first sample of the Danian.

Genus *Laeviheterohelix* NEDERBRAGT, 1991

Type species: *Guembelina pulchra* BROTZEN, 1936

Laeviheterohelix dentata STENESTAD, 1968

Pl. 6, fig. 10, 11; Pl. 16, fig. 16

1968. *Heterohelix dentata* STENESTAD; p. 67, 68, pl. 1, fig. 3-6, 8, 9; pl. 2, fig. 1-3.
1991. *Laeviheterohelix dentata* STENESTAD; NEDERBRAGT, p. 353, pl. 5, fig. 1-2.
2000. *Heterohelix dentata* STENESTAD; PETRIZZO, p. 500, text fig. 11, fig. 2.
2002. *Heterohelix dentata* STENESTAD; LUCIANI, p. 312, pl. 1, fig. 2.
2004. *Heterohelix dentata* STENESTAD; KELLER and PARDO, p. 97, pl. 1, fig. 19.
2004. Laevi*heterohelix dentata* STENESTAD; PREMOLI-SILVA and VERGA, p. 147, pl. 77, fig. 1-5.
2007. *Heterohelix dentata* STENESTAD; DARVISHZAD *et al*., p. 142, pl. 2, fig. 7.

Remarks:

Laeviheterohelix dentata is easily identified among the other biserial forms. It has a very compressed test and subquadrate to reniform chambers. Its periphery is acute to subacute and resembles a triangle. It can be differentiated from *L. glabrans* in having a more acute periphery.

Stratigraphic Distribution:

L. dentata ranges from the *Radotruncana calcarata* zone (Campanian) to the end of the *Abathomphalus mayaroensis* zone (K/P boundary) and extinct at K/P boundary according to Nederbragt (1991) and Premoli-Silva and Verga (2004). However there are also several studies stating that *L. dentata* survived into the Danian (Keller, 1988, 1989a, 1989b; Keller *et al*., 1995; Canudo *et al*., 1991; MacLeod and Keller, 1994; Pardo *et al*., 1996; Luciani, 1997, 2002; Pardo *et al*., 1999; Karoui-Yaakoub *et al*., 2002; Keller and Pardo, 2004; Paul, 2005). In this study *L. dentata* is quite common, appeared in the unzoned interval of Maastrichtian age and continued until the boundary.

***Laeviheterohelix glabrans* CUSHMAN, 1938**

Pl. 16, fig. 12-14

1938. *Guembelina glabrans* CUSHMAN; p. 15, pl. 3, fig. 1, 2.
1991. *Laeviheterohelix glabrans* CUSHMAN; NEDERBRAGT, p. 353, pl. 5, fig. 6.
1998. *Laeviheterohelix glabrans* CUSHMAN; ZEPEDA, p. 131, text fig. 10, fig. 7.
2003. *Laeviheterohelix glabrans* CUSHMAN; ABRAMOVICH *et al*., p. 8, pl. 2, fig. 6.
2004. *Laeviheterohelix glabrans* CUSHMAN; PREMOLI-SILVA and VERGA, p. 147, pl. 77, fig. 9, 10; p. 254, pl. 24, fig. 1, 2.

Remarks:

Laeviheterohelix glabrans is identified with its biserial and compressed test. Its periphery is subacute and its chambers are lentil-shaped in side view. It differs from *L. dentata* in having more highly arched chambers and less acute periphery.

Stratigraphic Distribution:

There are also two different views about the stratigraphic range of *L. glabrans*. One view is that the species lived from the *Globotruncana ventricosa* zone (Campanian) to the end of the *Abathomphalus mayaroensis* zone and extinct at K/P boundary (Nederbragt, 1991; Premoli-Silva and Verga, 2004). Another view claims that *L. glabrans* survived into the early Danian (Keller, 1988, 1989a, 1989b; Keller *et al*., 1995; Canudo *et al*., 1991; MacLeod and Keller, 1994; Pardo *et al*., 1996; Luciani, 1997, 2002; Pardo *et al*., 1999; Karoui-Yaakoub *et al*., 2002; Keller and Pardo, 2004; Paul, 2005). In this study *L. dentata* is quite common in the samples. It is found starting from the lower boundary of the *P. hariaensis* zone until the boundary and seen also in the first sample of Danian.

Genus *Planoglobulina* CUSHMAN, 1927

Type species: *Guembelina acervulinoides* EGGER, 1899

Planoglobulina acervulinoides EGGER, 1899

Pl. 8, fig. 1-5; Pl. 17, fig. 12

1899. *Guembelina acervulinoides* EGGER; p. 35, pl. 14, fig. 20.

1972. *Planoglobulina acervulinoides* EGGER; MARTIN, p. 81, pl. 3, fig. 3-6.

1972. *Planoglobulina brazoensis* MARTIN; p. 82, 83, pl. 3, fig. 7; pl. 4, fig. 1-2.

1988. *Planoglobulina brazoensis* MARTIN; KELLER, p. 250, pl. 1, fig. 5.

1991. *Planoglobulina acervulinoides* EGGER; NEDERBRAGT, p. 355, pl. 6, fig.5-6; p. 357, pl. 7, fig. 1.

1999. *Planoglobulina acervulinoides* EGGER; ÖZKAN-ALTINER and ÖZCAN, p. 292, text fig. 4, fig. 9.

2002. *Planoglobulina brazoensis* MARTIN; KELLER *et al*., p. 279, pl. 2, fig. 11.

2003. *Planoglobulina acervulinoides* EGGER; ABRAMOVICH *et al*., p. 14, pl. 4, fig. 11.

2003. *Planoglobulina brazoensis* MARTIN; ABRAMOVICH *et al*., p. 14, pl. 4, fig. 10.

2004. *Planoglobulina acervulinoides* EGGER; PREMOLI-SILVA and VERGA, p. 171, pl. 101, fig. 1-7; p. 261, pl. 31, fig. 6-11.

2004. *Planoglobulina brazoensis* MARTIN; PREMOLI-SILVA and VERGA, p. 172, pl. 102, fig. 1-4.

Remarks:

Planoglobulina acervulinoides is one of the common forms that show proliferation. In its initial part a biserial portion is observed. In the later stage multiserial chamberlets start to form and up to 6 sets are observed. Both biserial chambers and multiserial chamberlets are subglobular. Its surface is covered with distinct continuous or discontinuous costae. Although used quite common *P. brazoensis* has not been differentiated as a different species in this study. Martin (1972) differentiated *P. brazoensis* from *P. acervulinoides* in having a deeper test and less multiserial chamberlets. However Nederbragt (1991) interpreted such forms as end members of a continuous series of phenotypes of one species. In our taxonomical criteria both considered synonym based on the idea of Nederbragt (1991).

Stratigraphic Distribution:

The stratigraphic range of *P. acervulinoides* is from the middle part of the *Gansserina gansseri* zone (Late Campanian-Early Maastrichtian) to the top of the *Abathomphalus mayaroensis* zone (K/P boundary). In this study *P. acervulinoides* is very common in the samples and its first appearance datum has been defined as the lower boundary of the *P. acervulinoides* zone. *P. acervulinoides* continued until the K/P boundary and has also been seen in the first sample of the Danian.

Planoglobulina carseyae PLUMMER, 1931

Pl. 8, fig. 6; Pl. 17, fig. 9-11

1931. *Ventilabrella carseyae* PLUMMER; p. 178, 179, pl. 9, fig. 7-10.
1988. *Planoglobulina carseyae* PLUMMER; KELLER, p. 250, pl.1, fig. 16.
1991. *Planoglobulina carseyae* PLUMMER; NEDERBRAGT, p. 357, pl. 7, fig. 2, 3.
2003. *Planoglobulina carseyae* PLUMMER; ABRAMOVICH *et al*., p. 14, pl. 4, fig. 9.
2004. *Planoglobulina carseyae* PLUMMER; PREMOLI-SILVA and VERGA, p. 172, pl. 102, fig. 5; p. 173, pl. 103, fig. 1-5; p. 261, pl. 31, fig. 12, 13.

Remarks:

Planoglobulina carseyae has also biserial initial and multiserial later portions like the other species of *Planoglobulina* do. However, it differs from them in having a longer biserial portion than the multiserial portion. Its biserial chambers are followed only by one or two sets of multiserial chamberlets. It has a compressed and V-shaped test. Later chambers are arranged irregularly in the plane of biseriality forming a fully mature test that shows a fan-shaped appearance in the peripheral outline.

Stratigraphic Distribution:

Planoglobulina carseyae is also one of the forms that its stratigraphic range is still in debate. According to Nederbragt (1991) and Premoli-Silva and Verga (2004) *P. carseyae* is seen throughout the Maastrichtian and extinct at the K/P boundary. However some authors consider that *P. carseyae* is one of the survived species (Keller, 1988). In this study *P. carseyae* has been found from the beginning of the *P. acervulinoides* zone to the middle part of the *P. hariaensis* zone. When compared to *P. acervulinoides* this species is rather rare in the samples.

Genus *Pseudotextularia* RZEHAK, 1891

Type species: *Cuneolina elegans* RZEHAK, 1891

Pseudotextularia elegans RZEHAK, 1891

Pl. 7, fig. 1-4; Pl. 17, fig. 1-4

1891. *Cuneolina elegans* RZEHAK; p. 4.
1988. *Pseudotextularia elegans* RZEHAK; KELLER, p. 250, pl. 1, fig. 17.
1991. *Pseudotextularia elegans* RZEHAK; NEDERBRAGT, p. 363, pl. 10, fig. 1, 2.
1998. *Pseudotextularia elegans* RZEHAK; ZEPEDA, p. 132, text fig. 11, fig. 3, 4.
2000. *Pseudotextularia elegans* RZEHAK; ARENILLAS *et al*., p. 43, pl. 1, fig. 7, 8.
2002. *Pseudotextularia elegans* RZEHAK; KELLER *et al*., p. 280, pl. 3, fig. 5.
2003. *Pseudotextularia elegans* RZEHAK; ABDELGHANY, p. 399, text fig. 8, fig. 15.
2003. *Pseudotextularia elegans* RZEHAK; ABRAMOVICH *et al*., p. 14, pl. 4, fig. 2.

2004. *Pseudotextularia elegans* RZEHAK; PREMOLI-SILVA and VERGA, p. 185, pl. 115, fig. 1-3; p. 264, pl. 34, fig. 6-13.

2007. *Pseudotextularia elegans* RZEHAK; DARVISHZAD *et al*., p. 141, pl. 1, fig. 14.

Remarks:

The test of *Pseudotextularia elegans* is biserial throughout without chamber proliferation. In edge-view it has a bi-convex appearance. It is easily identified with its reniform chambers and coarse and continuous costae on its surface. It differs from the *P*. *nuttalli* in being much more coarsely costate and in having more compressed and reniform chambers.

Stratigraphic Distribution:

P. *elegans* is seen from the *G*. *havanensis* zone (Campanian) to the end of the *Abathomphalus mayaroensis* zone (K/P boundary). *P*. *elegans* is quite common in the samples and has been seen first in the unzoned part of the measured section and continued until the K/P boundary. It has been recorded even in the first sample of Paleocene.

***Pseudotextularia nuttalli* VOORWIJK, 1937**

Pl. 7, fig. 5-7; Pl. 17, fig. 4, 5

1937. *Guembelina nuttalli* VOORWIJK; p. 192, pl. 2, fig. 1-9.

1991. *Pseudotextularia nuttalli* VOORWIJK; NEDERBRAGT, p. 363, pl. 10, fig. 4, 6.

1998. *Pseudotextularia nuttalli* VOORWIJK; ZEPEDA, p. 132, text fig. 11, fig 6.

2000. *Pseudotextularia nuttalli* VOORWIJK; PETRIZZO, p. 500, text fig. 11, fig. 9.

2004. *Pseudotextularia nuttalli* VOORWIJK; PREMOLI-SILVA and VERGA, p. 186, pl. 116, fig. 3-5; p. 264, pl. 34, fig. 14.

Remarks:

The test of *Pseudotextularia nuttalli* is biconcave to biconvex in edge view. It resembles *P. elegans* in having chambers which are clearly deeper than wide. Hence, it is easy to differentiate them. Important difference between *P. nuttalli* and *P. elegans* is that *P. nuttalli* has ovate to subglobular chambers rather than reniform and that the costae of *P. nuttalli* are much finer. In side view *P. nuttalli* also resembles *Heterohelix* species. However in edge view it differs from *Heterohelix* species with its compressed, ovate and almost reniform chambers.

Stratigraphic Distribution:

P. nuttalli is recorded from the *Dicarinella concavata* zone (Coniacian) to the end of the *Abathomphalus mayaroensis* zone (K/P boundary). In this study this species has been one of the most common biserial forms, encountered in the unzoned part of Maastrichtian age and disappeared in the first sample of Danian.

Subfamily PSEUDOGUEMBELININAE ALIYULLA, 1977

Genus *Pseudoguembelina* BRONNIMANN and BROWN, 1953

Type species: *Guembelina excolata* CUSHMAN, 1926

Pseudoguembelina costulata CUSHMAN, 1938

Pl. 7, fig. 8, 9

1938. *Guembelina costulata* CUSHMAN; p. 16, 17, pl. 3, fig. 7-9.

1991. *Pseudoguembelina costulata* CUSHMAN; NEDERBRAGT, p. 359, pl. 8, fig. 3, 4.

2003. *Pseudoguembelina costulata* CUSHMAN; ABRAMOVICH *et al*., p. 8, pl. 2, fig. 12.

2004. *Pseudoguembelina costulata* CUSHMAN; PREMOLI-SILVA and VERGA, p. 179, pl. 109, fig. 3-6; p. 263, pl. 33, fig. 9-12.

2005. *Pseudoguembelina costulata* CUSHMAN; OBAIDALLA, p. 214, pl. 1, fig. 2.

Remarks:

Test of *Pseudoguembelina costulata* is biserial and slender. It is distinguished by its slightly reniform adult chambers and its continuous costae which follows the curvature of the chambers. *P. costulata* differs from *P. excolata* in having a narrower outline in side view.

Stratigraphic Distribution:

The stratigraphic distribution of *P. costulata* ranges from the beginning of the *Globotruncanita elevata* zone (Campanian) to the end of the *Abathomphalus mayaroensis* zone (K/P boundary). It was very rare and recorded within the *P. hariaensis* zone.

Pseudoguembelina excolata CUSHMAN, 1926

Pl. 17, fig. 8

1926. *Guembelina excolata* CUSHMAN; p. 20, pl. 2, fig. 9.

1991. *Pseudoguembelina excolata* CUSHMAN; NEDERBRAGT, p. 359, pl. 8, fig. 5.

2003. *Pseudoguembelina excolata* CUSHMAN; ABRAMOVICH *et al*., p. 6, pl. 1, fig. 7; p. 8, pl. 2, fig. 13.

2004. *Pseudoguembelina excolata* CUSHMAN; PREMOLI-SILVA and VERGA, p. 179, pl. 109, fig. 7-9; p. 263, pl. 33, fig. 13.

2007. *Pseudoguembelina excolata* CUSHMAN; MACLEOD *et al*., p. 107, text fig. 5, fig. J.

Remarks:

Pseudoguembelina excolata is also a biserial form possessing thick and continuous costae following the curvature of the chambers. *P. excolata* differs from *P. costulata* in having coarser costae, much broader test in side view and more rectangular adult chambers.

Stratigraphic Distribution:

The stratigraphic distribution of *P. excolata* ranges from the *G. havanensis* zone (Campanian) to the end of the *Abathomphalus mayaroensis* zone (K/P boundary). This species is very rare in the samples, and has been encountered first in the unzoned interval of Maastrichtian age and continued until the *P. hariaensis* zone.

Pseudoguembelina hariaensis NEDERBRAGT, 1991

Pl. 7, fig. 10-12; Pl. 17, fig. 7

1991. *Pseudoguembelina hariaensis* NEDERBRAGT; p. 359, pl. 8, fig. 6, 7; p. 361, pl. 9, fig. 1, 2.

2001. *Pseudoguembelina hariaensis* NEDERBRAGT; PETRIZZO, p. 855, text fig. 10, fig. 12, 13.

2002. *Pseudoguembelina hariaensis* NEDERBRAGT; KELLER *et al*., p. 279, pl. 2, fig. 12.

2003. *Pseudoguembelina hariaensis* NEDERBRAGT; ABRAMOVICH *et al*., p. 8, pl. 2, fig. 15

2005. *Pseudoguembelina hariaensis* NEDERBRAGT; OBAIDALLA, p. 214, pl. 1, fig. 3.

2004. *Pseudoguembelina hariaensis* NEDERBRAGT; PREMOLI-SILVA and VERGA, p. 180, pl. 110, fig. 1-4.

2007. *Pseudoguembelina hariaensis* NEDERBRAGT; DARVISHZAD *et al*., p. 142, pl. 2, fig. 2.

Remarks:

The biserial test of *Pseudoguembelina hariaensis* is followed by one or two, rarely more, sets of small multiserial chamberlets. Biserial part of the test is flaring throughout and sides of last few pairs of biserial chambers become subparallel. The test of *P. hariaensis* is also covered with costae like the other species of this genus. It differs from *P. palpebra* mainly in having thinner costae, less inflated chambers and more sets of multiserial chamberlets.

Stratigraphic Distribution:

The stratigraphic range of *P. hariaensis* is restricted to the uppermost part of the *Abathomphalus mayaroensis* zone (Latest Maastrichtian). In this study, it is found in the samples very close to the boundary and the taxon defines the

lower boundary of the last biozone of Maastrichtian. It is present until the boundary and also recorded in the first Paleocene sample.

Genus: *Racemiguembelina* MONTANARO GALLITELLI, 1957

Type species: *Guembelina fructicosa* EGGER, 1899

Racemiguembelina fructicosa EGGER, 1899

Pl. 8, fig. 7, 8; Pl. 17, fig. 13

1899. *Guembelina fructicosa* EGGER; p. 35, pl. 14, fig. 8, 9, 24.
1988. *Racemiguembelina fructicosa* EGGER; KELLER, p. 250, pl. 1, fig. 15.
1991. *Racemiguembelina fructicosa* EGGER; NEDERBRAGT, p. 363, pl. 10, fig. 5.
1998. *Racemiguembelina fructicosa* EGGER; ZEPEDA, p. 131, text fig. 10, fig. 2.
1999. *Racemiguembelina fructicosa* EGGER; ÖZKAN-ALTINER and ÖZCAN, p. 292, text fig. 4, fig. 10.
2002. *Racemiguembelina fructicosa* EGGER; KELLER *et al*., p. 280, pl. 3, fig. 2.
2003. *Racemiguembelina fructicosa* EGGER; ABRAMOVICH *et al*., p. 14, pl. 4, fig. 7, 8.
2004. *Racemiguembelina fructicosa* EGGER; CHACON *et al*., p. 590, text fig. 4, fig. M.
2004. *Racemiguembelina fructicosa* EGGER; PREMOLI-SILVA and VERGA, p. 187, pl. 117, fig. 1-6; p. 265, pl. 35, fig. 1-3.
2005. Racemiguembelina fructicosa EGGER; OBAIDALLA, p. 214, pl. 1, fig. 4.
2007. *Racemiguembelina fructicosa* EGGER; DARVISHZAD *et al*., p. 142, pl. 2, fig. 4.

Remarks:

Racemiguembelina fructicosa is easily differentiated from the other multiserial forms with its conical shape and multiserial chamberlets developing in 3-dimension after the initial biserial stage. In top view the outline of the taxon is seen like an ellipsoid. Main differences between *R. fructicosa* and *R. powelli* are that *R. fructicosa* has greater number of multiserial chamber sets and smaller chambers in multiserial stage than *R. powelli*.

Stratigraphic Distribution:

R. fructicosa is seen throughout *Abathomphalus mayaroensis* zone (Late Maastrichtian). In this study first appearance datum of this species marks the *R. fructicosa* zone. It disappears very close to the K/P boundary.

***Racemiguembelina powelli* SMITH and PESSAGNO, 1973**

Pl. 8, fig. 9; Pl. 17, fig. 14

1973. *Racemiguembelina powelli* SMITH and PESSAGNO; p. 35-37, pl. 11, fig. 4-12.
1991. *Racemiguembelina powelli* SMITH and PESSAGNO; NEDERBRAGT, p. 365, pl. 11, fig. 1.
2000. *Racemiguembelina powelli* SMITH and PESSAGNO; ARENILLAS *et al*., p. 208, pl. 1, fig. 1, 2.
2002. *Racemiguembelina powelli* SMITH and PESSAGNO; KELLER *et al*., p. 280, pl. 3, fig. 3.
2003. *Racemiguembelina powelli* SMITH and PESSAGNO; ABRAMOVICH *et al*., p. 14, pl. 4, fig. 5, 6.
2004. *Racemiguembelina powelli* SMITH and PESSAGNO; PREMOLI-SILVA and VERGA, p. 188, pl. 118, fig. 1-4.

Remarks:

Like *R. fructicosa*, *R. powelli* has also biserial and multiserial stages, a conical test and an ellipsoidal top view. However the number of multiserial chamber sets of *R. powelli* is less than the number of *R. fructicosa*. It has only 1 or 2 sets of multiserial chambers arranged in 3-dimension. The size of multiserial chambers is also larger in *R. powelli* than in *R. fructicosa*.

Stratigraphic Distribution:

The stratigraphic distribution of *R. powelli* ranges from the *Gansserina gansseri* zone (Late Campanian-Early Maastrichtian) to the end of the *Abathomphalus mayaroensis* zone (K/P boundary). In the studied samples *R. powelli* appears in the *P. acervulinoides* zone and disappears very close to the upper part of the *P. hariaensis* zone.

Family GLOBIGERINIDAE Carpenter, Parker, and Jones, 1862

Genus *Eoglobigerina* MOROZOVA, 1959

Type species: *Globigerina (Eoglobigerina) eobulloides* MOROZOVA, 1959

Eoglobigerina edita SUBBOTINA, 1953

Pl. 9, fig. 10-13

1953. *Globigerina edita* SUBBOTINA; p. 62, pl. 2, fig. 1a-c.

1996. *Eoglobigerina edita* SUBBOTINA; KOUTSOUUKOS, p. 331, text fig. 8, fig. 6, 7.

2005. *Eoglobigerina edita* SUBBOTINA; OBAIDALLA, p. 219, pl. 3, fig. 17.

Remarks:

Eoglobigerina edita is characterized by a moderately high trochospiral test with 4 to 5 globular chambers which increase gradually in size in the ultimate whorl, and a strongly lobate peripheral margin. The chambers of the early whorls are compactly arranged and closely packed together; those of the last whorl are arranged much more freely giving a scalloped appearance to the peripheral margin. This form can be differentiated from the other *Eoglobigerina* species with its turret-like dorsal surface which is due to the large size of the chambers in the earlier whorls.

Stratigraphic Distribution:

The stratigraphic distribution of *E. edita* is from the Pα zone (Early Paleocene) to the P1c zone (Early Paleocene) (Olsson *et al*., 1999). In this study we have defined this species within the *P. eugubina* (P1a) zone.

***Eoglobigerina eobulloides* MOROZOVA, 1959**

Pl. 9, fig. 5-9

1959. *Globigerina* (*Eoglobigerina*) *eobulloides* MOROZOVA; p. 1115, text fig. 1a-c.

1996. *Eoglobigerina eobulloides* MOROZOVA; KOUTSOUUKOS, p. 331, text fig. 8, fig. 3-5.

1999. *Eoglobigerina eobulloides* MOROZOVA; PARDO *et al*., p. 260, pl. 4, fig. 7, 8.

2005. *Eoglobigerina eobulloides* MOROZOVA; OBAIDALLA, p. 223, pl. 5, fig. 4.

2007. *Eoglobigerina eobulloides* MOROZOVA; MACLEOD *et al*., p. 107, text fig. 5, fig. T.

Remarks:

Eoglobigerina eobulloides is also one of the small forms of the genus *Eoglobigerina*. It has 4-5 globular chambers in the last whorl increasing moderately in size.

There are some uncertainties in the identification of this species and *Globigerina fringa* SUBBOTINA, 1950. Examination of the holotype under a light microscope shows it to be similar to *E. eobulloides* in general morphology and, thus, a possible senior synonym (Olsson *et al*., 1999). However, scanning electron micrographs (SEM) of the two species show that they are distinctly different species. *Globigerina fringa* has a coarsely cancellate wall similar to that of *Subbotina cancellata* BLOW, 1979 (Olsson *et al*., 1999). Therefore we have defined *Globigerina fringa* as a different species in our study.

According to Olsson *et al*. (1999) *E. eobulloides* is the same form with *Globigerina moskvini* SHUTSKAYA, 1953 and *E. eobulloides simplicissima* named by BLOW, 1979 is a four chambered form of *E. eobulloides*.

In our study we have used the original type description of the species made by Morozova and defined the species as *E. eobulloides* which have fairly trochospiral test, an open umbilicus, a lobate and oval outline and 4-5 distinctly spherical chambers in the last whorl showing rather slow increase in size.

Stratigraphic Distribution:

The stratigraphic distribution of *E. eobulloides* is from the P0 zone (Early Paleocene) to the P1 zone (Early Paleocene) (Olsson *et al*., 1999). In this study *E. eobulloides* has been defined from the *G. cretacea* (P0) zone to the end of the *P. eugubina* (P1a) zone.

Eoglobigerina fringa SUBBOTINA, 1950

Pl. 9, fig. 3, 4

1950. *Globigerina fringa* SUBBOTINA; p.104, pl. 5, fig. 19-21.

1988. *Globigerina fringa* SUBBOTINA; KELLER, p. 252, pl. 2, fig. 1.

1996. *Eoglobigerina fringa* SUBBOTINA; KOUTSOUUKOS, p. 331, text fig. 8, fig. 1, 2.

1999. *Eoglobigerina fringa* SUBBOTINA; PARDO *et al*., p. 260, pl. 4, fig. 9.

2002. *Eoglobigerina fringa* SUBBOTINA; KAROUI-YAAKOUB *et al*., p. 242, pl. 1, fig. 11.

2005. *Eoglobigerina fringa* SUBBOTINA; OBAIDALLA, p. 223, pl. 5, fig. 6.

2007. *Eoglobigerina fringa* SUBBOTINA; DARVISHZAD *et al*., p. 142, pl. 2, fig. 15.

Remarks:

Eoglobigerina fringa is one of the most important Danian forms. It has been defined by many authors as one of the first Paleocene forms and helped them to place the boundary. Subbotina (1950) defined the form as an extremely small form with a rounded and lobate periphery. It has four spherical, slightly compressed chambers in the last whorl showing a great increase in size. Olsson *et al*. (1999) criticized the original description and type level of the form and stated that the *Globigerina fringa* defined by Subbotina (1950) has a cancellate wall structure which would suggest a very advanced form for an Early Danian species. Olsson *et al*. (1999) believe that the form defined by the author belongs to the upper level of Danian. Therefore they suggest that four-chambered initial forms of Danian should be considered as a part of an *E. eobulloides* population. However we retain the species name *E. fringa* because we believe that *E. fringa* defined in the literature has distinguishable features. The authors, who preferred to use this species, have followed the original description of the form and there is a consistency in their observations. *E. fringa* differs from *E. eobulloides*

population in having less spherical chambers, lower trochospire and often less number of chambers.

Stratigraphic Distribution:

The stratigraphic distribution of *E. fringa* has been defined in the recent studies from the P0 zone (Early Paleocene) to the P1b-c (Early Paleocene) (Arenillas *et al*., 2000; Luciani, 2002; Karoui-Yaakoub *et al*., 2002). In this study it has been seen first in the initial samples of Paleocene and continued towards to the *P. eugubina* (P1a) zone.

Genus *Parasubbotina* OLSSON, HEMLEBEN, BERGGREN, and LIU 1992

Type species: *Globigerina pseudobulloides* PLUMMER, 1926

Parasubbotina pseudobulloides PLUMMER, 1926

Pl. 11, fig. 1, 2; Pl. 18, fig. 17-20

1926. *Globigerina pseudo-bulloides* PLUMMER; p. 133, pl. 8, fig. 9a-c.
1988. *Globigerina pseudobulloides* PLUMMER; KELLER, p. 256, pl. 3, fig. 2.
1996. *Parasubbotina pseudobulloides* PLUMMER; KOUTSOUUKOS, p. 333, text fig. 9, fig. 1-3.
2000. *Parasubbotina pseudobulloides* PLUMMER; ARENILLAS *et al*., p. 208, pl. 1, fig. 18, 19.
2002. *Parasubbotina pseudobulloides* PLUMMER; KAROUI-YAAKOUB *et al*., p. 242, pl. 2, fig 9.
2004. *Parasubbotina pseudobulloides* PLUMMER; ARENILLAS *et al*., p. 82, text fig. 4, fig. N.
2005. *Parasubbotina pseudobulloides* PLUMMER; OBAIDALLA, p. 219, pl. 3, fig. 1, 2.

2007. *Parasubbotina pseudobulloides* PLUMMER; DARVISHZAD *et al*., p. 142, pl. 2, fig. 17.

Remarks:

Parasubbotina pseudobulloides is one of the very important forms of Paleocene and identified easily with its very low trochospiral test, lobate and broadly rounded periphery and 5 chambers in the last convolution showing a very rapid size increase. Its globular chambers are slightly ovoid. It really resembles *Praemurica pseudoinconstans* but differs from it in having faster increase in chamber size and more lobate and inflated outline. This species is one of the Early Paleocene species which has a clear definition. Unlike most of the other Danian forms there is a consistency in the pictures of the form in several papers.

Stratigraphic Distribution:

The stratigraphic distribution of *P. pseudobulloides* is from the latest part of Pα zone (Early Paleocene) to the P3a zone (Early Late Paleocene) (Olsson *et al*., 1999). In this study it has been seen within the *P. eugubina* (P1a) zone.

Genus *Subbotina* BROTZEN and POZARYSKA, 1961

Type species: *Globigerina triloculinoides* PLUMMER, 1926

Subbotina triloculinoides PLUMMER, 1926

Pl. 11, fig. 4-9; Pl. 18, fig. 21-28

1926. *Globigerina triloculinoides* PLUMMER; p. 134, pl. 8, fig. 10a-b.
1996. *Subbotina triloculinoides* PLUMMER; KOUTSOUUKOS, p. 331, text fig. 8, fig. 15.
2000. *Subbotina triloculinoides* PLUMMER; ARENILLAS *et al*., p. 208, pl. 1, fig. 15.
2002. *Subbotina triloculinoides* PLUMMER; KAROUI-YAAKOUB *et al*., p. 242, pl. 2, fig. 12-16.
2004. *Subbotina triloculinoides* PLUMMER; ARENILLAS *et al*., p. 82, text fig. 4, fig. Q.
2005. *Subbotina triloculinoides* PLUMMER; OBAIDALLA, p. 221, pl. 4, fig. 6.
2007. *Subbotina triloculinoides* PLUMMER; MACLEOD *et al*., p. 107, text fig. 5, fig. A.

Remarks:

The main characteristic of *Subbotina triloculinoides* is its trilobate test with 3-3,5 chambers in the ultimate whorl which increase rapidly in size. The ultimate and highly globose chamber occupies up to 1/2 of the test. In other words, the size of the last chamber of *S. triloculinoides* is almost equal to the total size of the previous chambers. With its distinctly great last chamber it is really easily distinguished. *S. triloculinoides* is distinguished from *S. trivialis* with its higher increase in chamber size and smaller size of the chambers of the early whorl.

Stratigraphic Distribution:

The stratigraphic distribution of *S. triloculinoides* is from the P1b zone (Early Paleocene) to the P4 zone (Late Paleocene) (Olsson *et al*., 1999). In our work it is very common and identified throughout the *P. eugubina* (P1a) zone.

Subbotina trivialis SUBBOTINA, 1953

Pl. 11, fig. 10, 11

1953. *Globigerina trivialis* SUBBOTINA; p. 64, pl. 4, fig. 4a-c.
1996. *Subbotina trivialis* SUBBOTINA; KOUTSOUUKOS, p. 331, text fig. 8, fig. 13, 14.
1999. *Eoglobigerina trivialis* SUBBOTINA; PARDO *et al*., p. 260, pl. 4, fig. 11, 12.
2004. *Eoglobigerina trivialis* SUBBOTINA; ARENILLAS *et al*., p. 82, text fig. 4, fig. O, P.
2005. *Subbotina trivialis* SUBBOTINA; OBAIDALLA, p. 221, pl. 4, fig. 11.

Remarks:

The main characteristic of *Subbotina trivialis* is its 4-4,5 almost regular, spherical chambers in the last whorl which differ very slightly in size. The ultimate chamber is equal to, or slightly smaller than the penultimate one. The chambers are closely packed together and partially overlap each other. Because of these unique properties it is easy to identify this form from the other *Subbotina* species.

Stratigraphic Distribution:

The stratigraphic distribution of *S. trivialis* is from the Pα zone (Early Paleocene) to the P2 zone (Late Early Paleocene). In the studied samples it is

quite common and identified in the *G. cretacea* (P0) and *P. eugubina* (P1a) zones.

Genus *Globanomalina* HAQUE 1956

Type species: *Globanomalina ovalis* HAQUE, 1956

Globanomalina archeocompressa BLOW, 1979

Pl. 10, fig. 4-6

1979. *Globorotalia* (*Turborotalia*) *archeocompressa* BLOW; p. 1049, pl. 58, fig. 8-9.

1988. *Globorotalia archeocompressa* BLOW; KELLER, p. 252, pl. 2, fig. 19, 20.

2005. *Globanomalina archeocompressa* BLOW; OBAIDALLA, p. 221, pl. 4, fig. 12, 13.

Remarks:

Globanomalina archeocompressa is the first species of *Globanomalina* that appeared in the Early Danian and has a very small size like the other Danian species (less than 130 μm). It is identified with its low trochospiral test and 5 chambered last convolution. Most distinguishable character of the form is the compression of the subglobular to subrectangular chambers. Both spiral and umbilical view of the chambers are inflated and compressed. Another property that helped us to differentiate *G. archeocompressa* is its axial-apertural profile. In axial-apertural profile, the test appears biconcave (flattish spiral side) because of the depression of the initial spire below the level of the dorsal surfaces of the later chambers.

Stratigraphic Distribution:

The stratigraphic distribution of *G. archeocompressa* is from the P0 zone (Early Paleocene) to the P1b zone (Early Paleocene) (Olsson *et al*., 1999). In this study it has been identified in the *G. cretacea* (P0) and *P. eugubina* (P1a) zones.

Genus *Praemurica* OLSSON, HEMLEBEN, BERGGREN and LIU, 1992

Type species: *Globigerina (Eoglobigerina) taurica* MOROZOVA, 1961

Praemurica pseudoinconstans BLOW, 1979

Pl. 11, fig. 3

1979. *Globorotalia* (*Turborotalia*) *pseudoinconstans* BLOW; p. 1105, pl. 67, fig. 4

1996. *Praemurica pseudoinconstans* BLOW; KOUTSOUUKOS, p. 331, text fig. 8, fig. 1.

Remarks:

Praemurica pseudoinconstans is identified with its low trochospiral test and 5-6 chambers in the last whorl which increase gradually in size. The rate of growth in the chamber size is slightly faster towards to the final chambers. Its axial-apertural profile is almost biconvex with rounded peripheral margins. It resembles *P. pseudobulloides* however its equatorial profile is moderately lobulate and rate of increase in the chamber size is slower.

Stratigraphic Distribution:

The stratigraphic distribution of *P. pseudoinconstans* is from the Pα zone (Early Paleocene) to the P2 zone (Late Early Paleocene) (Olsson *et al*., 1999). In this study it has been identified within the *P. eugubina* (P1a) zone.

***Praemurica taurica* MOROZOVA, 1961**

Pl. 10, fig. 7, 8

1961. *Globigerina* (*Eoglobigerina*) *taurica* MOROZOVA; p. 10, fig. 5a-c.
1988. *Globigerina (Eoglobigerina) taurica* MOROZOVA; KELLER, p. 252, pl. 2, fig. 4, 5.
1996. *Praemurica taurica* MOROZOVA; KOUTSOUUKOS, p. 331, text fig. 8, fig. 8-9.
2002. *Praemurica taurica* MOROZOVA; KAROUI-YAAKOUB *et al*., p. 242, pl. 2, fig. 13.
2005. *Praemurica taurica* MOROZOVA; OBAIDALLA, p. 219, pl. 3, fig. 16.

Remarks:

Praemurica taurica is differentiated with its greater number of subspherical chambers in the last whorl (5-6), which increase rapidly and uniformly in size. In equatorial view it has a subpolygonal outline and in axial view equally biconvex appearance. One of the most important characteristics of the form is the nature of its last chamber which is asymmetrical, flattened at the apertural face and slightly shifted toward the umbilical surface. It is differentiated from the *P. pseudoinconstans* in having often greater number of chambers and less lobate and subpolygonal periphery.

Stratigraphic Distribution:

The stratigraphic distribution of *P. taurica* is from the P0 zone (Early Paleocene) to the P1b zone (Early Paleocene) (Olsson *et al*., 1999). In this study it has been recorded within the *P. eugubina* (P1a) zone.

Family GUEMBELITRIIDAE MONTANARO GALLITELLI, 1957

Genus *Guembelitria* CUSHMAN, 1933

Type species: *Guembelitria cretacea* CUSHMAN, 1933.

Guembelitria cretacea CUSHMAN, 1933

Pl. 12, fig. 1; Pl. 20, fig. 1-15

1933. *Guembelitria cretacea* CUSHMAN; p. 37, pl. 4, fig. 12 a, b.
1988. *Guembelitria cretacea* CUSHMAN; KELLER, p. 252, pl. 2, fig. 1.
2003. *Guembelitria cretacea* CUSHMAN; ABDELGHANY, p. 399, text fig. 8, fig. 12.
2004. *Guembelitria cretacea* CUSHMAN; ARENILLAS *et al*., p. 82, text fig. 4, fig. F.

Remarks:

Guembelitria cretacea is one of the most distinguishable species in the Late Maastrichtian and Early Danian with its triserial test. It has globular chambers, depressed sutures and large, semicircular or semi-elliptical aperture at the inner margin of the last-formed chamber. Although Olsson *et al*. (1999) consider all triserial species as variants of wide-ranging population of *G. cretacea*, there are other triserial *Guembelitria* forms defined in the literature. These are *G. trifolia*, *G. irregularis* and *G. danica*. *G. trifolia* is identified with its very short spire; *G. irregularis* with its irregularly stacked chambers and

G. danica with its highly regularly arranged chambers and elongate spires (Karoui-Yaakoub *et al*., 2002). In our study *Guembelitria* forms in the washed samples are very rare. However in the thin sections these triserial forms were very abundant (especially above the boundary) and easy to distinguish. Since we had very rare specimens in the washed samples and thin section views were inadequate to differentiate them in species level, all triserial forms identified in this study were classified as *G. cretacea* following the suggestion of Olsson *et al*. (1999).

Stratigraphic Distribution:

G. cretacea is one of the survived species and its stratigraphic distribution is from the *Dicarinella concavata* zone (Coniacian) to the P1b zone (Early Paleocene) (Olsson *et al*., 1999; Premoli-Silva and Verga, 2004). In our study we have defined this species throughout the whole section from the Maastrichtian to the Danian sediments. Above the boundary the abundance of this species shows a remarkable increase.

Genus *Globoconusa* KHALILOV, 1956

Type species: *Globoconusa conusa* KHALILOV, 1956 (= *Globigerina daubjergensis* BRONNIMANN, 1953)

Globoconusa daubjergensis BRONNIMANN, 1952

Pl. 10, fig. 2, 3; Pl. 18, fig. 10-16

1953. *Globigerina daubjergensis* BRONNIMANN; p. 340, text fig. 1.

1999. *Globastica daubjergensis* BRONNIMANN; PARDO *et al*., p. 260, pl. 4, fig. 10.

2002. *Globoconusa daubjergensis* BRONNIMANN; KAROUI-YAAKOUB *et al*., p. 242, pl. 2, fig. 14-15.

2007. *Globoconusa daubjergensis* BRONNIMANN; DARVISHZAD *et al*., p. 142, pl. 2, fig. 16.

Remarks:

Globoconusa daubjergensis is also one of the very small Danian forms. It has a high trochospiral test which is noticeably lobulate. Most important feature of the form is its 3-4 gradually increasing chambers in the dominant final whorl and distinctly pointed initial spire. *G. conusa* CHALILOV, 1956 resembles *G. daubjergensis*. Olsson *et al*. (1999) put *G. conusa* in the synonym list of *G. daubjergensis* and therefore we did not differentiate these two *Globoconusa* forms from each other.

Stratigraphic Distribution:

The stratigraphic distribution of *G. daubjergensis* is from the Pα zone (Early Paleocene) to the P1c zone (Early Paleocene) (Olsson *et al*., 1999). In this study it has been identified from the beginning of the *P. eugubina* (P1a) zone towards to the end of the measured section.

***Globoconusa minutula* LUTERBACHER and PREMOLI-SILVA, 1964**

Pl. 9, fig. 1, 2

1964. *Globigerina minutula* LUTERBACHER and PREMOLI-SILVA; pl. 2, fig. 5.

1988. *Globoconusa minutula* LUTERBACHER and PREMOLI-SILVA; BRINKHUIS and ZACHARIASSE, p. 163, pl. 2, fig. 1-7, 13 (non Luterbacher and Premoli-Silva, 1964); p. 179, pl. 3, fig. 10, 14 (non Luterbacher and Premoli-Silva, 1964).

2000. *Globoconusa minutula* LUTERBACHER and PREMOLI-SILVA; ARENILLAS *et al*., p. 209, pl. 2, fig. 6.

2005. *Globoconusa minutula* LUTERBACHER and PREMOLI-SILVA; OBAIDALLA, p. 223, pl. 5, fig. 2, 3.

Remarks:

Globoconusa minutula was first described by Luterbacher and Premoli-Silva in 1964 as *Globigerina minutula* along the Gubbio section together with *Globigerina eugubina*. The holotype drawing illustrates a very low trochospiral composed of 2-2,5 whorls. In the last whorl it has 3 chambers and the last chamber makes up the half of the test. It is a very minute form and has been identified by many authors as one of the first Danian species (Ben Abdelkader *et al*., 1997; Luciani, 1997; Arenillas *et al*., 2000; Obaidalla, 2005; Arenillas *et al*., 2006).

There is another form in the literature with the same taxon name. Some authors (Brinkhuis and Zachariasse, 1988; Smit, 1982) have described a high trochospiral species as *G. minutula*, which is obviously not the same form with the holotype described by Luterbacher and Premoli-Silva (1964). This type of high trochospiral "*Globoconusa minutula*" forms with a pointed initial portion has been placed as a synonym with *Parvularugoglobigerina extensa* BLOW, 1979 by Olsson *et al*. (1999). In our study we have used the holotype description of the form described by Luterbacher and Premoli-Silva (1964).

Stratigraphic Distribution:

The global stratigraphic range of *Globoconusa minutula* is not given in the main atlases; however the studies defined this species state the stratigraphic range as from the beginning of P0 zone to the Pα or P1a zones (Early Paleocene) (Luciani, 1997; Obaidalla, 2005). We have also found this species in the first samples of Paleocene towards to the lower portion of the *P. eugubina* (P1a) zone.

Genus *Parvularugoglobigerina* HOFKER, 1978

Type species: *Globigerina eugubina* Luterbacher and Premoli-Silva, 1964

Parvularugoglobigerina eugubina LUTERBACHER and PREMOLI-SILVA, 1964

Pl. 10, fig. 1

1964. *Globigerina eugubina* LUTERBACHER and PREMOLI-SILVA; p. 105, pl. 2, fig. 8a-c.

1988. *Globigerina eugubina* LUTERBACHER and PREMOLI-SILVA; KELLER, p. 252, pl. 2, fig. 8-10.

1997. *Parvularugoglobigerina eugubina* LUTERBACHER and PREMOLI-SILVA; LUCIANI, p. 811, text fig. 7, fig. 1-6.

1999. *Parvularugoglobigerina eugubina* LUTERBACHER and PREMOLI-SILVA; PARDO *et al*., p. 260, pl. 4, fig. 1, 2.

2000. *Parvularugoglobigerina eugubina* LUTERBACHER and PREMOLI-SILVA; ARENILLAS *et al*., p. 208, pl. 1, fig. 9, 10.

2002. *Parvularugoglobigerina eugubina* LUTERBACHER and PREMOLI-SILVA; KAROUI-YAAKOUB *et al*., p. 242, pl. 2, fig. 1-4.2005. *Parvularugoglobigerina eugubina* LUTERBACHER and PREMOLI-SILVA; OBAIDALLA, p. 219, pl. 3, fig. 9-11.

2004. *Parvulorugoglobigerina eugubina* LUTERBACHER and PREMOLI-SILVA; ARENILLAS *et al*., p. 82, text fig. 4, fig. J, K.

2007. *Parvularugoglobigerina eugubina* LUTERBACHER and PREMOLI-SILVA; MACLEOD *et al*., p. 107, text fig. 5, fig. D, E.

Remarks:

Parvularugoglobigerina eugubina exhibits extremely variable morphology (Olsson *et al*., 1999). In the holotype description it is stated that the

form is very small, low to moderately trochospiral and has 6 chambers in the final whorl that increase gradually in size. In our samples the most distinguishable characteristics of *P. eugubina* are its distinctly radial sutures on the umbilical side and its prominent final chamber that is distinctly protruding and occupying 1/4 to 1/5 of the test surface.

Stratigraphic Distribution:

The stratigraphic range of the form is generally given confined in the Pα zone (Early Paleocene) (Olsson *et al*., 1999). The first appearance datum of this form marks the beginning of the P1a zone in this study. On the other hand, the last appearance datum has not been encountered within the measured section.

Genus *Woodringina* LOEBLICH and TAPPAN, 1957

Type species: *Woodringina claytonensis* LOEBLICH and TAPPAN, 1957

Woodringina claytonensis LOEBLICH and TAPPAN, 1957

Pl. 19, fig. 7-16

1957. *Woodringina claytonensis* LOEBLICH and TAPPAN; B, p. 39, fig. 1a-d.
1996. *Woodringina claytonensis* LOEBLICH and TAPPAN; KOUTSOUUKOS, p. 327, text fig. 6, fig. 1-3.
2004. *Chiloguembelina claytonensis* LOEBLICH and TAPPAN; KELLER and PARDO, p. 97, pl. 1, fig. 15.
2005. *Woodringina claytonensis* LOEBLICH and TAPPAN; OBAIDALLA, p. 219, pl. 3, fig. 5.

Remarks:

Woodringina claytonensis is one of the first Danian biserial forms. Its tiny test is flaring rapidly and composed of 3-5 pairs of biserial chambers. The most distinguishable morphology of *W. claytonensis* is the slightly twisted plane of biseriality. Furthermore, in some of the species triseriality in the first portion of the test may be observed. It is differentiated from *W. hornerstownensis* in having less number of biserial pairs and more distinctly twisted biserial portion of the test.

Stratigraphic Distribution:

The stratigraphic distribution of *W. claytonensis* is from the P0 zone (Early Paleocene) to the P1b zone (Early Paleocene) (Olsson *et al*., 1999). In this study it is recorded from the beginning of the P1a zone and continued until the end of the section.

***Woodringina hornerstownensis* OLSSON, 1960**

Pl. 19, fig. 1-6; Pl. 12, fig. 2-4

1960. *Woodringina hornerstownensis* OLSSON; p. 29, pl. 4, fig. 18, 19.
1988. *Woodringina hornerstownensis* OLSSON; KELLER, p. 252, pl. 2, fig. 15.
1996. *Woodringina hornerstownensis* OLSSON; KOUTSOUUKOS, p. 327, text fig. 6, fig. 6-13.
1997. *Woodringina hornerstownensis* OLSSON; LUCIANI, p. 804, text fig. 3, fig. 17, 18.
1999. *Woodringina hornerstownensis* OLSSON; PARDO *et al*., p. 254, pl. 1, fig. 16.
2004. *Woodringina hornerstownensis* OLSSON; KELLER and PARDO, p. 97, pl. 1, fig. 16.

2005. *Woodringina hornerstownensis* OLSSON; OBAIDALLA, p. 219, pl. 3, fig. 3.

2007. *Woodringina hornerstownensis* OLSSON; MACLEOD *et al*., p. 107, text fig. 5, fig. I.

Remarks:

Woodringina hornerstownensis is distinguished with its small, elongate, biserial, slightly twisted and rather rapidly tapering test. Like in the *W. claytonensis* the initial part of the test may consists of a whorl of three chambers. It has a slender test, in other words the test is about twice as long as broad. *W. hornerstownensis* is differentiated from *W. claytonensis* in having less twisted biserial portion and more number of pairs. *Woodringina hornerstownensis* often has six or more pairs of biserial chambers, while *W. claytonensis* is usually limited to five or fewer.

Stratigraphic Distribution:

The stratigraphic distribution of *W. hornerstownensis* is given as from the Pα zone (Early Paleocene) to the P3b zone (Early Late Paleocene) in Olsson *et al*. (1999). However we see that some authors stated this species in the P0 zone already (Koutsoukos, 1996; Karoui-Yaakoub *et al*., 2002, Luciani, 2002). In our study we have also defined *W. hornerstownensis* in P0 zone first, and then recorded it until the last sample.

Family CHILOGUEMBELINIDAE REISS, 1963

Genus *Chiloguembelina* LOEBLICH and TAPPAN, 1956

Type species: *Chiloguembelina midwayensis* CUSHMAN

Chiloguembelina midwayensis CUSHMAN, 1940

Pl. 19, fig. 21-24

1940. *Guembelina midwayensis* CUSHMAN; p. 65, pl. 11, fig. 15.

2002. *Chiloguembelina midwayensis* CUSHMAN; KAROUI-YAAKOUB *et al*., p. 242, pl. 2, fig. 5.

2004. *Chiloguembelina midwayensis* CUSHMAN; KELLER and PARDO, p. 97, pl. 1, fig. 14.

2005. *Chiloguembelina midwayensis* CUSHMAN; OBAIDALLA, p. 219, pl. 3, fig. 4.

Remarks:

Chiloguembelina midwayensis is one of the Early Danian biserial forms. Its test is small, compressed, rapidly tapering and twice as long as broad. Most prominent attribute of *C. midwayensis* is its chamber shape and arrangment. The early chambers of the form are subspherical and successive chambers increase more rapidly in breadth than in height. Furthermore, each late-stage chamber crosses the coiling axis and overlaps the immediately preceding chamber.

Stratigraphic Distribution:

The stratigraphic distribution of *C. midwayensis* is from the Pα zone (Early Paleocene) to the P5 zone (Late Paleocene) (Olsson *et al*., 1999). In this study it is present within the P1a zone.

Chiloguembelina morsei KLINE, 1943

Pl. 19, fig. 17-20

1943. *Guembelina morsei* KLINE; p. 44, pl. 7, fig. 12.

1996. *Guembelina morsei* KLINE; KOUTSOUUKOS, p. 326, text fig. 6, fig. 24-25.

Remarks:

The test of the form is quite small like the other biserial forms of Early Paleocene. The chambers of the *Chiloguembelina morsei* are regularly tapering with greatest breadth at apertural end. Successive chambers of the overlap especially in late ontogeny stage, however this overlap is not obvious as in the *C. midwayensis*. The most important diffrence between *Chiloguembelina morsei* and *C. midwayensis* is that the former has a narrower test and more globular chambers.

Stratigraphic Distribution:

The stratigraphic distribution of *C. morsei* is from the Pα zone (Early Paleocene) to the P1c zone (Early Paleocene) (Olsson *et al*., 1999). In this study it has been observed within the *G. cretacea* (P0) and *P. eugubina* (P1a) zones.

Family HETEROHELICIDAE CUSHMAN, 1927

Genus *Zeauvigerina* FINLAY, 1939

Type Species: *Zeauvigerina zelandica* FINLAY, 1939, p. 541-542, pl. 69, fig. 4a.

Zeauvigerina waiparaensis JENKINS, 1966

Pl. 12, fig. 6, 7; Pl. 19, fig. 25

1966. *Chiloguembelina waiparaensis* JENKINS; p. 1095, pl. 1, fig. 1-6.

1999. *Chiloguembelina waiparaensis* JENKINS; PARDO *et al*., p. 256, pl. 2, fig. 1-4.

2004. *Chiloguembelina waiparaensis* JENKINS; KELLER and PARDO, p. 97, pl. 1, fig. 11, 12.

Remarks:

Zeauvigerina waiparaensis is one of the Early Danian minute biserial forms and distinguished by its irregular outline of the test and uneven biserial chamber addition. Besides the terminal oval-shaped aperture is seen only in this species among the all Danian biserial forms.

Stratigraphic Distribution:

The stratigraphic distribution of this from is from the Late Maastrichtian to the P5 zone (Late Paleocene) (Olsson *et al*., 1999). In this study it has not been encountered in the Late Maastrichtian samples. It has been first recorded in the *G*. *cretacea* (P0) zone and seen also in the first samples of the *P*. *eugubina* (P1a) zone.

CHAPTER 7

DISCUSSION AND CONCLUSIONS

In this study K/P boundary in the Haymana basin (Central Anatolia, Turkey) was examined with a multidisciplinary approach. Biostratigraphical, mineralogical and facies changes across the boundary were investigated and accordingly a sequence stratigraphical model was conducted. A 29.41 m thick section was measured and 90 samples throughout the section were analyzed.

K/P boundary is one of the most important global events that the world undergone. At the boundary a mass extinction occurred and this global event is one of the five big mass extinctions that the world suffered (Raup and Sepkoski, 1982). Many marine organisms were affected intensely including the planktonic foraminifera. The change in the planktonic foraminifera is one of the best and most applicable methods in order to mark the K/P boundary. For this reason, biostratigraphy and chronostratigraphy of this study was established based on the variations in the planktonic foraminiferal genera. Since the sampling interval plays a crucial role in the determination of the planktonic foraminiferal biozones across the boundary, samples were collected with a cm-scale sampling interval. From the 2 m interval including the boundary level 30 samples were collected and analyzed.

A detailed taxonomical study was carried out based on the coiling mode, peripheral shape, shape-arrangement and number of the chambers, presence or absence of keels, number of the keels and sutural properties of the species. Accordingly 14 genera and 47 species in the Late Cretaceous; 10 genera and 17 species in the Early Paleocene were identified. All the large, ornamented and keeled forms of the genera *Globotruncana*, *Globotruncanita*, *Globotruncanella*, *Rugoglobigerina*, *Racemiguembelina*, *Pseudotextularia*, and *Planoglobulina* are

extinct, whereas minute and delicate first Danian forms of the genera *Globoconusa*, *Eoglobigerina Globanomalina*, and *Woodringina* appeared at the boundary. K/P boundary in this study was placed based on the first appearance of the Paleocene forms, i.e. at the extinction horizon of the Cretaceous forms.

Some Cretaceous species were observed in the first Danian sample within a 20 cm interval. These are *Globotruncana arca*, *Globotruncana orientalis*, *Globotruncanita pettersi*, *Globotruncanita stuartiformis*, *Rugoglobigerina hexacamerata*, *Rugoglobigerina pennyi*, *Rugoglobigerina rugosa*, *Globigerinelloides prairiehillensis*, *Globigerinelloides* sp., *Heterohelix globulosa*, *Heterohelix punctulata*, *Pseudotextularia elegans*, *Pseudotextularia nuttalli*, *Planoglobulina acervulinoides*, *Pseudoguembelina hariaensis*, *Laeviheterohelix glabrans*, *Hedbergella holmdelensis*, *Hedbergella monmouthensis*, and *Guembelitria cretacea*. It is difficult to conclude whether these species are reworked or survived species. Species survivorship concept across the K/P boundary has been discussed by various authors and this subject is still in debate. However, many recent studies agree that all the large, complex, ornamented, tropical Cretaceous forms like globotruncanids, racemiguembelinids and rugoglobigerinids are extinct at the boundary; and small, robust, dwarfed forms like heterohelicids, pseudotextularids, hedbergellids and guembelitrids survived across the boundary (Keller, 1988, 1989a, 1989b; Keller *et al*., 1995; Canudo *et al*., 1991; MacLeod and Keller, 1994; Pardo *et al*., 1996; Luciani, 1997, 2002; Pardo *et al*., 1999; Karoui-Yaakoub *et al*., 2002; Keller and Pardo, 2004; Paul, 2005). Therefore it might be considered that in our section, small cosmopolitan surface-water dweller forms such as *Heterohelix*, *Laeviheterohelix*, *Pseudoguembelina*, *Globigerinelloides*, *Hedbergella* and *Guembelitria* in the first Danian sample are survived species. On the other hand, keeled deeper dwellers and larger forms like *Globotruncana*, *Globotruncanita*, *Rugoglobigerina* and *Planoglobulina* in the first Danian samples should be considered as reworked species.

Based on the first and last appearances of the key planktonic species 5 biozones were established in this study. These are from older to younger: *Planoglobulina acervulinoides* zone, *Racemiguembelina fructicosa* zone, *Pseudoguembelina hariaensis* zone for the Late Maastrichtian; *Guembelitria cretacea* (P0) zone and *Parvulorugoglobigerina eugubina* (P1a) zone for the Early Danian. This study is the one of the most detailed biostratigraphic study across the K/P boundary beds in Turkey and defines the Early Danian P0 and P1a planktonic foraminiferal biozones for the first time.

In order to detect the mineralogical changes across the boundary bulk and clay mineralogy of 12 samples collected from the 2 m interval including the boundary were analyzed by using X-ray diffractometry (XRD). Calcite, detrital minerals like quartz, plagioclase and K-feldspar, and the clay minerals comprising the smectite group montmorillonite and chlorite are the main components of the rocks. Calcite content averages between 33 to 70% in volume, whereas total percentage of the clay minerals made up approximately 17 to 30%. Quartz is a minor element for some of the samples with the 3% volume but its percentage can reach to 20% for some of the samples. The relative percentages of the plagioclase and K-feldspar range between 3 to 14%. There are also some amphiboles, illite and smectite-chlorite mixed layers in the samples with very minor amounts.

In our section, a marked drop in carbonate content (11%) is recorded at the base of the P0 zone. However, the percentage of calcium carbonate is still too high (39%) at the boundary for properly defining the boundary clay. This behavior of calcium carbonate could indicate that the carbonate/clastic sedimentation ratio in the measured section does not purely reflect the primary productivity of carbonate plankton and but also related to sea-level fluctuations and terrestrial sediment input related to tectonic pulses. When calcite drops at the boundary beds, an increase in the detrital minerals like quartz and feldspars are seen. This opposite relation may be explained with the sea-level fluctuations and related changes in the rate of terrestrial influx to the basin.

There is an increase in the clay minerals, namely smectite and chlorite in the boundary beds. They both reach their maximum percentage volumes approximately 25 cm above the boundary, at the base of P1a zone. Smectite group minerals commonly associated with weathering and transport (Flügel, 2004). Therefore, the increase in the smectites can be explained with the increase in sediment influx around the boundary. This result can also be correlated with the increase in chlorite, quartz and feldspars. The increase in the detrital and clay minerals and the simultaneous decrease in the calcite mineral can also be explained with the low production of carbonate related to the extinction of the calcareous microfossils around the boundary.

A detailed microfacies analysis was carried out in order to find out the depositional history of the measured section and 10 microfacies type were determined. The results of the microfacies analyses show that the deposition took place in a slope to basin environment. The section begins with packstones, grainstones, wackestones and floatstones composed of numerous large benthic foraminifera, calcareous red algae, echinodermata and mollusks fragments, bryozoans; and few planktonic foraminifera. Then silty marls with benthic and planktonic foraminifera and calcareous red algae deposited. Towards the K/P boundary silty limestones with benthic and planktonic foraminifera are seen. Just at the boundary beds a great number of large green clay minerals were encountered showing prominent similarities with the clay minerals found in different K/P boundary beds in various localities of the world. Besides, some spheroid grains were recognized which resemble microtektites. In order to investigate their origin further research is needed.

Based on the microfacies analyses and field observations sequence stratigraphical framework throughout the measured section was conducted. The lowermost part of the section is represented with a highstand systems tract (HST). According to our observations carbonates are prograding into the basin during highstand shedding when the accommodation is not enough for their growth. Above the HST a type 2 sequence boundary is seen and shelf margin

wedge (SMW) beds are represented with silty limestone rich in quartz, planktonic and benthic foraminifera and ammonites. Overlying silty marl succession deposited in the transgressive systems tract (TST) and towards to the boundary carbonates enter into the system again indicating the beginning of the new HST. Based on this model K/P boundary beds are coinciding in the transition of the TST to HST, namely a maximum flooding surface (MFS).

Based on the Haq *et al*. (1987) eustatic sea-level curve and the curve proposed by Keller and Stinnesbeck (1996) showing the sea-level fluctuations at the K/P transition, a transgression marks the end of the Maastrichtian and maximum flooding coincides with the K/P boundary. This shows that the K/P section in the Haymana basin was recorded with very similar depositional patterns with the other localities of the world. This is an evidence that the eustatic sea-level control overprints the tectonic controls in the Haymana basin. XRD results also support an eustatic sea-level fall in Early Danian showing an increase in the detrital minerals.

This study delineated the K/P transition in a tectonically active, fore arc Haymana basin in the Central Anatolia and showed that K/P boundary has been recorded in a similar pattern with the many other K/P sections around the world in terms of planktonic foraminiferal, mineralogical and sea-level changes. In order to detect the triggering mechanism of the mass extinction across the boundary a further research is being to plan in the future. Platinum-group element iridium showing significant positive anomalies at the K/P boundary sections is an evidence for an extraterrestrial impact. An iridium analysis on the boundary samples will show whether the Haymana basin was affected from the Chicxulub impact (Alvarez *et al*., 1988) or not. Besides, the magnetostratigraphy of the section will be investigated across the measured section. For the magnetostratigraphy, the section has already been sampled and it is aimed to determine the normal and reverse zones across the measured section and correlate the results with the data already obtained.

REFERENCES

Abramovich, S., Keller, G., 2003. Planktic foraminiferal response to the latest Maastrichtian abrupt warm event: a case study from South Atlantic DSDP Site 525A. Mar. Micropaleontology., 48, 225-249.

Abramovich, S., Almogi-Labin, A., Benjamini, C., 1998. Decline of the Maastrichtian pelagic ecosystem based on planktic foraminifera assemblage change: implications for the terminal Cretaceous faunal crisis. Geology, 26, 63-66.

Abramovich, S., Keller, G., Stüben, D., Berner, Z., 2003. Characterization of Late Campanian and Maastrichtian planktonic foraminiferal depth habitats and vital activities based on stable isotopes. Palaeogeography, Palaeoclimatology, Palaeoecology, 202, 1-29.

Abdelghany, O., 2003. Late Campanian-Maastrichtian foraminifera from the Simsima Formation on the western side of the Northern Oman Mountains. Cretaceous Research, 24, 391–405.

Adatte, T., Rumley, G., 1989. Sedimentology and mineralogy of Valanginian and Hauterivian in the stratotypic region (Jura mountains, Switzerland). In: Wiedmann, J. (Ed.), Cretaceous of the Western Tethys Proceedings 3rd International Cretaceous Symposium. Scheizerbart'sche Verlagsbuchandlhung, Stuttgart, 329-351.

Adatte, T., Keller, G., Stinnesbeck, W., 2002a. Late Cretaceous to early Paleocene climate and sea-level fluctuations: the Tunisian record. Palaeogeography, Palaeoclimatology, Palaeoecology, 178, 165–196.

Adatte, T., Keller, G., Burns, S., Stoykova, K. H., Ivanov, M. I., Vangelov, D., Kramar, U., Stüben, D., 2002b. Paleoenvironment across the Cretaceous-Tertiary transition in eastern Bulgaria. Geol. Soc. Am. Spec. Pap., 356, 231– 251.

Akarsu, İ., 1971. II. Bölge AR/TPO/747 nolu sahanın terk raporu. Pet. İş. Gen. Md., Ankara.

Akyazı, M., Özgen, N., İnan, N., 1998. Adriyatik platformu ve Torid platformu'nda bentik foraminiferlerle K/T geçişinin karşılaştırılması. Türkiye Jeoloji Bülteni, 41/2, 165-175.

Alvarez, L. W., Alvarez, W., Asaro, F., Michel, H. V., 1980. Extraterrestrial cause for the Cretaceous–Tertiary extinction. Science, 208, 1095–1108.

Ando, H., 2003. Stratigraphic correlation of Upper Cretaceous to Paleocene forearc basin sediments in Northeast Japan: cyclic sedimentation and basin evolution. Journal of Asian Earth Sciences, 21, 921–935.

Arawaka, Y., Li, X., Ebihara, M., Meriç, E., Tansel, İ., Bargu, S., Koral, H., Matsumaru, K., 2003. Element profiles and Ir concentration of Cretaceous-Tertiary (K-T) boundary layers at Medetli, Gölpazari, northwestern Turkey. Geochemical Journal, 37, 681-693.

Arenillas, I., Arz, J. A., Molina, E., Dupuis, C., 2000. The Cretaceous/Paleogene (K/P) boundary at Aïn Settara, Tunisia: sudden catastrophic mass extinction in planktic foraminifera, Journal of Foraminiferal Research, 30, 202–218.

Arenillas, I., Arz, J. A., Molina, E., 2004. A new high-resolution planktic foraminiferal zonation and subzonation for the lower Danian. Lethaia, 37, 79–95.

Arenillas, I., Arz, J. A., Grajales-Nishimura, J. M., Murillo-Muñetón, G., Alvarez, W., Camargo-Zanoguera, A., Molina, E., Rosales-Domínguez, C., 2006. Chicxulub impact event is Cretaceous/Paleogene boundary in age: New micropaleontological evidence. Earth and Planetary Science Letters, 249, 241–257.

Arıkan, Y., 1975. Tuzgölü havzasının jeolojisi ve petrol imkanları. MTA Bülteni, 85, 17-38.

Aydemir, A., Ateş, A., 2006. Structural interpretation of the Tuzgölü and Haymana basins, Central Anatolia, Turkey, using seismic, gravity and aeromagnetic data. Earth Planets Space, 58, 951-961.

Babazadeh, S. A., Robaszynski, F., Courme, M. D., 2007. New biostratigraphic data from Cretaceous planktic foraminifera in Sahlabad province, eastern Iran. Geobios, 40, 445–454.

Bailey, E., B., McCallien, W. J., 1953. Ankara mélange and the Anatolian thrust. Royal Society of London Philosophical Transactions, 62, 403-442.

Baum, G., R., Vail, P., R., 1988. Sequence stratigraphic concepts applied to Paleogene outcrops, Gulf and Atlantic basins. In: Wilgus, C.K., Posamentier, H., Ross, C.A., Kendall, C.G. (Eds.), Sea-Level Changes: An Integrated Approach. Soc. Econ. Paleontol. Mineral. Spec. Publ., 42, 309-327.

Bayhan, E., 2007. Clay mineralogy of the Upper Cretaceous-Lower Tertiary sedimentary sequences of the Kalecik Region (Central Anatolia, Turkey). Yerbilimleri, Hacettepe Üniversitesi Yerbilimleri Uygulama ve Araştırma Merkezi Dergisi, 28/2, 127-136.

Bayhan, E., Gökçen, S. L., 1990. ‘Ankara virgasyonu’ Üst Kretase-Alt Tersiyer havzalarının petrolojik karşılaştırılması. MTA Bülteni, 11, 101-110.

Ben Abdelkader, O., Ben Salem, H., Donze, P., Maamouri, A. L., Meon, H., Robin, E., Rocchia, R., Froget, L., 1997. The K/T stratotype section of El Kef (Tunisia): events and biotic turnovers. Geobios, 21, 235-245.

Berggren, W., A., Kent, D., V., Swisher, C., C., Aubry, M., P., 1995. A revised Cenozoic geochronology and chronostratigraphy. SEPM, Special Publication, 54, 129-212.

Berner, R., A., 1971. Principles of chemical sedimentology. International Series in the Earth and Planetary Sciences, McGraw-Hill Book Company, 240 p.

Bertle, R., J., Suttner, T., J., 2005. New biostratigraphic data for the Chikkim Formation (Cretaceous, Tethyan Himalaya, India). Cretaceous Research, 26, 882-894.

Blow, W., H., 1979. The Cainozoic Globigerinida. 3 Vols., Brill, Leiden. 1413 p.

Blumenthal, M., 1942. Ankara şimalbatısındaki Bağlum ve Yakacık dolayları jeolojisi. MTA report archive no. 447, Ankara.

Bolli, H., M., 1966. Zonation of Cretaceous to Paleocene marine sediments based on planktonic foraminifera. Boletino Informativo Asociacion Venezolana de Geologia, Mineria y Petroleo, 9, 3-32.

Bozkaya, Ö., Yalçın, H., 1991a. Hekimhan doğu ve güney kesimindeki Üst Kretase-Tersiyer yaşlı sedimanter birimlerin mineralojisi ve jeokimyası. Türkiye Jeoloji Kurultayı Bülteni, 6, 234-252.

Bozkaya, Ö., Yalçın, H., 1991b. An approach to the Upper Cretaceous-Tertiary transition by using clay and carbonate mineralogy, Malatya-Hekimhan province, Eastern Turkey. Proc. 7th Euroclay Conf. Dresden, Greifswald, 141-146.

Bozkaya, Ö., Yalçın, H., 1992. Hekimhan havzası (Kuzeybatı Malatya) Üst Kretase-Tersiyer istifinin jeolojisi. TPJD Bülteni, 4/I, 59-80.

Brinkhuis, H., Zachariasse, W. J., 1988. Dinoflagellate cysts, sea-level changes and planktonic foraminifers across the Cretaceous-Tertiary boundary at El Haria, Northwest Tunisia. Marine Micropaleontology, 13, 153-191.

Brönnimann, P., 1952. Globigerinidae from the Upper Cretaceous (Cenomanian-Maestrichtian) of Trinidad, B.W.I. Bull. Am. Paleontol., 34, 1-70.

Catuneanu, O., 2006. Principles of sequence stratigraphy. Elsevier, Amsterdam, 375 p.

Canudo, J. I., 1997. El Kef blind test I results. Mar. Micropaleontol., 29, 73-76.

Canudo, J. I., Keller, G., Molina, E., 1991. Cretaceous–Tertiary boundary extinction pattern and faunal turnover at Agost and Caravaca, SE Spain. Mar. Micropaleontol., 17, 319–341.

Carlisle, D. B., Braman, D. R., 1991. Nanometre-size diamonds in the Cretaceous/Tertiary boundary clay of Alberta. Nature, 352, 708–709.

Chacon, B., Martin-Chivelet, J., Graefe, K. U., 2004. Latest Santonian to latest Maastrichtian planktic foraminifera and biostratigraphy of the hemipelagic successions of the Prebetic Zone (Murcia and Alicante provinces, south-east Spain) Cretaceous Research 25, 585-601.

Chamley, H., 1989. Clay Sedimentology. Springer-Verlag, Berlin, 623 p.

Chaput, E., 1932. Observations géologiques en Asie Mineure: Le Crétacé supérieur dans l'Anatolie Centrale. C. R. A. S., 194, 1960-1961.

Chaput, E., 1935a. L'Eocene du plateau de Galatie (Anatolie Centrale). C. R. A. S., 200, 767-768.

Chaput, E., 1935b. Les plissements Tertiare de l'Anatolie Centrale. C. R. A. S., 201, 1404-1405.

Chaput, E., 1936. Voyages d'études géologiques et géomorphologiques en Turquie. Mém. Inst. Françaiş D'Archaéo. İstanbul, II, 312 p.

Claeys, P., Kiessling, W., Alvarez, W., 2002. Distribution of Chicxulub ejecta at the Cretaceous-Tertiary boundary, in Koeberl, C., and MacLeod, K. G., eds., Catastrophic Events and Mass Extinctions: Impacts and Beyond: Boulder, Colorado, Geological Society of America Special Paper, 356, 55–68.

Coccioni, R., Marsili, A., 2007. The response of benthic foraminifera to the K–Pg boundary biotic crisis at Elles (northwestern Tunisia). Palaeogeography, Palaeoclimatology, Palaeoecology, doi:10.1016/j.palaeo.2007.02.046.

Coccioni, R., Luciani, V., Marsili, A., 2006. Cretaceous oceanic anoxic events and radially elongated chambered planktonic foraminifera: Paleoecological and paleoceanographic implications. Palaeogeography, Palaeoclimatology, Palaeoecology, 235, 66–92.

Coe, A., L., 2003. The sedimentary record of sea-level change. Cambridge University Press, 288 p.

Coşkun, B., Özdemir, A., Işık, V., 1990. Haymana-Mandıra-Dereköy arasındaki sahanın petrol imkanları. TPJD Bülteni, 2, 135-143.

Cowie, J. W., Zieger, W., Remane, J., 1989. Stratigraphic Commission accelerates progress, 1984–1989. Episodes, 112, 79–83.

Çemen, İ., Göncüoğlu, M. C., Dirik, K., 1999. Structural evolution of the Tuzgölü basin in Central Anatolia, Turkey. The Journal of Geology, 107, 693-706.

Çetin, H., Demirel, İ. H., Gökçen, S. L., 1986. Haymana'nın (SW Ankara) doğusu ve batısındaki Üst Kretase-Alt Tersiyer istifinin sedimantolojik ve sedimanter petrolojik incelemesi. TJK Bülteni, 29/2, 21-33.

Çiner, A., 1992. Sediméntologie et stratigraphie séquentielle du bassin d'Haymana à l'Eocene moyen Turquie. PhD Thesis, l'Univ. Louis Pasteur, France, 190 p.

Çiner, A., 1993. Geology of Haymana Basin (U. Cretaceous – M. Eocene); Central Anatolia, Turkey. 6th International Meeting and Training School on IGCP Project 269, Middle East Technical University, Field Trip Guide Book, 21 p.

Çiner, A., 1996. Distribution of small scale sedimentary cycles throughout several selected Basins. Tr. J. of Earth Sciences, 5, 25-37.

Çiner, A., Deynoux, M., Koşun, E., Gündoğdu, N., 1993a. Yamak türbidit karmaşığının (YTK) sekansiyel stratigrafik analizi: Haymana Baseni (Orta Eosen). Sekans Stratigrafisi, Sedimantoloji Çalışma Grubu Özel Yayını, 1, 53-70.

Çiner, A., Deynoux, M., Koşun, E., Gündoğdu, N., 1993b. Beldede örgülü-delta karmaşığının (BÖDK) sekans stratigrafik analizi: Polatlı-Haymana baseni (Orta Eosen) Orta Anadolu. Yerbilimleri, 16, 67-92.

Çiner, A., Deynoux, M., Ricou, S., Koşun, E. 1996a. Cyclicity in the middle Eocene Çayraz Carbonate Formation, Haymana Basin, Central Anatolia. Palaeogeography, Palaeoclimatology, Palaeoecology, 121, 313-329.

Çiner, A., Deynoux, M., Koşun, E., 1996b. Cyclicity in the Middle Eocene Yamak turbidite complex of the Haymana basin, Central Anatolia, Turkey. Geol. Rundschau., 85, 669-682.

Dağer, Z., Öztümer, E., Sirel, E., Yazlak, Ö., 1963. Ankara civarında birkaç stratigrafik kesit. TJK Bülteni, 8/1-2, 84-95.

Darvishzad, B., Ghasemi-Nejad, E., Ghourchaei, S., Keller, G., 2007. Planktonic foraminiferal biostratigraphy and faunal turnover across the Cretaceous-Tertiary boundary in Southwestern Iran. Journal of Sciences, Islamic Republic of Iran, 18/2, 139-149.

Demirel, H. İ., Şahbaz, A., 1994. Haymana, Paşadağ-Aladağ havzalarının petrofasiyes ve provenans karakteristikleri ile petrol potansiyeli. Türkiye 10. Petrol Kongresi ve Sergisi (Geology), 5-19.

Dizer, A., 1964. Sur quelques alveolines de l'Eocene de Turquie. Revue de Micropaléontologie, 7, 265-279.

Dizer, A., 1968. Etude micropaléntologique du nummulitique de Haymana (Turquie). Revue de Micropaléontologie, 11, 13-21.

Dizer, A., Meriç, E., 1981. Kuzeybati Anadolu'da Üst Kretase-Paleosen Biyostratigrafisi. MTA Bülteni, 95-96, 149-163.

Donovan, A., D., Baum, G., R., Blechschmidt, G., L., Loutit, T., S., Pflum, C., E., Vail, P., R., 1988. Sequence stratigraphic setting of the Cretaceous-Tertiary boundary in central Alabama. In: Wilgus, C.K., Posamentier, H., Ross, C.A., Kendall, C.G. (Eds.), Sea-Level Changes: An Integrated Approach. Soc. Econ. Paleontol. Mineral. Spec. Publ., 42, 299-307.

Dunham, R., J., 1962. Classification of carbonate rocks according to the depositional texture in: Ham, W. E. (ed.): Classification of carbonate rocks. A symposium. AAPG Memoir 1, 108-171.

Duru, M., Gökçen, N., 1990. Polatlı (GB Ankara) güneyi Monsiyen-Küiziyen istifinin ostrakod biyostratigrafisi ve ortamsal yorumu. MTA Bülteni, 110, 165-174.

Egeran, N., Lahn, E., 1951. Kuzey ve Orta Anadolu'nun tektonik durumu hakkında not. MTA Bülteni, 41, 23-28.

Ekdale, A., A., Bromley, R., G., 1984. Sedimentology and ichnology of the Cretaceous- Tertiary boundary in Denmark; implications for the causes of the terminal Cretaceous extinction. Journal of Sedimentary Petrology, 54, 681-703.

El Azabi, M. H., El Araby, A., 2000. Depositional cycles: an approach to the sequence stratigraphy of the Dakhla Formation, west Dakhla-Farafra stretch, Western Desert, Egypt. Journal of African Earth Sciences, 30/4, 971-996.

El Gadi, M., S., M., Brookfield, M., E., 1999. Open carbonate ramp facies, microfacies and paleoenvironments of the Gramame Formation (Maastrichtian), Pernambuco-Paraiba Basin, Northeastern Brazil. Journal of South American Earth Sciences, 12, 411-433.

El Kadiri, K., Serrano, F., Hlila, R., Liemlahi, H., Chalouan, A., Lopez-Garrido, A., C., Guerra-Merchan, A., Sanz-de-Galdeano, C., Kerzazi, K., El Mrihi, A., 2005. Lithostratigraphy and sedimentology of the latest Cretaceous-early Burdigalian Tamezzakht succession (Northern Rif, Morocco): consequences for its sequence stratigraphic interpretation. Facies, 50, 477–503.

Ellis, B., Messina, A., 1941–2004. Catalogue of Micropaleontology, Catalogue of Foraminifera. American Museum of Natural History, Special Publication.

Embry, A., F., Klovan J., E., 1971. A late Devonian reef tract on northeastern Banks Island N.W.T. Bulletin Canadian Petrol. Geol., 19, 730-781.

Emery, D., Myers, K., J., 1996. Sequence Stratigraphy. Blackwell Science, 297 p.

Erol, O., 1961. Ankara bölgesinin tektonik gelişmesi. TJK Bülteni, 7/1, 57-85.

Fornaciari, E., Giusberti, L., Luciani, V., Tateo, F., Agnini, C., Backman, J., Oddone, M., Rio, D., 2007. An expanded Cretaceous−Tertiary transition in a pelagic setting of the Southern Alps (central-western Tethys) Palaeogeography, Palaeoclimatology, Palaeoecology, 255, 98–131.

Fourquin, C., 1975. L'anatolie du Nord-Ouest, marge méridionale du continent europeén, histoire paléogéographique, tectonique et magmatique durant le Secondaire et Tertiare. Bull. Soc. Géol. France, 7, 1058-1070.

Flügel, E., 2004. Microfacies of carbonate rocks: analysis, interpretation and application. Springer, 976 p.

Gebhardt, H., 1999. Middle to Upper Miocene benthonic foraminiferal palaeoecology of the Tap Marls (Alicante Province, SE Spain) and its palaeoceanographic implications. Palaeogeography, Palaeoclimatology, Palaeoecology, 145, 141–156.

Geel, T., 2000. Recognition of stratigraphic sequences in carbonate platform and slope deposits: empirical models based on microfacies analysis of Palaeogene deposits in southeastern Spain. Palaeogeography, Palaeoclimatology, Palaeoecology, 155, 211-238.

Ginsburg, R. N., 1997a. An attempt to resolve the controversy over the end-Cretaceous extinction of planktic foraminifera at El Kef, Tunisia using a blind test. Mar. Micropaleontol., 29, 65 – 103.

Ginsburg, R. N., 1997b. Not so blind El Kef Test – Reply. Mar. Micropaleontol., 32, 399.

Gökçen, S. L., 1976. Haymana güneyinin sedimentolojik incelemesi. I. Stratigrafik birimler ve tektonik. Yerbilimleri, 2, 161-201.

Gökçen, S., L., 1977. Sedimentology and provenance of resedimented deposits in part of the Haymana basin-Central Anatolia. Yerbilimleri, 3, 13-23.

Gökçen, S. L., 1978. Haymana (GB Ankara) güneyindeki tortul istifinin sedimanter petrolojik incelenmesi. MTA Bülteni, 89, 99-115.

Gökçen, S. L., Kelling, G., 1983. The Paleogene Yamak sand-rich submarine-fan complex, Haymana basin, Turkey. Sedimentary Geology, 34, 219-243.

Görmüş, M., Karaman, E., 1992. Facies changes and new stratigraphical data in the Cretaceous – Tertiary boundary around Söbüdağ (Çünür – Isparta). Geosound, 21, 43- 57.

Görür, N., 1981. Tuzgölü-Haymana havzasının stratigrafik analizi. TJK, İç Anadolunun Jeolojisi Simpozyumu, Ankara, 60-66.

Görür, N., Oktay, F. Y., Seymen, İ., Şengör, A. M. C., 1984. Paleotectonic evolution of the Tuzgölü Basin complex, central Turkey: Sedimentary record of the neo-tethyan closure. In: Dixon J. ve Robertson A. H. F. (eds), The Geological Evolution of the Eastern Mediterranean. Spec. Pub. 17, Geol. Soc. London, 467-481.

Görür, N., Tüysüz, O., Şengör, A. M. C., 1998. Tectonic evolution of the Central Anatolian basins. International Geology Review, 40, 831-850.

Graciansky de, P., C., Hardenbol, J., Jacquin, T., Vail, P., R., (Eds.), 1998. Mesozoic and Cenozoic sequence stratigraphy of European basins. SEPM (Society of Sedimentary Geology) Special Publication, 60, p. 786.

Green, O. R., 2001. A Manual of Practical Laboratory and Field Techniques in Palaeobiology. Kluwer Academic Publishers, Dordrecht.

Güngör, A., 1975. Ankara-Haymana bölgesi Eoseninde bulunan Campanile Bayle (In Fischer), 1884, cinsine ait türlerin etüdü. MTA Bülteni, 84, 30-34.

Güray, A., 2006. Campanian-Maastrichtian planktonic foraminiferal investigation and biostratigraphy (Kokaksu Section, Bartın, NW Anatolia): Remarks on the Cretaceous paleoceanography based on quantitative data. M.Sc.Thesis, Middle East Technical University, 244 p.

Güvenç, T., 1973. Gaziantep-Kilis bölgesi stratigrafisi. Ege Üniv. Fen Fak. Jeoloji Kürsüsü, Bornova.

Hallam, A., Wignall, P., B., 1999. Mass extinctions and sea-level changes. Earth-Science Reviews, 48, 217–250.

Hancock, J., M., Kauffman, E., G., 1979. The great transgressions of the late Cretaceous. Journal of the Geological Society, London, 136, 175-186.

Hart, M., B., Feist, S., E., Hakansson, E., Heinberg, C., Price, G., D., Leng, M., J., Watkinson, M., P., 2005. The Cretaceous–Palaeogene boundary succession at Stevns Klint, Denmark: Foraminifers and stable isotope stratigraphy. Palaeogeography, Palaeoclimatology, Palaeoecology, 224, 6-26.

Haq, B., U., Hardenbol, J., Vail, P., R., 1987. Chronology of fluctuating sea-levels since the Triassic. Science, 235, 1156-1167.

Haq, B., U., Hardenbol, J., Vail, P., R., 1988. Mesozoic and Cenozoic chronostratigraphy and cycles of sea-level change. In: Wilgus, C.K., Hastings, B.S., Kendall, C.G.St.C., Posamentier, H.W., Ross, C.A., van Wagoner, J.C. (Eds.), Sea-Level Changes: An Integrated Approach, SEPM (Society for Sedimentary Geology), Special Publications, 42, 71–108.

Heldt, M., Bachmann, M., Lehmann, J., 2008. Microfacies, biostratigraphy, and geochemistry of the hemipelagic Barremian–Aptian in north-central Tunisia: Influence of the OAE 1a on the southern Tethys margin. Palaeogeography, Palaeoclimatology, Palaeoecology, 261, 246–260

Hildebrand, A. R., Boynton, W. V., 1990. Proximal Cretaceous–Tertiary boundary impact deposits in the Caribbean. Science, 248, 843–847.

Horowitz, A., S., Potter, P., E., 1971. Introductory petrography of fossils. Springer Verlag, Heidelberg, Berlin, 302 p.

Hultberg, S., U., Malmgren, B., A., 1986. Dinoflagellate and planktonic foraminiferal paleobathymetrical indices in the Boreal uppermost Cretaceous. Micropaleontology, 32, 316-323.

Hüseynov, A., 2007. Sedimentary cyclicity in the Upper Cretaceous successions of the Haymana Basin (Turkey): depositional sequences as response to relative sea-level changes. M.Sc. Thesis, Middle East Technical University, 120 p.

ICS, 2003. Consolidated Annual Report for 2003. International Commission on Stratigraphy, International Union of Geological Sciences.

İnan, N., Temiz, H., 1992. Niksar (Tokat) yöresinde Kretase/Tersiyer geçişinin litostratigrafik ve biyostratigrafik özellikleri. Türkiye Jeoloji Bülteni, 35, 39-47.

İnan, N., İnan, S., Kurt, İ., 1999. Doğu Pontidler'de uyumlu bentik K/T geçişi: Tonya formasyonunun (GB Trabzon) Şahinkaya üyesi. Türkiye Jeoloji Bülteni, 42/2, 63-67.

Karoui-Yaakoub, N., Zaghbib-Turki, D., Keller, G., 2002. The Cretaceous-Tertiary (K-T) mass extinction in planktic foraminifera at Elles I and El Melah, Tunisia. Palaeogeography, Palaeoclimatology, Palaeoecology, 178, 233 – 255.

Kassab, A. S., Zakhera M. S., Obaidalla N. A., 2004. Integrated biostratigraphy of the Campanian–Maastrichtian transition in the Nile Valley, Southern Egypt. Journal of African Earth Sciences, 39, 429–434.

Kaya, M., 1997. Niksar – Tokat yöresindeki Üst Kretase – Paleosen yaşlı Kırandağ ve Düdenyaylası formasyonlarının foraminifer içeriği. Türkiye Jeoloji Bülteni, 40/2, 85-100.

Kaymakçı, N., 2000. Tectono-stratigraphical evolution of the Çankırı Basin (Central Anatolia, Turkey). Geologica Ultraictina, no. 190, 247 p.

Keller, G., 1988. Extinction, survivorship and evolution of planktic foraminifera across the Cretaceous/Tertiary boundary at El Kef Tunisia. Marine Micropaleontology, 13, 239–263.

Keller, G., 1989a. Extended Cretaceous/Tertiary boundary extinctions and delayed population changes in planktonic foraminifera from Brazos River, Texas. Paleoceanography, 4, 287-332.

Keller, G., 1989b. Extended period of extinctions across the Cretaceous/Tertiary boundary in planktonic foraminifera of continental shelf sections: Implications for impact and volcanism theories. Geol. Soc. Am. Bull., 101, 1408-1419.

Keller, G., 1993. The Cretaceous Tertiary boundary transition in the Antarctic Ocean and its global implications. Marine Micropaleontology, 21, 1–45.

Keller, G., 1996. The K-T mass extinction in planktonic foraminifera: Biotic constraints for catastrophe theories. In: McLeod, N., Keller, G. (eds.), Cretaceous-Tertiary mass extinction: biotic and environmental changes. W. W. Norton & Company, New York-London, 49–84.

Keller, G., 1997. Analysis of El-Kef blind test I. Marine Micropaleontology, 29, 89-93.

Keller, G., 2001. The end-cretaceous mass extinction in the marine realm: year 2000 assessment. Planetary and Space Science, 49, 817–830.

Keller, G., Stinnesbeck, W., 1996. Sea-level changes, clastic deposits, and megatsunamis across the Cretaceous-Tertiary boundary. In: MacLeod, N., Keller, G. (Eds.), Cretaceous/Tertiary Boundary Mass Extinction: Biotic and Environmental Changes. W.W. Norton, New York, 415-450.

Keller, G., Pardo, A., 2004. Disaster opportunists Guembelitrinidae: index for environmental catastrophes. Marine Micropaleontology, 53, 83 – 116.

Keller, G., Barrera, E., Schmitz, B., Mattson, E., 1993. Gradual mass extinction, species survivorship and long-term environmental changes across the Cretaceous Tertiary boundary in high latitudes. Geol. Soc. Am. Bull., 105, 979–997.

Keller, G., Stinnesbeck, W., Lopez-Oliva, J. G., 1994. Age, deposition and biotic effects of the Cretaceous-Tertiary boundary event at Mimbral, NE Mexico. Palaios, 9, 144–157.

Keller, G., Adatte, T., Stinnesbeck, W., Stüben, D., Berner, Z., 2001. Age, chemo- and biostratigraphy of Haiti spherule rich deposits: a multi-event K-T scenario. Can. J. Earth Sci., 38, 197-227.

Keller, G., Adatte, T., Stinnesbeck, W., Luciani, V., Karoui-Yaakoub, N., Zaghbib-Turki, D., 2002. Paleoecology of the Cretaceous–Tertiary mass extinction in planktonic foraminifera. Palaeogeogr. Palaeoclimatol. Palaeoecol., 178, 257–297.

Keller, G., Stinnesbeck, W., Adatte, T., Stüben, D., 2003. Multiple impacts across the Cretaceous–Tertiaty boundary. Earth-Science Reviews, 62, 327– 363.

Knitter, H., 1979. Eine verbesserte Methode zur Gewinnung von Mikrofosilien aus harten, nicht schlammbaren Kalken. Geol. Bl. Nor-Bayern, 29, 182 – 186.

Koçyiğit, A., 1991. An example of an accretionary forearc basin from Central Anatolia and its implications for the history of subduction of Neo-Tethys in Turkey. Geological Society of American Bulletin, 103, 22-36.

Koçyiğit, A., Lünel, T., 1987. Geology and tectonic setting of Alcı region, Ankara. Middle East Technical University Journal of Pure and Applied Sciences, 20, 35-57.

Koçyiğit, A., Özkan, S., Rojay, B., 1988. Examples of the forearc basin remnants at the active margin of northern Neo-Tethys: development and emplacement ages of the Anatolian Nappe, Turkey. Middle East Technical University Journal of Pure and Applied Sciences, 3, 183-210.

Koutsoukos, E.A.M., 1996. Phenotypic experiments into new pelagic niches in early Danian planktonic foraminifera: aftermath of the K/T boundary event. In: M.B. HART (Editor), Biotic Recovery from Mass Extinction Events, Geological Society, Special Publication, London, 102, 319-335.

Koutsoukos, E. A. M., 2006. The Cretaceous-Paleogene Boundary at the Poty Section, NE Brazil: foraminiferal record and sequence of events-a review. Anuário do Instituto de Geociências, UFRJ, 29/1, 95-107.

Lahn, E., 1949. Orta Anadolu'nun jeolojisi hakkında, TJK Bülteni, 1, 1.

Li, L., Keller, G., 1998. Maastrichtian climate, productivity and faunal turnovers in planktic foraminifera in South Atlantic DSDP Sites 525A and 21. Marine Micropaleontology, 33, 55-86.

Lipps, J. H., 1997. The Cretaceous-Tertiary boundary: the El Kef blind test. Marine Micropaleontology, 29, 65 – 66.

Lirer, F., 2000. A new technique for retrieving calcareous microfossils from lithified lime deposits. Micropaleontology 46, 365–369.

Liu, G., Olsson, R., K., 1992. Evolutionary radiation of microperforate planktic foraminifera following the K-T mass extinction event. J. Foraminiferal Res. 22, 328–346.

Loeblich, A., R., Jr. and Tappan, H., 1988. Foraminiferal genera and their classification. Von Nostrand Reinhold Company, New York, 2v, 970 p.

Lokman, K., Lahn, D., 1946. Haymana bölgesi jeolojisi. MTA Bülteni, 36, 292-300.

Loucks, R., G., Sarg, J., F., (Eds.), 1991. Carbonate sequence stratigraphy: Recent developments and applications. AAPG, Memoir 57, Tulsa, Oklohama.Luciani, V., 1997. Planktonic foraminiferal turnover across the Cretaceous–Tertiary boundary in the Vajont valley (southern Alps, northern Italy). Cretaceous Research, 18, 799– 821.

Luciani, V., 1997. Planktonic foraminiferal turnover across the Cretaceous–Tertiary boundary in the Vajont valley (Southern Alps, northern Italy). Cretaceous Research, 18, 799– 821.

Luciani, V., 2002. High-resolution planktonic foraminiferal analysis from the Cretaceous-Tertiary boundary at Ain Settera (Tunisia): evidence of an extended mass extinction. Palaeogeography, Palaeoclimatology, Palaeoecology, 178, 299 – 319.

Luterbacher, H. P., Premoli-Silva, I., 1964. Biostratigrafia del limite cretaceo–terziario nell'Appennino centrale. Rivista Italiana di Paleontologia, 70, 67–117.

MacLeod, N., Keller, G., 1991. How complete are Cretaceous/Tertiary boundary sections? A chronostratigraphic estimate based on graphic correlation: Geological Society of America Bulletin, 103, 1439–1457.

Macleod, N., Keller, G., 1994. Comparative biogeographic analysis of planktonic foraminiferal survivorship across Cretaceous/Tertiary (K/T) boundary. Paleobiology, 20, 2, 143-177.

MacLeod, N., Keller, G., (Eds.), 1996. Cretaceous-Tertiary Mass Extinctions; Biotic and Environmental Changes. W.W. Norton and Company, New York, 575 p.

MacLeod, K. G., Whitney, D. L., Huber, B. T., Koeberl, C., 2007. Impact and extinction in remarkably complete Cretaceous-Tertiary boundary sections from Demerara Rise, tropical western North Atlantic. Geological Society of America Bulletin, 119, 1/2, 101 – 115.

Martin, S., E., 1972. Reexamination of the upper Cretaceous planktonic foraminiferal genera *Planoglobulina* and *Ventilabrella* Cushman. Journal of Foraminiferal Research., 2/2, 73-92.

Martinez-Ruiz, F., Ortega-Huertas, M., Kroon, D., Smit, J., Palomo-Delgado, I., Rocchia, R., 2001. Geochemistry of the Cretaceous–Tertiary boundary at Blake Nose (ODP Leg l7lB). In: Kroon, D., Norris, R.D., Klaus, A. (Eds.), Western North Atlantic Paleogene and Cretaceous Paleoceanography. Geol. Soc., London, 131– 148.

Martinez-Ruiz, F., Ortega-Huertas, M., Rivas, P., 2006. Rare earth element composition as evidence of the precursor material of Cretaceous-Tertiary boundary sediments at distal sections. Chemical Geology, 232, 1-11.

Masters, B., A., 1997. El Kef blind test II results. Mar. Micropaleontology, 29, 77-79.

Matsumaru, K., 1997. On Pseudorbitoides Trechmanni Douville (orbitoidal foraminifera) from Turkey. Revue de Micropaleontologie, 40, 339-346.

Matsumoto, T., 1980. Inter-regional correlation of transgressions and regressions in the Cretaceous period. Cretaceous Research, 1, 359-373.

Meriç, E., Görür, N., 1979-80. Haymana-Polatlı havzasındaki Çaldağ kireçtaşının kireçtaşının yaş konağı. MTA Bülteni, 93/94, 137-142.

Meriç, E., Oktay, F. Y., Toker, V., Tansel, İ., Duru, M., 1987. Adıyaman yöresi Üst Kreta se- Eosen istifinin sedimanter jeolojisi ve biyostratigrafisi (foraminifer, nannoplankton ostrakod). Türkiye Jeoloji Bülteni, 30, 19-32.

Mitchum, R., M., Vail, P., R., Thomson, S. 1977. Seismic stratigraphy and global changes of sea-level, Part 2: The depositional sequences as a basic unit of for stratigraphic analysis. Applications to Hydrocarbon Exploration. AAPG Memoir, 26, 53-62.

Molina, E., Arenillas, I., Arz, J. A., 1996. The Cretaceous/Tertiary boundary mass extinction in planktic foraminifera at Agost, Spain. Revue de Micropaleontologie, 39, 225– 243.

Morris, R.W., 1971. Upper Cretaceous Foraminifera from the Upper Mancos Formation, the Mesaverde Group, and the Basal Lewis Formation, Northwestern Colorado. Micropaleontology, 17/3, 257-296.

Mount, J., 1985. Mixed siliciclastic and carbonate sediments: a proposed first-order textural and compositional classification. Sedimentology, 32, 435-442.

Nagy, J., Johansen, H. O., 1991. Delta-influenced foraminiferal assemblages from the Jurassic (Toarcian-Bajocian) of the Northern North Sea. Micropaleontology, 37/1, 1-40.

Nederbragt, A., J., 1991. Late Cretaceous biostratigraphy and development of Heterohelicidae (planktic foraminifera). Micropaleontology, 37, 4, 329 –372.

Nederbragt, A., J., 1998. Quantitative biogeography of late Maastrichtian planktic foraminifera. Micropaleontology, 44/4, 385 – 412.

Neumann, A., C., Macintyre, I., 1985. Reef response to sea-level rise: keep-up, catch-up or give-up. In: Proceedings of the Fifth International Coral Reef Congress, 1985, Tahiti, 3, 105-110.

Nielsen, J. K., Jakobsen, S. L., 2004. Extraction of calcareous macrofossils from the Upper Cretaceous white chalk and other sedimentary carbonates in Denmark and Sweden: the acid-hot water method and the waterblasting technique. Palaeontologia Electronica 7/4, 1-11.

Norman, T., 1973. Ankara Yahşıhan bölgesinde Üst Kretase-Alt Tersiyer sedimantasyonu. TJK Bülteni, 16, 41-66.

Norman, T., Rad, M. R., 1971. Çayraz (Haymana) civarının Horhor (Eosen) formasyonunda alttan üste doğru doku parametrelerinde ve ağır mineral bolluk derecelerinde değişmeler. TJK Bülteni, 14/2, 205-225.

Norman, T., Gökçen, S. L., Şenalp, M., 1980. Sedimentation pattern in Central Anatolia at the Cretaceous-Tertiary boundary. Cretaceous Research, 1, 61-84.

Ocakoğlu, F., Çiner, A., 1995. Sedimentary evolution of the Orhaniye-Güvenç (NW Ankara) continental deposits during Paleocene-Early Eocene. Türkiye Jeoloji Bülteni, 38/2, 41-53.

Obaidalla, N.A., 2000. Planktonic foraminiferal biostratigraphy and faunal turnover events during the Late Cretaceous-early Tertiary along the Rea Sea coast, Egypt. Journal of African Earth Sciences, 31, 571-595.

Obaidalla, N. A., 2005. Complete Cretaceous/Paleogene (K/P) boundary section at Wadi Nukhul, southwestern Sinai, Egypt: inference from planktic foraminiferal biostratigraphy. Revue de Paléobiologie, 24/1, 201 – 224.

Okay, A. İ., Tansel, İ., Tüysüz, O., 2001. Obduction, subduction and collision as reflected in the Upper Cretaceous-Lower Eocene sedimentary record of western Turkey. Geol. Mag., 138, 117-142.

Olsson, R., K., 1964. Late Cretaceous planktonic foraminifera from New Jersey and Delaware. Micropaleontology, 10/2, 157-188.

Olsson, R. K., 1997. El Kef blind test III results. Mar. Micropaleontol., 29, 80-84.

Olsson, R. K., Hemleben, C., Berggren, W. A., and Huber, B. T., 1999. Atlas of Paleocene planktonic foraminifera. Smithsonian Contributions to Paleobiology, 85, 252 p.

Orue-Etxebarria, X., 1997. El Kef blind test IV results. Mar. Micropaleontol., 29, 85-88.

Özcan, E., 2002. Cuisian orthophragminid assemblages (*Discocyclina*, *Orbitoclypeus* and *Nemkovella*) from the Haymana-Polatlı Basin (Central Turkey): biometry and description of two new taxa. Eclogae geol. Helv., 95, 75-97.

Özcan, E., Özkan-Altıner, S., 1997. Late Campanian-Maastrichtian evolution of orbitoid foraminifera in Haymana basin succession (Ankara, Central Turkey). Revue de Paléobiologie, 16/1, 271-290.

Özcan, E., Özkan-Altıner, S. 1999. The genus *Lepidorbitoides* and *Orbitoides*: Evolution and stratigraphic significance in some Anatolian basins (Turkey). Geological Journal, 34/3, 275-286.

Özcan, E., Özkan-Altıner, S., 2001. Description of an early ontogenetic evolutionary step in *Lepidorbitoides*: *Lepidorbitoides bisambergensis asymmetrica* subsp. n., Early Maastrichtian (Central Turkey). Rivista Italiana di Paleontologia e Stratigrafia, 107, 137-144.

Özcan, E., Sirel, E., Özkan-Altıner, S., Çolakoğlu, S., 2001. Late Paleocene Orthophragminae (foraminifera) from the Haymana-Polatlı Basin, Central Turkey) and description of a new taxon, *Orbitoclypeus haymanaensis*. Micropaleontology, 47/4, 339-357.

Özer, S., 1986. İç Anadolu Bölgesi rudist paleontolojisi ve paleobiyocoğrafyası. Dokuz Eylül Üniversitesi Fen Bilimleri Enstitüsü, Araştırma Raporları, 1-14.

Özer, S., Sözbilir, H., Özkar, İ., Toker, V., Sarı, B., 2001. Stratigraphy of Upper Cretaceous – Paleogene sequences in the southern and eastern Menderes Massif (western Turkey). Int. J. Earth Sciences, 89, 852-866.

Özkan, S., 1985. Maastrichtian planktonic foraminifera and stratigraphy of Germav Formation, Gercüş area, Southeast Turkey. M.Sc. Thesis, Middle East Technical University, 273 p.

Özkan, S., Altıner, D., 1987. Maastrichtian planktonic foraminifera from the Germav Formation in Gercüş area (SE Anatolia, Turkey), with notes on the suprageneric classification of globotruncanids. Revue de Paléobiologie, 6/2, 261 – 277.

Özkan-Altıner, S., Özcan, E., 1997. Microfacies variations around Cretaceous-Tertiary boundary: an integrated zonation of calcareous nannofossil, planktonic foraminifera and benthonic foraminifera, Project no. TÜBİTAK-YDABÇAG-69.

Özkan-Altıner, S., Özcan, E., 1999. Upper Cretaceous planktonic foraminiferal biostratigraphy from NW Turkey: calibration of the stratigraphic ranges of larger benthonic foraminifera. Geological Journal, 34/3, 287-301.

Pardo, A., Ortiz, N., Keller, G., 1996. Latest Maastrichtian foraminiferal turnover and its environmental implications at Agost, Spain, in MacLeod, N., and Keller, G., eds., Cretaceous-Tertiary mass extinction: New York, W.W. Norton and Co., p. 139–172.

Pardo, A., Adatte, T., Keller, G., Oberhänsli, H., 1999. Paleoenvironmental changes across the K–T transition in Koshak (Kazakstan) based on planktic foraminifera and clay minerals. Palaeogeogr. Palaeoclimat. Palaeoecol., 154, 247– 273.

Paul, C., R., C., 2005. Interpreting bioevents: What exactly did happen to planktonic foraminifers across the Cretaceous–Tertiary boundary?. Palaeogeography, Palaeoclimatology, Palaeoecology, 224, 291– 310.

Pessagno, E., A., Jr., 1967. Upper Cretaceous planktonic foraminifera from the western Gulf Coastal Plain. Paleontographica Americana, 5, 245-445.

Petrizzo, M. R., 2000. Upper Turonian–lower Campanian planktonic foraminifera from southern mid–high latitudes (Exmouth Plateau, NW Australia): biostratigraphy and taxonomic notes. Cretaceous Research, 21, 479–505.

Petrizzo, M. R., 2001. Late Cretaceous planktonic foraminifera from Kerguelen Plateau (ODP Leg 183): new data to improve the Southern Ocean biozonation. Cretaceous Research, 22, 829–855.

Peypouquet, J., P., Grousset, F., Mourguiart, P., 1986. Paleoceanography of the Mesogean Sea based on ostracods of the northern Tunisian continental shelf between the Late Cretaceous and Early Paleogene. Geologische Rundschau, 75, 159-174.

Posamentier, H., W., Jervey, M., T., Vail, P., R., 1988. Eustatic controls on clastic Deposition I - Conceptual framework. Sea-Level Changes - An Integrated Approach. The Society of Economic Paleontologist and Mineralogists, Special Publication, 42, 109-124.

Postuma, J., A., 1971. Manual of planktonic foraminifera. Elsevier Publishing Company, 420 p.

Premoli-Silva, I., Verga, D., 2004. Practical manual of Cretaceous Planktonic Foraminifera. International School on Planktonic Foraminifera, 3. Course: Cretaceous. Verga & Rettori eds. Universities of Perugia and Milan, Tipografia Pontefelcino, Perugia (Italy), 283 p.

Raup, D. M., Sepkoski, J. J., 1982. Mass extinction in the marine fossil record. Science, 215, 1501-1503.

Reckamp, J., U., Özbey, S., 1960. Petroleum geology of Temelli and Kuştepe structures, Polatlı area. Pet. İş. Gen. Md., Ankara.

Rigo de Righi, M., Cortesini, A., 1959. Regional studies in central Anatolian basin. Progress Report 1, Turkish Gulf Oil Co., Pet. İş. Gen. Md., Ankara.

Robaszynski, F., 1998. Cretaceous planktonic foraminiferal biozonation in Exxon chart 2000.

Robaszynski, F., Caron, M., Gonzalez Donoso, J. M., Wonders, A. H. & The European Working Group on Planktonic Foraminifera, 1984. Atlas of Late Cretaceous globotruncanids. Revue de Micropaléontologie, 26, 145–305.

Robin, E., Boclet, D., Bonté, P., Froguet, L., Jéhanno, C., Rocchia, R., 1991. The stratigraphic distribution of Ni-rich spinels in Cretaceous–Tertiary boundary rocks at El Kef (Tunisia), Caravaca (Spain) and Hole 761C (Leg 122). Earth Planet. Sci. Lett., 107, 715–721.

Rojay, B., Süzen, L., 1997. Tectonostratigraphic evolution of the Cretaceous dynamic basins on accretionary ophiolitihic melange prism, SW of Ankara region. TPJD Bülteni, 9/1, 1-12.

Rojay, B., Yalınız, K., Altıner, D., 2001. Age and origin of some pillow basalts from Ankara mélange and their tectonic implications to the evolution of northern branch of Neotethys, Central Anatolia. Turkish Journal of Earth Sciences, 10, 93-102.

Rojay, B., Altıner, D., Özkan-Altıner, S., Önen, P., James, S., Thirwall, M., 2004. Geodynamic significance of the Cretaceous pillow basalts from North Anatolian Mélange Belt (Central Anatolia, Turkey): geochemical and paleontological constrains. Geodynamica Acta, 17/5, 349-361.

Said, R., Kenawy, A., 1956. Upper Cretaceous and Lower Tertiary Foraminifera from Northern Sinai, Egypt. Micropaleontology, 2/2, 105-173.

Saner, S., 1980. Batı Pontidlerin ve komşu havzaların oluşumlarının levha tektoniği kuramı ile açıklanması, Kuzeybatı Türkiye. MTA Bülteni, 93/94, 1-19.

Sarg, J. F., 1988. Carbonate sequence stratigraphy. In: Sea-level Changes: An integrated approach. Wilgus, C. K., Hastings, B. S. *et al*. (eds.), The Society of Economic Paleontologist and Mineralogist, Special Publication, 42, 155-181.

Schlager, W., 2005. Carbonate sedimentology and sequence stratigraphy. SEPM (Society of Sedimentary Geology) Concepts in Sedimentology and Paleontology, n. 8, Tulsa, Oklahoma, 200 p.

Schmidt, G., C., 1960. AR/MEM/365-266-367 sahalarının nihai terk raporu. Pet. İş. Gen. Md., Ankara.

Scholle, P., A., Ulmer-Scholle, D., S., 2003. A color guide to the petrography of carbonates rocks: grains, textures, porosity, diagenesis. AAPG Memoir 77, Tulsa, Oklahoma, USA, 474 p.

Schulte, P., Speijer, R., Mai, H., Kontny, A., 2006. The Cretaceous–Paleogene (K/P) boundary at Brazos, Texas: sequence stratigraphy, depositional events and the Chicxulub impact. Sediment. Geol., 184, 77–109.

Shukolyukov, A., Lugmair, G. W., 1998. Isotopic evidence for the Cretaceous/Tertiary impactor and its type. Science, 282, 927–929.

Sirel, E., 1975. Polatlı (GB Ankara) güneyinin stratigrafisi. TJK Bülteni, 18/2, 181-192.

Sirel, E., 1976a. Polatlı (GB Ankara) güneyinde bulunan *Alveolina*, *Nummulites*, *Ranikothalia* ve *Assilina* cinslerinin bazı türlerinin sistematik inclemeleri. TJK Bülteni, 19/2, 89-103.

Sirel, E., 1976b. Description of six new species of the *Alveolina* found in the South of Polatlı (SW Ankara) region. TJK Bülteni, 19, 19-22.

Sirel, E., 1976c. Haymana (G Ankara) yöresi İlerdiyen, Küiziyen ve Lütesiyen'deki *Nummulites*, *Assilina* ve *Alveolina* cinslerinin bazı türlerinin tanımlamaları ve stratigrafik dağılımları. TJK Bülteni, 19, 31-44.

Sirel, E., 1998. Foraminiferal description and biostratigraphy of the Paleocene-Lower Eocene shallow-water limestones and discussion on the Cretaceous-Tertiary boundary in Turkey. General Directorate of the Mineral Research and Exploration, Monography Series, 2, 117 p.

Sirel, E., 1999. Four new genera (*Haymanella*, *Kayseriella*, *Elazigella* and *Orduella*) and one new species of Hottingerina form the Paleocene of Turkey. Micropaleontology, 45/2, 113-137.

Sirel, E., Gündüz, H., 1976. Description and stratigraphic distribution of some species the genera *Nummulites*, *Assilina* and *Alveolina* from the Ilerdian, Cuisian and Lutetian of Haymana region. TJK Bülteni, 19, 33-44.

Sirel, E., Dağer, Z., Sözeri, B., 1986. Some biostratigraphic and paleogeographic observations on the Cretaceous-Tertiary boundary in the Haymana-Polatlı region (Central Turkey) in Walliser O. (ed) Global Bioevents. Lecture Notes in Earth Sciences, 8, 385-396.

Sloss, L., L., 1963. Sequences in the cratonic interior of North America. Geological Society of America Bull., 74, 93-114.

Smit, J., 1977. Discovery of a planktonic foraminiferal association between the *Abathomphalus mayaroensis* Zone and the *'Globigerina' eugubina* Zone at the Cretaceous/Tertiary boundary in the Barranco del Gredero (Caravaca, SE Spain): A preliminary report. Proc. K. Ned. Akad. Wet., 80, 280-301.

Smit, J., 1982. Extinction and evolution of planktonic foraminifera after a major impact at the Cretaceous/Tertiary boundary. Geol. Soc. Am. Spec. Pap., 190, 329–352.

Smit, J., 1990. Meteorite impact, extinctions and the Cretaceous-Tertiary Boundary. Geol. Mijnb., 69, 187-204.

Smit, J., 1999. The global stratigraphy of the Cretaceous–Tertiary boundary impact ejecta. Annual Review of Earth and Planetary Sciences, 27, 75–113.

Smit, J., Hertogen, J., 1980. An extraterrestrial event at the Cretaceous–Tertiary boundary. Nature, 285, 198–200.

Smit, J., Nederbragt, A. J., 1997. Analysis of the El Kef blind test II. Mar. Micropaleontol., 29, 94-100.

Smith, R. K., Buzas M. A., 1986. Microdistribution of foraminifera in a single bed of the monterey formation, Monterey County, California. Smithsonian Contributions to Paleobiology, no. 60, Smithsonian Institution Press, City of Washington.

Speijer, R., P., Van der Zwaan, G., J., 1996. Extinction and survivorship of southern Tethyan benthic foraminifera across the Cretaceous/Paleogene boundary. In: Hart, M.B. (Ed.), Biotic Recovery from Mass Extinction Events, Special Publication, Geological Society of London, London, United Kingdom, 102, 343–371.

Stinnesbeck, W., Keller, G., Adatte, T., Lopez-Oliva, J.,G., MacLeod, N., 1996. Cretaceous-Tertiary boundary clastic deposits in Northeastern Mexico: Impact Tsunami or sealevel lowstand. In: MacLeod, N., Keller, G. (Eds.), Cretaceous/Cretaceous/Tertiary Boundary Mass Extinction: Biotic and Environmental Changes. W.W. Norton, New York, 471-517.

Stüben, D., Kramar, U., Harting, M., Stinnesbeck, W., and Keller, G., 2005. High-resolution geochemical record of Cretaceous-Tertiary boundary sections in Mexico: new constraints on the K-T and Chicxulub events: Geochimica et Cosmochimica Acta, 69, 2559– 2579.

Şenalp, M., Gökçen, S. L., 1978. Sedimentological studies of the oil-saturated sandstones of the Haymana Region (SW Ankara). TJK Bülteni, 21/1, 87-94.

Şengör, A. M. C., Yılmaz, Y., 1981. Tethyan evolution of Turkey: a plate tectonic approach. Tectonophysics, 75, 181-241.

Şengüler, İ., Hakyemez, A., Satır, M., 1999. Analysis of Cretaceous/Tertiary hemipelagic successions on the western coast of the Black Sea (Turkey); implications for the Cretaceous-Tertiary boundary problem. Journal of Conference Abstracts, Cambridge Publications, Cambridge, United Kingdom, 4/1, 271.

Tansel, İ., 1989. Ağva (İstanbul) yöresinde Geç Kretase – Paleosen sınırı ve Paleosen biyostratigrafisi. TPJD Bülteni, 1/3, 211-218.

Tantawy, A. A., Keller, G., Adatte, T., Stinnesbeck, W., Kassab, A., and Schulte, P., 2001. Maastrichtian to Paleocene depositional environment of the Dakhla Formation, Western Desert, Egypt: sedimentology, mineralogy, and integrated micro-and macrofossil biostratigraphies. Cretaceous Research, 22, 795-827.

Toker, V., 1975. Haymana yöresinin (SW Ankara) planktonik foraminifera ve nannoplanktonlarla biyostratigrafik incelenmesi. PhD. Thesis, Ankara Üniversitesi Fen Fakültesi, 1-57.

Toker, V., 1977. Haymana ve Kavak formasyonlarındaki planktonik foraminifera ve nannoplanktonlar. TBTAK VI. Bilim Kongresi, 57-70.

Toker, V., 1979. Haymana yöresi (GB Ankara) Üst Kretase planktonik foraminiferaları ve biyostratigrafi incelemesi. TJK Bülteni, 22, 121-132.

Toker, V., 1980. Haymana yöresi (GB Ankara) nannoplankton biyostratigrafisi. TJK Bülteni, 23/2, 165-178.

Toker, V., 1981. Haymana yöresi (GB Ankara) Tersiyer oluşuklarının planktonik foraminiferlerle biyostratigrafik incelemesi. KTÜ Yer Bilimleri Dergisi, Jeoloji 1, 2, 115-126.

Ünalan, G., Yüksel, V., Tekeli, T., Gönenç, O., Seyirt, Z., Hüseyin, S., 1976. Haymana-Polatlı yöresinin (Güneybatı Ankara) Üst Kretase-Alt Tersiyer stratigrafisi ve paleocoğrafik evrimi. TJK Bülteni, 19, 159-176.

Vail, P., R., Mitchum, J., R., 1977. Seismic stratigraphy and global changes of sea-level, Part 1: Overview-Applications to Hydrocarbon Exploration. AAPG Memoir, 26, 63-81.

Vail, P., R., Mitchum, R., M., Thompson, S., 1977. Seismic stratigraphy and global changes of sea-level, Part 4: Global cycles of relative changes of the sea-level, in payton, C. E., eds., seismic stratigraphy. Application to Hydrocarbon Exploration. AAPG Memoir, 26, 83-97.

Vail, P., R., Hardenbol, J., Todd, R., G., 1984. Jurassic unconformities, chronostratigraphy and sea-level changes from seismic stratigraphy. In: Interregional Unconformities and Hydrocarbon Exploration (ed. By J. S Schlee). Memoir of the AAPG, Tulsa, 33, 129-144.

Van Wagoner, J., C., Posamentier, H., W., Mithchum, R., M., Vail, P., R., Sarg, J., F., Loutit, T., S., Hardenbol, J., 1988. An overview of the fundamentals of sequence stratigraphy and key definitions. Sea-Level Changes-An Integrated Approach. The Society of Economic Paleontologist and Mineralogist, Special Publication, 42, 40-44.

Verga, D., Premoli-Silva, I., 2003. Early Cretaceous planktonic foraminifera from the Tethys: the small, few-chambered representatives of the genus Globigerinelloides. Cretaceous Research, 24, 305–334.

Yakar, H., 1993. Late Campanian-Early Paleocene planktic foraminiferal taxonomy and biostratigraphy in the Adıyaman Region (SE Anatolia). M.Sc. Thesis, Middle East Technical University, 290 p.

Yalçın, H., Bozkaya, Ö., 1996. A new discovery of the Cretaceous/Tertiary boundary from the Tethyan belt, Hekimhan Basin, Turkey: mineralogical and geochemical evidence. International Geology Review, 38, 759-767.

Yalçın, H., İnan, N., 1992a. Tecer formasyonunda (Sivas) Kretase-Tersiyer geçişine paleontolojîk, mineralojik ve jeokimyasal yaklaşımlar. Türkiye Jeoloji Bülteni, 35, 95-102.

Yalçın, H., İnan, N., 1992b. Paleontological features and mineralogical – geochemical changes of the Cretaceous/Tertiary transition at Iğdır formation, Koyulhisar – Sivas, Turkey. Geosound, First International Symposium on Eastern Mediterranean Geology Special Issue, 39-55.

Yan, Y., Xia, B., Lin, G., Cui, X., Hu, X., Yan, P ., Zhang, F., 2006. Geochemistry of the sedimentary rocks from the Nanxiong Basin, South China and implications for provenance, paleoenvironment and paleoclimate at the K/T boundary. Sedimentary Geology, 197, 1-2, 127-140.

Yıldız, A., Toker, V., 1995. Gürün Yöresi (Sivas) Konakpınar formasyonu K/T sınırı. TJK Bülteni, 10, 11-24.

Yıldız, A., Gürel, A., 2005. Palaeontological, diagenetic and facies characteristics of Cretaceous/Paleogene boundary sediments in the Ordu, Yavuzlu and Uzunisa areas, Eastern Pontides, NE Turkey. Cretaceous Research, 26, 329-341.

Yıldız, A., Karahasan, G., Demircan, H., Toker, V., 2000. Kalecik (Ankara) güneydoğusu Alt Maastrichtiyen-Paleosen biyostratigrafisi ve paleoekolojisi. Yerbilimleri, Hacettepe Üniversitesi Yerbilimleri Uygulama ve Araştırma Merkezi Bülteni, 22, 247-259.

Yıldız, A., Ayyıldız, T., Sonel, N., 2001. Tuzgölü havzası kuzeybatısı (Karahoca- Mangaldağ – Yeşilyurt – Sarıhalit bölgesi) Üst Maastrihtiyen-Paleosen biyostratigrafisi ve paleoekolojisi. Yerbilimleri, Hacettepe Üniversitesi Yerbilimleri Uygulama ve Araştırma Merkezi Bülteni, 23, 33-52.

Yüksel, S., 1970. Etude géologique de la region d'Haymana (Turquie Centrale). Thèse Fac. Sci. Univ. De Nancy, 1-179.

Weaver, C., E., 1989. Clays, muds and shales. In: Development in Sedimentology, 44, Elsevier, Amsterdam, 819 p.

Weimer, P., Posamentier, H., W., (Eds.), 1993. Siliciclastic sequence stratigraphy: Recent developments and applications. AAPG, Memoir 58, Tulsa, Oklohama.

Wilson, J., L., 1975. Carbonate facies in geologic history. Springer-Verlag, New York, 469 p.

Zepeda, M. A., 1998. Planktonic foraminiferal diversity, equitability and biostratigraphy of the uppermost Campanian–Maastrichtian, ODP Leg 122, Hole 762C, Exmouth Plateau, NW Australia, eastern Indian Ocean. Cretaceous Research, 19, 117–152.

Web Site References:

Chronos.org, Georgescu, M., D., Chronos Services, An Interactive Guide to Planktonic Foraminifera: A. Cretaceous taxa, http://services.chronos.org/guideplankforam/index.htm, August 2008

Chronos.org, Mesozoic and Paleocene Planktonic Foraminiferal Working Groups, Chronos Portal, Foraminiferal Databases, http://portal.chronos.org/gridsphere/gridsphere?cid=res_taxondb, August 2008

Vrije Universiteit Amsterdam, Smit, J., Microkrystites from the K/T Boundary, http://www.geo.vu.nl/~smit/microkrystites/microkrystites.html, August 2008

APPENDIX

PLATES 1-12 are SEM images, PLATES 13-20 are thin section photographs

PLATE 1

Scale bar = 100 μm

Figure 1: *Globotruncana arca* CUSHMAN, sample no. KTS 1, *P. hariaensis* zone, **a.** spiral view, **b.** side view, **c.** umbilical view

Figure 2: *Globotruncana arca* CUSHMAN, sample no. KTS 2, *P. hariaensis* zone, umbilical view

Figure 3: *Globotruncana orientalis* EL NAGGAR, sample no. KTS 5, *P. hariaensis* zone, **a.** spiral view, **b.** spiral view, **c.** side view

Figure 4: *Globotruncana orientalis* EL NAGGAR, sample no. KTS 5, *P. hariaensis* zone, **a.** spiral view, **b.** spiral view, **c.** side view

Figure 5: *Globotruncana orientalis* EL NAGGAR, sample no. KTS 4, *P. hariaensis* zone, **a.** spiral view, **b.** side view, **c.** umbilical view

PLATE 1

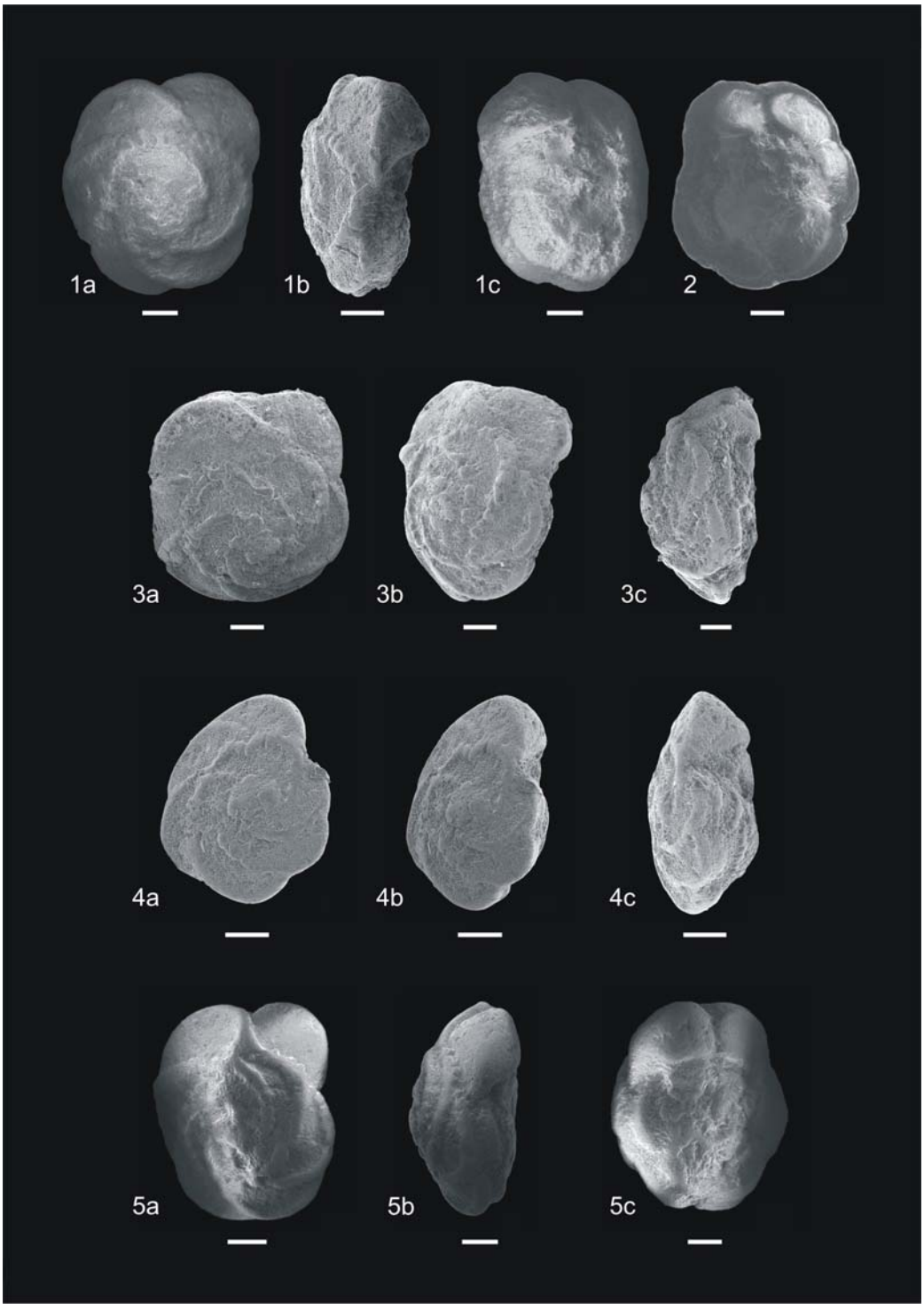

PLATE 2

Scale bar = 100 μm

Figure 1: *Globotruncana orientalis* EL NAGGAR, sample no. HSE 46, *P. hariaensis* zone, spiral view

Figure 2: *Globotruncana orientalis* EL NAGGAR, sample no. KTS 5, *P. hariaensis* zone, umbilical view

Figure 3: *Globotruncana mariei* BANNER and BLOW, sample no. KTS 5, *P. hariaensis* zone, spiral view

Figure 4: *Globotruncana mariei* BANNER and BLOW, sample no. KTS 5, *P. hariaensis* zone, side view

Figure 5: *Globotruncana mariei* BANNER and BLOW, sample no. HSE 46, *P. hariaensis* zone, **a.** spiral view, **b.** side view, **c.** umbilical view

Figure 6: *Globotruncana dupeublei* CARON *et al*., sample no. KTS 1, *P. hariaensis* zone, **a.** spiral view, **b.** spiral view, **c.** spiral view

Figure 7: *Globotruncana aegyptiaca* NAKKADY, sample no. KTS 2, *P. hariaensis* zone, spiral view

Figure 8: *Globotruncana aegyptiaca* NAKKADY, sample no. KTS 1, *P. hariaensis* zone, umbilical view

Figure 9: *Globotruncana esnehensis* NAKKADY, sample no. KTS 1, *P. hariaensis* zone, spiral view

PLATE 2

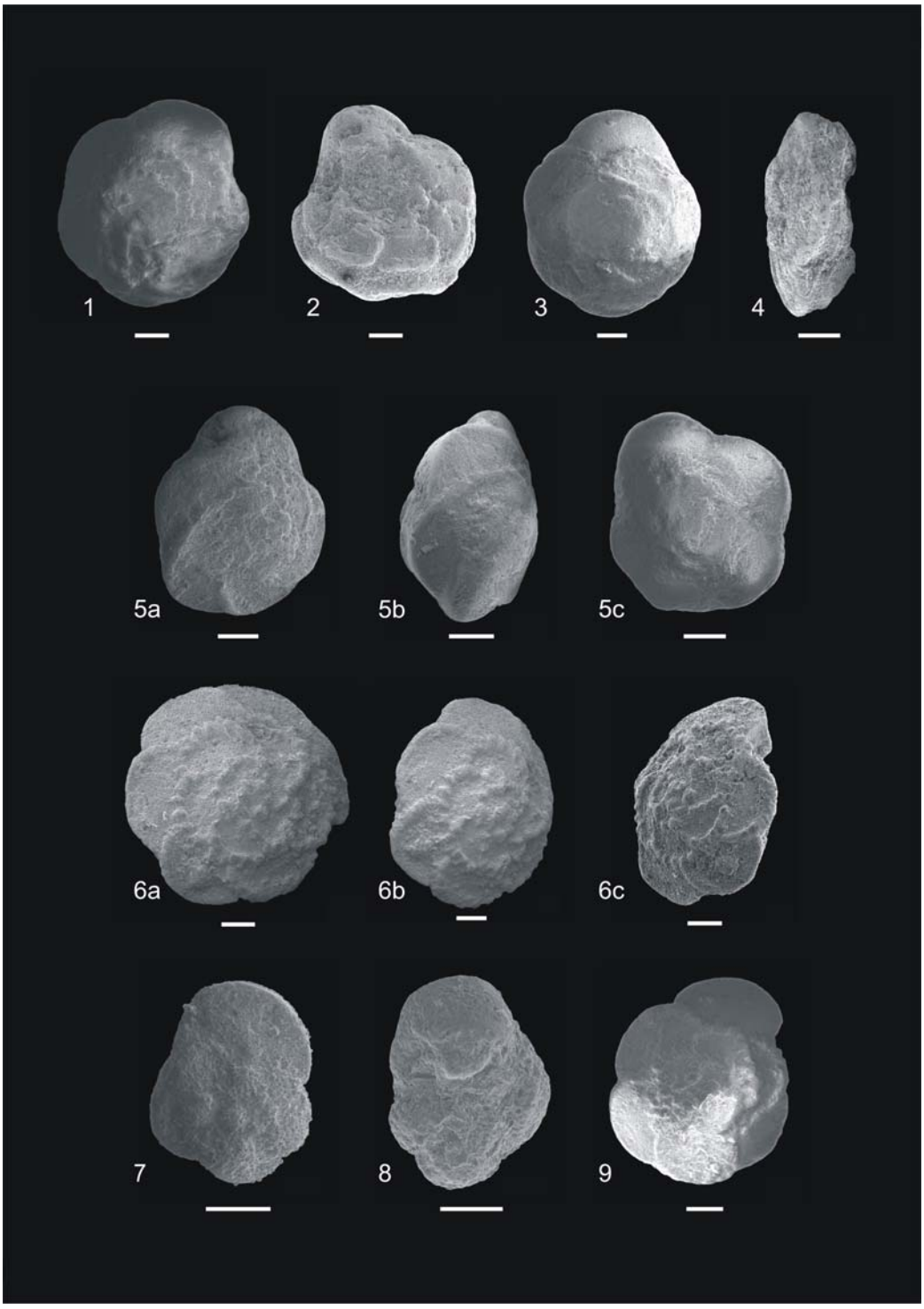

PLATE 3

Scale bar = 100 µm

Figure 1: *Contusotruncana walfischensis* TODD, sample no. KTS 1, *P. hariaensis* zone, **a.** spiral view, **b.** spiral view, **c.** side view

Figure 2: *Globotruncanita angulata* TILEV, sample no. KTS 2, *P. hariaensis* zone, **a.** spiral view, **b.** side view

Figure 3: *Globotruncanita angulata* TILEV, sample no. KTS 5, *P. hariaensis* zone, spiral view

Figure 4: *Globotruncanita pettersi* GANDOLFI, sample no. KTS 4, *P. hariaensis* zone, **a.** spiral view, **b.** umbilical view, **c.** side view

Figure 5: *Globotruncana stuarti* de LAPPARENT, sample no. KTS 5, *P. hariaensis* zone, **a.** spiral view, **b.** side view

Figure 6: *Globotruncanita stuartiformis* DALBIEZ, sample no. KTS 5, *P. hariaensis* zone, **a.** spiral view, **b.** spiral view, **c.** side view

PLATE 3

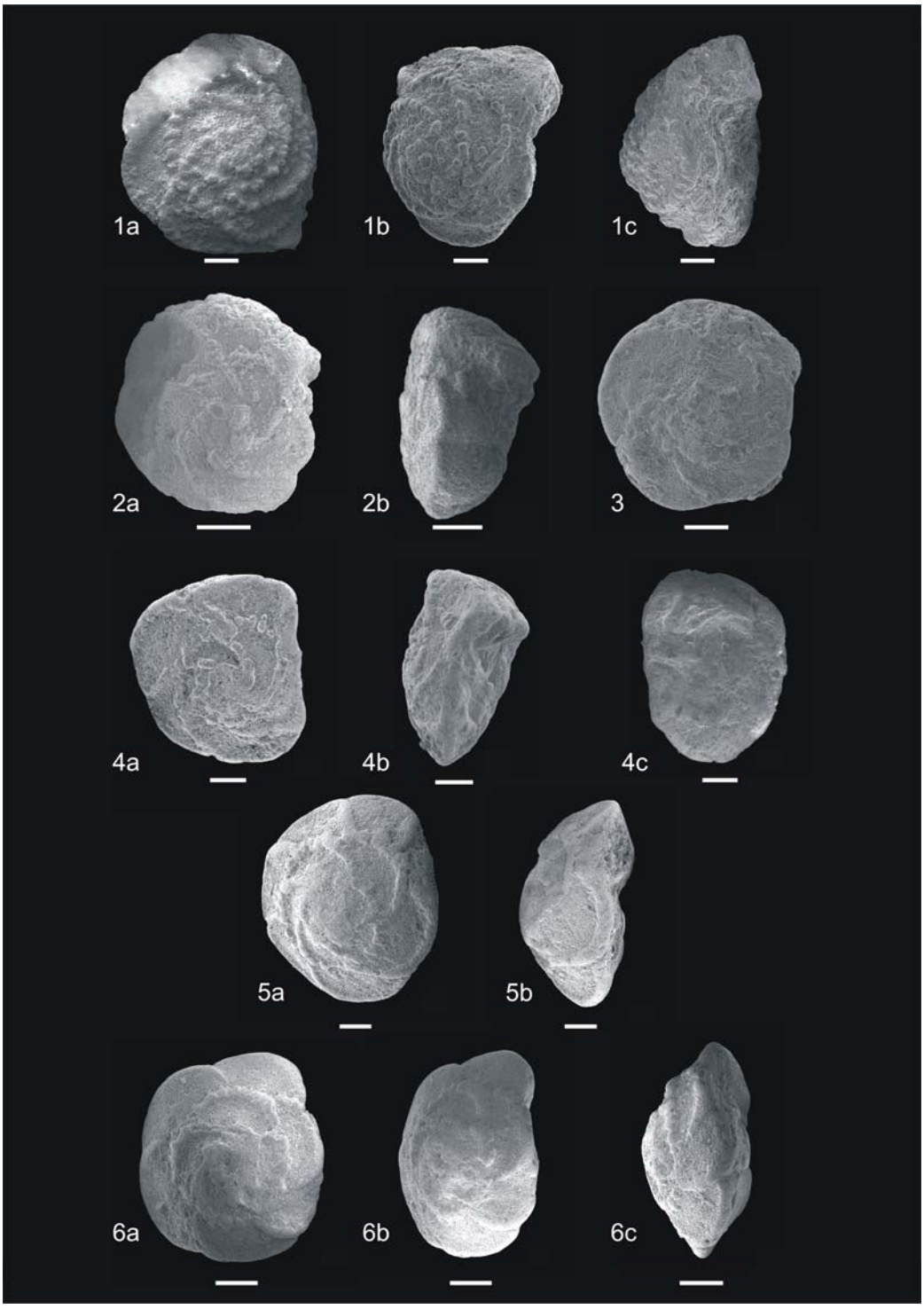

PLATE 4

Scale bar = 100 μm

Figure 1: *Rugoglobigerina hexacamerata* BRONNIMANN, sample no. KTS 2, *P. hariaensis* zone, spiral view

Figure 2: *Rugoglobigerina pennyi* BRONNIMANN, sample no. KTS 3, *P. hariaensis* zone, spiral view

Figure 3: *Rugoglobigerina rugosa* PLUMMER - *Rugoglobigerina macrocephala* BRONNIMANN transition, sample no. HSE 46, *P. hariaensis* zone, umbilical view

Figure 4: *Rugoglobigerina rugosa* PLUMMER, sample no. KTS 4, *P. hariaensis* zone, **a.** spiral view, **b.** side view, **c.** umbilical view

Figure 5: *Rugoglobigerina rugosa* PLUMMER, sample no. KTS 5, *P. hariaensis* zone, umbilical view

Figure 6: *Rugoglobigerina rugosa* PLUMMER, sample no. KTS 1, *P. hariaensis* zone, spiral view

Figure 7: *Globotruncanella havanensis* VOORWIJK, sample no. KTS 3, *P. hariaensis* zone, umbilical view

Figure 8: *Globotruncanella havanensis* VOORWIJK, sample no. KTS 2, *P. hariaensis* zone, spiral view

Figure 9: *Globotruncanella minuta* CARON, sample no. KTS 2, *P. hariaensis* zone, spiral view

Figure 10: *Globotruncanella petaloidea* GANDOLFI, sample no. KTS 3, *P. hariaensis* zone, spiral view

Figure 11: *Globotruncanella petaloidea* GANDOLFI, sample no. KTS 1, *P. hariaensis* zone, side view

Figure 12: *Globotruncanella petaloidea* GANDOLFI, sample no. KTS 2, *P. hariaensis* zone, **a.** umbilical view, **b.** side view,

PLATE 4

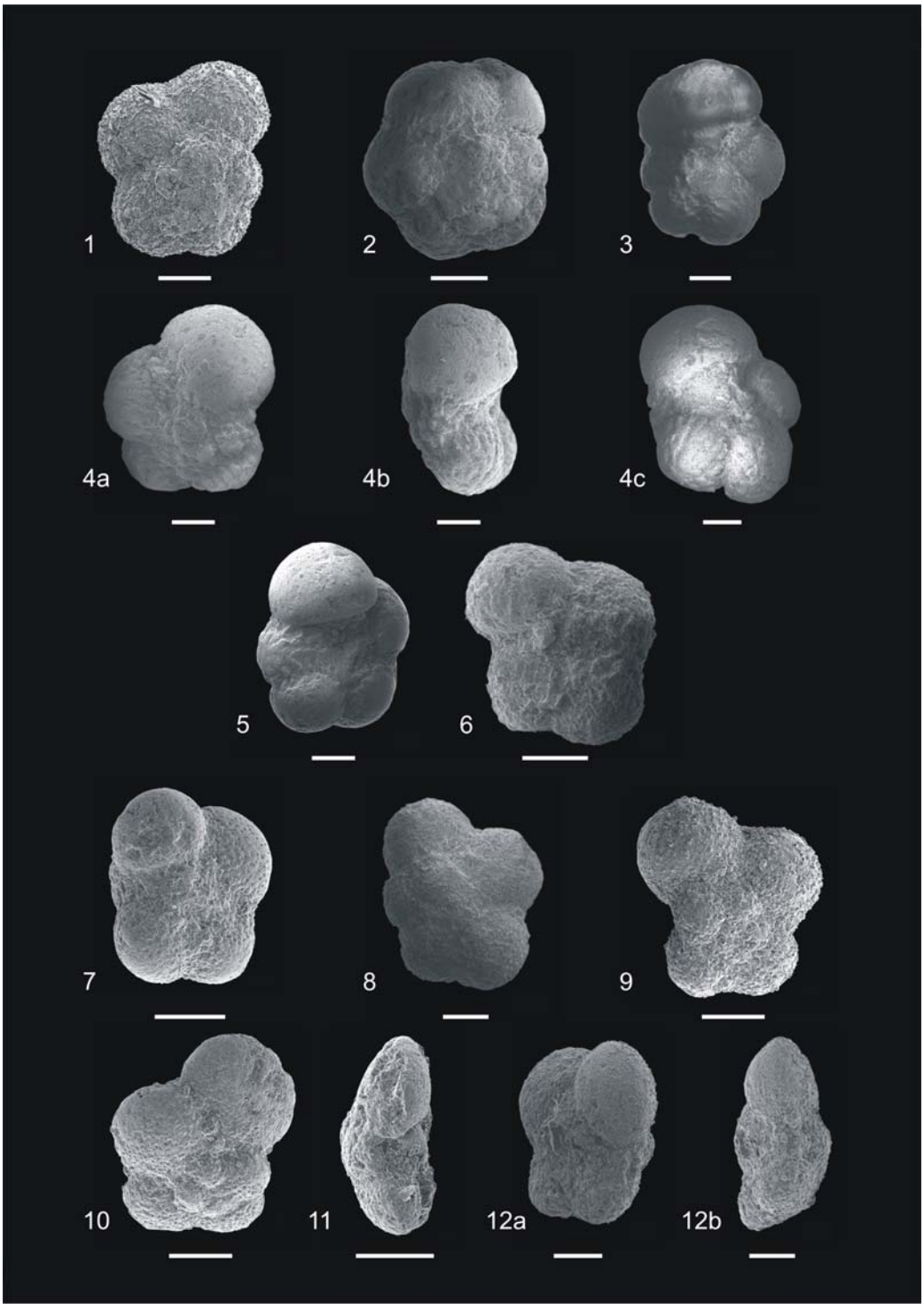

PLATE 5

Scale bar = 100 μm

Figure 1: *Globigerinelloides alvarezi* ETERNOD OLVERA, sample no. KTS 2, *P. hariaensis* zone, spiral view

Figure 2: *Globigerinelloides prairiehillensis* PESSAGNO, sample no. KTS 5, *P. hariaensis* zone, umbilical view

Figure 3: *Globigerinelloides messinae* BRONNIMANN, sample no. KTS 1, *P. hariaensis* zone, umbilical view

Figure 4: *Globigerinelloides multispinus* LALICKER, sample no. KTS 2, *P. hariaensis* zone, side view

Figure 5: *Globigerinelloides subcarinatus* BRONNIMANN, sample no. HSE 46, *P. hariaensis* zone, spiral view

Figure 6: *Globigerinelloides subcarinatus* BRONNIMANN, sample no. KTS 1, *P. hariaensis* zone, **a.** spiral view, **b.** side view

Figure 7: *Globigerinelloides* sp., sample no. KTS 14, *P. hariaensis* zone, spiral view

Figure 8: *Hedbergella monmouthensis* OLSSON, sample no. KTS 6, *P. hariaensis* zone, **a.** spiral view, **b.** side view, **c.** umbilical view

Figure 9: *Hedbergella monmouthensis* OLSSON, sample no. KTS 2, *P. hariaensis* zone, spiral view

Figure 10: *Hedbergella holmdelensis* OLSSON, sample no. KTS 2, *P. hariaensis* zone, **a.** spiral view, **b.** side view, **c.** umbilical view

Figure 11: *Hedbergella holmdelensis* OLSSON, sample no. KTS 2, *P. hariaensis* zone, spiral view

PLATE 5

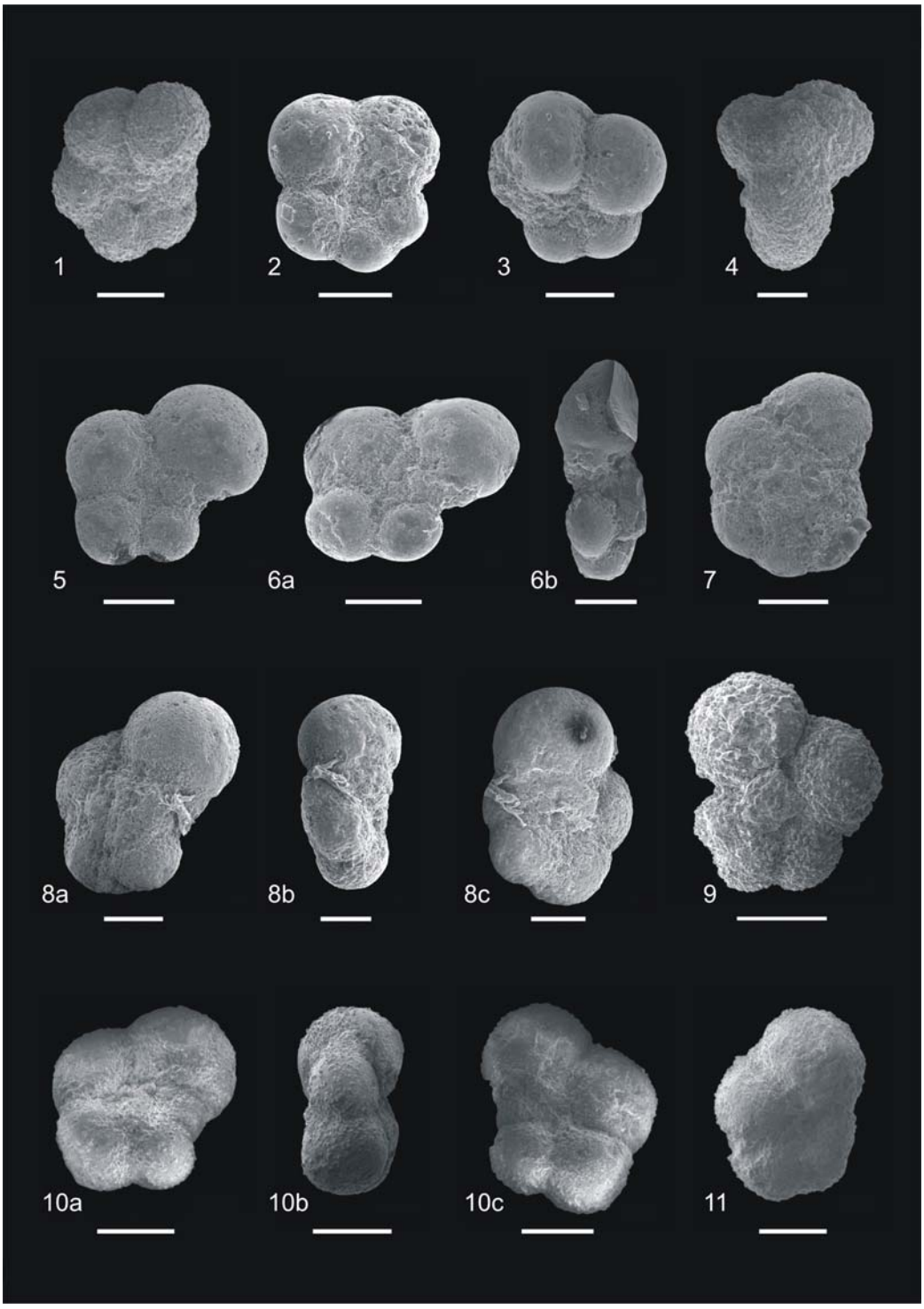

PLATE 6

Scale bar = 100 μm

Figure 1: *Heterohelix globulosa* EHRENBERG, sample no. KTS 2, *P. hariaensis* zone, side view

Figure 2: *Heterohelix globulosa* EHRENBERG, sample no. KTS 3, *P. hariaensis* zone, side view

Figure 3: *Heterohelix globulosa* EHRENBERG, sample no. HSE 46, *P. hariaensis* zone, side view

Figure 4: *Heterohelix globulosa* EHRENBERG, sample no. KTS 5, *P. hariaensis* zone, side view

Figure 5: *Heterohelix globulosa* EHRENBERG (*Heterohelix striata* cf. EHRENBERG), sample no. KTS 2, *P. hariaensis* zone, side view

Figure 6: *Heterohelix globulosa* EHRENBERG, sample no. KTS 5, *P. hariaensis* zone, side view

Figure 7: *Heterohelix navarroensis* LOEBLICH, sample no. KTS 5, *P. hariaensis* zone, side view

Figure 8: *Heterohelix labellosa* NEDERBRAGT, sample no. KTS 2, *P. hariaensis* zone, side view

Figure 9: *Heterohelix punctulata* CUSHMAN, sample no. KTS 2, *P. hariaensis* zone, side view

Figure 10: *Laeviheterohelix dentata* STENESTAD, sample no. KTS 2, *P. hariaensis* zone, side view

Figure 11: *Laeviheterohelix dentata* STENESTAD, sample no. KTS 1, *P. hariaensis* zone, side view

Figure 12: *Laeviheterohelix glabrans* CUSHMAN, sample no. HSE 46, *P. hariaensis* zone, side view

Figure 13: *Laeviheterohelix glabrans* CUSHMAN, KTS 14, *P. hariaensis* zone, **a.** side view, **b.** edge view

Figure 14: *Laeviheterohelix glabrans* CUSHMAN, KTS 3, *P. hariaensis* zone, **a.** side view, **b.** edge view

PLATE 6

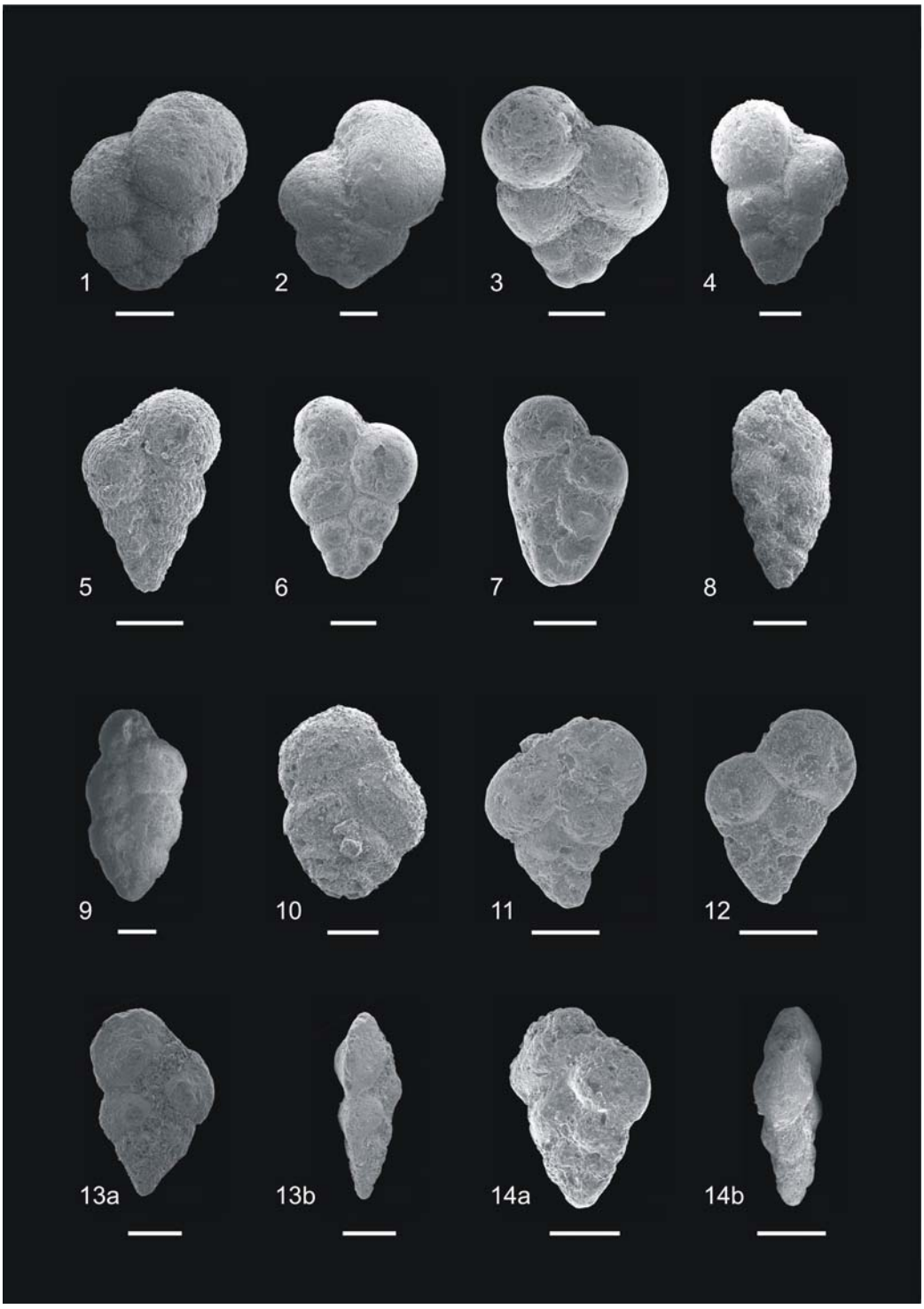

PLATE 7

Scale bar = 100 μm

Figure 1: *Pseudotextularia elegans* RZEHAK, sample no. KTS 3, *P. hariaensis* zone, edge view

Figure 2: *Pseudotextularia elegans* RZEHAK, sample no. KTS 5, *P. hariaensis* zone, edge view

Figure 3: *Pseudotextularia elegans* RZEHAK, sample no. KTS 5, *P. hariaensis* zone, **a.** side view, **b.** edge view

Figure 4: *Pseudotextularia elegans* RZEHAK, sample no. KTS 5, *P. hariaensis* zone, edge view

Figure 5: *Pseudotextularia nuttalli* VOORWIJK, sample no. KTS 5, *P. hariaensis* zone, edge view

Figure 6: *Pseudotextularia nuttalli* VOORWIJK, sample no. HSE 46, *P. hariaensis* zone, side view

Figure 7: *Pseudotextularia nuttalli* VOORWIJK, sample no. KTS 5, *P. hariaensis* zone, edge view

Figure 8: *Pseudoguembelina costulata* CUSHMAN, sample no. KTS 1, *P. hariaensis* zone, side view

Figure 9: *Pseudoguembelina costulata* CUSHMAN, sample no. KTS 3, *P. hariaensis* zone, side view

Figure 10: *Pseudoguembelina hariaensis* NEDERBRAGT, sample no. KTS 14, *P. hariaensis* zone, side view

Figure 11: *Pseudoguembelina hariaensis* NEDERBRAGT, sample no. KTS 2, *P. hariaensis* zone, side view

Figure 12: *Pseudoguembelina hariaensis* NEDERBRAGT, sample no. HSE 46, *P. hariaensis* zone, side view

PLATE 7

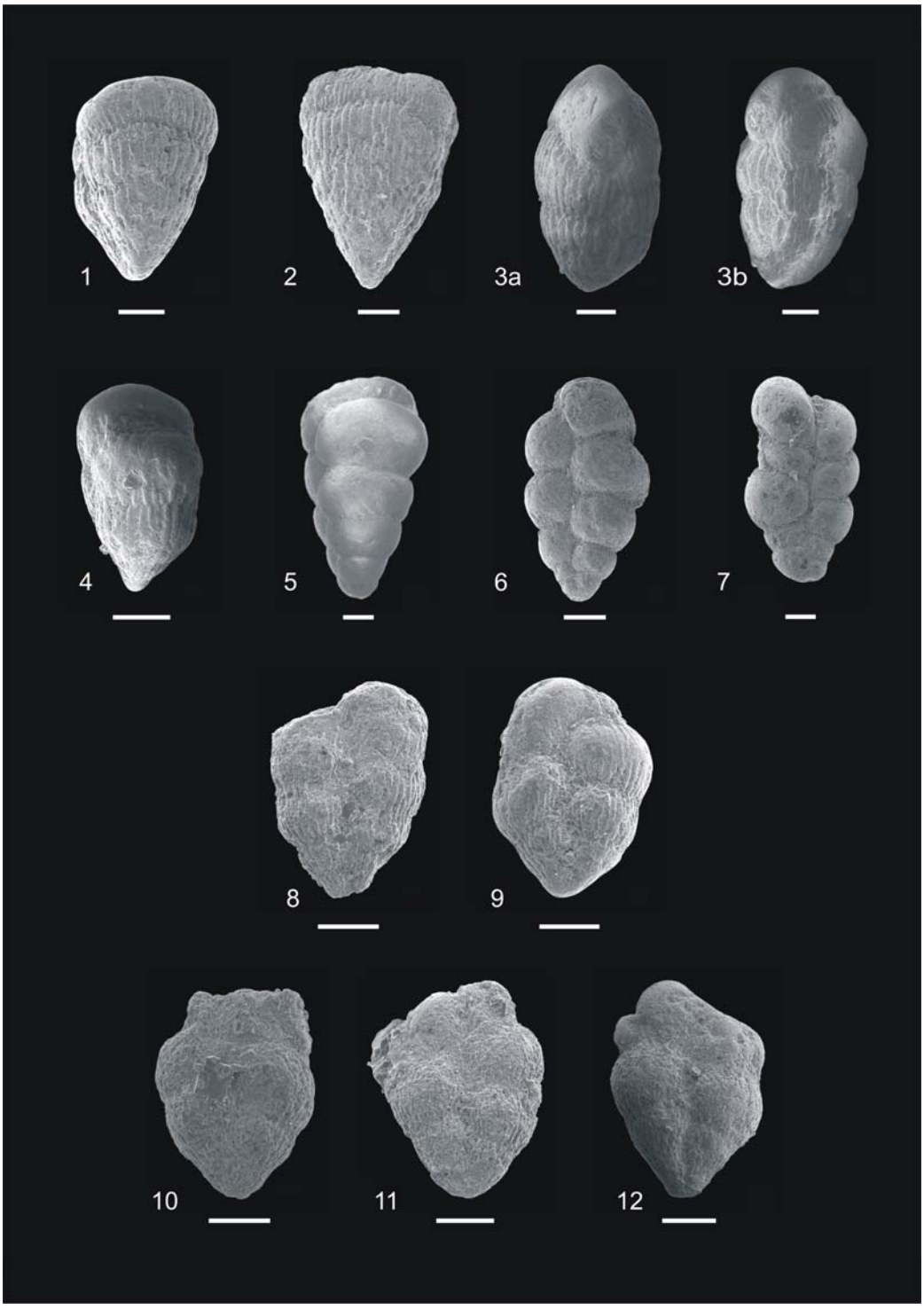

PLATE 8

Scale bar = 100 μm

Figure 1: *Planoglobulina acervulinoides* EGGER, sample no. KTS 1, *P. hariaensis* zone, side view

Figure 2: *Planoglobulina acervulinoides* EGGER, sample no. KTS 1, *P. hariaensis* zone, **a.** side view, **b.** edge view

Figure 3: *Planoglobulina acervulinoides* EGGER, sample no. KTS 5, *P. hariaensis* zone, side view

Figure 4: *Planoglobulina acervulinoides* EGGER, sample no. HSE 46, *P. hariaensis* zone, side view

Figure 5: *Planoglobulina acervulinoides* EGGER, sample no. HSE 46, *P. hariaensis* zone, side view

Figure 6: *Planoglobulina carseyae* PLUMMER, sample no. KTS 2, *P. hariaensis* zone, side view

Figure 7: *Racemiguembelina fructicosa* EGGER, sample no. HSE 46, *P. hariaensis* zone, side view

Figure 8: *Racemiguembelina fructicosa* EGGER, sample no. HSE 46, *P. hariaensis* zone, side view

Figure 9: *Racemiguembelina powelli* SMITH and PESSAGNO, sample no. HSE 46, *P. hariaensis* zone, **a.** side view, **b.** top view

PLATE 8

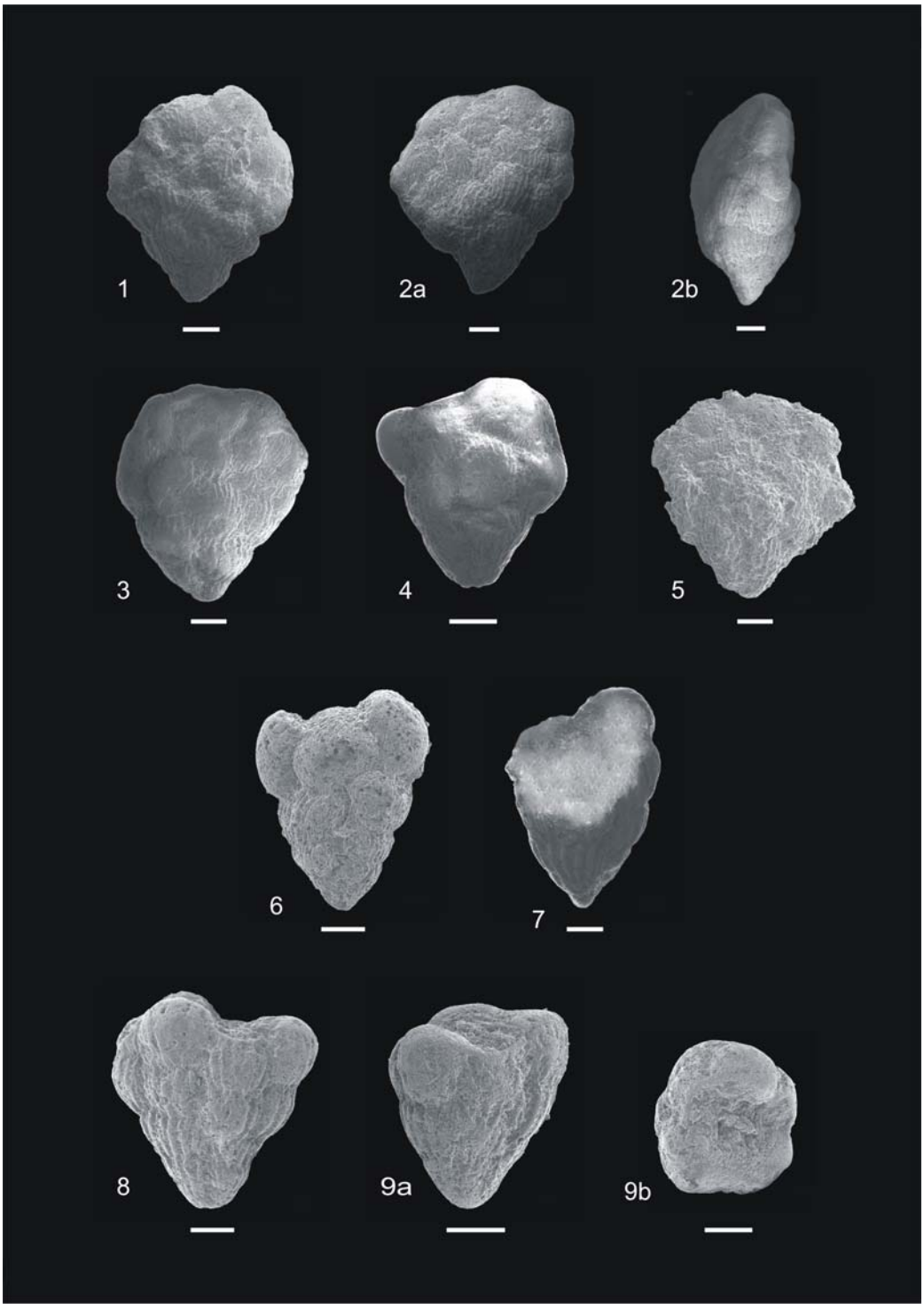

PLATE 9

Scale bar = 100 μm

Figure 1: *Globoconusa minutula* LUTERBACHER and PREMOLI-SILVA, sample no. KTS 14, P0 zone, **a.** spiral view, **b.** side view

Figure 2: *Globoconusa minutula* LUTERBACHER and PREMOLI-SILVA, sample no. KTS 19, P1a zone, spiral view

Figure 3: *Eoglobigerina fringa* SUBBOTINA, sample no. KTS 16, P1a zone, spiral view

Figure 4: *Eoglobigerina fringa* SUBBOTINA, sample no. KTS 16, P1a zone, umbilical view

Figure 5: *Eoglobigerina eobulloides* MOROZOVA, sample no. KTS 27, P1a zone, umbilical view

Figure 6: *Eoglobigerina eobulloides* MOROZOVA, sample no. KTS 27, P1a zone, spiral view

Figure 7: *Eoglobigerina eobulloides* MOROZOVA, sample no. KTS 27, P1a zone, umbilical view

Figure 8: *Eoglobigerina eobulloides* MOROZOVA, sample no. KTS 19, P1a zone, spiral view

Figure 9: *Eoglobigerina eobulloides* MOROZOVA, sample no. KTS 19, P1a zone, umbilical view

Figure 10: *Eoglobigerina edita* SUBBOTINA, sample no. KTS 27, P1a zone, spiral view

Figure 11: *Eoglobigerina edita* SUBBOTINA, sample no. KTS 27, P1a zone, spiral view

Figure 12: *Eoglobigerina edita* SUBBOTINA, sample no. KTS 27, P1a zone, spiral view

Figure 13: *Eoglobigerina edita* SUBBOTINA, sample no. KTS 27, P1a zone, spiral view

PLATE 9

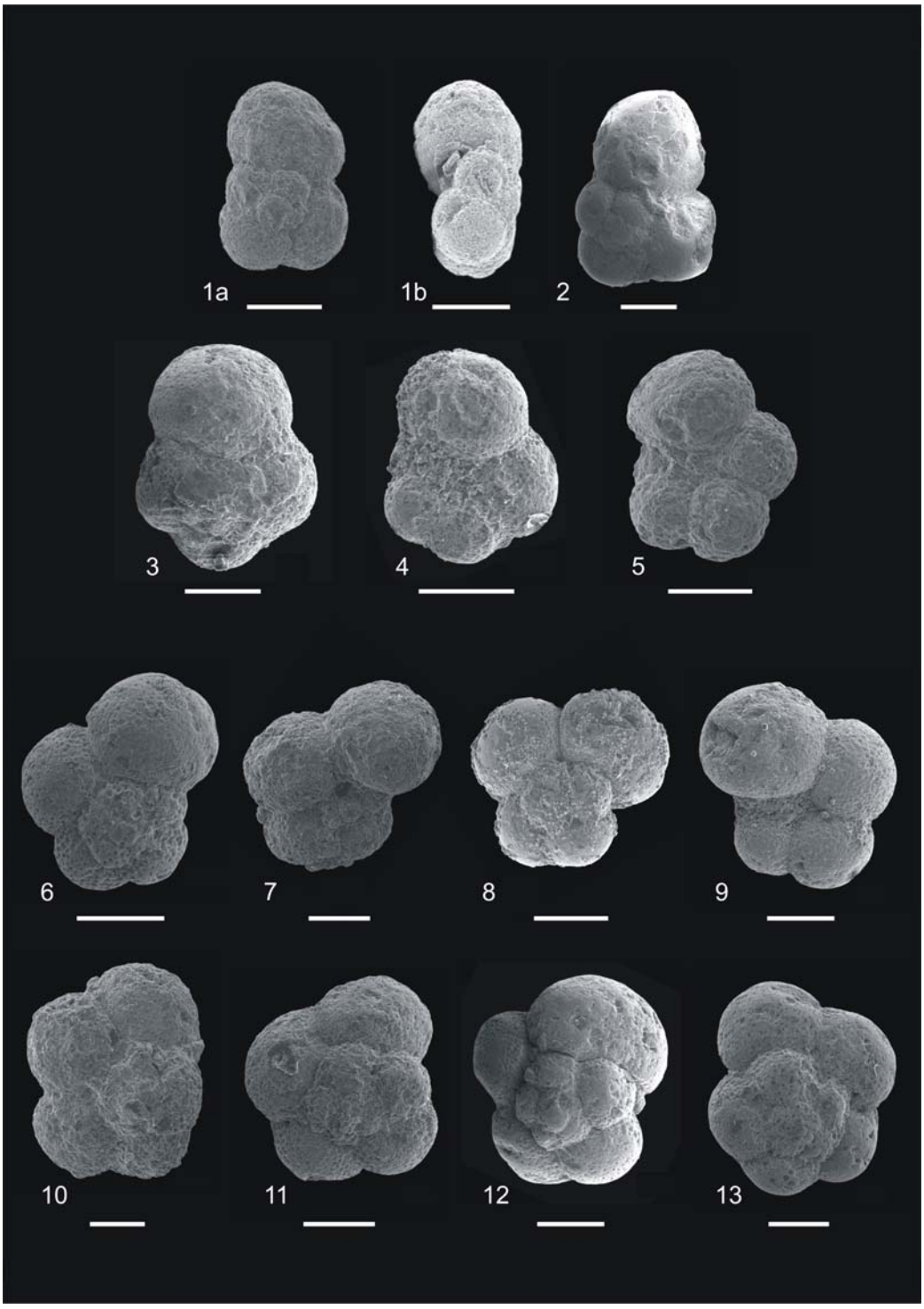

PLATE 10

Scale bar = 100 μm

Figure 1: *Parvularugoglobigerina eugubina* LUTERBACHER and PREMOLI-SILVA, sample no. KTS 16, P1a zone, spiral view

Figure 2: *Globoconusa daubjergensis* BRONNIMANN, sample no. KTS 16, P1a zone, spiral view

Figure 3: *Globoconusa daubjergensis* BRONNIMANN, sample no. KTS 27, P1a zone, spiral view

Figure 4: *Globanomalina archeocompressa* BLOW, sample no. KTS 17, P1a zone, **a.** spiral view, **b.** side view

Figure 5: *Globanomalina archeocompressa* BLOW, sample no. KTS 27, P1a zone, **a.** spiral view, **b.** side view

Figure 6: *Globanomalina archeocompressa* BLOW, sample no. HSE 55, P1a zone, spiral view

Figure 7: *Praemurica taurica* MOROZOVA, sample no. KTS 27, P1a zone, spiral view

Figure 8: *Praemurica taurica* MOROZOVA, sample no. KTS 16, P1a zone, umbilical view

PLATE 10

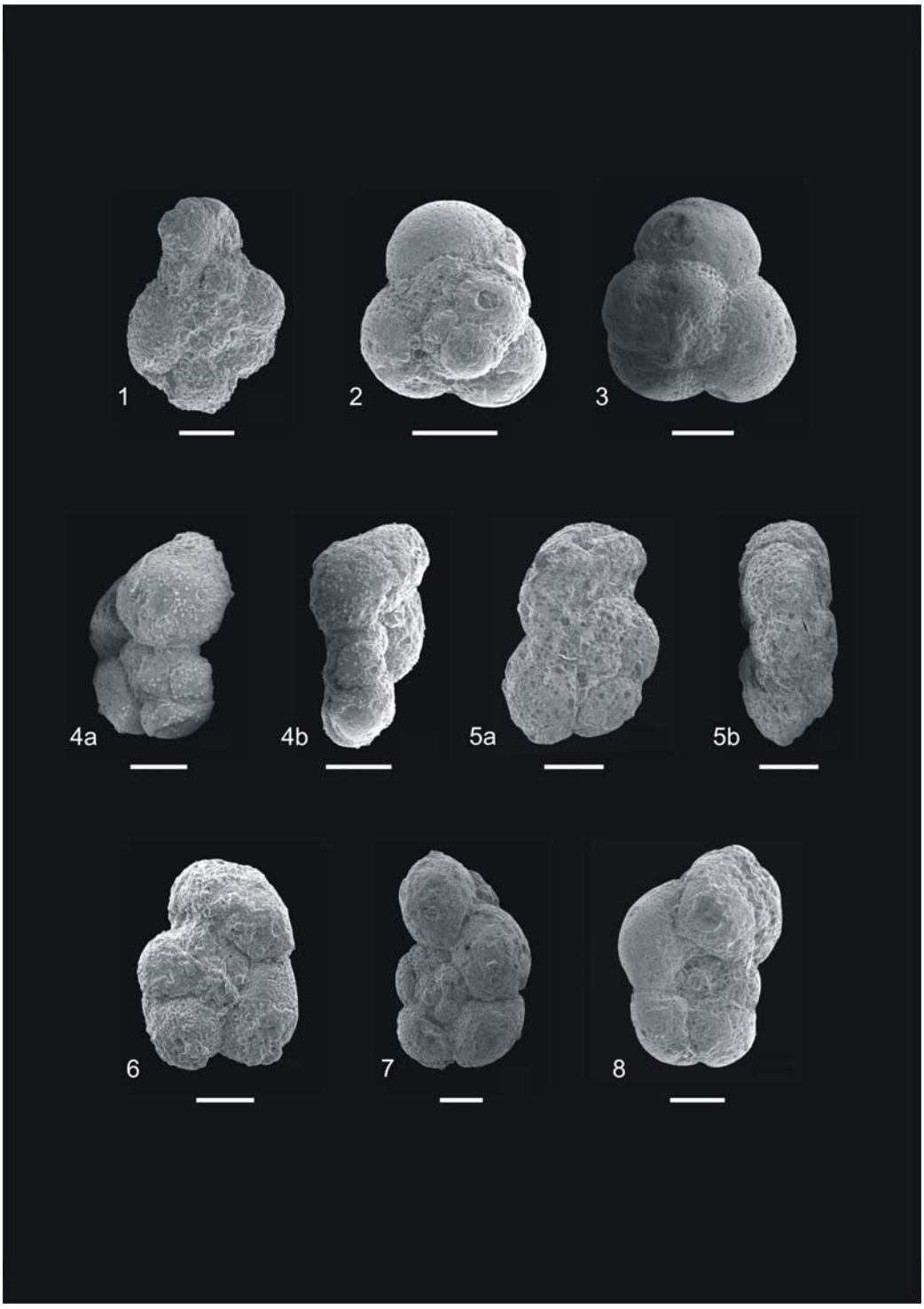

PLATE 11

Scale bar = 100 μm

Figure 1: *Parasubbotina pseudobulloides* PLUMMER, sample no. KTS 16, P1a zone, spiral view

Figure 2: *Parasubbotina pseudobulloides* PLUMMER, sample no. KTS 19, P1a zone, umbilical view

Figure 3: *Praemurica pseudoinconstans* BLOW, sample no. KTS 27, P1a zone, spiral view

Figure 4: *Subbotina triloculinoides* PLUMMER, sample no. KTS 16, P1a zone, spiral view

Figure 5: *Subbotina triloculinoides* PLUMMER, sample no. KTS 27, P1a zone, spiral view

Figure 6: *Subbotina triloculinoides* PLUMMER, sample no. KTS 19, P1a zone, spiral view

Figure 7: *Subbotina triloculinoides* PLUMMER, sample no. KTS 16, P1a zone, spiral view

Figure 8: *Subbotina triloculinoides* PLUMMER, sample no. KTS 19, P1a zone, side view

Figure 9: *Subbotina triloculinoides* PLUMMER, sample no. KTS 19, P1a zone, umbilical view

Figure 10: *Subbotina trivialis* SUBBOTINA, sample no. KTS 17, P1a zone, spiral view

Figure 11: *Subbotina trivialis* SUBBOTINA, sample no. KTS 27, P1a zone, umbilical view

PLATE 11

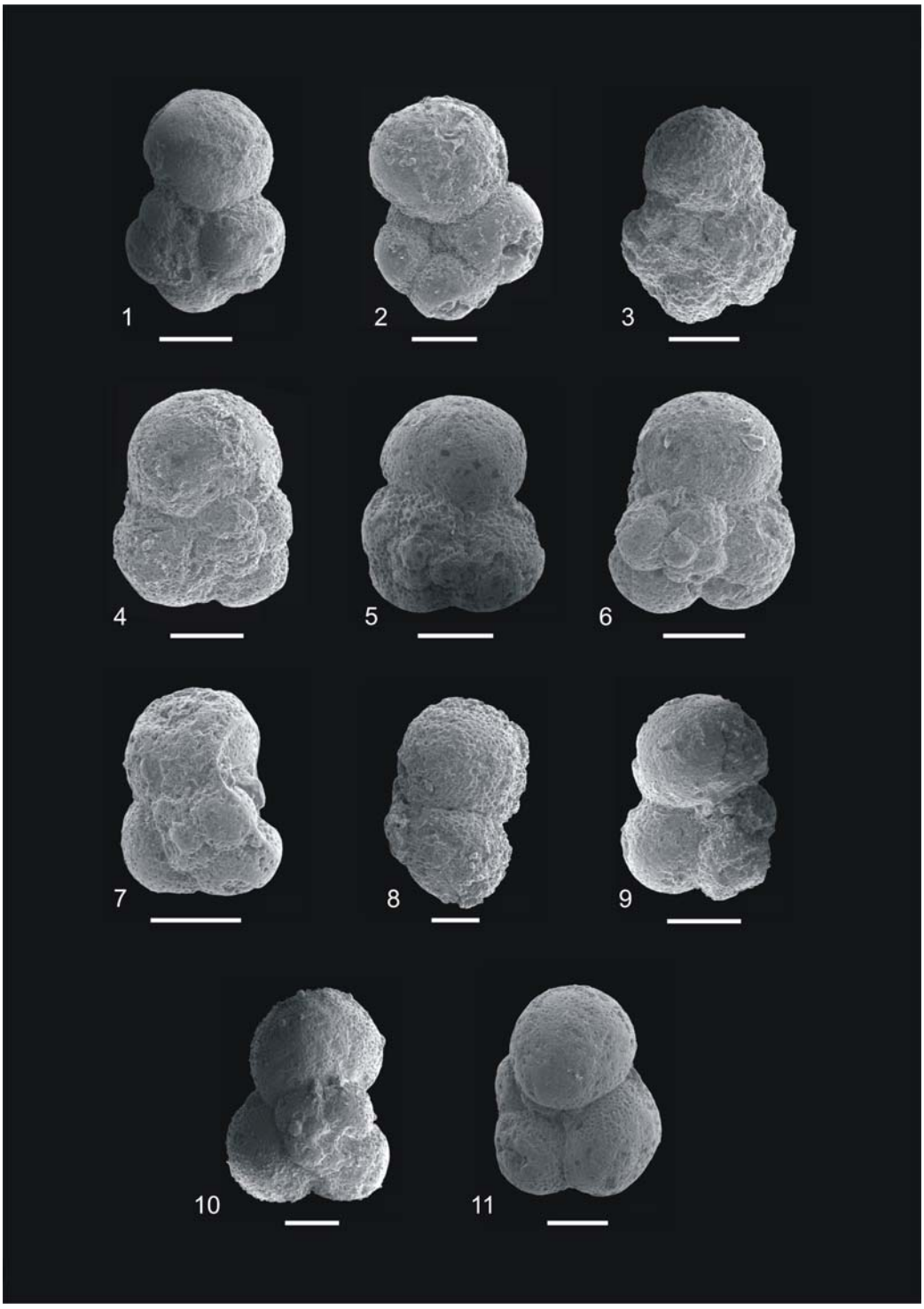

PLATE 12

Scale bar = 50 µm

Figure 1: *Guembelitria cretacea* CUSHMAN, sample no. HSE 60, P1a zone, side view

Figure 2: *Woodringina hornerstownensis* OLSSON, sample no. KTS 14, P1a zone, side view

Figure 3: *Woodringina hornerstownensis* OLSSON, sample no. KTS 16, P1a zone, side view

Figure 4: *Woodringina hornerstownensis* OLSSON, sample no. HSE 52, P1a zone, side view

Figure 5: *Chiloguembelina* sp., sample no. KTS 16, P1a zone, side view

Figure 6: *Zeauvigerina waiparaensis* JENKINS, sample no. KTS 16, P1a zone, side view

Figure 7: *Zeauvigerina waiparaensis* JENKINS, sample no. KTS 15, P1a zone, side view

PLATE 12

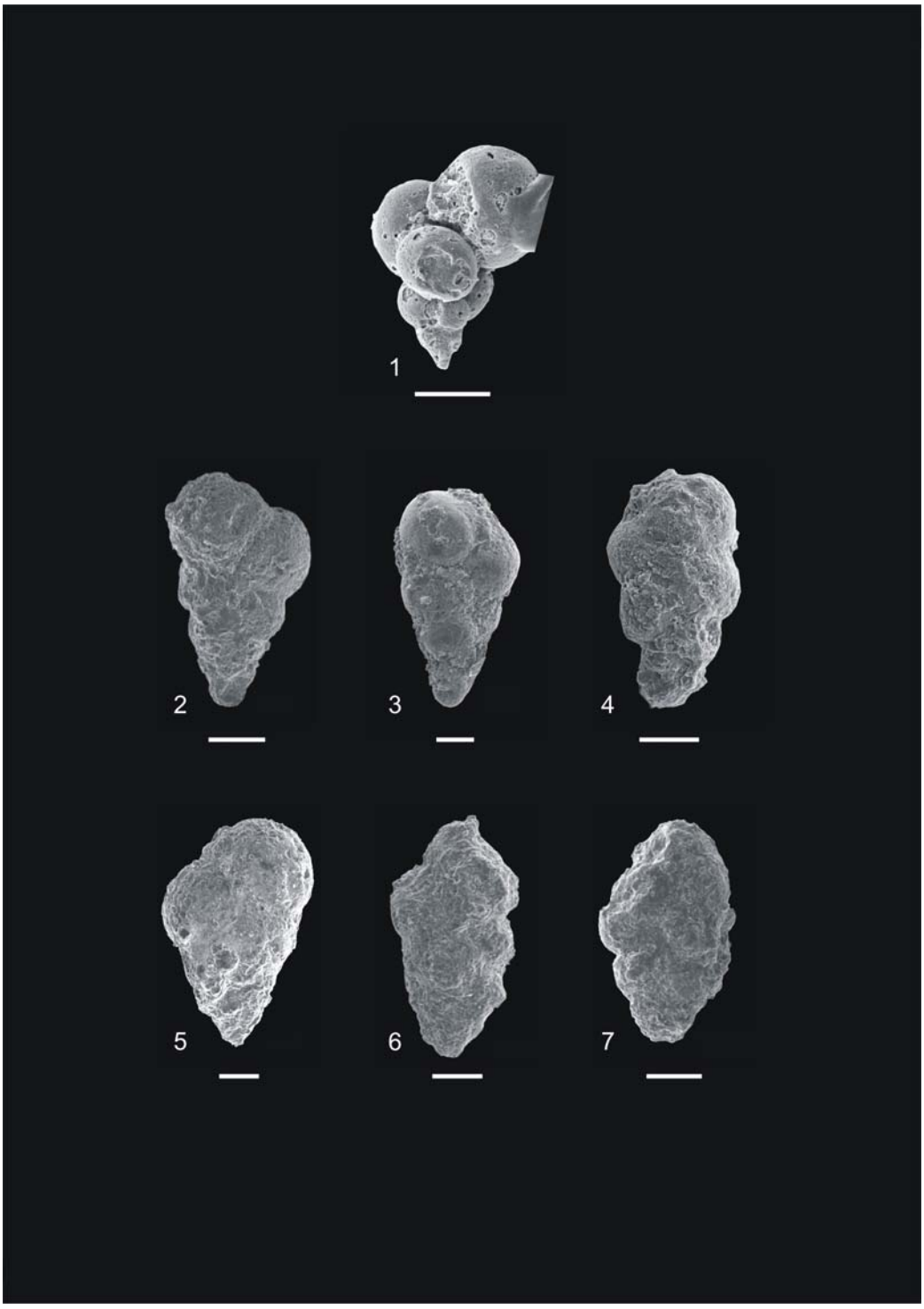

PLATE 13

Figure 1: *Globotruncana arca* CUSHMAN, sample no. KTS 1, *P. hariaensis* zone, X65

Figure 2: *Globotruncana arca* CUSHMAN, sample no. KTS 10, *P. hariaensis* zone, X49

Figure 3: *Globotruncana arca* CUSHMAN, sample no. KTS 11, *P. hariaensis* zone, X71

Figure 4: *Globotruncana arca* CUSHMAN, sample no. KTS 3, *P. hariaensis* zone, X73

Figure 5: *Globotruncana mariei* BANNER and BLOW, sample no. HSE 41, *R. fructicosa* zone, X96

Figure 6: *Globotruncana mariei* BANNER and BLOW, sample no. HSE 40, *P. acervulinoides* zone, X87

Figure 7: *Globotruncana hilli* PESSAGNO, sample no. KTS 12, *P. hariaensis* zone, X118

Figure 8: *Globotruncana hilli* PESSAGNO, sample no. KTS 2, *P. hariaensis* zone, X154

Figure 9: *Globotruncana hilli* PESSAGNO, sample no. HSE 46, *P. hariaensis* zone, X113

Figure 10: *Globotruncana falsostuarti* SIGAL, sample no. HSE 24, unzoned, X81

Figure 11: *Globotruncana falsostuarti* SIGAL, sample no. KTS 12, *P. hariaensis* zone, X70

Figure 12: *Globotruncana falsostuarti* SIGAL, sample no. KTS 12, *P. hariaensis* zone, X98

Figure 13: *Contusotruncana contusa* CUSHMAN, sample no. HSE 23, unzoned, X36

Figure 14: *Contusotruncana walfischensis* TODD, sample no. KTS 10, *P. hariaensis* zone, X83

Figure 15: *Contusotruncana walfischensis* TODD, sample no. KTS 3, *P. hariaensis* zone, X55

Figure 16: *Globotruncanita conica* WHITE, sample no. KTS 11, *P. hariaensis* zone, X39

Figure 17: *Globotruncanita conica* WHITE, sample no. HSE 45, *P. hariaensis* zone, X50

Figure 18: *Globotruncana stuarti* de LAPPARENT, sample no. HSE 17, unzoned, X90

Figure 19: *Globotruncana stuarti* de LAPPARENT, sample no. HSE 23, unzoned, X71

Figure 20: *Globotruncana stuarti* de LAPPARENT, sample no. HSE 19, unzoned, X92

Figure 21: *Globotruncanita stuartiformis* DALBIEZ, sample no. HSE 21, unzoned, X70

Figure 22: *Globotruncanita stuartiformis* DALBIEZ, sample no. HSE 19, unzoned, X97

Figure 23: *Globotruncanita stuartiformis* DALBIEZ, sample no. HSE 33, unzoned, X92

Figure 24: *Globotruncanita stuartiformis* DALBIEZ, sample no. HSE 39, *P. acervulinoides* zone, X84

Figure 25: *Globotruncanita stuartiformis* DALBIEZ, sample no. HSE 39, *P. acervulinoides* zone, X75

Figure 26: *Globotruncanita stuartiformis* DALBIEZ, sample no. HSE 25, unzoned, X111

Figure 27: *Globotruncanita stuartiformis* DALBIEZ, sample no. HSE 3, unzoned, X68

Figure 28: *Globotruncanita angulata* TILEV, sample no. HSE 39, *P. acervulinoides* zone, X75

PLATE 13

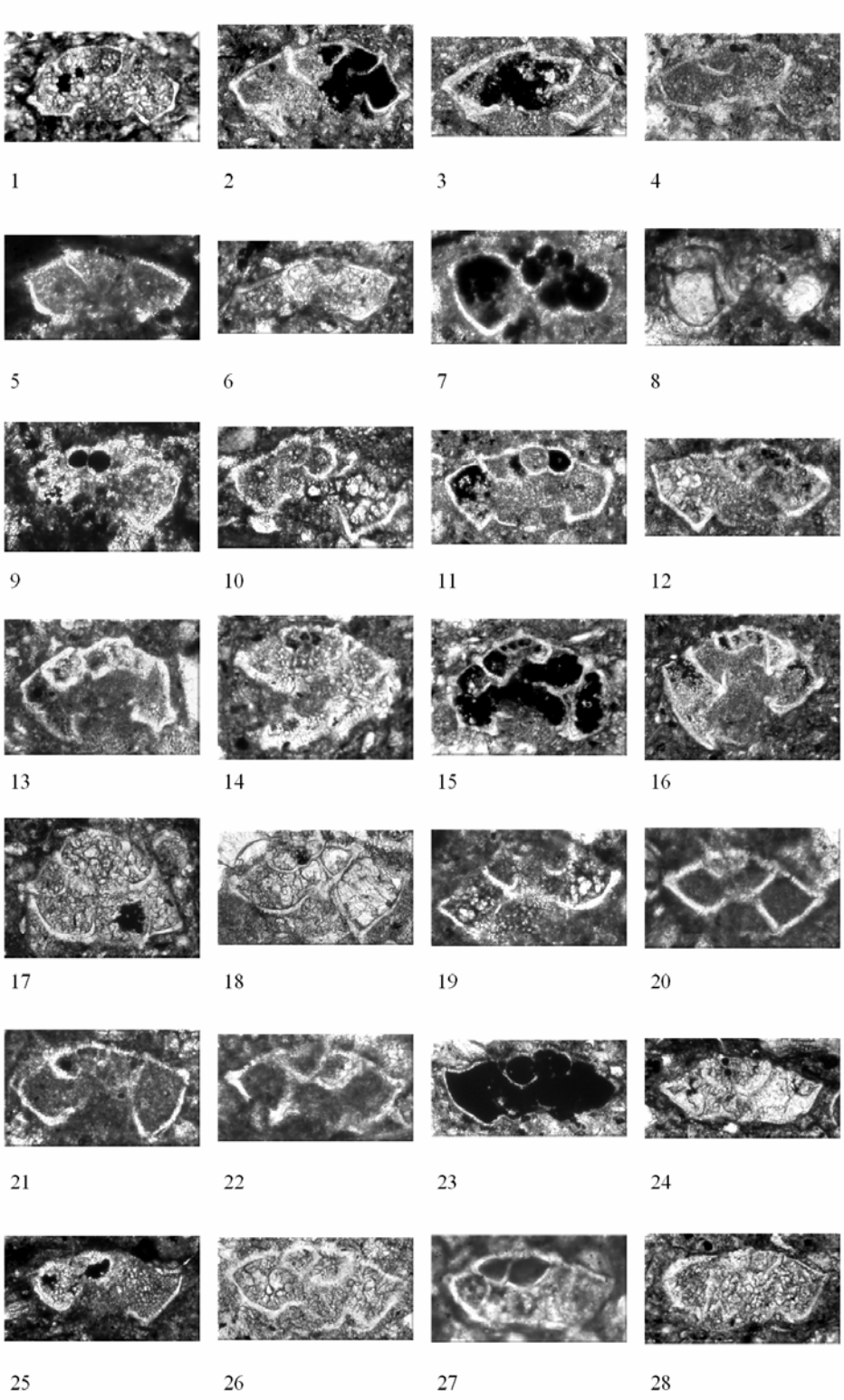

PLATE 14

Figure 1: *Rugoglobigerina hexacamerata* BRONNIMANN, sample no. KTS 7, *P. hariaensis* zone, X150

Figure 2: *Rugoglobigerina hexacamerata* BRONNIMANN, sample no. HSE 25, unzoned, X121

Figure 3: *Rugoglobigerina macrocephala* BRONNIMANN, sample no. HSE 36, *P. acervulinoides* zone, X78

Figure 4: *Rugoglobigerina macrocephala* BRONNIMANN, sample no. HSE 47, *P. hariaensis* zone, X100

Figure 5: *Rugoglobigerina milamensis* SMITH and PESSAGNO, sample no. HSE 2, unzoned, X87

Figure 6: *Rugoglobigerina pennyi* BRONNIMANN, sample no. KTS 11, *P. hariaensis* zone, X106

Figure 7: *Rugoglobigerina pennyi* BRONNIMANN, sample no. HSE 24, unzoned, X134

Figure 8: *Rugoglobigerina rugosa* PLUMMER, sample no. KTS 9, *P. hariaensis* zone, X131

Figure 9: *Rugoglobigerina rugosa* PLUMMER, sample no. KTS 7, *P. hariaensis* zone, X124

Figure 10: *Globotruncanella havanensis* VOORWIJK, sample no. KTS 5, *P. hariaensis* zone, X180

Figure 11: *Globotruncanella havanensis* VOORWIJK, sample no. HSE 16, unzoned, X171

Figure 12: *Globotruncanella petaloidea* GANDOLFI, sample no. KTS 12, *P. hariaensis* zone, X116

Figure 13: *Globotruncanella minuta* CARON, sample no. KTS 4, *P. hariaensis* zone, X96

Figure 14: *Hedbergella monmouthensis* OLSSON, sample no. KTS 5, *P. hariaensis* zone, X142

Figure 15: *Hedbergella monmouthensis* OLSSON, sample no. KTS 2, *P. hariaensis* zone, X175

Figure 16: *Hedbergella monmouthensis* OLSSON, sample no. HSE 49, *P. hariaensis* zone, X150

Figure 17: *Hedbergella monmouthensis* OLSSON, sample no. HSE 1, unzoned, X88

Figure 18: *Hedbergella monmouthensis* OLSSON, sample no. KTS 13, *P. hariaensis* zone, X110

Figure 19: *Hedbergella monmouthensis* OLSSON, sample no. KTS 3, *P. hariaensis* zone, X100

Figure 20: *Hedbergella monmouthensis* OLSSON, sample no. KTS 1, *P. hariaensis* zone, X118

Figure 21: *Hedbergella holmdelensis* OLSSON, sample no. HSE 25, unzoned, X100

Figure 22: *Hedbergella holmdelensis* OLSSON, sample no. KTS 5, *P. hariaensis* zone, X208

Figure 23: *Hedbergella holmdelensis* OLSSON, sample no. KTS 5, *P. hariaensis* zone, X176

Figure 24: *Hedbergella holmdelensis* OLSSON, sample no. HSE 46, *P. hariaensis* zone, X158

Figure 25: *Hedbergella holmdelensis* OLSSON, sample no. HSE 48, *P. hariaensis* zone, X133

Figure 26: *Hedbergella holmdelensis* OLSSON, sample no. HSE 46, *P. hariaensis* zone, X233

Figure 27: *Hedbergella holmdelensis* OLSSON, sample no. KTS 12, *P. hariaensis* zone, X154

Figure 28: *Hedbergella holmdelensis* OLSSON, sample no. HSE 44, *R. fructicosa* zone, X151

PLATE 14

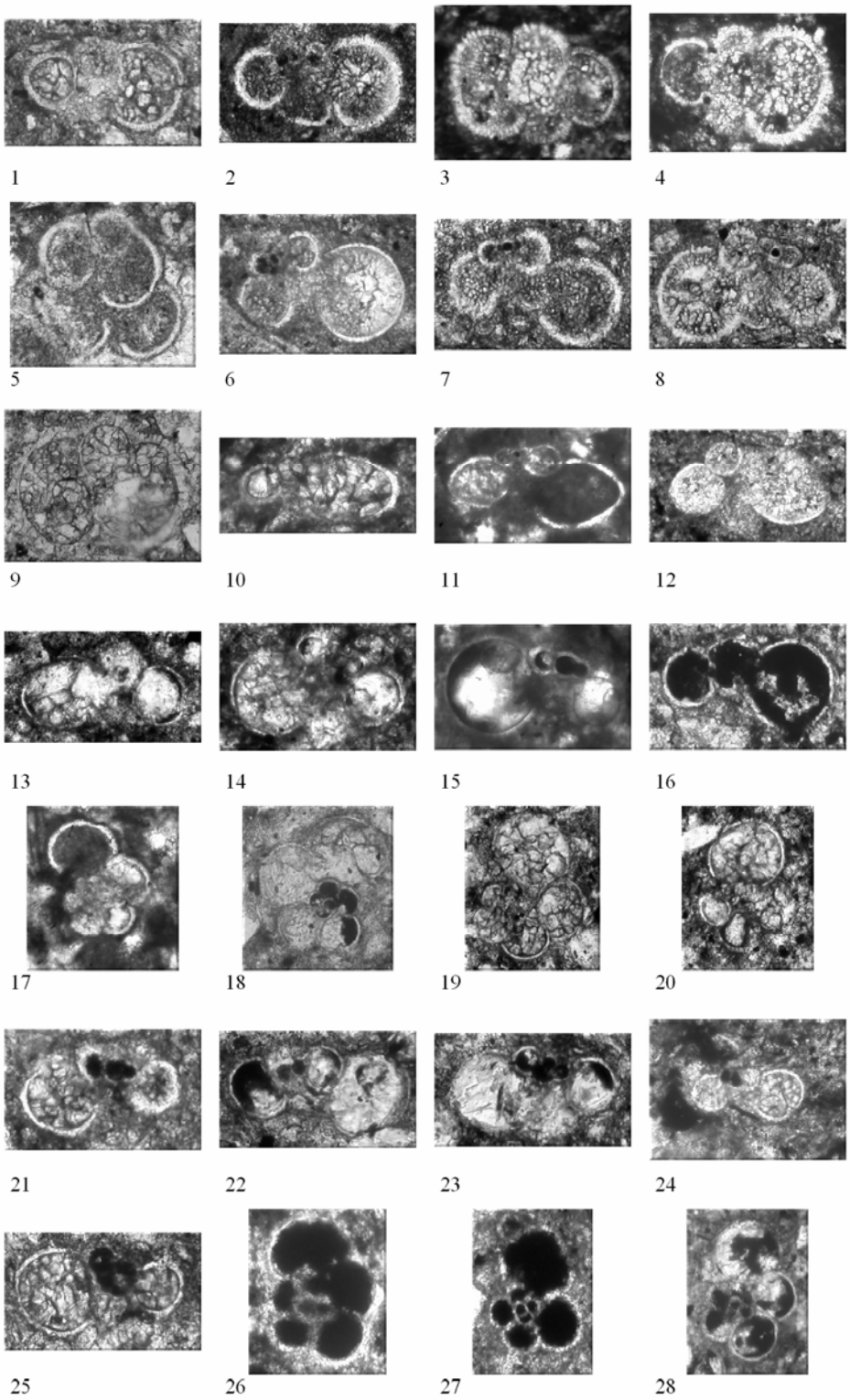

PLATE 15

Figure 1: *Globigerinelloides alvarezi* ETERNOD OLVERA, sample no. HSE 17, unzoned, X272

Figure 2: *Globigerinelloides alvarezi* ETERNOD OLVERA, sample no. HSE 25, unzoned, X315

Figure 3: *Globigerinelloides alvarezi* ETERNOD OLVERA, sample no. HSE 49, *P. hariaensis* zone, X180

Figure 4: *Globigerinelloides alvarezi* ETERNOD OLVERA, sample no. KTS 9, *P. hariaensis* zone, X417

Figure 5: *Globigerinelloides alvarezi* ETERNOD OLVERA, sample no. KTS 3, *P. hariaensis* zone, X206

Figure 6: *Globigerinelloides messinae* BRONNIMANN, sample no. HSE 42, *R. fructicosa* zone, X196

Figure 7: *Globigerinelloides messinae* BRONNIMANN, sample no. HSE 49, *P. hariaensis* zone, X387

Figure 8: *Globigerinelloides messinae* BRONNIMANN, sample no. KTS 10, *P. hariaensis* zone, X180

Figure 9: *Globigerinelloides prairiehillensis* PESSAGNO, sample no. HSE 41, *R. fructicosa* zone, X328

Figure 10: *Globigerinelloides prairiehillensis* PESSAGNO, sample no. HSE 33, unzoned, X180

Figure 11: *Globigerinelloides prairiehillensis* PESSAGNO, sample no. HSE 47, *R. fructicosa* zone, X328

Figure 12: *Globigerinelloides prairiehillensis* PESSAGNO, sample no. KTS 2, *R. fructicosa* zone, X240

Figure 13: *Globigerinelloides prairiehillensis* PESSAGNO, sample no. HSE 38, *P. acervulinoides* zone, X232

Figure 14: *Globigerinelloides prairiehillensis* PESSAGNO, sample no. HSE 48, *P. hariaensis* zone, X193

Figure 15: *Globigerinelloides prairiehillensis* PESSAGNO, sample no. HSE 47, *P. hariaensis* zone, X277

Figure 16: *Globigerinelloides prairiehillensis* PESSAGNO, sample no. KTS 9, *P. hariaensis* zone, X194

Figure 17: *Globigerinelloides subcarinatus* BRONNIMANN, sample no. HSE 47, *P. hariaensis* zone, X182

Figure 18: *Globigerinelloides subcarinatus* BRONNIMANN, sample no. HSE 47, *P. hariaensis* zone, X213

PLATE 15

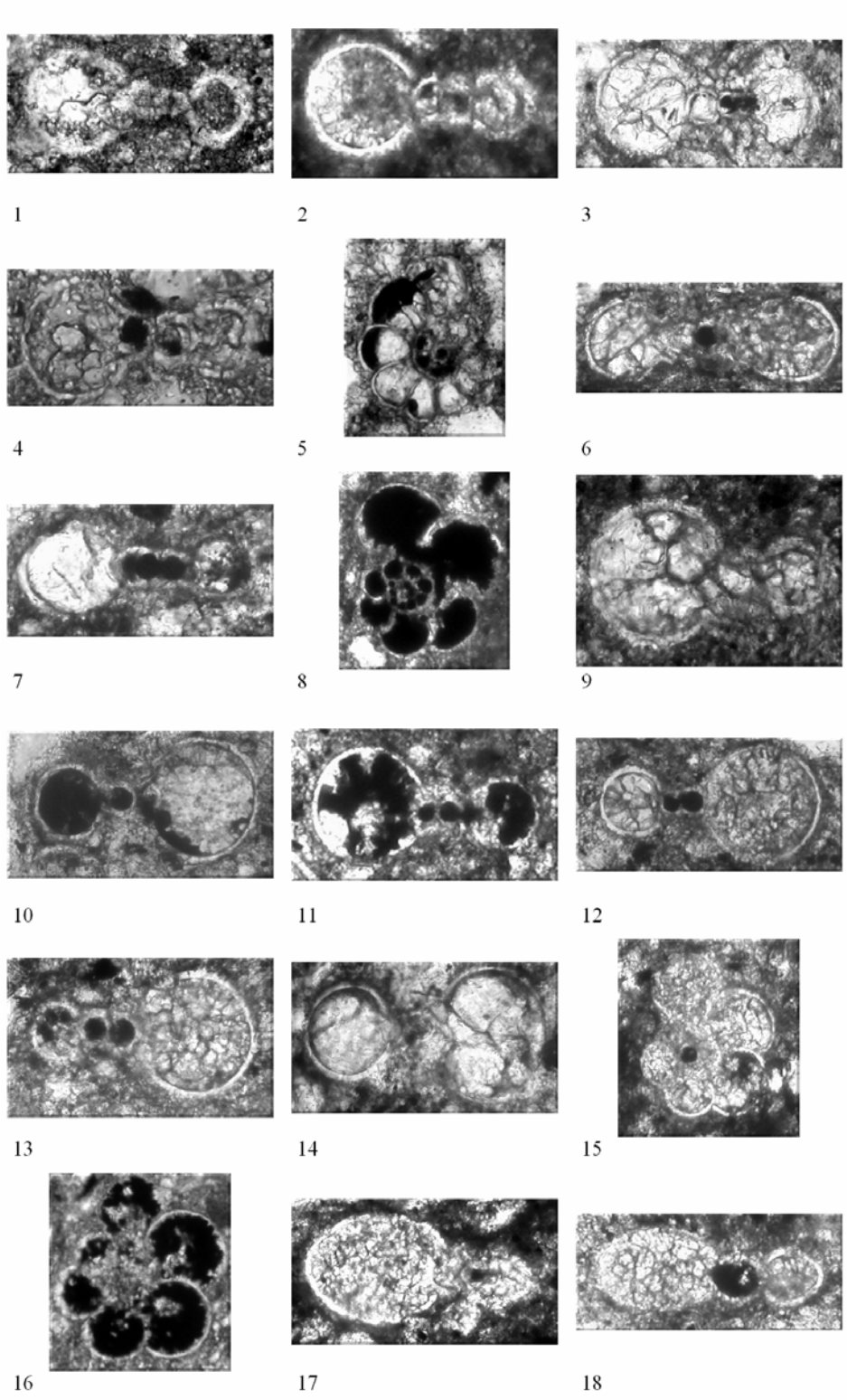

PLATE 16

Figure 1: *Heterohelix globulosa* EHRENBERG, sample no. KTS 9, *P. hariaensis* zone, X130

Figure 2: *Heterohelix globulosa* EHRENBERG, sample no. KTS 1, *P. hariaensis* zone, X148

Figure 3: *Heterohelix globulosa* EHRENBERG, sample no. HSE 33, unzoned, X154

Figure 4: *Heterohelix globulosa* EHRENBERG, sample no. HSE 43, *P. acervulinoides zone*, X148

Figure 5: *Heterohelix globulosa* EHRENBERG, sample no. HSE 45, *P. hariaensis* zone, X269

Figure 6: *Heterohelix globulosa* EHRENBERG, sample no. HSE 49, *P. hariaensis* zone, X330

Figure 7: *Heterohelix globulosa* EHRENBERG, sample no. KTS 1, *P. hariaensis* zone, X576

Figure 8: *Heterohelix navarroensis* LOEBLICH, sample no. KTS 2, *P. hariaensis* zone, X167

Figure 9: *Heterohelix navarroensis* LOEBLICH, sample no. KTS 2, *P. hariaensis* zone, X273

Figure 10: *Heterohelix navarroensis* LOEBLICH, sample no. HSE 46, *P. hariaensis* zone, X245

Figure 11: *Heterohelix navarroensis* LOEBLICH, sample no. KTS 2, *P. hariaensis* zone, X234

Figure 12: *Heterohelix navarroensis* LOEBLICH, sample no. HSE 30, unzoned, X187

Figure 13: *Heterohelix punctulata* CUSHMAN, sample no. KTS 8, *P. hariaensis* zone, X159

Figure 14: *Heterohelix labellosa* NEDERBRAGT, sample no. HSE 19, unzoned, X177

Figure 15: *Heterohelix labellosa* NEDERBRAGT, sample no. HSE 31, unzoned, X106

Figure 16: *Laeviheterohelix dentata* STENESTAD, sample no. HSE 45, *P. hariaensis* zone, X324

PLATE 16

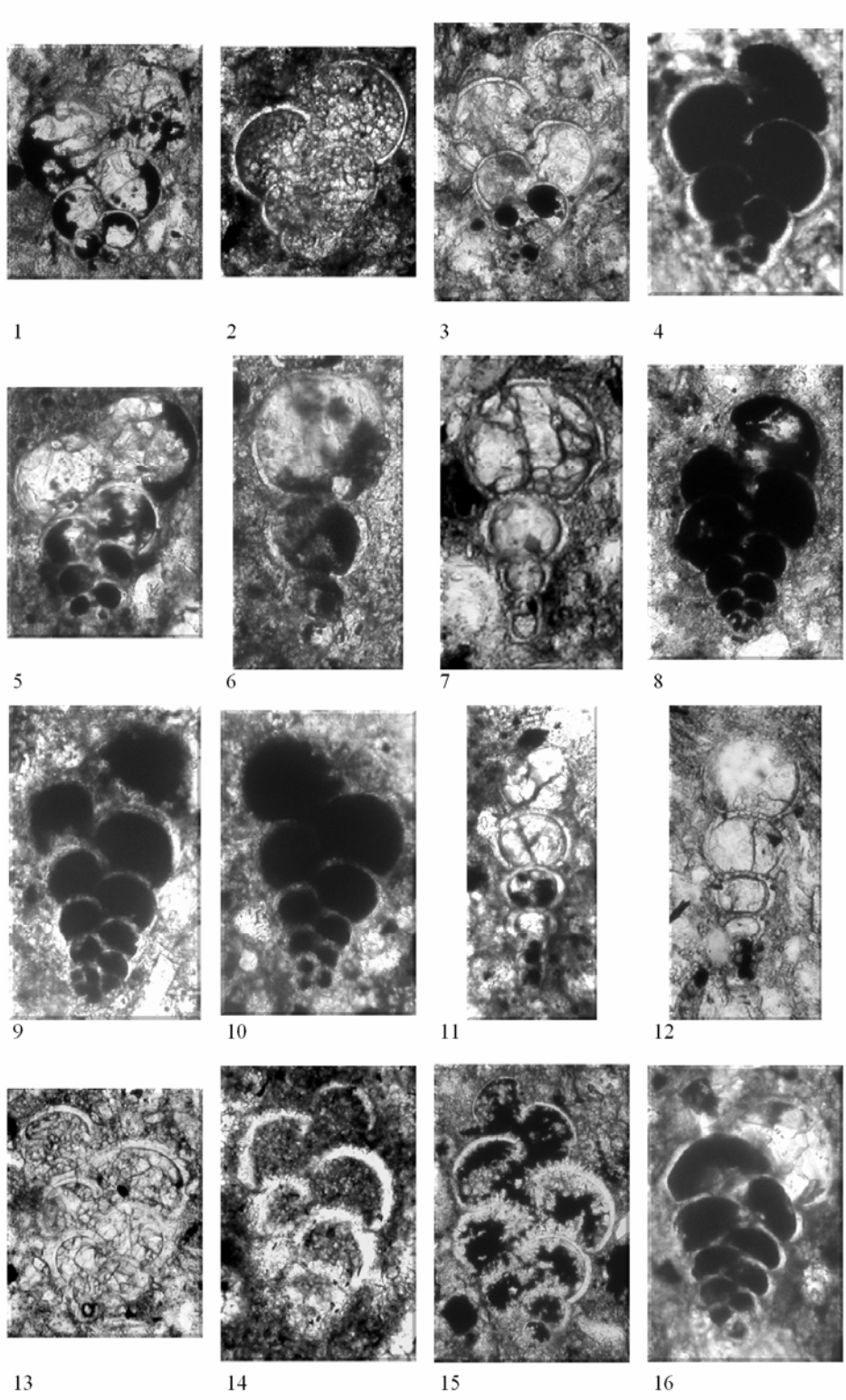

PLATE 17

Figure 1: *Pseudotextularia elegans* RZEHAK, sample no. HSE 41, *R. fructicosa* zone, X104

Figure 2: *Pseudotextularia elegans* RZEHAK, sample no. KTS 4, *P. hariaensis* zone, X88

Figure 3: *Pseudotextularia elegans* RZEHAK, sample no. HSE 47, *P. hariaensis* zone, X152

Figure 4: *Pseudotextularia nuttalli* VOORWIJK, sample no. HSE 36, *R. fructicosa* zone, X103

Figure 5: *Pseudotextularia nuttalli* VOORWIJK, sample no. HSE 39, *R. fructicosa* zone, X131

Figure 6: *Pseudoguembelina* sp., sample no. KTS 9, *P. hariaensis* zone, X

Figure 7: *Pseudoguembelina hariaensis* NEDERBRAGT, sample no. HSE 39, *R. fructicosa* zone, X80

Figure 8: *Pseudoguembelina excolata* CUSHMAN, sample no. HSE 25, unzoned, X114

Figure 9: *Planoglobulina carseyae* PLUMMER, sample no. KTS 6, *P. hariaensis* zone, X171

Figure 10: *Planoglobulina carseyae* PLUMMER, sample no. KTS 7, *P. hariaensis* zone, X117

Figure 11: *Planoglobulina carseyae* PLUMMER, sample no. KTS 6, *P. hariaensis* zone, X93

Figure 12: *Planoglobulina acervulinoides* EGGER, sample no. HSE 45, *P. hariaensis* zone, X86

Figure 13: *Racemiguembelina fructicosa* EGGER, sample no. HSE 47, *P. hariaensis* zone, X84

Figure 14: *Racemiguembelina powelli* SMITH and PESSAGNO, sample no. HSE 47, *P. hariaensis* zone, X89

Figure 15: *Racemiguembelina* sp., sample no. HSE 46, *P. hariaensis* zone, X125

PLATE 17

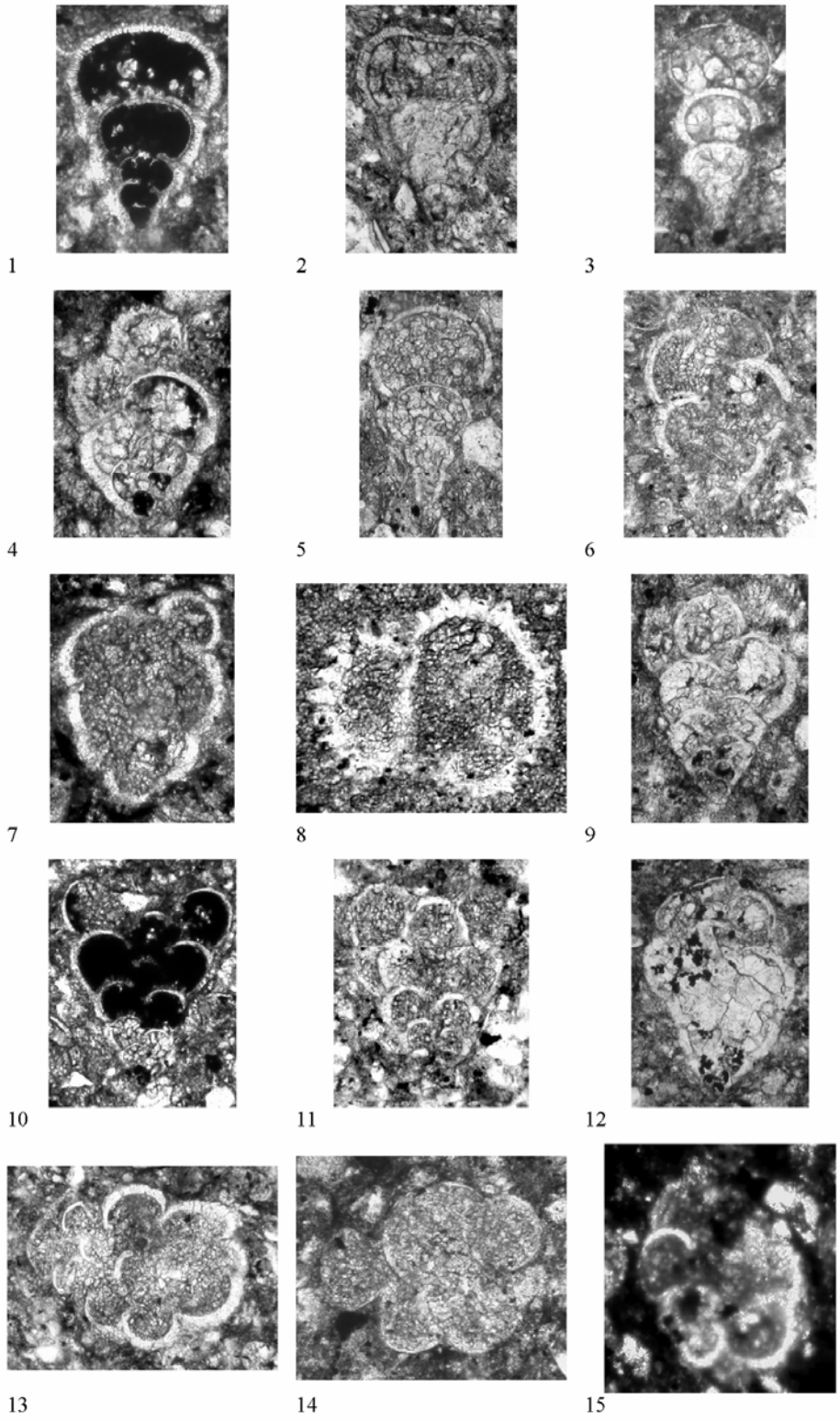

PLATE 18

Figure 1: *Eoglobigerina* sp., sample no. KTS 20, P1a zone, X177

Figure 2: *Eoglobigerina* sp., sample no. HSE 59, P1a zone, X102

Figure 3: *Eoglobigerina* sp., sample no. KTS 18, P1a zone, X101

Figure 4: *Eoglobigerina* sp., sample no. KTS 22, P1a zone, X195

Figure 5: *Eoglobigerina* sp., sample no. KTS 19, P1a zone, X176

Figure 6: *Eoglobigerina* sp., sample no. KTS 26, P1a zone, X175

Figure 7: *Eoglobigerina* sp., sample no. HSE 51, P0 zone, X130

Figure 8: *Eoglobigerina* sp., sample no. HSE 56, P1a zone, X117

Figure 9: *Eoglobigerina* sp., sample no. KTS 27, P1a zone, X120

Figure 10: *Globoconusa daubjergensis* BRONNIMANN, sample no. KTS 23, P1a zone, X137

Figure 11: *Globoconusa daubjergensis* BRONNIMANN, sample no. KTS 29, P1a zone, X153

Figure 12: *Globoconusa daubjergensis* BRONNIMANN, sample no. KTS 28, P1a zone, X100

Figure 13: *Globoconusa daubjergensis* BRONNIMANN, sample no. KTS 21, P1a zone, X106

Figure 14: *Globoconusa daubjergensis* BRONNIMANN, sample no. HSE 60, P1a zone, X144

Figure 15: *Globoconusa daubjergensis* BRONNIMANN, sample no. HSE 54, P1a zone, X300

Figure 16: *Globoconusa daubjergensis* BRONNIMANN, sample no. KTS 16, P1a zone, X163

Figure 17: *Parasubbotina pseudobulloides* PLUMMER, sample no. KTS 18, P1a zone, X85

Figure 18: *Parasubbotina pseudobulloides* PLUMMER, sample no. KTS 20, P1a zone, X96

Figure 19: *Parasubbotina pseudobulloides* PLUMMER, sample no. HSE 53, P1a zone, X98

Figure 20: *Parasubbotina pseudobulloides* PLUMMER, sample no. HSE 56, P1a zone, X143

Figure 21: *Subbotina triloculinoides* PLUMMER, sample no. HSE 60, P1a zone, X137

Figure 22: *Subbotina triloculinoides* PLUMMER, sample no. HSE 60, P1a zone, X262

Figure 23: *Subbotina triloculinoides* PLUMMER, sample no. HSE 53, P1a zone, X156

Figure 24: *Subbotina triloculinoides* PLUMMER, sample no. HSE 58, P1a zone, X73

Figure 25: *Subbotina triloculinoides* PLUMMER, sample no. KTS 26, P1a zone, X175

Figure 26: *Subbotina triloculinoides* PLUMMER, sample no. HSE 60, P1a zone, X152

Figure 27: *Subbotina triloculinoides* PLUMMER, sample no. KTS 21, P1a zone, X148

Figure 28: *Subbotina triloculinoides* PLUMMER, sample no. HSE 56, P1a zone, X118

PLATE 18

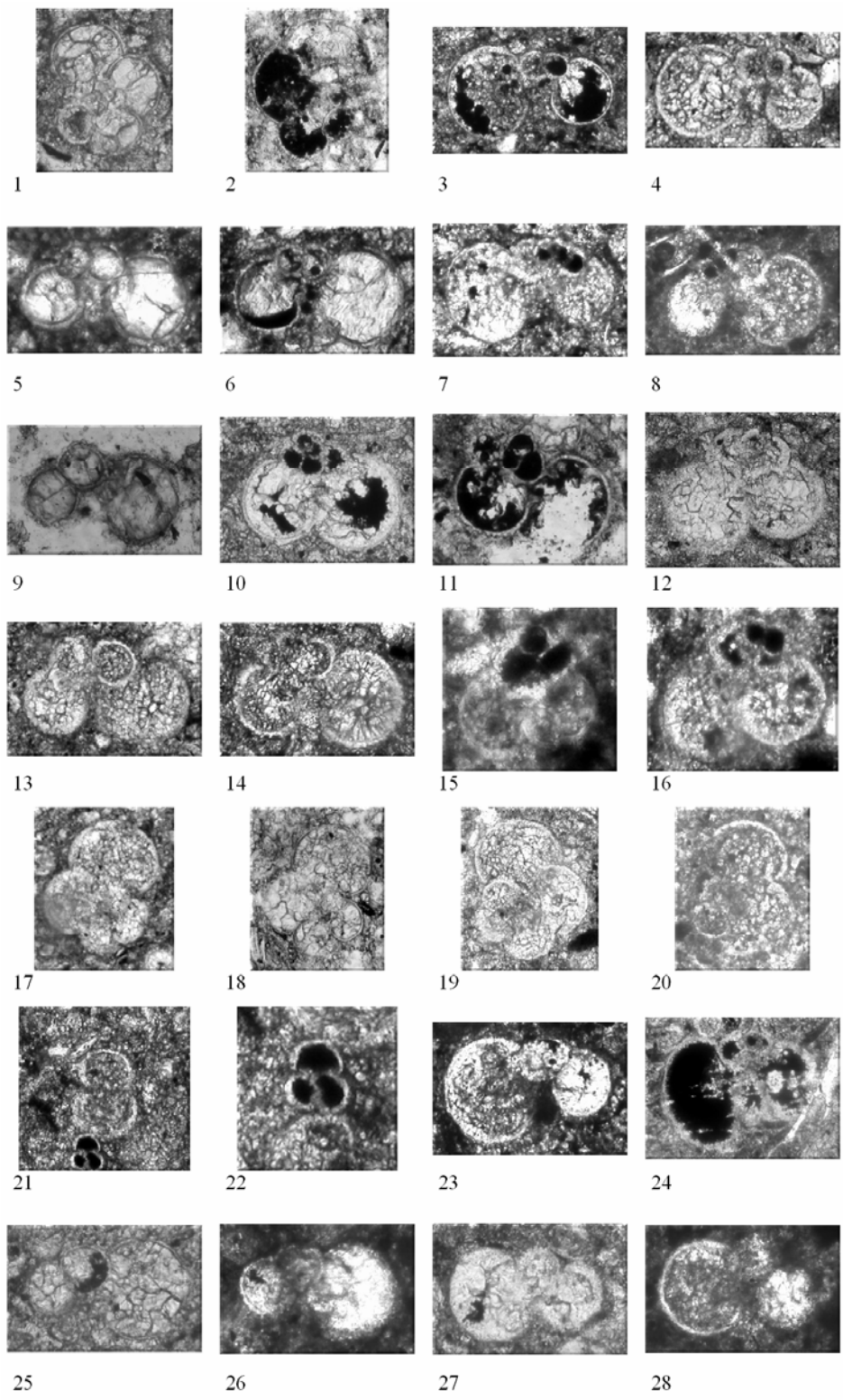

PLATE 19

Figure 1: *Woodringina hornerstownensis* OLSSON, sample no. KTS 27, P1a zone, X253

Figure 2: *Woodringina hornerstownensis* OLSSON, sample no. KTS 19, P1a zone, X196

Figure 3: *Woodringina hornerstownensis* OLSSON, sample no. KTS 27, P1a zone, X283

Figure 4: *Woodringina hornerstownensis* OLSSON, sample no. HSE 59, P1a zone, X261

Figure 5: *Woodringina hornerstownensis* OLSSON, sample no. KTS 27, P1a zone, X121

Figure 6: *Woodringina hornerstownensis* OLSSON, sample no. HSE 60, P1a zone, X144

Figure 7: *Woodringina claytonensis* LOEBLICH and TAPPAN, sample no. KTS 27, P1a zone, X252

Figure 8: *Woodringina claytonensis* LOEBLICH and TAPPAN, sample no. HSE 57, P1a zone, X190

Figure 9: *Woodringina claytonensis* LOEBLICH and TAPPAN, sample no. HSE 52, P1a zone, X225

Figure 10: *Woodringina claytonensis* LOEBLICH and TAPPAN, sample no. KTS 25, P1a zone, X196

Figure 11: *Woodringina claytonensis* LOEBLICH and TAPPAN, sample no. KTS 19, P1a zone, X234

Figure 12: *Woodringina claytonensis* LOEBLICH and TAPPAN, sample no. KTS 22, P1a zone, X165

Figure 13: *Woodringina claytonensis* LOEBLICH and TAPPAN, sample no. KTS 21, P1a zone, X185

Figure 14: *Woodringina claytonensis* LOEBLICH and TAPPAN, sample no. KTS 19, P1a zone, X160

Figure 15: *Woodringina claytonensis* LOEBLICH and TAPPAN, sample no. HSE 52, P1a zone, X224

Figure 16: *Woodringina claytonensis* LOEBLICH and TAPPAN, sample no. HSE 55, P1a zone, X240

Figure 17: *Chiloguembelina morsei* KLINE, sample no. HSE 51, P1a zone, X141

Figure 18: *Chiloguembelina morsei* KLINE, sample no. KTS 21, P1a zone, X450

Figure 19: *Chiloguembelina morsei* KLINE, sample no. KTS 18, P1a zone, X504

Figure 20: *Chiloguembelina morsei* KLINE, sample no. KTS 27, P1a zone, X284

Figure 21: *Chiloguembelina midwayensis* CUSHMAN, sample no. HSE 55, P1a zone, X285

Figure 22: *Chiloguembelina midwayensis* CUSHMAN, sample no. KTS 21, P1a zone, X368

Figure 23: *Chiloguembelina midwayensis* CUSHMAN, sample no. HSE 53, P1a zone, X184

Figure 24: *Chiloguembelina midwayensis* CUSHMAN, sample no. KTS 20, P1a zone, X422

Figure 25: *Zeauvigerina waiparaensis* JENKINS, sample no. KTS 17, P1a zone, X177

PLATE 19

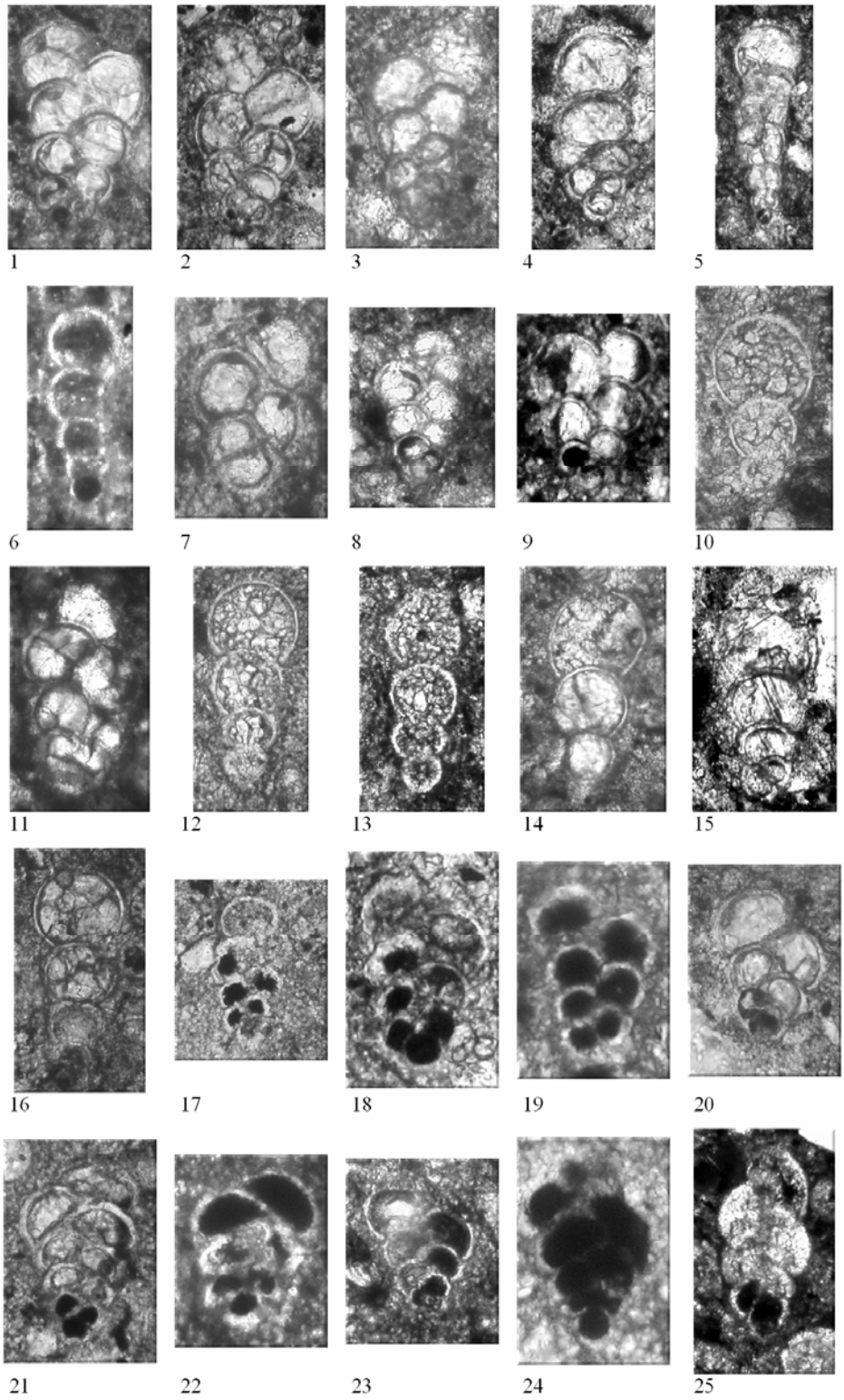

PLATE 20

Figure 1: *Guembelitria cretacea* CUSHMAN, sample no. KTS 27, P1a zone, X165

Figure 2: *Guembelitria cretacea* CUSHMAN, sample no. HSE 59, P1a zone, X425

Figure 3: *Guembelitria cretacea* CUSHMAN, sample no. HSE 54, P1a zone, X340

Figure 4: *Guembelitria cretacea* CUSHMAN, sample no. HSE 53, P1a zone, X368

Figure 5: *Guembelitria cretacea* CUSHMAN, sample no. HSE 53, P1a zone, X268

Figure 6: *Guembelitria cretacea* CUSHMAN, sample no. KTS 24, P1a zone, X354

Figure 7: *Guembelitria cretacea* CUSHMAN, sample no. KTS 18, P1a zone, X338

Figure 8: *Guembelitria cretacea* CUSHMAN, sample no. HSE 56, P1a zone, X235

Figure 9: *Guembelitria cretacea* CUSHMAN, sample no. HSE 57, P1a zone, X192

Figure 10: *Guembelitria cretacea* CUSHMAN, sample no. HSE 54, P1a zone, X234

Figure 11: *Guembelitria cretacea* CUSHMAN, sample no. HSE 56, P1a zone, X264

Figure 12: *Guembelitria cretacea* CUSHMAN, sample no. HSE 53, P1a zone, X504

Figure 13: *Guembelitria cretacea* CUSHMAN, sample no. KTS 10, P1a zone, X345

Figure 14: *Guembelitria cretacea* CUSHMAN, sample no. KTS 17, P1a zone, X287

Figure 15: *Guembelitria cretacea* CUSHMAN, sample no. KTS 24, P1a zone, X397

PLATE 20